Coordination Chemistry Reviews 254 (2010) 2096–2180

Contents lists available at ScienceDirect

Coordination Chemistry Reviews

journal homepage: www.elsevier.com/locate/ccr

Review

1,10-Phenanthroline: A versatile building block for the construction of ligands for various purposes

Andrea Bencini [a,*], Vito Lippolis [b,**]

[a] Dipartimento di Chimica "Ugo Schiff", Università degli Studi di Firenze, Polo Scientifico, Via della Lastruccia 3, 50019 Sesto Fiorentino, Florence, Italy
[b] Dipartimento di Chimica Inorganica ed Analitica, Università degli Studi di Cagliari, S.S. 554 bivio per Sestu, 09042 Monserrato, CA, Italy

Contents

Abbreviations: Phen, 1,10-phenanthroline; en, ethylenediamine; bpy, 2,2′-bipyridine; tpy, 2,2′ ;6′,6″-terpyridine; MLCT, metal-to-ligand charge-transfer; *N*-MeIm, 1-methylimidazole; manisyl, 4-methoxy-2,6-dimethylphenyl; neocuproine, 2,9-dimethyl-1,10-phenanthroline; 2,3-dpp, 2,3-*bis*(2-pyridyl)pyrazine; tren, *tris*(2-aminoethyl)amine; BNPP, *bis*(*p*-nitrophenyl)phosphate; HPNP, 2-hydroxypropyl-4-nitrophenyl phosphate; ISE, ion-selective electrode; SLM, supported liquid membrane; tbtpy, 4′-(3,5-di-*tert*-butylphenyl)-2,2′ ;6′,2″-terpyridine; 4,4′-dmbp, 4,4′-dimethyl-2,2′-bipyridine; 4,7-dpphen, 4,7-diphenyl-1,10-phenanthroline; MC, metal centred; LC, ligand centred; ECL, electrogenerated chemiluminescence; py, pyridine; PET, photoinduced electron transfer; cyclitol, cyclohexane diol; cbz, benzyloxycarbonyl; CD, circular dichroism; EtB, ethydium bromide; dppz, dipyrido[3,2-a:2′,3-c]phenazine; phi, 9,10-phenanthrenequinone diimine; dpq, dipyrido[3,2-*f*:2′,3′-h]quinoxaline; dppf, 1,10-bis(diphenylphosphino)ferrocene; gmp, 4-(guanidylmethyl)-1,10-phenanthroline; TAP, 1,4,5,8-tetraazaphenanthrene; HAT, 1,4,5,8,9,12-hexaazatriphenylene; bpz, 2,2′-bipyrazine; DMTr, 4,4′-dimethoxytrityl; TSU, *N*,*N*,*N*′,*N*′-tetramethyl(succinimido) uronium tetrafluoroborate; FRET, fluorescence resonance energy transfer; cyclen, 1,4,7,10-tetraazacyclododecane; 2,9-dpphen, 2,9-diphenyl-1,10-phenanthroline; HETPHEN, heterolopetic phenanthroline metal complexes; HETTAP, heteroleptic terpyridine and phenanthroline metal complexes; DOSY, diffusion ordered spectroscopy; DABCO, 1,4-diazabicyclo[2.2.2]octane.

* Corresponding author. Tel.: +39 055 4573371; fax: +39 055 4573364.
** Corresponding author. Tel.: +39 070 6754467; fax: +39 070 6754456.
E-mail addresses: andrea.bencini@unifi.it (A. Bencini), lippolis@unica.it (V. Lippolis).

0010-8545/$ – see front matter
doi:10.1016/j.ccr.2010.04.008

ARTICLE INFO

Article history:
Received 16 February 2010
Accepted 11 April 2010
Available online 24 April 2010

Keywords:
Phenanthroline
Coordination chemistry
Supramolecular chemistry
Sensors
DNA binders

ABSTRACT

This review will cover the developments in the chemistry of phenanthroline-based ligands in the last 10–15 years. 1,10-Phenanthroline (phen) is a classic ligand in coordination chemistry, which couples versatility in metal ion binding with peculiar properties of its complexes. For instance, metal complexes with phenanthroline can be featured by an intense luminescence or can interact with DNA in an intercalative fashion inducing, in some cases, DNA cleavage. For this reason a number of phenanthroline-containing ligands has been recently synthesized by inserting phenanthroline within open-chain or macrocyclic backbone, in order to develop new molecular chemosensors for metal cations and anions, ionophores as well as new intercalating agents for polynucleotides. Furthermore, phenanthroline is rigid and its insertion within cyclic or acyclic structures can impart to the resulting ligand a high degree of pre-organization, affording selective complexing agents. This review will discuss on the coordination, luminescence and intercalating and/or DNA cleaving properties as well as on analytical applications of metal complexes with phenanthroline-based ligands. Particular attention will be devoted to macrocyclic receptors or open-chain ligands that, beside the phenanthroline nitrogen atoms, contain other donor atoms able to interact with the metal cations or anions.

1. Introduction

1,10-Phenanthroline (phen) is a classic chelating bidentate ligand for transition metal ions that has played an important role in the development of coordination chemistry [1–3] and still continues to be of considerable interest as versatile starting material for organic, inorganic and supramolecular chemistry. Phen is a rigid planar, hydrophobic, electron-poor heteroaromatic system whose nitrogen atoms are beautifully placed to act cooperatively in cation binding. These structural features determine its coordination ability toward metal ions.

The phen ligand behaves as a weak base in aqueous solution, the protonation constant being 4.95 log units [4,5]. Its basicity is remarkably lower than aliphatic diamines, such as ethylenediamine (en) ($\log K = 10.65$ and 8.04 for successive addition of acidic protons to en) [6], in agreement with the electron-poor characteristics of the heteroaromatic rings and to the consequent lower σ-donor ability of its nitrogen atoms [7]. Nevertheless, phen displays a noticeable coordination ability for transition metal cations. Phen easily forms in aqueous solution octahedral complexes of the type $[M(phen)(H_2O)_4]^{2+}$, $[M(phen)_2(H_2O)_2]^{2+}$ and $[M(phen)_3]^{2+}$ with first-row transition metal cations. The stability of the $[M(phen)]^{2+}$ complexes follows the Irving–Williams sequence, their formation constants spanning from 4.13 ($[Mn(phen)]^{2+}$) to 9.25 ($[Cu(phen)]^{2+}$) log units [4]. Despite the low σ-donor ability of the heteroaromatic nitrogen atoms, the stability of these complexes is somewhat higher than that found for the corresponding complexes with en. In fact, the complexes with phen exhibit a larger entropic contribution to complex stabilization than en, mainly due to the hydrophobic nature of phen and to the consequent larger desolvation of metal cations upon complex formation [4,5]. At the same time, the poorer σ-donor ability of the heteroaromatic nitrogen atoms is compensated by the ability of phen to behave as π-acceptor [4,5]. In consequence, the complexes $[M(phen)_x]^{2+}$ in aqueous solution (M = first-row transition metal, $x = 1–3$) are generally stabilized by a favourable enthalpic contribution, similar to that reported for the corresponding complexes with en, accounting for the formation of a couple of strong coordination bonds [4,5,7]. Only the complex $[Fe(phen)_3]^{2+}$ displays an enthalpic contribution remarkably larger than that found for $[Fe(en)_3]^{2+}$, due to the low-spin stabilizing d^6 electronic configuration of Fe^{2+} in the former complex.

Compared to the parent 2,2′-bipyridine (bpy) and 2,2′; 6′,6″-terpyridine (tpy) systems (Scheme 1), phen is characterized by two inward-pointing nitrogen donor atoms being held juxtaposed and, therefore, pre-organized for strong and entropically favoured metal binding.

A similar disposition of the nitrogen donors in bpy and tpy can be disrupted by the free rotation about the bond(s) linking the heteroaromatic six-membered rings.

Taking advantages of these structural features (planarity, rigidity and hydrophobicity) phen derivatives and their metal complexes have been used, for example, as intercalating or groove binding agents for DNA and RNA [2,8,9]. Some metal complexes are also able to efficiently cleave the DNA backbone and nowadays the complex $[Cu(phen)_2]^{2+}$ is commonly used in molecular biology as DNA cleaving reagent [9].

The photophysical properties of phen have been subject of a number of studies since the fifties and will be only shortly accounted here. A more detailed discussion can be found in Refs. [10–12]. Phen is essentially characterized in aqueous solution by UV absorptions at 229 and 265 nm, the latter attributed to a $\pi–\pi^*$ transition to the lowest-energy excited singlet state, $^1\pi\pi^*$ [10,11]. Excitation at 307 nm originates a fluorescence emission band at 380 nm, due to radiative decay of the $^1\pi\pi^*$ state. More interestingly, these spectroscopic features are modulated by appropriate substituents on the phen framework and pH changes, *i.e.*, by protonation of the heteroaromatic nitrogen atoms. The UV spectrum recorded at pH 4, where phen is in its monoprotonated form, $(phenH)^+$, shows a *ca.* 8 nm red shift of the absorption band at 265 nm [10], attributed to some charge-transfer character of the $\pi–\pi^*$ transition (*i.e.*, the LUMO has a higher electron density on the nitrogen atoms than the HOMO). Monoprotonation of phen leads to the disappearance of the emission band at 380 nm and to the formation of a new emission broad red-shifted band at *ca.* 410 nm,

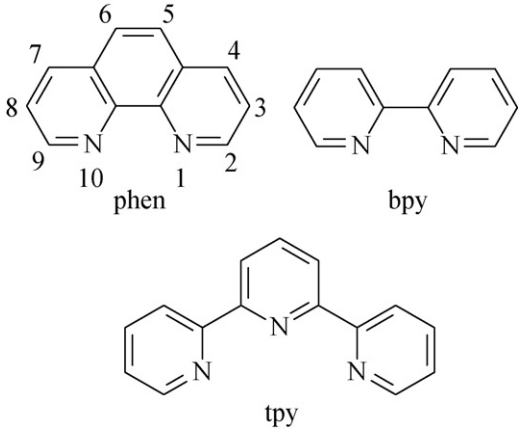

Scheme 1.

accounting for stabilization of the lowest-energy $^1\pi\pi^*$ state by protonation of the heteroaromatic nitrogen atoms because of its charge-transfer character [10,11].

Another distinct property of this class of chelating agents, phen and bpy, in particular, is their π-electron deficiency that makes them excellent π acceptors capable of stabilizing metal ions in lower oxidation states. Furthermore, due to the presence of low-energy π^* orbitals of the ligand, metal complexes can be characterized by strong metal-to-ligand charge-transfer (MLCT) absorption bands in the visible spectrum and red-shifted fluorescent emissions [13,14].

Due to the combination in phen of these distinct structural and chemical properties, metal complexes with phen-based ligands have been actively studied since the seventies for their catalytic, redox, photochemical and photophysical properties [3,13–17] and, therefore, more recently, as building units for the construction of efficient luminescent materials and even photoswitchable molecular devices [12,18,19]. In the last two decades, functionalized phen derivatives have also heavily been exploited by chemists involved with molecular recognition and sensing [3,20], DNA/RNA binding/cleavage [2,8,9] and molecular self-assembling. Many extraordinary molecular architectures such as catenanes, rotaxanes and knots owe their appearance in the literature thank to the coordinating properties of phen [21]. Far from the intention to write a seminal review, in this work we intend to cover the most recent (10–15 years) and relevant aspects of the synthetic and coordination chemistry of phen-based ligands, cyclic and non cyclic, characterized by additional coordinating groups, and their use for the development of ligands for different purposes, in particular, luminescent materials, efficient receptors and new molecular chemosensors for metal cations and anions, as well as new intercalating agents for polynucleotides. In the last part of the review, a brief outline of the most recent trends in self-assembling and material chemistry using the phen group will be given. Polycyclic heteroaromatic fused systems featuring phen moieties will not be considered. The main aim of this work, however, is to show the reader how versatile phen can be and, how useful its derivatives are as building blocks for various purposes.

2. Synthesis and metal binding properties of phenanthroline-based ligands

The increasing interest in the chemistry of phen derivatives has prompted the development of efficient synthetic procedures for the chemical functionalization of the phen nucleus at the various ring positions. The symmetric synthetic manipulation at the 2,9-positions to prepare more elaborate phen-based structures represents the most preferred strategy. Symmetric substitution at the 3,8-, 4,7- and 5,6-positions are less common and even less numerous are unsymmetrical functionalizations of the phen. In this section, the main synthetic and coordination chemistry aspects of recently reported, relatively simple phen-based ligands will be reviewed by paying particular attention to the goals the many researchers intended to achieve with their synthesis. This first section can also be considered as an introduction to the following sections in which the development of more complex and multifunctional systems will be considered in more details in relation to the specific task they have been designed for.

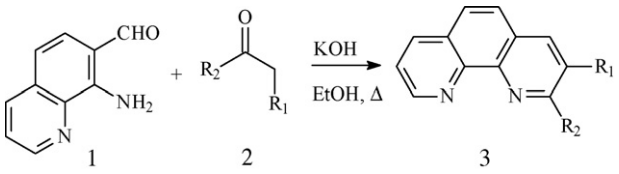

Scheme 2.

2.1. 2-Mono- or 2,9-disubstituted 1,10-phenanthroline derivatives (open-chain ligands)

Phen derivatives bearing substituents at the 2-position can be directly prepared through the Friedländer condensation. In this classical reaction, an *o*-aminoaldehyde such as the 8-amino-7-quinolinecarbaldehyde (**1**) condenses with an enolizable ketone, **2**, with concomitant loss of water, according to Scheme 2.

This useful and versatile method has recently been extensively applied by Thummel and co-workers for the construction of a great variety of symmetrical phen-based bridging ligands of different denticity featuring two proximal 1,10-phenanthrolin-2-yl units and a central (hetero)aromatic linker, such as **4**–**7** (Scheme 3) [22–30].

These ligands allow the preparation of mono- and dinuclear metal complexes, in particular Ru^{2+} complexes, whose photo- and electrochemical properties mainly depend on the degree of communication between the metal centres which can be finely tuned by changing the size, shape and binding properties of the central linker [24–30].

Thummel and co-workers have also used the Friedländer condensation for the preparation of the unsymmetrical terdentate ligands **8**–**10** (Scheme 4) [31–33].

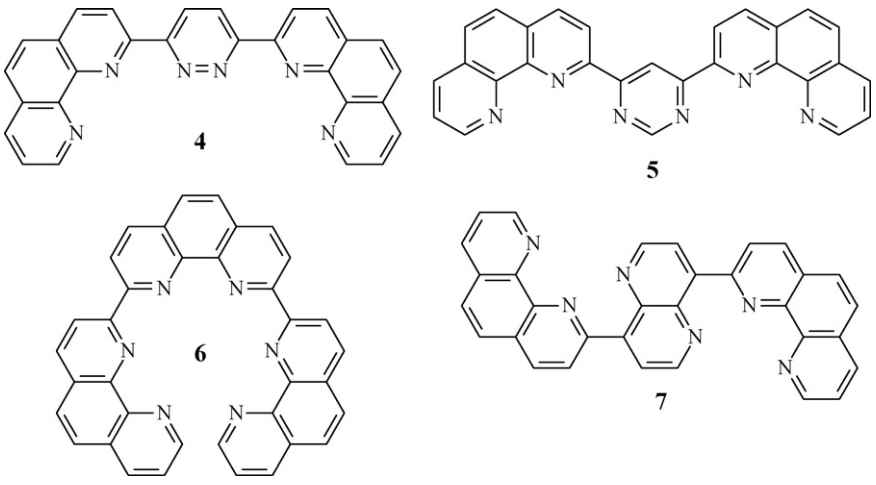

Scheme 3.

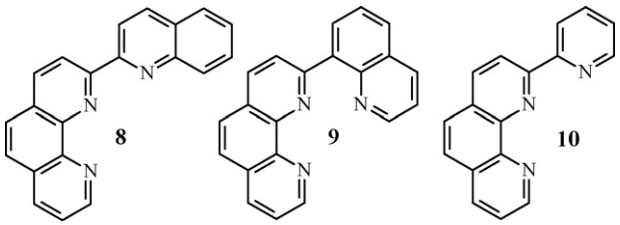

Scheme 4.

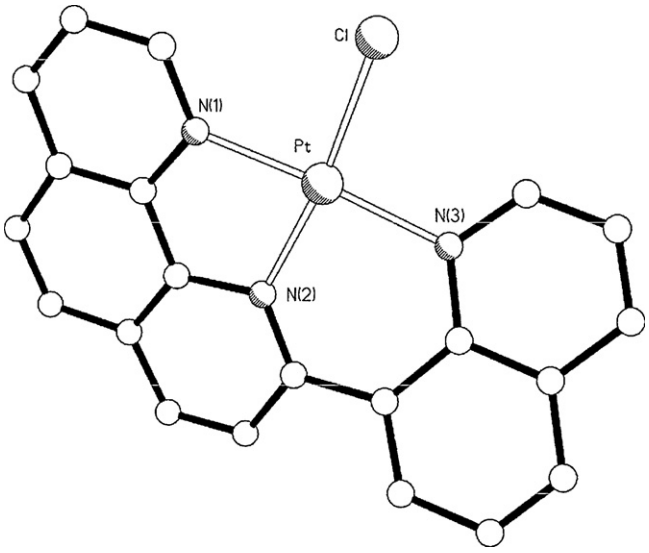

Fig. 1. ORTEP view of the complex cation [Pt(**9**)Cl]$^+$ [33]. H-atoms are omitted for clarity. In this and other similar figures, the X-ray data are taken from the Cambridge Crystallographic Data Centre (CCDC).

As contrary to what observed for the complex [Pt(tpy)Cl]$^+$, the corresponding platinum(II) complexes of the tpy-like ligands **8**–**10** shown in Scheme 4 are photoluminescent in fluid solutions of dichloromethane and, therefore, could represent more useful DNA intercalators and protein probes. It is commonly accepted that excited-state lifetimes of platinum(II) polypyridine complexes are strongly reduced because of the presence of thermally accessible d–d excited-states which promote non-radiative decay processes.

In the emissive complexes [Pt(**9**)Cl]$^+$ (see Fig. 1) and [Pt(**10**)Cl]$^+$, d–d excited-states become less accessible due to a higher degree of planarity of the ligands which strengthen the metal-ligand σ bond, and due to their fused-ring structure and more extended π system that lower the energy of the MLCT absorption [33–35].

A very efficient method for the synthesis of 2,9-diaryl-1,10-phenanthrolines was developed by Sauvage and co-workers in the early eighties and consists of a nucleophilic addition at the 2,9-position of the phen nucleus of an appropriate aryllithium reagent followed by an oxidative re-aromatization [36]. This synthetic method has been crucial for the development of topological interesting and fascinating molecular architectures such as catenanes, rotaxanes and knots [21], but it has also been used for the synthesis of less complicated tetradentate and tridentate ligands such as **11**–**13** (Scheme 5), featuring, respectively, the phen nucleus bearing phenolic moieties at the 2,9-positions (**11**) [37–39] or at the 2-position (**12**) [40], and a 2-dimethylaminophenyl group at the 2-position (**13**) [41].

The iron(III) complexes [Fe(**11**-2H)Cl]$_2$·2DMSO and [Fe(**11**-2H)(*N*-MeIm)$_2$](ClO$_4$) (*N*-MeIm = 1-methylimidazole) have been synthesized and structural characterized [37]. While in [Fe(**11**-2H)Cl]$_2$ (see Fig. 2b) two [Fe(**11**-2H)Cl] units are bridged by two oxygen atoms of the phenolate ligands, in [Fe(**11**-2H)(*N*-MeIm)$_2$]$^+$ (see Fig. 2a) the Fe^{3+} ion is in a *pseudo*-octahedral coordination environment with the donor atom from the deprotonated ligand occupying the equatorial positions, and the two *N*-MeIm ligands occupying the axial positions. Both complexes are reported to catalyze the electrochemical reduction of carbon dioxide to a mixture of carbon monoxide, formate and oxalate, with formate being the major product [37].

The square-planar platinum(II) complex of the structural analogues of **11** featuring also phenyl groups at the 4,7-positions is highly luminescent in solution and has been employed as electrophosphorescent dopant in multilayer OLEDs [39].

The presence of bulky *tert*-butyl substituents in **12** prevents dimerization of the corresponding copper(II) complexes, and the neutral cupric complexes [Cu(**12**-H)(CF$_3$SO$_3$)] and [Cu(**12**-H)Cl] have been isolated and, the former, structurally characterized [40]. This complex shows a strongly distorted coordination geometry at the metal centre; furthermore, electrochemical properties and affinity for alcohol and alcoholate ligands make these monophenolate–copper(II) complexes potential models of galactose oxidase [40].

The terdentate ligand **13** (Scheme 5) can be considered a structural analogous of **10**; however, its 1:1 complex [Pd(**13**)Cl]$^+$ is not perfectly square-planar as [Pt(**10**)Cl]$^+$ and shows a dihedral twist angle of about 40° between the phenyl and the phen fragments of the ligand [41]. The homoleptic copper(I) complex [Cu(**13**)$_2$]$^+$ has also been prepared and structurally characterized [42]. This complex shows a highly distorted tetrahedral structure in which only the phen moieties of the two ligands units are coordinated to the metal centre, while the 2-dimethylaminophenyl fragments are pendant. [Cu(**13**)$_2$]$^+$ is not emissive probably because the metal centre is only partially locked into a *pseudo*-tetrahedral environment and, therefore, quenching of the excited state may occur either *via* formation of a five-coordinate exciplex with solvent and counter-ion, or *via* an intramolecular exciplex formation from transient coordination of the pendant amino groups (see below) [42].

The Sauvage's method [36] has also been extensively used by Schmittel and co-workers for the preparation of sterically encumbered phen ligands such as **14** characterized by the presence of bulky aryl substituents in the 2,9-positions (Scheme 6).

Ligands of this type have been used to selectively prepare kinetically locked heteroleptic *bis*(phen) complexes of different metal ions, in particular Cu$^+$, Ag$^+$, and Zn^{2+}. In fact, the presence of bulky

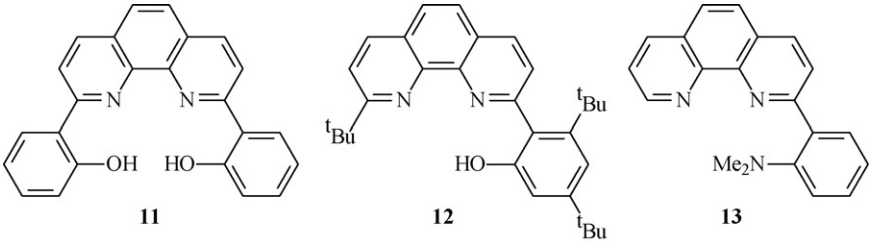

Scheme 5.

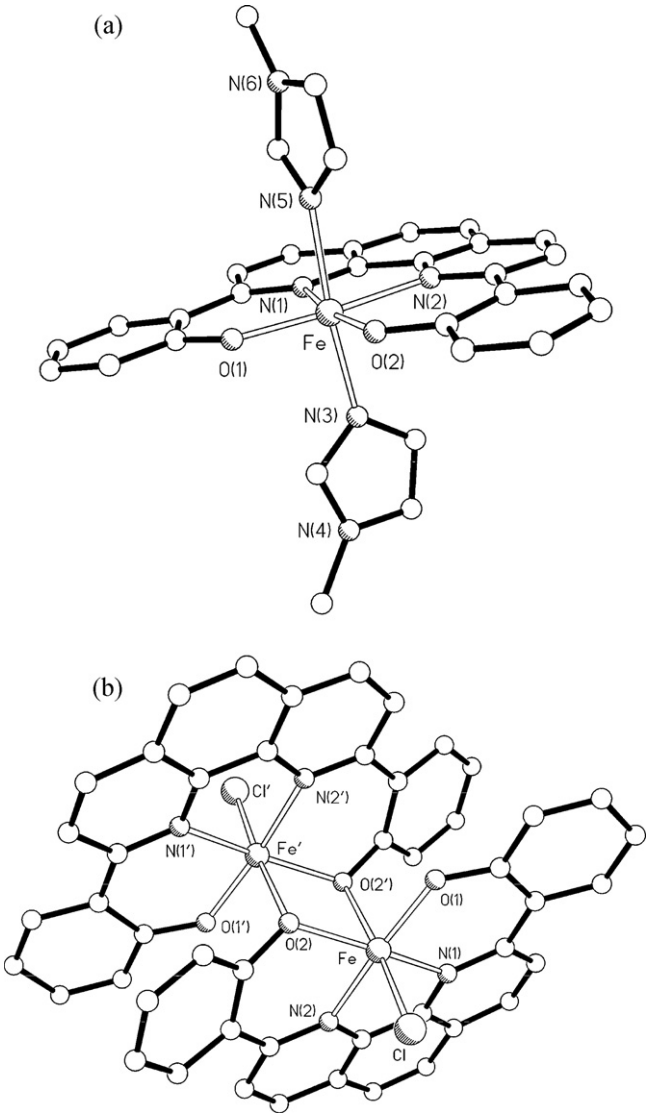

Fig. 2. ORTEP view of [Fe(**11**-2H)(*N*-MeIm)$_2$]$^+$ (a) and [Fe(**11**-2H)Cl]$_2$ (b) [37]. H-atoms are omitted for clarity.

aryl groups at the 2,9-positions in **14** prevents the thermodynamically favoured formation of homoleptic [M(**14**)$_2$]$^{n+}$ complexes, but it allows the combination of the fragment [M(**14**)]$^{n+}$ with less sterically demanding ligands including phen, to afford heteroleptic complexes. This concept has found ample use in the controlled self-assembly of polynuclear supramolecular frameworks such as

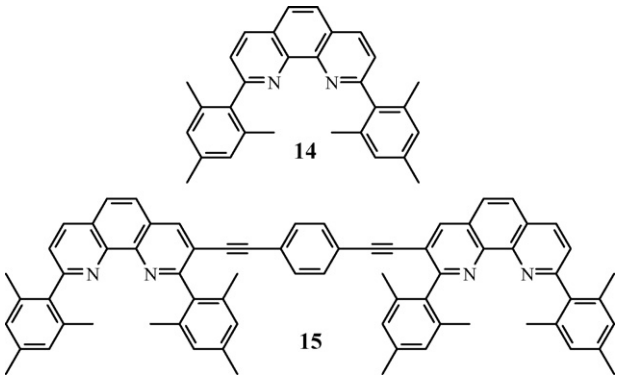

Scheme 6.

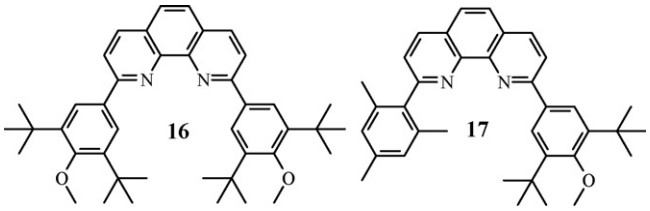

Scheme 7.

nanosized ladders and racks, grids, boxes, dumbbells and other topologies, by implementing sterically encumbered phen moieties in multiple ligands such as **15** (see Section 6) [43–53].

Interestingly, the homoleptic 1:2 Cu$^+$ complexes of **16** and **17** (Scheme 7), could be prepared by Schmittel and Armaroli, and resulted kinetically locked by the bulky *tert*-butylphenyl substituents: once formed, it did not exchange ligands even when phen was added in excess [54].

Furthermore, the bulky aryl substituents at the 2,9-positions of the phen nucleus in **16** and **17** hampered a flattening distortion from the *pseudo*-tetrahedral coordination environment in the corresponding homoleptic Cu$^+$ complexes, with interesting consequences for the absorption and luminescence properties of these species. In particular [Cu(**17**)$_2$]$^+$ is the first example of a copper(I) complex with phenylphenanthroline ligands emitting at 77 K in dichloromethane [54].

In order to reduce non-radiative deactivation pathways in *pseudo*-tetrahedral copper(I) complexes of phen derivatives, due to flattening distortion of the coordination geometry and/or exciplex quenching of the excited state in polar donor solvents *via* formation of transient five-coordinate species [14,55,56], Sherrill and co-workers have synthesized, according to Scheme 8, a series of tetradentate ligands featuring the phen nucleus functionalized at the 2,9-positions with coordinating biaryl substituents, capable to enforce a locked *pseudo*-tetrahedral (C_2-symmetry) coordination environment at the Cu$^+$ metal centre [57].

The synthesis of **21** and **22** was accomplished *via* Suzuki cross-coupling of 2,9-dichloro-1,10-phenanthroline (**20**) [58] with the appropriate aryl-boronic acid pinacol ester [57]; however, despite the rigid architecture of these ligands, coordinative rearrangements occurred in the excited state of the corresponding 1:1 copper(I) complexes leading to non-radiative deactivation *via* exciplex quenching and flattening distortions [57,59].

A similar cross-coupling reaction between **20** and 2-(tri-*n*-butyl-stannyl)pyridine was employed by Zong and Thummel for the preparation of **23** [60] which represents a structural analogous of quaterpyridine **24** but with much less conformational freedom (Scheme 9). In fact, while **24** can act as bridging ligand and binds two Ru^{2+} centres in a bidentate fashion by assuming a helical conformation [61], the highly pre-organized **23** coordinates Ru^{2+} in a tetradentate porphyrin-like fashion by occupying the equatorial plane of a *pseudo*-octahedral coordination sphere in *trans*-[Rh(**23**)(4-X-py)$_2$]$^{2+}$ complexes (py = pyridine, X = NMe$_2$, Me, CF$_3$) [60].

The complexing properties of **23** towards an extended series of metal ions differing in size and charge have been recently studied in aqueous solution and in the solid state by Thummel and Hancock [62]. Despite **23** does not have a cavity as do macrocyclic ligands, it demonstrates a remarkable macrocycle-like thermodynamic stability in 1:1 complexes with metal ions having an ionic radius of about 1.0 Å, in particular Cd^{2+} and Bi^{3+} [62]. This size selectivity of **23** is not only determined by its highly pre-organized cleft, but also by the possibility to form three rigid five-membered chelate rings which is recognized to favour complexation to larger metal ions over smaller ones (see below) [63]. Significantly, **23** also exhibits

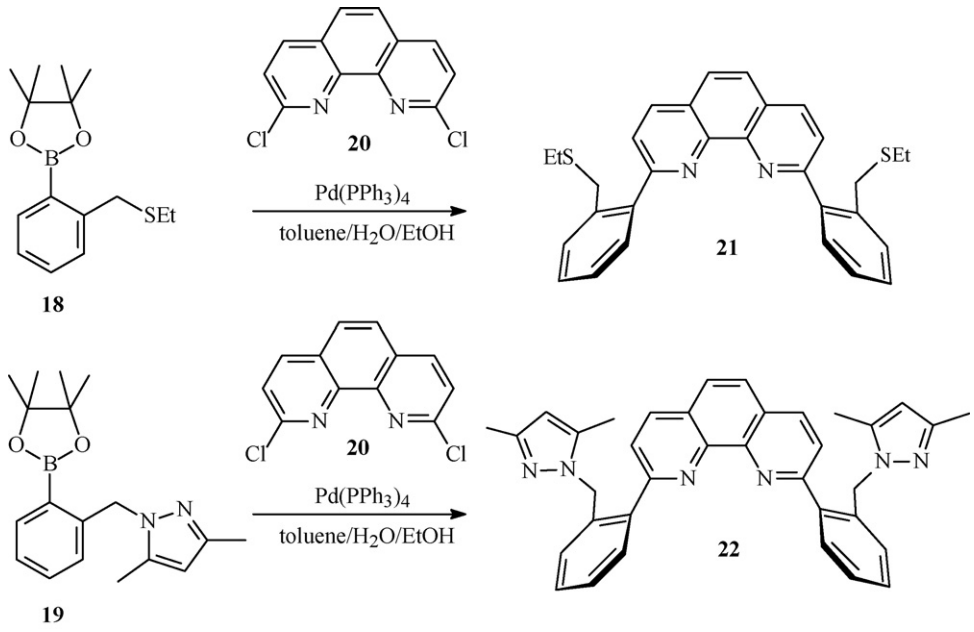

Scheme 8.

a remarkable selective CHEF (chelation enhancement of fluorescence) effect in the presence of Cd^{2+}, whereas no CHEF effect is observed in the presence of the smaller Zn^{2+} [62] (these aspects will be discussed more in details in the following sections dedicated to recognition and sensing).

It is well known that symmetric substitution with aromatic residues at the 2,9-positions is particularly effective to improve the fluorescence performance of phen [12]. Very recently, Siegel and co-workers have synthesized a 3 × 3 array of dimanisyl substituted 2-pyridyl-1,10-phenanthroline isomers (manisyl = 4-methoxy-2,6-dimethylphenyl) of general formula **25** (Scheme 10) by using a palladium catalyzed cross-coupling of appropriate organozinc halides and heterocyclic halides [64,65]. This systematic variation of the substitution pattern at the tpy-like backbone with manisyl groups α, β, and γ to the external nitrogen atoms has rendered possible a systematic investigation of the structural–fluorescence

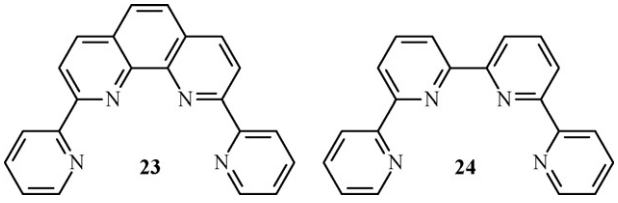

Scheme 9.

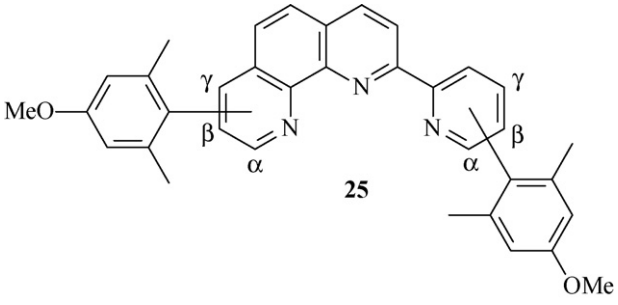

Scheme 10.

relationship in this congruent class of compounds [66]. Siegel and co-workers discovered that these manisyl-substituted pyridyl-phenanthrolines possess dual emissive states: a weakly emissive excited state similar to the $^1\pi\pi^*$ state of phen, and a strongly emissive charge-transfer state (CT*) dependent on the manisyl regiochemistry and solvent polarity. In particular, the members of the β-family having a manisyl group in β-position relative to the pyridyl nitrogen, show a highly emissive "pure" CT* state in polar solvents (EtOH, MeCN), while emission from the locally excited state mainly localized on the phen backbone becomes prevalent in non-polar solvents (cyclohexane, ether).

The possible use of these compounds as building blocks for the assembly of topological chiral structures *via* octahedral transition metals templates is under consideration.

The most used starting material for the preparation of 2-mono- or 2,9-disubstituted phen derivatives is the commercially available 2,9-dimethyl-1,10-phenanthroline (neocuproine). According to Scheme 11, neocuproine (**26**) can be easily converted *via* well established procedures [67–69], into a whole range of derivatives which represent either useful synthons for the development of polydentate and macrocyclic ligands incorporating the phen subunit, or polydentate ligands themselves.

In particular, the coordination properties of 1,10-phenanthroline-2,9-dicarboxylic acid (**27**) have very recently been the subject of a renewed interest [70–73]. In fact, analogously to **23**, this ligand binds very strongly, in its deprotonated form, large metal ions with an ionic radius of about 1.0 Å and charges higher than 2 + [$\log K_1$ = 16.1 (Gd^{3+}), 19.7 (In^{3+}), 20.0 (Fe^{3+}), 26.2 (Bi^{3+}), 25.7 (Th^{4+}) in aqueous solutions], due to the high level of pre-organization determined by the rigidity of the phen backbone, and to the possibility of imposing three five-membered chelate rings at the metal centre. Solution studies are well backed up by structural data as in the complexes of **27** with small metal ions such as Ni^{2+} and Cu^{2+} one carboxylate is left uncoordinated [73–76], while in complexes of larger metal ions such as UO_2^{2+}, Th^{4+}, Eu^{3+} and Tb^{3+} the deprotonated ligand coordinates through all four donor atoms [70–73]. Further evidence of this preference of **27** for larger metal ions (ionic radius of about 1.0 Å) is represented either by the formation of 1:1 and 1:2 metal-to-ligand complexes in water between derivatives of **27** and europium(III) [77,78], or

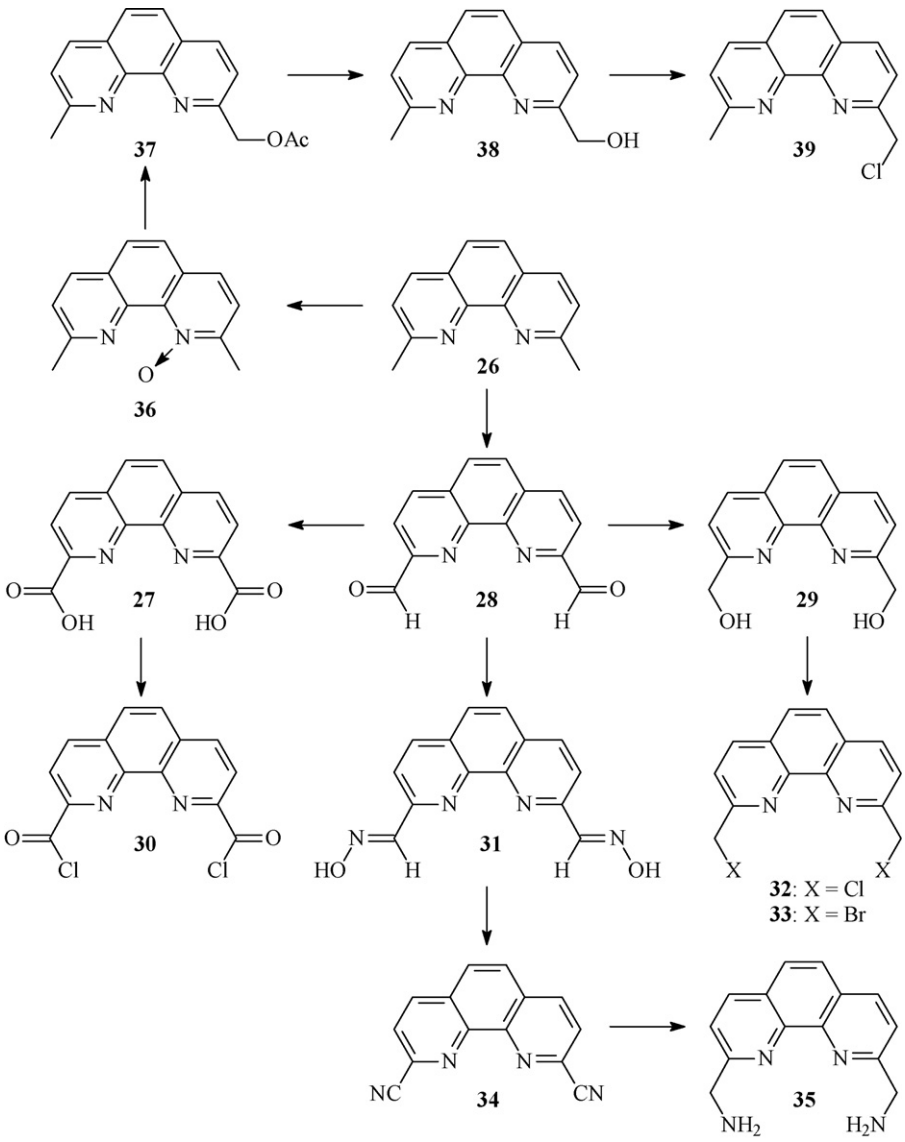

Scheme 11.

by the ability of lanthanide(III) ions to promote the hydrolysis of 4,7-diphenyl-1,10-phenanthroline-2,9-dicarboxylic acid esters to the corresponding acids [79].

The sharp band at 247 nm in the electronic spectra of **27** complexes in water solutions is a good indicator of whether or not the metal ion is coordinated to all four donor atoms of the ligand.

In fact, this band is absent for the complexes with small metal ions but present for the complexes with larger metal ions [72]. Fluorescence studies show a CHEF effect in the complexes with **27** following the order $Y^{3+} > La^{3+} > Lu^{3+}$; on the other hand, heavy metal ions (In^{3+}, Bi^{3+}) and metal ions with partially filled d or f orbitals (Fe^{3+}, Gd^{3+}, Tb^{3+}, Yb^{3+}) induces an almost complete quenching of the fluorescence emission of the ligand. In the case of Al^{3+} a strong broad emission is observed at about 450 nm, tentatively assigned to the formation of an exciplex in solution between two complex units [72]. Analogously to **27**, also **29** (Scheme 11) demonstrates a high level of pre-organization and a metal ion selectivity for larger metal ions [$\log K_1$ = 6.2 (Gd^{3+}), 9.1 (In^{3+}), 6.3 (Fe^{3+}), 8.3 (Bi^{3+}), 8.4 (Th^{4+}) in aqueous solutions] with increases in $\log K_1$ as much as 5.5 log units compared to analogous phen complexes [80,81].

However, complexes of **29** with larger metal ions are less stable than complexes of **27** in agreement with the fact that alcoholic oxygen atoms are much weaker bases than the carboxylates ones [80,81]. From a structural and spectroscopic point of view both **27** and **29** show strict similarity, with the preference to behave as tetradentate ligands for larger metal ions and as terdentate ligands for smaller metal ions, and with fluorescence induced enhancement or quenching effects controlled by the same factors, strictly related to the nature of the added metal ions.

The coordination properties of **27** and **29** and their size-based recognition ability towards metal ions are determined by their high level of pre-organization, which is comparable if not superior to that of macrocyclic ligands or cryptands, and could find interesting applications in separation and transport processes involving actinides and lanthanide ions.

Recently, Helquist and co-workers have reported on the SmI_2-promoted direct coupling of phen with an appropriate epoxide to generate the chiral (hydroxyalkyl)phenanthrolines **40** and **41** (Scheme 12) to be possibly used in metal-catalyzed enantioselective reactions [82].

On testing the coordination properties of **41**, the authors have isolated and structurally characterized its 1:1 Cu^{2+} and Zn^{2+} complexes as triflate salts. In contrast to what observed for the complexes of **29** with small-sized metal ions, in both these com-

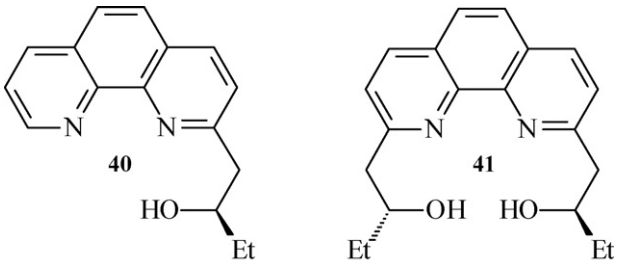

Scheme 12.

plexes, **41** behaves as tetradentate ligand forming with the metal centres two six-membered and one five-membered chelate rings.

1,10-Phenanthroline-2,9-dicarboxylic acyl chloride **30** (Scheme 11) has extensively been used in the past as starting material for the construction of macrocyclic ligands, in particular crown ethers incorporating the phen unit with endotopic coordination sites (see Section 2.1.1). Quite recently, **30** has been used as starting material for the preparation of the polytopic ligand **42** containing three different coordination domains: phen, tpy and diazacrown-ether subunits (Scheme 13) [83].

Compound **42** can afford complexes with different nuclearity and architectures depending on the metal ions used and the procedure followed. In particular, the reaction of **42** with 1 equiv. of Zn^{2+} affords the mononuclear discrete complex cation $[Zn(\mathbf{42})]^{2+}$ in which the metal centre is coordinated by the tpy ends of the polytopic ligand to give a metallocyclic species. On the other hand, the reaction of **42** with the complexes $[Ru(bpy)_2Cl_2]$ or $[Cl_2Ru\{(\mu\text{-}2,3\text{-}dpp)Ru(bpy)_2\}_2]^{4+}$ (2,3-dpp = 2,3-*bis*(2-pyridyl)pyrazine) affords the dinuclear complex $[(bpy)_2Ru(\mu\text{-}\mathbf{42})Ru(bpy)_2]^{4+}$ and the hexanuclear complex $[\{(\mu\text{-}2,3\text{-}dpp)Ru(bpy)_2\}_2Ru(\mu\text{-}\mathbf{42})Ru\{(\mu\text{-}2,3\text{-}dpp)Ru(bpy)_2\}_2]^{12+}$, respectively, in which the tpy subunits bind the metal centres and the phen site is left uncoordinated because it is sterically hindered. The ruthenium complexes exhibit MLCT luminescence both in MeCN solution and in butyronitrile rigid matrix at 77 K. The photophysical data indicate that the $[Ru(bpy)_2]^{2+}$ and the dendritic $[Ru\{(\mu\text{-}2,3\text{-}dpp)Ru(bpy)_2\}_2]^{6+}$ fragments appended to the tpy ends of the polytopic ligand **42** behave as independent components of the multicomponent system [83].

Quite recently, excess of 1,10-phenanthroline-2-carboxylic acyl chloride **43** [84], has been condensed with *tris*(2-aminoethyl)amine (tren) to give the nonadentate tripodal ligand **44** (Scheme 14) [85]. This ligand encapsulates lanthanide ions in a slightly distorted tricapped, trigonal prismatic coordination environment *via* the six nitrogen atoms of the phen arms and the three amide oxygen atoms (see Fig. 3 for the case of Nd^{3+}).

The three carbonyl groups which all point outside in the free ligand, rotate upon complexation to lanthanide ions to assume a *cis*-position relative the phen nitrogen atoms, thus forming three tridentate arms which bind the metal ion in a nearly planar mode.

Solution-state NMR studies show that in acetonitrile solution lanthanide complexes of **44** exists as discrete rigid and kinetically inert C_3-symmetric 1:1 species. However, bimetallic and trimetallic species are formed in the presence of excess lanthanide ions, whereas mononuclear *bis*-**44** complexes are formed in the presence of excess ligand. Studies of the luminescent properties of the lanthanide complexes of **44** are under progress [85].

1,10-Phenanthroline-2-carboxylic acyl chloride **43** is also a key intermediate for the preparation of 2-formyl, 2-acetyl and 2-benzoyl-1,10-phenanthroline derivatives [84,86]. Condensation of these aldehydes and ketones with appropriate substituted anilines in the presence of *p*-toluensulfonic acid afforded tridentate 2-imino-1,10-phenanthrolinyl ligands of general formula **45** (Scheme 15) [86–88].

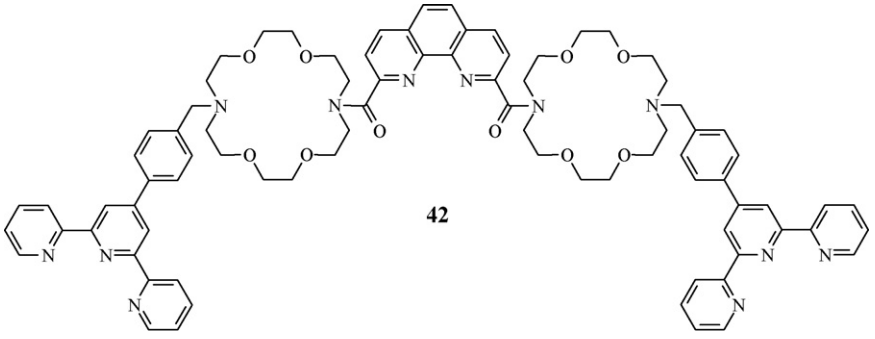

Scheme 13.

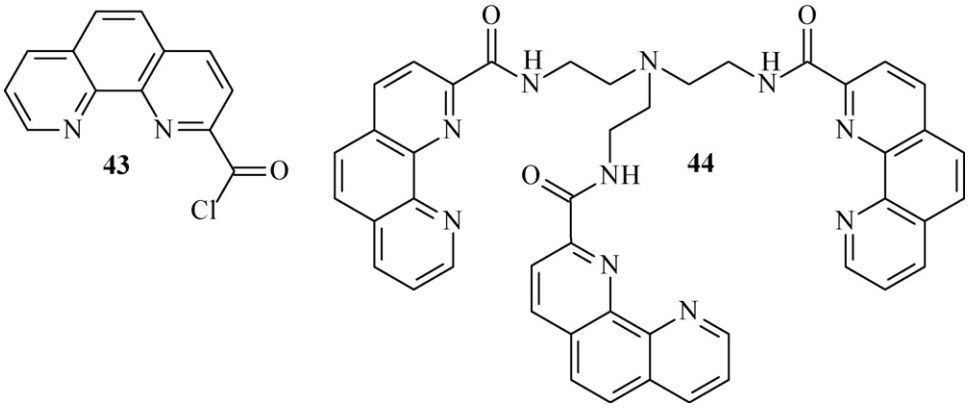

Scheme 14.

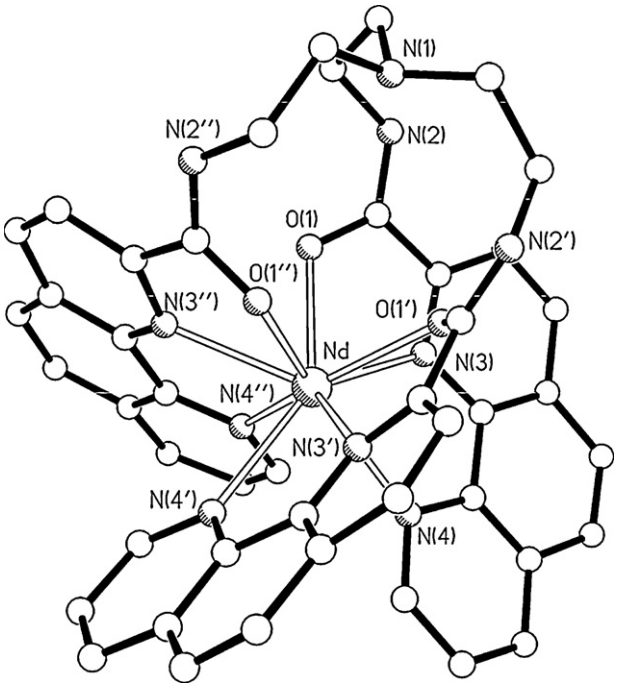

Fig. 3. ORTEP view of the complex cation [Nd(**44**)]$^{3+}$ [85]. H-atoms are omitted for clarity.

A series of iron(II), cobalt(II) and nickel(II) complexes with these ligands of general formula **46** (Scheme 15) has been synthesized, and many of them also crystallographically characterized. They all feature a distorted trigonal bipyramidal coordination geometry around the metal centre in which the nitrogen of the phenanthrolinyl moiety next to the imino-group and two halide ligands compose the equatorial plane [86–88]. These complexes show catalytic activities for ethylene oligomerization, the iron(II)- and the cobalt(II)-complexes being the most and the less active, respectively. Steric and electronic effects of the coordinative ligands finely tune the catalytic activity and the properties of the products in terms of distribution of oligomers.

More recently, Sun and co-workers have reported the synthesis 2-(benzimidazol-2-yl)-1,10-phenanthroline derivatives, **47**, and the corresponding nickel(II)-complexes (**48**), as new catalysts for ethylene oligomerization (Scheme 16). The key step for the preparation of these ligands is the condensation reaction of 2-carboxylic-1,10-phenanthroline acids with *o*-phenylenediamine [89].

2,9-Diformyl-1,10-phenanthroline (**28**) (Scheme 11) is also a good starting material for the preparation of more sophisticated ligands through the formation of Schiff bases. Quite recently, hexadentate hydrazonic ligands **49** and **50** (Scheme 17) have been

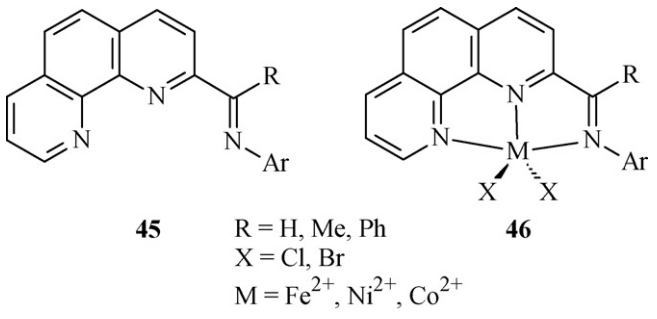

Scheme 15.

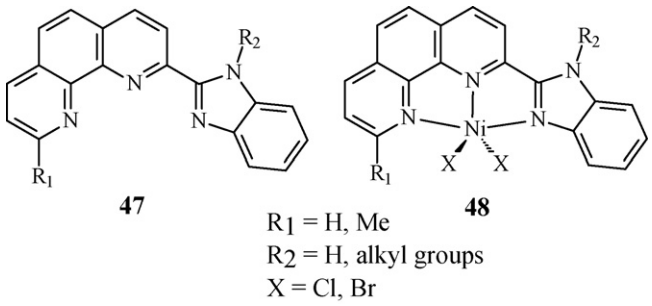

Scheme 16.

synthesized by direct condensation of **28** with the appropriate hydrazines [90,91]. Analogous ligands can be obtained by reacting 2,9-dihydrazino-1,10-phenanthroline, easily obtainable from **20** (Scheme 8) by reaction with hydrazine, with 2 equiv. of the appropriate carboxaldehyde [92].

These ligands mix the rigidity imposed by the central phen moiety with the flexibility of the hydrazonic arms and can accommodate in their large cavity large post-transition and rare-earth metal ions [90,91].

2-Cyano-1,10-phenanthroline **51**, beside being the precursor of 1,10-phenanthroline-2-carboxylic acyl chloride (**43**) (Scheme 14) [84], was recently used as starting material for the preparation of 2-(2-alkyl-2*H*-tetrazol-5-yl)-1,10-phenanthroline derivatives **53** *via* reaction with sodium azide and zinc bromide to give the tetrazolyl derivative **52** [93], followed by alkylation in the presence of KOH (Scheme 18) [94].

The coordination properties of the final terdentate ligands towards iron(II) were then studied. The basic molecular moiety of the resulting compounds is the distorted octahedral Fe^{2+} core chelated by two unsymmetrical tridentate 2-tetrazolyl-1,10-phenanthroline ligands in *mer* mode [94]. The temperature dependence of the magnetic susceptibility of these 2:1 ligand-to-metal complexes was studied and the results indicated diverse and complicated spin-crossover behaviours dependent on the nature of the alkyl chains, solvent molecules and anions [94].

The reaction between 1,10-phenanthroline-5,6-dione **54** and the carboxamidrazone **55** (obtainable from **51** by reaction with hydrazine) [95] gives the 1,2,4-triazine **56**, which can be converted into **57** following an inverse-type Diels–Alder reaction with norborna-2,5-diene and extrusion of molecular nitrogen (Scheme 19) [96].

Ligand **57** contains two possible complexing sites. Specific coordination of [Ru(bpy)$_2$Cl$_2$] to the less hindered 1,5,12-triazatriphenylene unit leaves the phen binding site free to be occupied by the smaller silver(I) ion to give the tri-heteronuclear complex **58** (Scheme 20) [97].

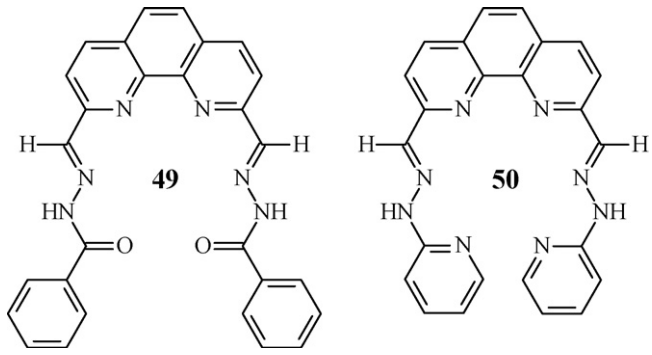

Scheme 17.

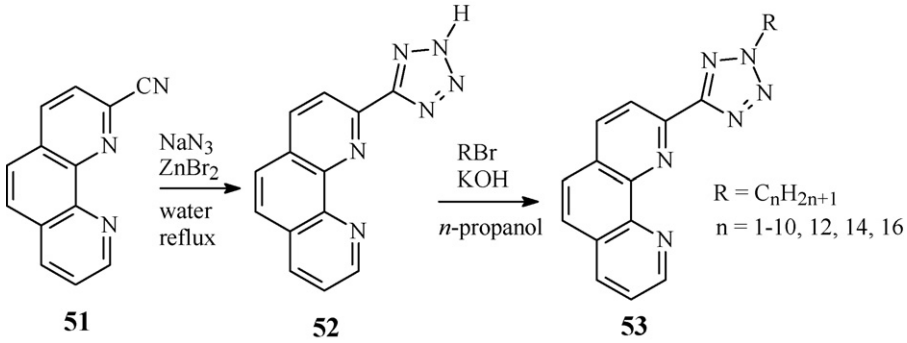

Scheme 18.

The method established by Case [95] for the preparation 1,2,5-triazine rings and used by Sauer [96,97] for the synthesis of **56**, was also adopted for the synthesis of **59**–**61** (Scheme 21) [98].

Homoleptic and tpy-heteroleptic Ru^{2+} complexes of these three ligands have been synthesized and their electrochemical and spectroscopic properties compared to those of $[Ru(tpy)_2]^{2+}$ [98].

As a matter of fact, 2-halomethyl- or 2,9-*bis*(halomethyl)-1,10-phenanthrolines such as **32**, **33** and **39** in Scheme 11 are the most used neocuproine (**26**) derivatives as starting materials for more complex functionalizations. The first two have been extensively used for the synthesis of macrocyclic ligands incorporating the phen nucleus with endotopic coordination sites, as discussed in the next section. However, **32**, **33** and **39** have also been used for the synthesis of open-chain ligands. In particular, following the work of Hodgson [99], recently Stack and co-workers, in an effort to study the interaction of small-molecules copper(I) complexes with dioxygen, have synthesized the unsymmetrical phen- and pyrazolyl-based terdentate ligand **62** (Scheme 22) by reacting **39** with 3,5-dimethylpyrazole in a phase transfer coupling [100].

The study of the oxidative processes involving simple copper(I)–O_2 complexes, is useful to understand the mechanism of action of Cu-containing metalloenzymes and, therefore, to develop

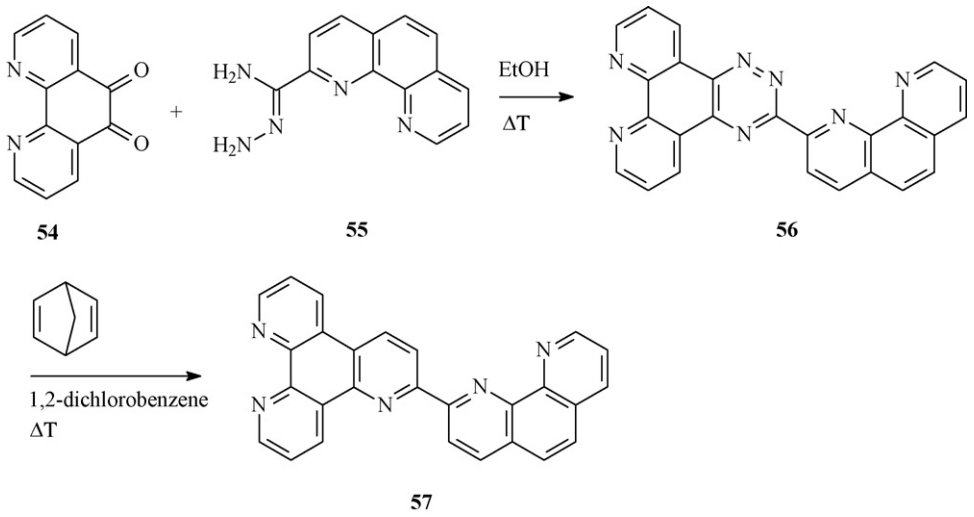

Scheme 19.

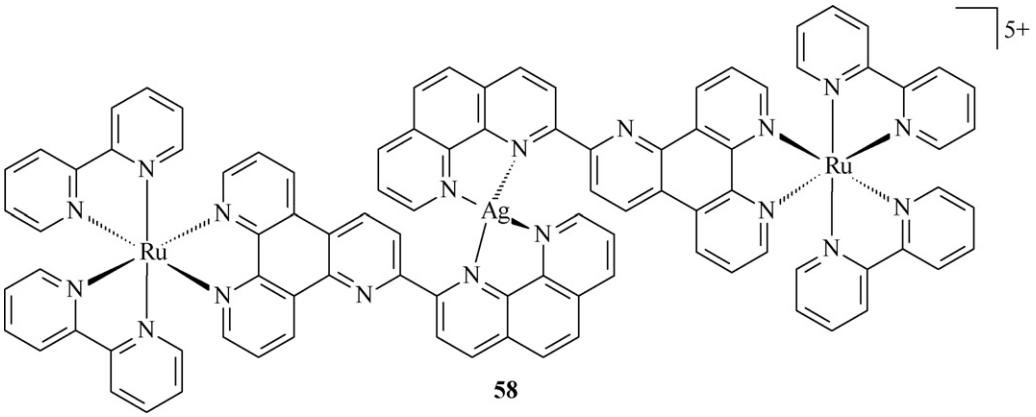

Scheme 20.

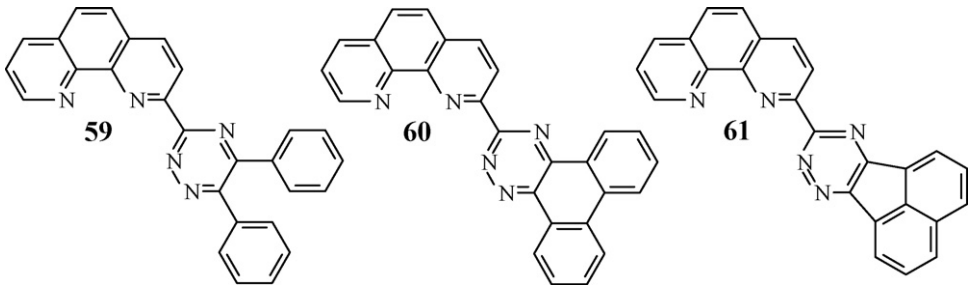

Scheme 21.

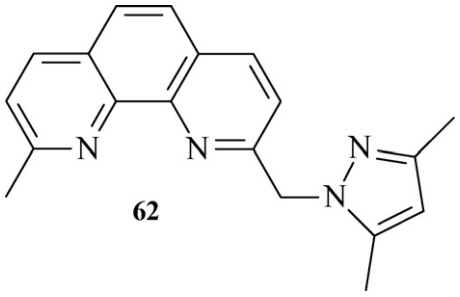

Scheme 22.

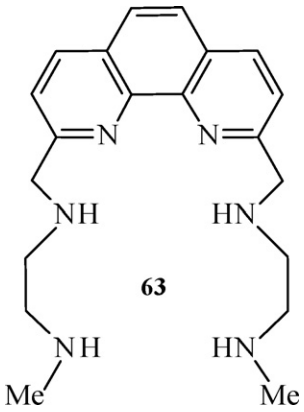

Scheme 23.

bio-inspired Cu-oxidation catalysts. It is well known that, in order to have the reduction of O_2 by copper(I)-phen derivative complexes, it is necessary to preclude *bis*-phen derivatives chelation at a Cu^+ centre [101]. Both the cupric and the cuprous complexes of **62** have been isolated and crystallographically characterized. In the former, the copper(II) centre adopts a five-coordinate distorted trigonal bipyramidal geometry involving the three N-donor atoms from the ligand, an acetonitrile N-donor and a triflate oxygen atom (see Fig. 4a). The copper(I) complex of **62** is a non-symmetric dimer in which two ligand units bridge two Cu^+ centres; one cuprous centre is complexed in a trigonal planar geometry and the other in a distorted tetrahedral environmental due to the participation of an acetonitrile molecule to coordination (see Fig. 4b).

Interestingly, despite the cuprous complex being redox inactive, it reacted with dioxygen to form the cupric complex upon exposure to air and over 1 h.

Aliphatic polyamine side arms have also been attached to the 2,9-positions of phen. The simplest example is represented by ligand **63** (Scheme 23) obtained by reaction of 2,9-*bis*(bromomethyl)-1-10-phenanthroline (**33**) (Scheme 11) with tosylated *N*-methyl-ethylenediamine, followed by removal of the tosyl groups in a HBr/CH_3COOH mixture.

This ligand contains a cleft, delimited by phen and the two side arms, where metal cations can be conveniently accommodated. As a consequence, **63** forms stable mononuclear complexes with Cu^{2+}, Zn^{2+}, Cd^{2+} and Pb^{2+} in aqueous solutions and, in the case of Cu^{2+}, also dinuclear complexes [102,103]. A potentiometric and calorimetric study on metal coordination by **63** pointed out that the stabilization of its complexes is essentially due to a favourable entropic contribution, due to the large desolvation of the metal cations upon their encapsulation and to the consequent increase in translational entropy. Conversely, the enthalpic contributions to metal complexation are rather low when compared to those usually found for metal complexation by linear

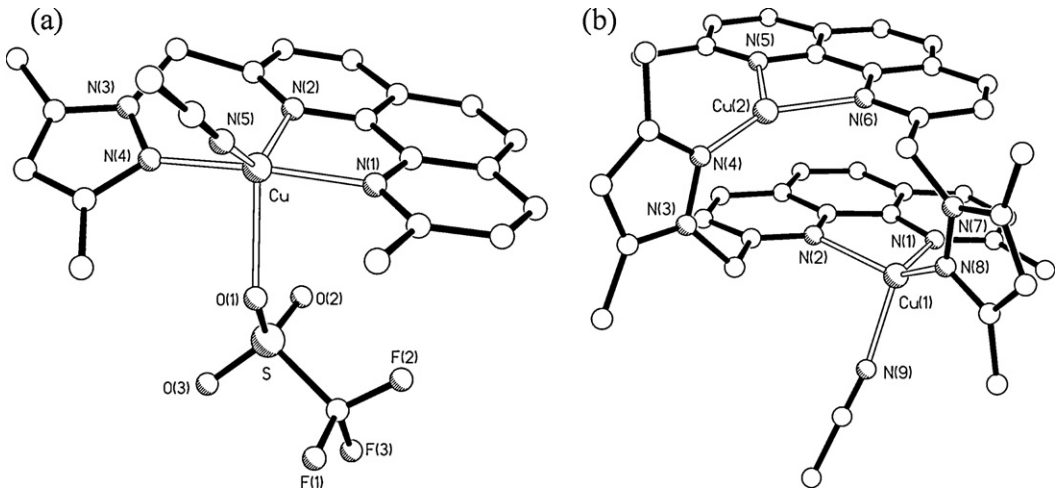

Fig. 4. ORTEP view of the complex cation $[Cu(\mathbf{62})(CF_3SO_3)(MeCN)]^+$ (a) and $[Cu_2(\mathbf{62})_2(MeCN)_2]^{2+}$ (b) [100]. H-atoms are omitted for clarity.

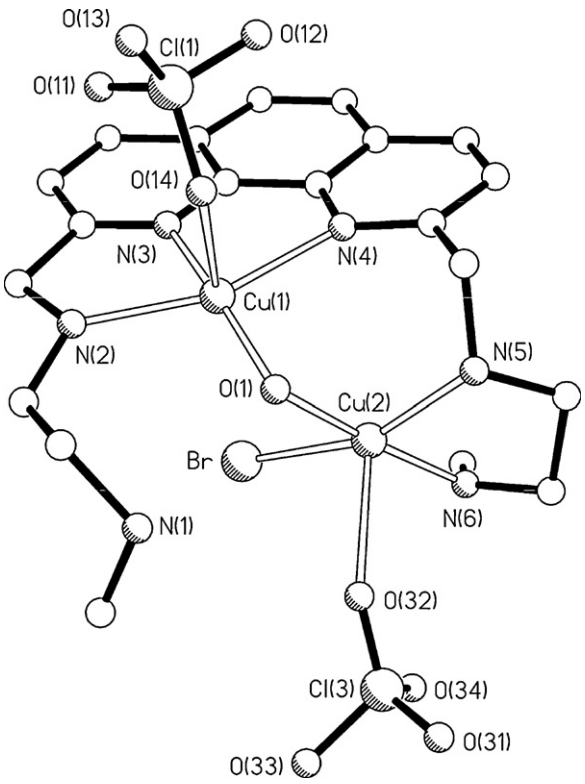

Fig. 5. ORTEP view of the complex cation $[Cu_2(H\mathbf{63})(\mu\text{-}OH)(ClO_4)_2Br]^+$ [102]. H-atoms are omitted for clarity.

aliphatic hexa-amines, such as 1,14-*bis*(methylamino)-3,6,9,12,-tetrazatetradecane or 1,4,7,10,13,16-hexaazadecane. This result was rationalized considering that the ligand backbone of **63** is stiffened by the presence of the phen moiety, resulting in an enthalpic cost in the process of ligand rearrangement upon coordination to the metal cations. Furthermore, stiffening of the ligand could also preclude the simultaneous involvement of all donor atoms in metal coordination. The mononuclear $[Cu(\mathbf{63})]^{2+}$ complex can also add a second metal ion, giving a dinuclear Cu^{2+} complex in aqueous solution. Of note, the main species present in solution from slightly acidic to alkaline pH values, are the hydroxo-complexes $[Cu_2(\mathbf{63})(OH)]^{3+}$ and $[Cu_2(\mathbf{63})(OH)_2]^{2+}$. The stabilization of these species was attributed to a bridging coordination mode of hydroxide anion, as actually found in the crystal structure of the complex cation $[Cu_2(H\mathbf{63})(\mu\text{-}OH)(ClO_4)_2Br]^+$, which shows the $[Cu_2(\mu\text{-}OH)(ClO_4)_2Br]^+$ core embedded within the ligand cleft (see Fig. 5). Interestingly, one of the four aliphatic nitrogen donors of **63** is not coordinated and, instead, is protonated [102].

Fusi and co-workers have recently reported the synthesis of the branched ligand **64** featuring two diethylenetriamine units connected on the central nitrogen atom by a phen nucleus (Scheme 24) [104].

The synthesis consists of attaching two *N*,*N*-*bis*(2-phthalimidoethyl)amine groups to the 2,9-*bis*(bromomethyl)-1,10-phenanthroline, **33**, followed by removal of the phthaloyl groups in acidic conditions [104].

Ligand **64** behaves as ditopic unsymmetrical compartmental ligand and is able to form mono- and dinuclear complexes with both Cu^{2+} and Zn^{2+}. In fact, the phen moiety with both nitrogen atoms, and one dien unit imposes a pentacoordination environment to the first metal ion (see Fig. 6).

The second dien unit can be easily protonated in the mononuclear complexes while binds the second metal in the dinuclear species (see Fig. 7). The role of each binding area is fast exchanging

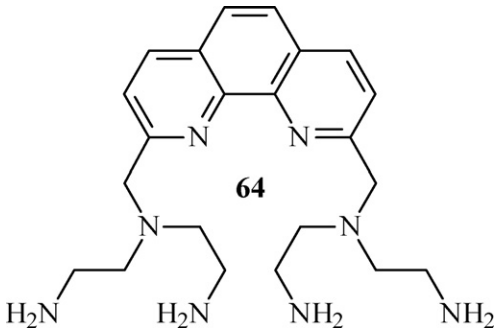

Scheme 24.

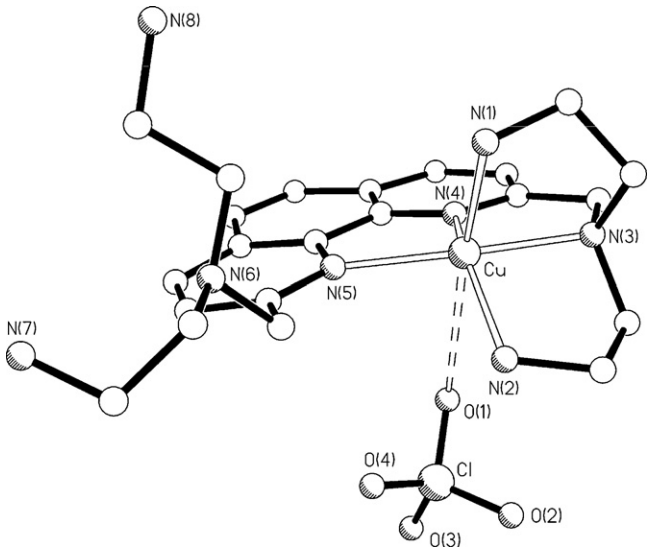

Fig. 6. ORTEP view of the complex cation $[Cu(\mathbf{64})ClO_4]^+$ [104]. H-atoms are omitted for clarity.

in aqueous solution, at least on the ^1H NMR time scale. Furthermore, both binding units of **64** do not saturate the coordination requirements of Zn^{2+} and Cu^{2+} which, therefore, can coordinate exogenous ligands such as hydroxide, chloride and perchlorate anions as well as water molecules, and possibly also anionic guests of biological relevance.

Ligand **64** is structurally analogous of **66**, obtained by reacting **32** with 1,4,7-triazacyclo[5.2.1.^{04,10}]decane (**65**) followed by standard procedures for deprotection of the secondary nitrogen atoms (Scheme 25) [105,106].

No crystal structures of metal complexes are known for **66**, however potentiometric data in water solution allow to draw some similarities and differences in the coordination chemistry of **64** and **66** with Zn^{2+} and Cu^{2+} [104,105]: (i) both ligands can form mono- and dinuclear complexes; (ii) **64** shows stability constants that are more than 3 logarithmic units higher in the formation of mononuclear species; (iii) mononuclear species with **64** do

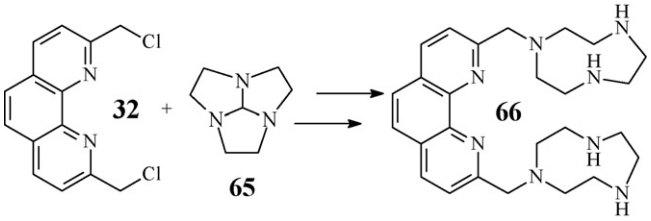

Scheme 25.

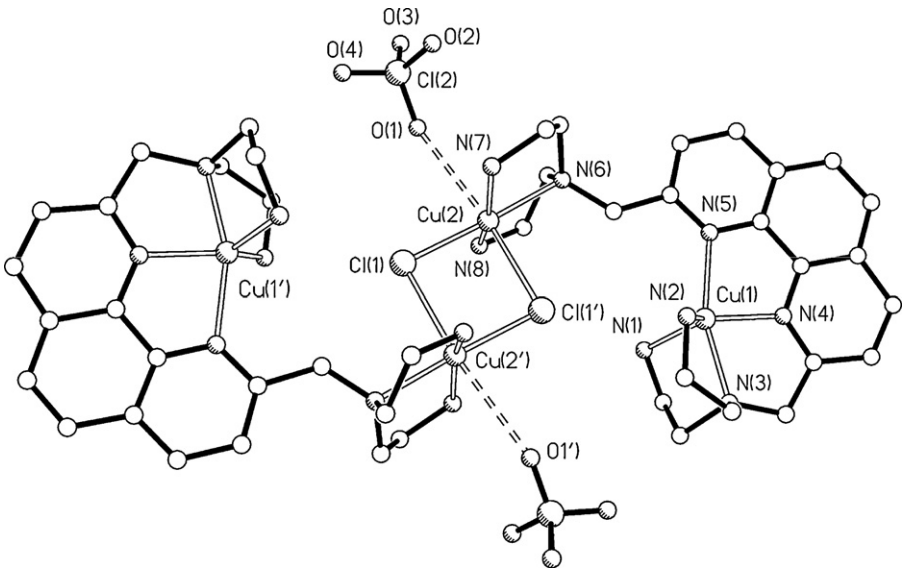

Fig. 7. ORTEP view of the complex cation $[Cu_2(\mathbf{64})(Cl)ClO_4]^{2+}$ in its dimeric form [104]. H-atoms are omitted for clarity.

not easily form hydroxylated species while this is favoured with **66**; (iv) **64** gives stable $[M_2(\mathbf{64})]^{4+}$ dinuclear species while for **66** only hydroxylated dinuclear species were found in solution. These differences have been attributed to the different degree of flexibility of the polyamine pendant arms in 2,9-positions of the phen unit in the two ligands [104]. Interestingly, the hydroxylated dinuclear zinc(II) complexes $[Zn_2(\mathbf{66})(OH)_2]^{2+}$ and $[Zn_2(\mathbf{66})(OH)_3]^{+}$ promote the hydrolysis of *bis*(*p*-nitrophenyl)phosphate (BNPP, a DNA model) with the two metal centres acting cooperatively [105], while the dinuclear complex $[Zn_2(\mathbf{66})]^{4+}$ appears also to promote at pH 7.6 the hydrolysis of 2-hydroxypropyl-4-nitrophenyl phosphate (HPNP, an RNA model) with the metal centres acting nearly independently [106].

Starting from **39** (Scheme 11), Quici and co-workers have synthesized the water soluble ligand **68** featuring a single phen unit as chromophore and a diethylenetriamine tetracarboxylic unit as hosting site for lanthanide ions. The key step in the synthetic procedure is once again the alkylation process of a secondary amino group (in **67**) with **39** (Scheme 26). The authors intended with this system to sensitize the luminescence of lanthanide ions employing the phen moiety as antenna for light absorption and subsequent energy-transfer to the available manifold of the metal-centred excited levels [107].

Luminescence measurements indicated the formation of very stable 1:1 lanthanide(III) complexes of **68** in water, with a high efficiency for the sensitized emission in the visible region in air equilibrated water for the Eu^{3+} and Tb^{3+} complexes. This behaviour is largely determined not only by the photophysical properties of the phen moiety and, therefore, by the efficiency of the antenna-to-cation sensitization step, but also by the binding properties of the phen moiety: in fact, the phen unit, by completing the coordination sphere of the metal cation, avoids the interaction of water molecules with it, and prevents the water-induced non-radiative quenching of the populated metal-centred luminescent level.

Analogous results (highly luminescent lanthanide(III) complexes) have been achieved by the same authors by using similar two-component ligand systems **69** and **70** containing the 1,4,7,10-tetraazacyclododecane-1,4,7-triacetic acid as hosting unit for lanthanide cations and an appended functionalized phen as chromophore for the antenna effect (Scheme 27). Also these ligands feature nine binding sites and can complete the first coordination sphere of the metal ion in a somehow water-free rigid coordination environment [108–110].

Neocuproine (**26**) can also be selectively deprotonated at one of the methyl groups with lithium diisopropylamide to generate the corresponding carboanion, which can be made to react with alkyl halogenides. This synthetic strategy was adopted for the preparation of the phen-based bridging ligands **71** and **72** (Scheme 28). The study of the coordination properties of these two ligands toward copper(I) revealed the formation of both the discrete dimeric $[Cu_2(\mathbf{71})_2]^{2+}$ complex and the polymeric $[\mathbf{72}(Cu(\mathbf{72}))_n]^{n+}$ assembly [111].

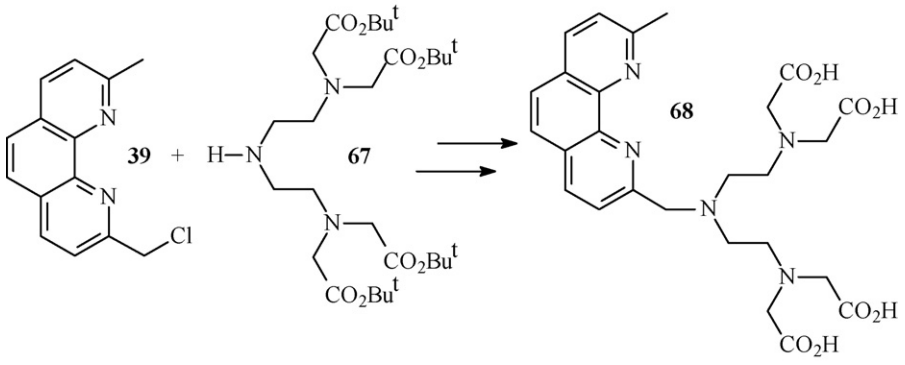

Scheme 26.

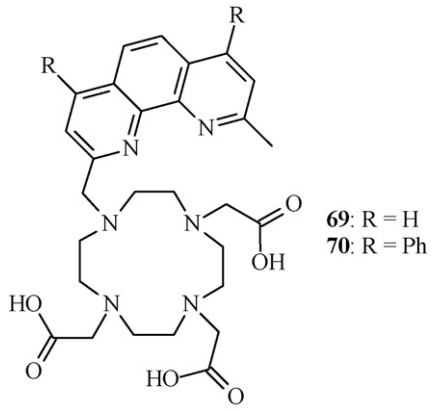

Scheme 27.

A similar synthetic strategy was adopted by Armaroli and co-workers to prepare the fullerene-substituted phen ligand **73** (Scheme 29) [112]. The hybrid heteroleptic copper(I) complexes **74** and **75** were prepared starting from **73** and studied in order to ascertain any possible electronic interactions between the fullerene subunit and the metal complexed moiety.

Electrochemical studies indicated some ground-state electronic interactions between the two units in both complexes. Interestingly, while in **75** both the photoexcited copper(I)-complexed unit and the fullerene moiety are quenched by the presence of the ferrocene unit, in **74** excitation of the copper(I)-complexed unit shows that the strongly emitting triplet metal-to-ligand charge-transfer excited state is quenched by the fullerene moiety [112].

Phen derivatives containing heteroatoms at the 2- or 2,9-positions are much rarer in the literature. Particularly interesting is the tetradentate 2,9-*bis*(diphenylphosphino)-1,10-phenanthroline ligand **76**, which has been used by Catalano and co-workers for the construction of Au^{+}-, Pd^{0}-, and Pt^{0}-metallocryptands whose internal pockets can effectively encapsulate closed-shell heavy metal ions, Tl^{+}, Hg^{0}, Hg_2^{2+}, Pb^{2+}, through strong metallophilic interactions

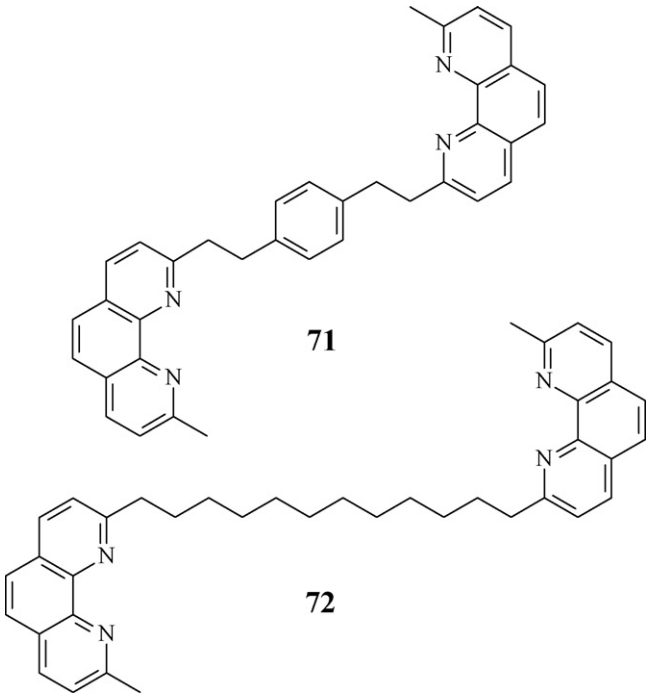

Scheme 28.

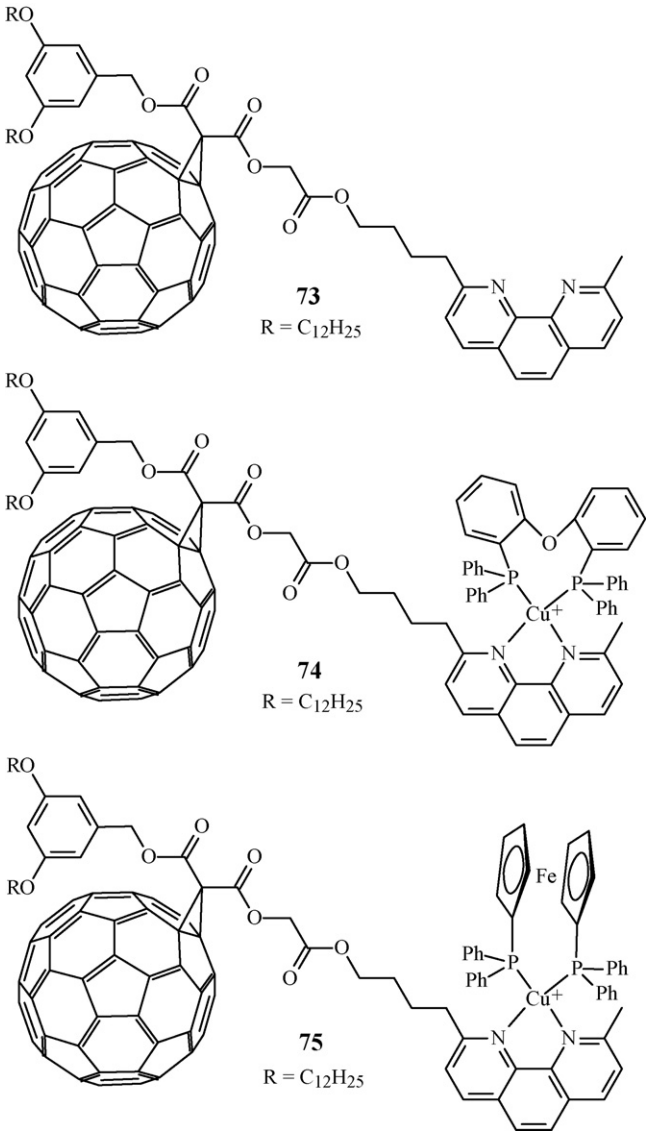

Scheme 29.

to give supramolecular systems of general formula **77** (Scheme 30) [113–118].

In particular, the complex cation $[Au_2Tl(\mathbf{76})_3]^{3+}$ is characterized by a strong emission at about 600 nm in MeCN attributed to a strong Au–Tl interactions [117].

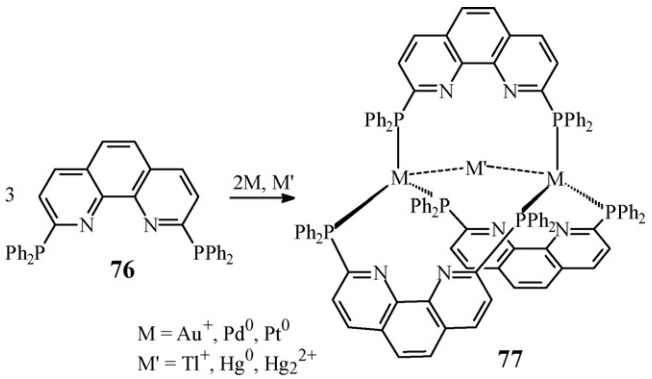

Scheme 30.

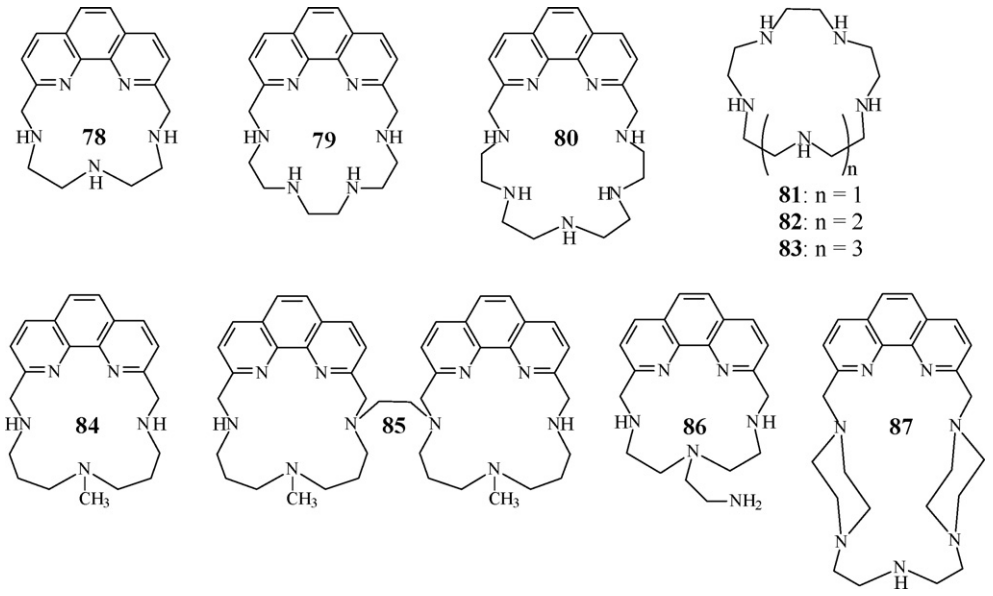

Scheme 31.

2.1.1. Macrocyclic ligands incorporating the 1,10-phenanthroline unit with endotopic coordination sites

In the eighties, functionalization at the 2,9-positions of the phen has been extensively considered for the construction of phen-based macrocycles with *endo*-coordination sites, especially crown ethers, cryptands, spherands, and bridged calix[4]arenes [119–128], and particularly in connections with the possibility of obtaining threaded and interlocked species like rotaxanes and catenanes [21,129–134]. These studies have been fundamental for the subsequent development of many other fields of supramolecular chemistry such as molecular machines, molecular switches, molecular logic gates and memory devices [19]. More recently, medium-sized polyaza- and mixed thia-aza macrocyclic systems incorporating the phen unit have been developed mainly in connection with the possibility of obtaining selective ionophores or receptors for metal ions and anions. In this section the main synthetic and coordination chemistry aspects of some of these recently synthesized macrocycles will be reviewed including some analytical applications, while systems specifically designed to perform selective host-guest recognition functions will be considered in the next sections.

2.1.2. Polyazamacrocycles

In the last 15 years Bencini, Bianchi and Paoletti have synthesized several polyamine macrocycles (Scheme 31) containing a phen moiety as integral part of the cyclic framework, with the aim to investigate the effects of the insertion of this heteroaromatic unit on the coordination properties of polyazamacrocyclic ligands [135–145]. The ligands were synthesized by cyclization of 2,9-*bis*(bromomethyl)-1,10-phenanthroline (**33**) with the disodium salt of the appropriate tosylated polyamine. The resulting tosylated macrocycles were then deprotected in HBr/CH_3COOH mixture [135,141]. Only **84** was obtained by template condensation of 2,9-diformyl-1,10-phenanthroline (**28**) with *N*-methyl-*N*,*N*-*bis*(3-aminopropyl)amine in the presence of $MnCl_2$, followed by reduction *in situ* of the resulting diimine [142].

Indeed, the presence of the rigid phen unit has a profound influence on the coordination ability of these ligands towards transition and post-transition metal cations as well as on the structural features of their complexes. Potentiometric titrations in aqueous solution pointed out that ligands **78**–**80** form noticeably less stable mononuclear complexes with Cu^{2+} [102,135,136], Ni^{2+} [137], Co^{2+} [137], Zn^{2+} [138,139], and Cd^{2+} [140], than aliphatic macrocycles with the same number of nitrogen donors, but containing an en moiety which replaces the phen unit (**81**–**83** in Scheme 31). This behaviour was ascribed to the stiffening of the macrocyclic structure of **78**–**80**. In fact, the presence of a large and rigid heteroaromatic unit does not allow all the nitrogen donors to achieve an optimal arrangement around the metal ions. This suggestion was confirmed by the resolution of crystal structures of the complexes with these metal cations, which unequivocally showed that some amine groups are not bound to the metal. For instance, the crystal structure of the complex $[Zn(\mathbf{78})(H_2O)]^{2+}$ (see Fig. 8a) shows that Zn^{2+} is bound to only three of five nitrogen donors, while the two benzylic nitrogen atoms, adjacent to phen, are not involved in metal coordination [138]. The metal achieves a tetrahedral coordination environment only thanks to binding to an exogenous water molecule. Similarly, in the complex $[Ni(\mathbf{79})(H_2O)]^{2+}$ (see Fig. 8b), the Ni^{2+} cation is bound to five nitrogen donors, one of which interacting at rather long distance (>2.3 Å), and to a water molecule in a resulting strongly distorted octahedral coordination geometry [137]. The presence of at least one benzylic amine group not bound to the metal cation is a peculiar feature of the complexes with first-row transition metal cations. In fact, binding of the metal cation to the heteroaromatic nitrogen atoms does not allow their simultaneous interaction with both the amine groups adjacent to the phen moiety.

The presence of nitrogen donors not bound or weakly bound to the metal cations was confirmed by the marked tendency of the complexes $[M(L)]^{2+}$ (L = **78**–**80**) to protonate in aqueous solutions, affording $[M(HL)]^{3+}$ or $[M(H_2L)]^{4+}$ species, as generally found in complexes with ligands containing amine groups scarcely interacting with the metal centres [135–140].

Among the metal ions investigated, only Pb^{2+} displayed an opposite behaviour, giving more stable complexes with **78**–**80** than with **81**–**83** [141]. This was attributed to the better binding ability of the phen nitrogen atoms toward large and soft metal cations, such as Pb^{2+}, with respect to aliphatic amine groups. Furthermore, the larger dimension allows this metal cation to better interact with the ligand donors, as confirmed by the crystal structure of the complexes with **78** and **80**. This hypothesis was corroborated by a calorimetric study, which showed that the higher stability of the Pb^{2+} complexes with **78**–**80** is essentially due to a more favourable enthalpic contribution, in agreement with an overall stronger inter-

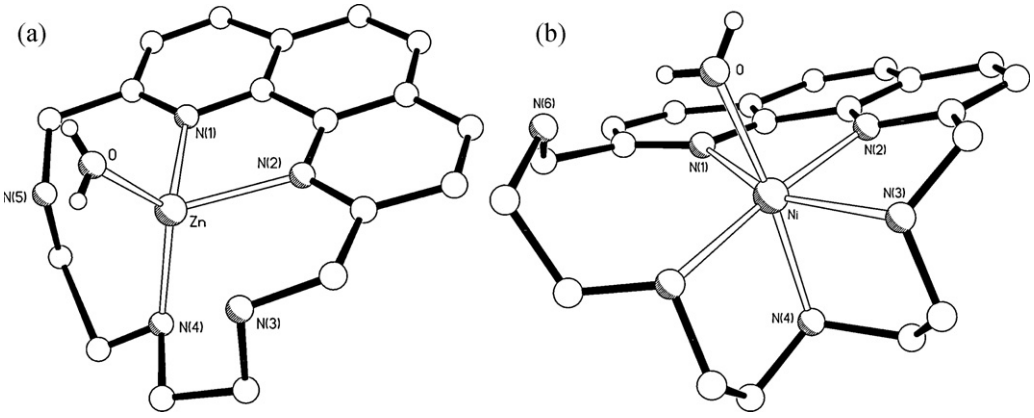

Fig. 8. ORTEP view of the complex cation $[Zn(\mathbf{78})(H_2O)]^{2+}$ (a) [138] and $[Ni(\mathbf{79})(H_2O)]^{2+}$ (b) [137]. H-atoms are omitted for clarity.

action of the set of donor atoms in the complexes with **78**–**80** than in the complexes with their aliphatic counterparts **81**–**83**.

Replacement of the ethylenic chains separating the amine groups with propylenic ones, like in **84** [142], increases the flexibility of the ligands, but does not give beneficial effect on the stability of the complexes. In fact, the increased N–M–N bond angle, as a result of the larger bite of propylenic chains, reduces the binding ability of the amine groups and the overall stability of the complexes, in particular with first row transition metal cations [142,145].

Similarly, stiffening of these phen-containing macrocycles by replacing two en units with two piperazine moieties lead to a marked decrease of the stability of the complexes [135]. For instance, the formation constant of the mononuclear complex $[Cu(\mathbf{87})]^{2+}$ was *ca.* six orders of magnitude lower than that of the corresponding complex with **80**. Actually, the crystal structure of the protonated complex $[Cu(H_2\mathbf{87})(NCS)_2]^{2+}$ showed that the metal is coordinated by the phen unit and one adjacent benzylic nitrogen (see Fig. 9), leaving a zone of the macrocycle available for the coordination of a second metal. As a consequence, the mononuclear complex can add a second Cu^{2+} ion to form a dinuclear species in aqueous solution. The crystal structure of the complex cation $[Cu_2(\mathbf{87})(\mu\text{-OH})(H_2O)(ClO_4)]^{2+}$ showed the assembly of a $[Cu_2(\mu\text{-OH})]^{3+}$ core within the macrocyclic cavity (see Fig. 9), as often observed when two metal cations are forced to stay at short distances (2.5–3.5 Å) by their encapsulation in a rather small macrocyclic cavity [144]. The piperazine rings, which were found in their stable chair conformation in the mononuclear complex $[Cu(H_2\mathbf{87})(NCS)_2]^{2+}$, are forced to assume the less energetically favourable boat conformation in the dinuclear copper(II) complex in order to participate to the coordination of the two metal ions.

Like **87**, the heptazamacrocycle **80** was also able to form dinuclear complexes in aqueous solution with small transition metal cations, such as Cu^{2+} [135] or Zn^{2+} [139]. Beside encapsulation of two metal cations within a single macrocyclic cavity, dinuclear metal complexes were also obtained by synthesizing *bis*-macrocyclic ligands containing two mono-macrocyclic units **84** linked by an appropriate bridge. This is the case of **85**, which was obtained by reaction of **84** with 1,2-dibromoethane [142]. As expected, this ligand is able to form stable mono- and dinuclear

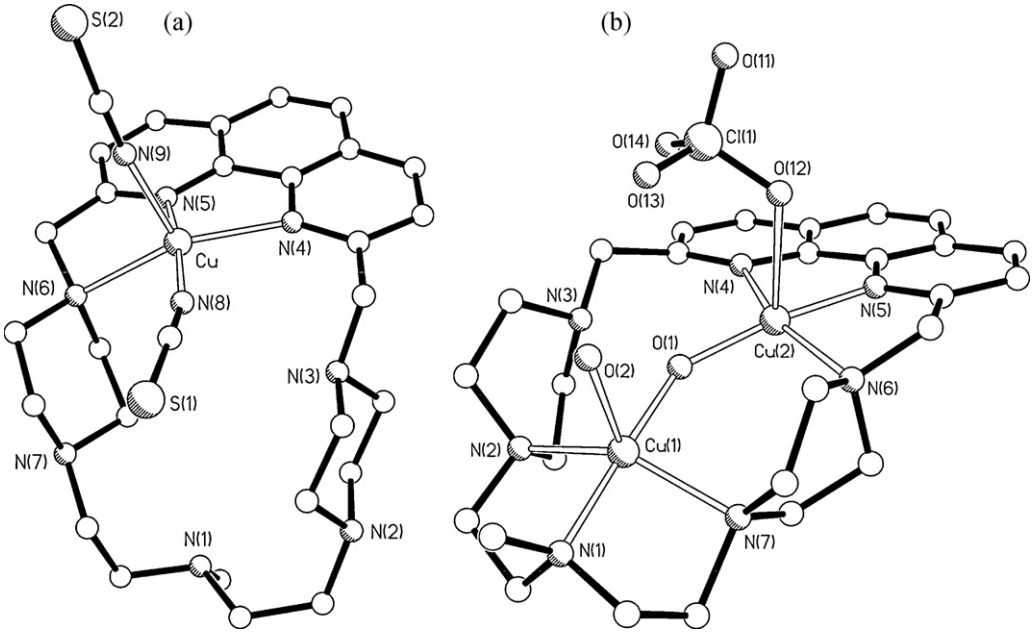

Fig. 9. ORTEP view of the complex cation $[Cu(H_2\mathbf{87})(NCS)_2]^{2+}$ (a) and $[Cu_2(\mathbf{87})(\mu\text{-OH})(H_2O)(ClO_4)]^{2+}$ (b) [135]. H-atoms are omitted for clarity.

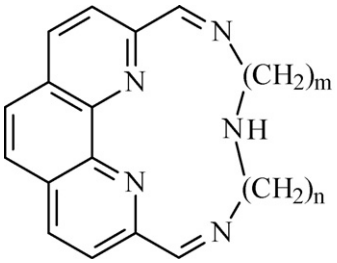

88: n = 2; m = 3
89: n = 3; m = 3
90: n = 3; m = 4

Scheme 32.

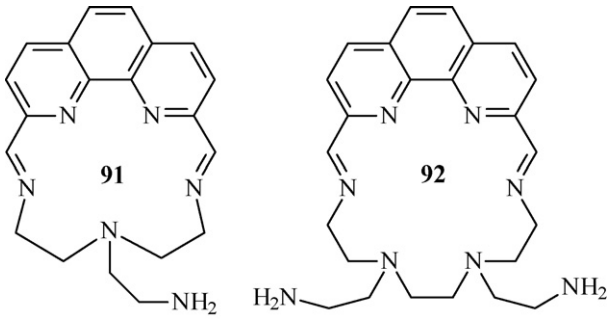

Scheme 33.

metal complexes in aqueous solution with first row transition and post-transition metal cations. While in the mononuclear complexes the metal cation is sandwiched between two **84** cyclic moieties, in the dinuclear complexes each metal ion is independently coordinated by a single macrocyclic unit.

García-España and co-workers have recently reported the synthesis of a polyamine macrocycle similar to **80**, but featuring propylenic chains between the benzylic nitrogen atoms and the adjacent amine groups [146,147]. The analysis of Cu^{2+} complexation revealed that this ligand forms in aqueous solution protonated mononuclear complexes of the type $[Cu(H_xL)]^{(x+2)+}$ ($x = 1–4$) [146]. UV–vis measurements pointed out that the coordination mode of the ligand is modulated by its protonation state. In fact, the metal is bound to the aliphatic amine groups in the $[Cu(HL)]^{3+}$ complex. Extensive protonation of the polyamine chain prevents this binding mode and the metal results to be coordinated by the phen nitrogen atoms in the di-, tri- and tetraprotonated forms of the complex. The analysis of the dynamics of Cu^{2+} movement between the polyamine and the phen binding moieties revealed that the process involves the formation of an intermediate containing the metal partly coordinated by both donor subunits. This ligand can also form in aqueous solution both mono- and dinuclear Zn^{2+} complexes, featured by coordination environments not saturated by the ligand donors. In consequence, facile deprotonation of Zn^{2+}-coordinated water molecules occurs in solution affording hydroxo complexes, which resulted to be efficient hydrolytic agents for the carboxy and phosphate ester bond of *p*-nitrophenylacetate and BNPP. In the case of BNPP, the hydrolytic mechanism takes place *via* an associative mechanism involving the interaction of the phosphate group with Zn^{2+} and simultaneous π-stacking pairing between phen and the nitrophenyl groups of the substrate [147].

Recently, Keypour and co-workers have reported the synthesis of a series of N_5 Schiff-base macrocyclic ligands, **88**–**90** (Scheme 32), *via* [1 + 1] cyclocondensation of 2,9-diformyl-1,10-phenanthroline (**28**) and appropriate linear triamines at the Cd^{2+} cation template [148].

The complexes of general formula $[Cd(L)Cl]^+$ (L = **88**–**90**) were characterized by a variety of methods; in particular, the complex $[Cd(\mathbf{88})Cl]^+$ resulted to have a one-dimensional polymeric structure in which each metal centre is seven-coordinated in a pentagonal-bipyramidal coordination geometry with the five nitrogen atoms from the macrocyclic ligand in the equatorial plane and two bridging chloride ligands in the axial positions.

Following the same synthetic procedures, the Mn^{2+} complexes with the branched ligands **91** and **92** (Scheme 33) were also prepared [149]. In the solid state the complex cation $[Mn(\mathbf{92})]^{2+}$ adopts a slightly distorted hexagonal bipyramid geometry with the metal centre located within the hexa-aza macrocyclic framework and the two pendant arms coordinating in the axial positions [149].

2.1.3. Mixed-donor macrocyclic systems

In the last 10 years, Lippolis and co-workers have been engaged in the development of mixed N/O/S-donor macrocycles structurally similar to the polyazamacrocycles described above, with the aim to combine the peculiar coordination properties of phen with those of aliphatic thioether crown. In particular, the cyclization reaction under diluted conditions between 2,9-*bis*(chloromethyl)-1,10-phenanthroline (**32**) easily obtainable from neocuproine (**26**) (Scheme 11), and the appropriate dithiol in DMF in the presence of Cs_2CO_3 allows the preparation of the macrocyclic ligands **93**–**101** (Scheme 34) in reasonably good yields [150–156]. For the preparation of **101**, similarly to the approach adopted for the synthesis of the polyazamacrocycles described above, **32** was cyclized with *N*,*N*′-*bis*(*p*-tolylsulfonyl)-*bis*(2-aminoethyl)sulfide-*N*,*N*′-disodium salt followed by deprotection of the secondary nitrogen atoms [156]. The basic coordination chemistry of these ligands has been extensively studied at the solid state and in solution towards different metal ions: some d^8 transition metal ions (Ni^{2+}, Pd^{2+}, Pt^{2+}, Ru^{2+}, Rh^{3+}), Cu^{2+} and d^{10} transition and post-transition metal ions (Cu^+, Ag^+, Cd^{2+}, Hg^{2+}, Pb^{2+}).

From a structurally point of view, the main feature in the isolated 1:1 metal complexes of these ligands is the folded conformation of the coordinated ligands, with the S-donors (**93**–**95**) or N-donors (**101**) adjacent to the phen moiety acquiring *endo*-dentate orientations for metal binding, and the aliphatic portion of the ring tilted over the plane of the heteroaromatic sub-unit [150–162], as exemplified by the structures of the complex cations $[Ni(\mathbf{93})MeCN]^{2+}$ [150] and $[Cu(\mathbf{93})Cl(PPh_3)]$ [155], reported in Fig. 10.

In some cases, dinuclear complexes have been isolated and structurally characterized featuring exogenous ligands bridging the two metal centres from the coordination hemisphere left free by the macrocyclic ligand [150,153,156,158].

For example, by reacting $[Ni(\mathbf{93})MeCN]^{2+}$ with F^-, the formation of a dinuclear Ni^{2+} species was observed both in solution and in the solid state, and single crystals corresponding to the formulation $[\{Ni(\mathbf{93})\}_2F][BF_4]_3{\cdot}MeCN{\cdot}H_2O$ were grown and studied by X-ray diffraction [158]. In this single F-bridged Ni^{2+}-dimer (the second of this type ever reported, and the first magnetically characterized showing a significant antiferromagnetic exchange) the phen moieties of the two $[Ni(\mathbf{93})]^{2+}$ units face each other and lie on almost parallel planes at a mean distance of about 3.70 Å (see Fig. 11). However, the $[Ni(\mathbf{93})]^{2+}$ units are rotated with respect to each other along the Ni-Ni′ axis and the projection of one phen moiety does not superimpose on the top of the other. The weak π–π interaction between the phen moieties in $[\{Ni(\mathbf{93})\}_2F]^{3+}$ might explain why only mononuclear Ni^{2+} complexes are isolated from the reaction of $[Ni(\mathbf{93})(MeCN)]^{2+}$ with the bigger Cl^-, Br^-, and I^- halogenide anions [150,157,159]. Indeed, an almost linear μ-Cl, μ-Br, μ-I bridge between two $[Ni(\mathbf{93})]^{2+}$ units would set the two phen moieties too far away from each other, thus hampering any π–π interaction between the two aromatic systems.

In the case of **93**–**95**, fluorimetric and conductometric measurements showed in some cases the formation in solution of 1:2 metal-to-ligand complexes [153,154]; however, only compound

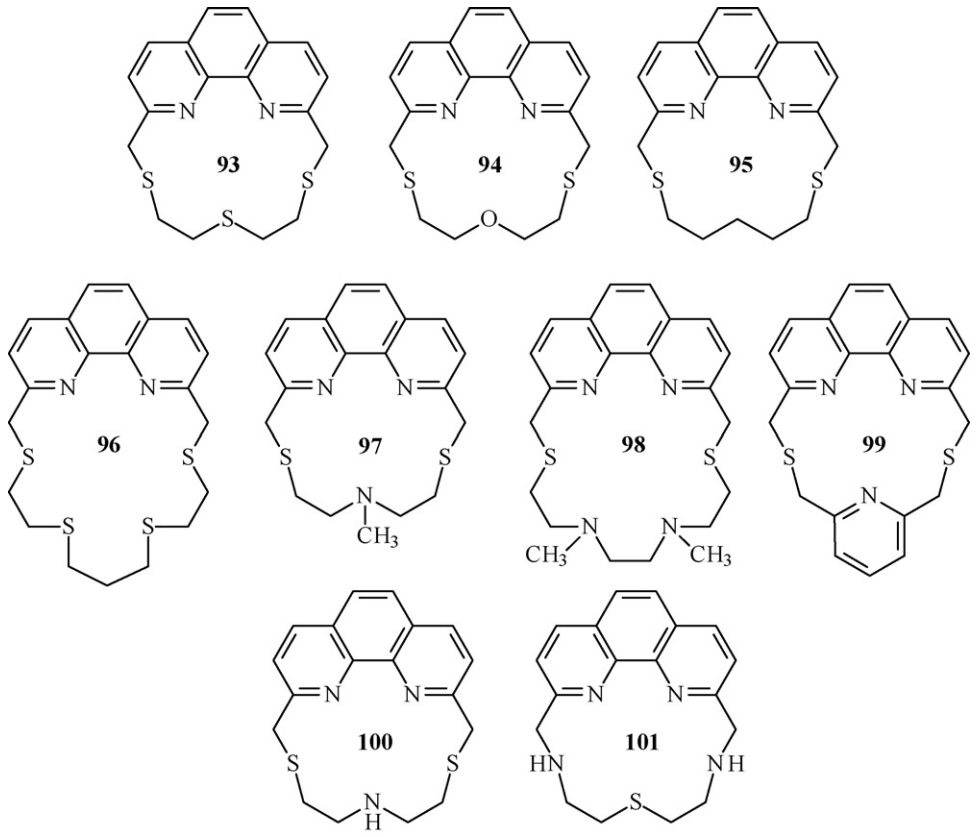

Scheme 34.

[Pb(**95**)](ClO$_4$)$_2$·MeCN was characterized by X-ray diffraction analysis [153]. In the complex cation [Pb(**95**)$_2$]$^{2+}$ the metal centre is sandwiched between two symmetry-related molecule of **95** reaching an overall [4N + 4S] eight-coordination (see Fig. 12) [153].

Complexation of Pb^{2+}, Cd^{2+}, Hg^{2+}, Cu^{2+} and Ag^{+} with **93**–**98** was studied by means of spectrofluorimetric, spectrophotometric and conductometric titrations in MeCN or EtOH solutions [153–155,162]; despite the measured 1:1 formation constants resulted of the same order of magnitude for the metal ions considered with the various macrocyclic systems, some of the ligands proved to be extremely selective neutral carriers when incorporated into organic membranes and involved in transport processes. Analytical applications of phen derivatives, mainly crown ether containing systems, have mainly regarded the construction of ion-

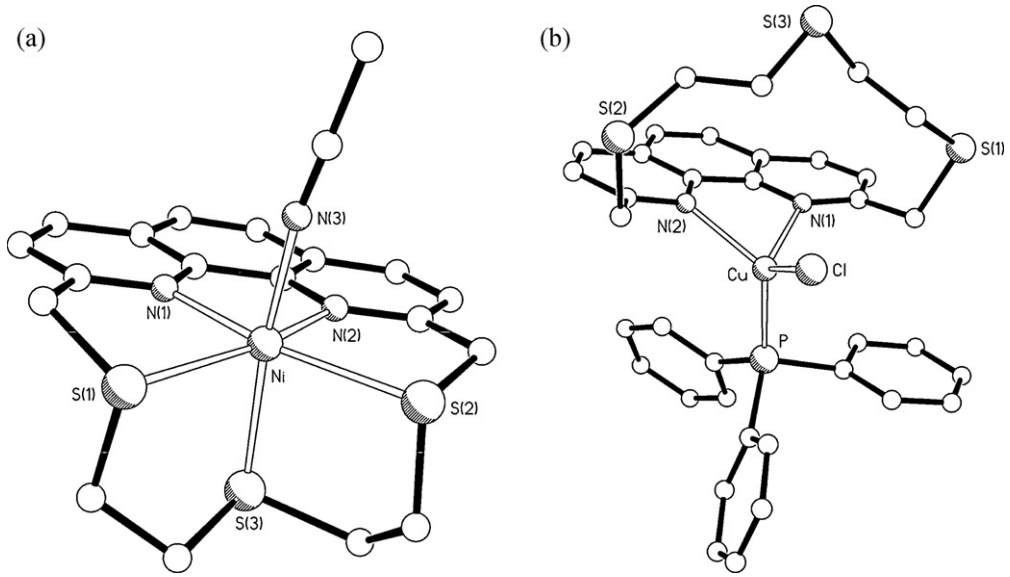

Fig. 10. ORTEP view of the complex cation [Ni(**93**)MeCN]$^{2+}$ (a) [150] and of [Cu(**93**)Cl(PPh$_3$)] (b) [155].

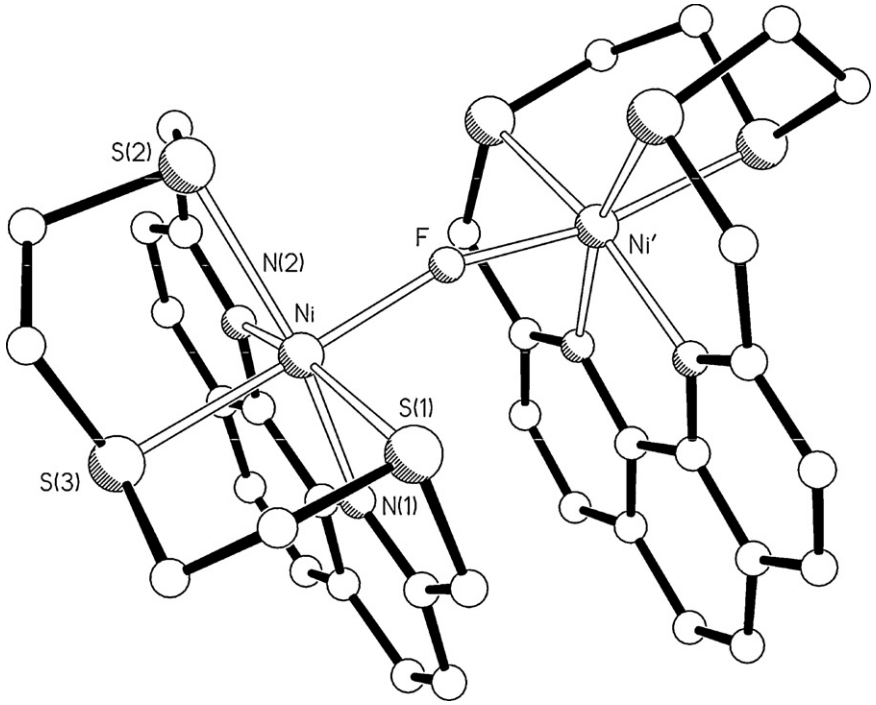

Fig. 11. ORTEP view of the complex cation $[\{Ni(\mathbf{93})\}_2F]^{3+}$ [158]. H-atoms are omitted for clarity.

selective electrodes (ISEs) and separation systems for alkali metal ions, and in particular Li^+ [20,163]. Using **93**, **95** and **97** it has been possible to built highly selective Cu^{2+} and Ag^+ ion polyvinyl chloride (PVC)-membrane electrodes characterized by low detection limits and a Nernstian behaviour over a wide concentration range, thus demonstrating the importance of transport dynamics, beside structural features of a carrier and the thermodynamic stability of its complexes in determining the potentiometric selectivity of ISEs [164–166]. In particular, a PVC-membrane electrode based on **93** resulted very selective for Cu^{2+} [164], while ISEs based on **95** and **97** resulted very selective for Ag^+ [165,166]. A very Nd^{3+}-selective ISE was instead constructed using **99** as neutral carrier [152]. Compounds **93**–**95** were also used as neutral ion carriers in the preparation of supported liquid membranes (SLMs) for selective transport and separation procedures of Ag^+ [167,168]. Surprisingly, under these new experimental conditions [a microporous polypropylene (PP) membrane as a supporting medium to hold a nitro-phenyl octyl ether (NPOE) solution containing the carrier], **94** resulted to be the most efficient carrier for the selective transport of silver(I) from a feed solution to a stripping one. Maximum transport, nearly 90% in three hours time, was observed in the presence of 0.01 M picric acid in the feeding solution with a [picric acid]/[Ag^+] ratio of about 100, and 0.03 M thiosulfate ion as scavenger for the transported Ag^+ in the stripping solution. Transport experiments were made with Mg^{2+}, Ca^{2+}, Sr^{2+}, Ba^{2+}, Co^{2+}, Ni^{2+}, Zn^{2+}, Cu^{2+}, Cd^{2+}, Pb^{2+}, and Hg^{2+} present initially at $[M^{2+}]/[Ag^+] \geq 5$ in the feed solution. None of these metal ions used interferes with the transport of silver(I) ion through the SLM system, even at such high $[M^{2+}]/[Ag^+]$ ratios up to 100 [167,168].

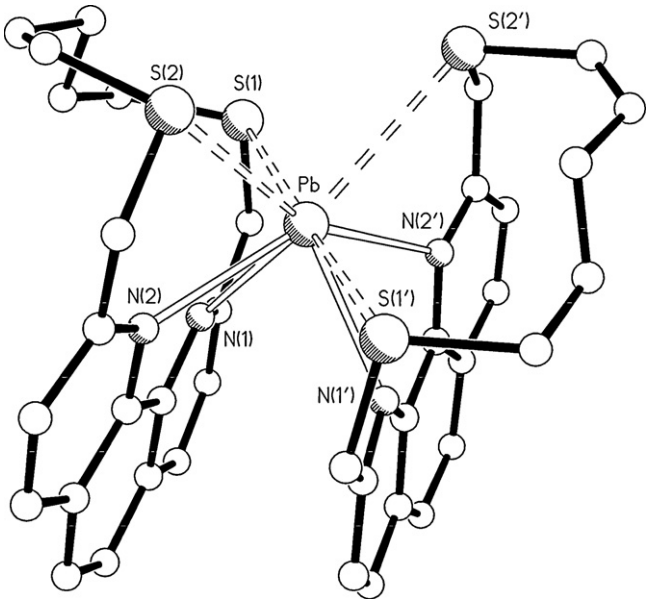

Fig. 12. ORTEP view of the complex cation $[Pb(\mathbf{95})_2]^{2+}$ [153]. H-atoms are omitted for clarity.

The macrocyclic ligands **93**–**95**, **97**, **99**, **100** were also tested as extractants for liquid–liquid $H_2O/CHCl_3$ extraction of a series of metal ions showing borderline or soft acid characters [156]. The main results are summarized in Fig. 13. In single ion experiments under comparable conditions, all ligands show a nearly quantitative Ag^+ extraction, independently of the different donor sets in the macrocyclic framework. In the case of Cu^{2+} only **99** shows a high ability to transfer this metal ion from the aqueous to the organic phase (see Fig. 13a).

Competitive experiments carried out on aqueous solutions containing equimolar concentrations of Ag^+, Cu^{2+} and Hg^{2+} and using $CHCl_3$ solutions of the ligands having the same concentration of the metals, showed a significant decrease of the Ag^+ extraction, which suggests a strong mutual influence on the extraction of Cu^{2+} and Hg^{2+}. The extraction of silver(I) is still favoured in the presence of copper(II) but not in the presence of mercury(II) (see Fig. 13b) [156].

Therefore, it appears clear that macrocyclic ligands, **93**–**95**, **99** and **100** can manifest different ability as receptors in recognition process depending on the chemical situation in which they oper-

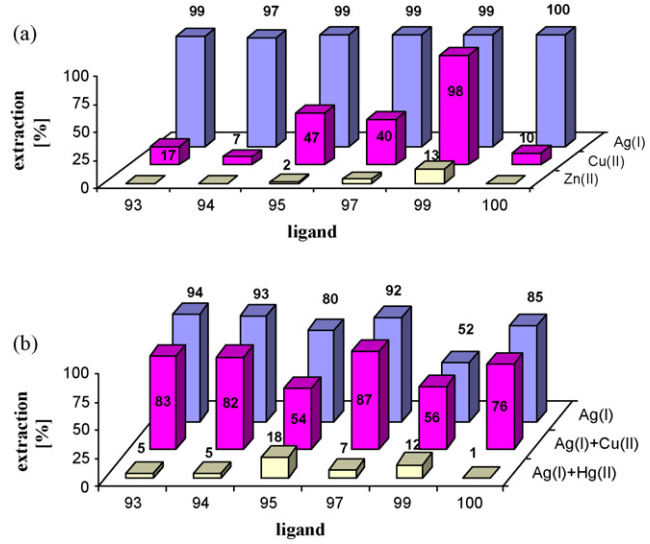

Fig. 13. Extraction of Ag^+, Cu^{2+} and Zn^{2+} by **93**–**95**, **97**, **99**, **100**; $[M^{n+}] = 1 \times 10^{-4}$ M in H_2O, $[NaClO_4]$ 1×10^{-3} M, pH 6.1, $[L] = 1 \times 10^{-3}$ M in $CHCl_3$ (a). Extraction of Ag^+ alone by **93**–**95**, **97**, **99**, **100** and in the presence of Cu^{2+} and Hg^{2+}; $[M^{n+}] = 1 \times 10^{-4}$ M in H_2O, $[NaClO_4]$ 1×10^{-3} M, pH 3.1, $[L] = 1 \times 10^{-4}$ M in $CHCl_3$ (b) [156].

ate, and this can stimulate their application for different analytical applications by employing different techniques.

Ligand **100** has been further functionalized with an anthracenylmethyl pendant arm to give **102** (Scheme 35) [169].

Interestingly, this ligand showed a selective binding for the UO_2^{2+} ion, which resulted in the formation of a 2:1 ligand-to-metal complex and a pronounced chelation enhancement of fluorescence. Because of these properties, **102** was employed as neutral ion carrier for the construction of a plasticized PVC membrane-based ion selective electrode for the determination of uranyl ion, and this electrode was used in flow injection potentiometry for the selective measurement of UO_2^{2+} in trace level [169].

2.2. Other types of 1,10-phenanthroline functionalizations

As already mentioned at the beginning of Section 2, the synthetic manipulation at the 3,8-, 4,7- and 5,6-positions of the phen nucleus are more difficult to be achieved and much less synthetic options are available. Below the most relevant and recent functionalization at these positions of the phen are discussed.

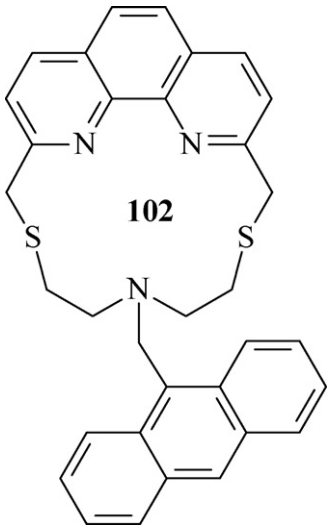

Scheme 35.

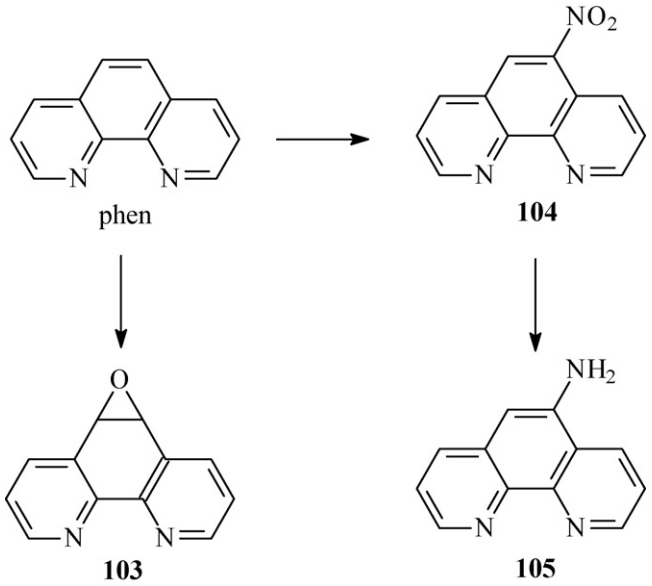

Scheme 36.

2.2.1. 5-Mono- or 5,6-disubstituted 1,10-phenanthroline derivatives

The 5- and 6-positions of phen are the most susceptible to electrophilic substitutions. Reaction with commercial bleach under phase-transfer conditions can afford, in good yield, 5,6-epoxy-1,10-phenanthroline (**103**) which represents a good intermediate for functionalization of the 5-position of phen with different binding sites for analytes (Scheme 36) [170]. Furthermore, direct nitration of phen with an HNO_3/H_2SO_4 mixture followed by reduction of the obtained 5-nitro-1,10-phenanthroline (**104**) affords 5-amino-1,10-phenanthroline (**105**) (Scheme 36) [171].

Compound **105** has been extensively used as starting material for the preparation of selective receptors for anionic, cationic and neutral species as it will be discussed in the next sections. Very recently, **105** has also been appropriately manipulated to facilitate covalent attachment of the phen unit and its complexes with europium(III) (**106** in Scheme 37) or other rare-earth metal ions onto the surface of silica substrates [171,172–174], or Merrifield resin [175], thus affording organic-inorganic hybrid luminescent materials.

In particular, functionalized silica nanotubes as **107** (Scheme 37) showed a selective quenching of the fluorescence emission of the phen moieties attached on the surface upon addition of Cu^{2+}, in agreement with the high affinity of this metal ion for the nitrogen atoms of phen-based ligands [176,177].

Starting from **105**, Keyes and co-workers have synthesized the photoactive complex **108** (Scheme 38), in which the phen nucleus is linked at the 5-position *via* a secondary amine to the 6-position of the primary (narrower) rim of β-cyclodextrin and then coordinated to a photosensitizing ruthenium(II) polypyridyl moiety [178]. Initially, the authors demonstrated the ability of the β-cyclodextrin moiety to support electronic communication between the ruthenium(II) centre and a hydroxo bridged Mn^{3+} dimer anchored at the wider rim [178]. Subsequently, they demonstrated the pH sensitivity of the luminescence of **108**, which resulted modulated by protonation/deprotonation processes at the amine bridge; furthermore, strong host–guest binding of **108** to anthraquinone and anthraquinone-2-carboxylic acid resulted in a concomitant and efficient quenching of the Ru^{2+}-based MLCT emission [179].

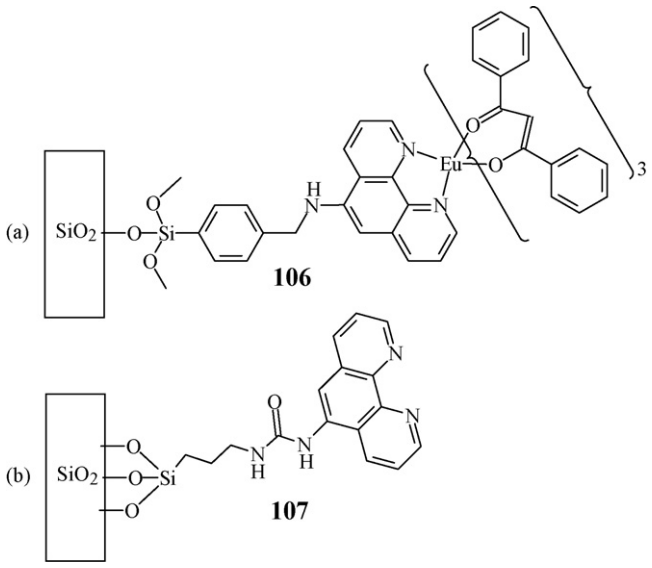

Scheme 37.

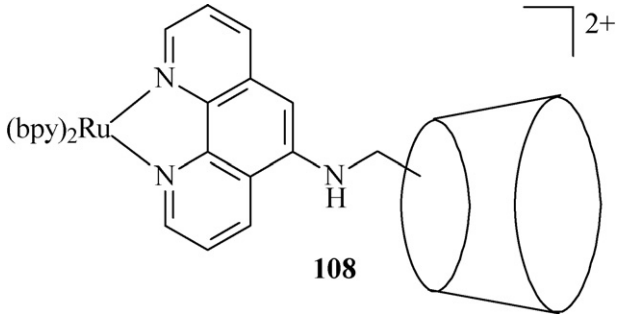

Scheme 38.

Gunnlaugsson and co-workers have developed the cationic tetraamide phen-based europium(III) complex **109** (Scheme 39) [180–182].

Unlike the systems developed by Quici and Accorsi (see Scheme 27, Section 2.1), in **109** the phen moiety is used both as an antenna sensitizing chromophore for the indirect population of the europium(III) excited state, and as a metal ion coordinating ligand. Indeed, the phen antenna is capable of sensitizing the europium(III) excited state, but the lanthanide luminescence is highly pH-dependent, being reversibly quenched in both acidic and basic media following an OFF–ON–OFF bell-shaped luminescence-

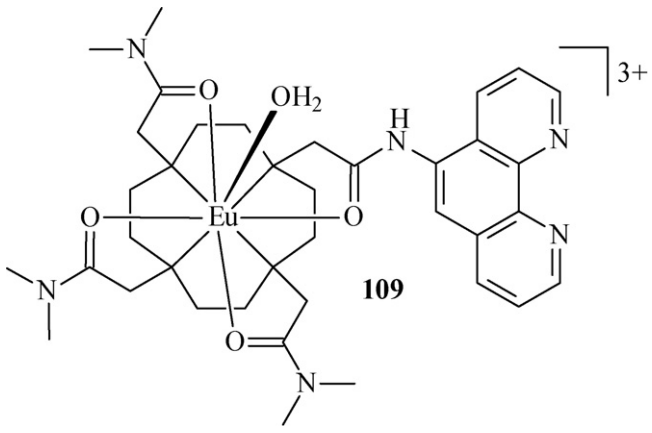

Scheme 39.

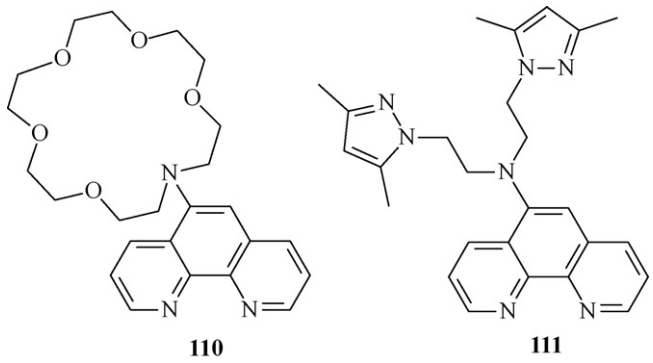

Scheme 40.

pH profile [180,182]. Furthermore, titrations of **109** with Cu^{2+}, Co^{2+}, and Fe^{2+} at pH 7.4 revealed the formation in solution of tri- and tetra-nuclear mixed f–d complexes, with concomitant quenching of both the fluorescence emission arising from the phen moiety, and the delayed Eu^{3+} emission. Interestingly, addition of EDTA to a fully quenched solution of these mixed polynuclear complexes re-instated the phen and Eu^{3+} centred emissions [181,182]. Recently, Gunnlaugsson has also developed mixed lanthanide-transition-metal supramolecular systems similar to **109** in which europium(III) is replaced by neodymium(III) or ytterbium(III), and the phen moiety is coordinated to a ruthenium(II)-$(bpy)_2$ unit [183,184]. Both complexes give sensitized lanthanide luminescence in the NIR region upon excitation of the $[Ru(phen)(bpy)_2]^{2+}$ triplet MLCT band, but for both complexes neither the MLCT nor the NIR emissions were modulated in the presence of DNA [183]. Interestingly, by replacing the ancillary $[Ru(phen)(bpy)_2]^{2+}$ moiety with the stronger DNA binding system $[Ru(phen)_3]^{2+}$, in the case of the Yb^{3+} complex, the Yb^{3+}-centred NIR emission resulted switched OFF upon binding to DNA at pH 7.4, while the MLCT emission slightly increased [184].

Reaction of 5,6-epoxy-1,10-phenanthroline (**103**) with a variety of nucleophiles results in hydroxy-dihydro intermediates that upon dehydration can afford not only 5-substituted phen derivatives useful for further manipulations [170], but also interesting ditopic ligands featuring the phen nucleus derivatized at the 5-position with chelating groups. For example, the systems **110** and **111** (Scheme 40) were prepared following this approach [170,185]. In particular, the rhenium(I) complex [*fac*-Re(**110**)$(CO)_3$Cl] is luminescent and its intensity emission undergoes a remarkable increase upon treatment with Pb^{2+} [170].

On the other hand, the luminescence intensity emission of the complex $[Ru(bpy)_2(\mathbf{111})]^{2+}$ in MeCN solution results partially quenched by the addition of Cu^{2+} up to a 1:1 molar ratio, and the residual luminescence of the resulting mixture is further diminished by NO addition [185]. This behaviour could represent a good starting point for the development of new photoluminescence systems which may serve as NO sensors.

As a further example, 5,6-epoxy-1,10-phenanthroline (**103**) can be easily converted to the 5-cyano-1,10-phenanthroline (**112**) by stirring at room temperature with excess KCN in water, or to the 5-dimethylamino derivative (**114**) by reaction with the appropriate nucleophile followed by dehydratation of the intermediate in the presence of NaH [170,186]; subsequent hydrolysis of **112** under basic conditions affords the 5-carboxy-1,10-phenanthroline (**113**) (Scheme 41) [186].

A series of pH-sensitive luminescent rhenium(I) and ruthenium(II) complexes of **113**, such as [Re(**113**)$(CO)_3$CN] and $[Ru(\mathbf{113})_3]^{2+}$ have been recently prepared [186].

All complexes show a sigmoidal monotonic increase in both luminescent intensity and lifetime of the excited form as the pH

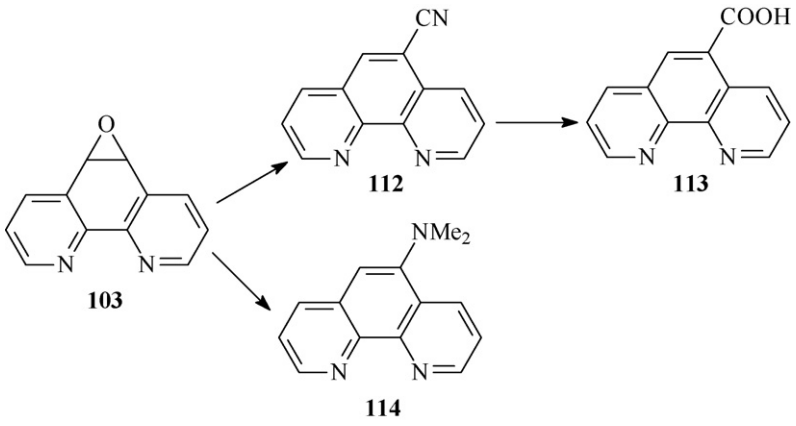

Scheme 41.

increases from 2 to 9. In particular, like the free ligand, the deprotonated form of the complex is the stronger emitter species for all complexes prepared which, therefore, could be used as pH-sensing probes.

Another useful synthon for interesting functionalizations at the 5,6-positions of phen is 5,6-diamino-1,10-phenanthroline (**117**) (Scheme 42). Two main procedures are reported in the literature for the synthesis of this compound; they respectively comprise: (i) amination of 5-nitro-1,10-phenanthroline (**104**) with hydroxylamine in strongly basic conditions followed by reduction of the formed 5-nitro-6-amino-1,10-phenanthroline (**116**) [187]; (ii) conversion of 5,6-dione-1,10-phenanthroline (**54**) to the dioxime derivative **115**, followed by catalytic reduction [188].

Starting from **117**, the heteroditopic ligand **118** and its complexes **119** and **120** (Scheme 43) have been recently synthesized [189]. The bridging ligand **118** combines two of the most used ligands in coordination chemistry, *i.e.*, phen and a N_2O_2 tetradentate Schiff-base salophenic cavity. This ligand was built to covalently tether the photosensitizer unit ($[Ru(bpy)_3]^{2+}$) to a first-row transition metal complex, in order to study the possible reduction (oxidation) of the latter following an oxidative (reductive) quenching pathway of the triplet MLCT excited state of the former.

Interestingly, as compared to the parent lumophore $[Ru(bpy)_3]^{2+}$, the luminescence of **119** is characterized by a fast quenching of the triplet excited state due to intramolecular electron transfer from the metal centre to the salophen unit and generation of a long lived charge-separated state featuring a phenoxyl radical. The presence of Cu^{2+} in the salophenic cavity of the ligand (complex **120** in Scheme 43), enhances the quenching process [189].

5,6-Dione-1,10-phenanthroline (**54**) can easily be reduced electrochemically or chemically to produce 5,6-dihydroxy-1,10-phenanthroline (**121**) (Scheme 44) [190].

The reaction of **121** with various poly(ethylene)glycol-ditosylates affords, in good yield, a series of ditopic macrocyclic ligands (**122**–**124** in Scheme 45), conceptually similar to **118**, which incorporate an externally-directed phen binding site (exotopic) available for the attachment, for example, of a $[Ru(bpy)_2]^{2+}$ fragment, and an adjacent crown ether unit capable of binding alkali metal ions [191].

$[Ru(bpy)_2(\mathbf{122})]^{2+}$, $[Re(\mathbf{122})(CO)_3Cl]$ and $[Ru(\mathbf{122})(CN)_4]^{2-}$ show increasing binding constants (evaluated by NMR spectroscopy) for K^+, in agreement with the presence of an important effect of the host complex charge on the interaction with the cationic guest [192].

The low absolute values for the K^+ binding constants across the series of Ru^{2+} and Re^+ complexes, mainly determined by the poor electron-donating ability of the oxygen atoms directly attached to

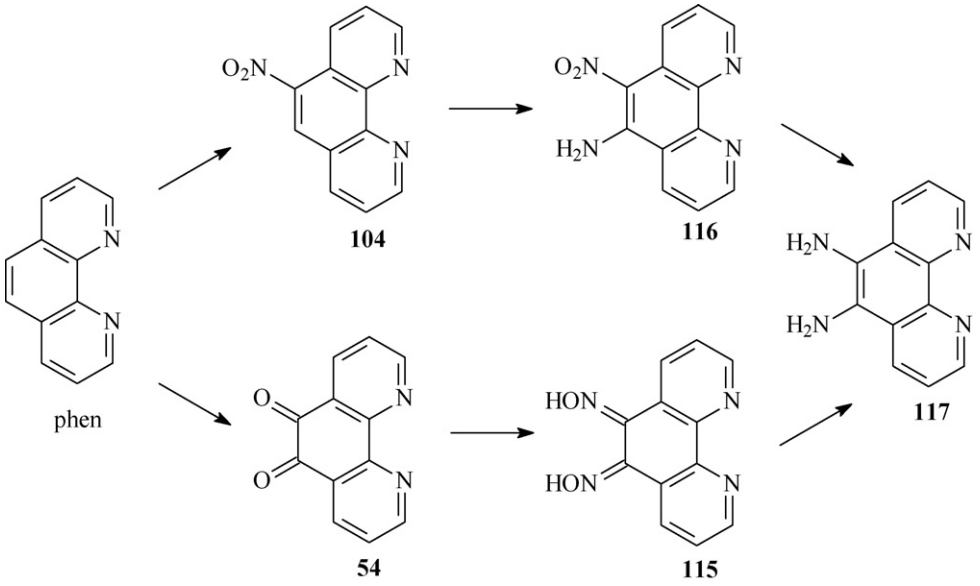

Scheme 42.

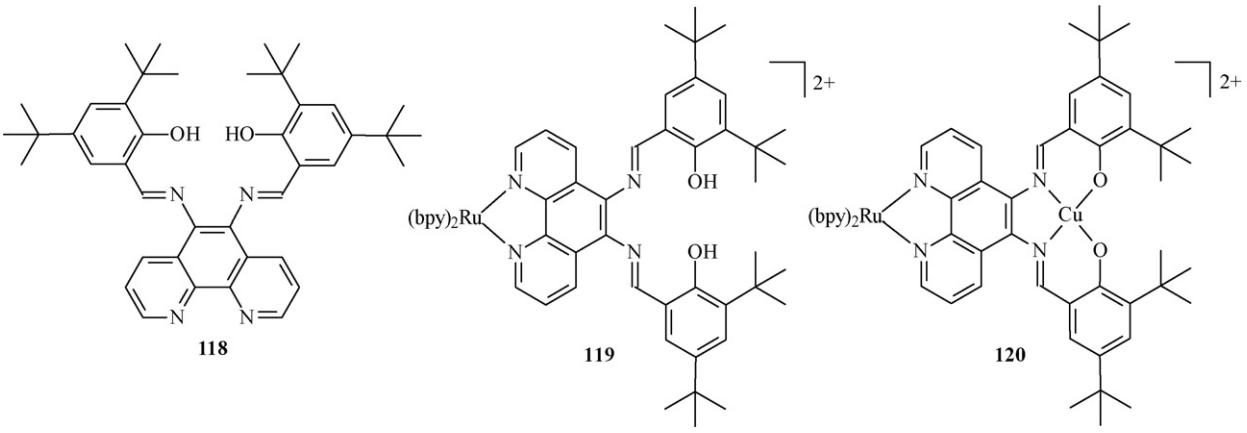

Scheme 43.

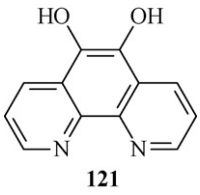

Scheme 44.

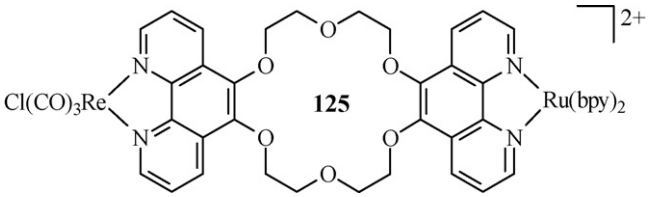

Scheme 46.

the strongly electron-withdrawing complexed phen moiety, preclude any effect on the luminescence from the triplet MLCT excited state of the Ru^{2+}-, Re^{+}-diimine chromophores. Instead, Ba^{2+} with its higher charge density shows strong binding to [Re(**122**)$(CO)_3$Cl] and [Re(**124**)$(CO)_3$Cl] with concomitant 50% quenching of the triplet MLCT luminescence intensity of the host complexes [192]. Interestingly, both [Re(**123**)$(CO)_3$Cl] and [Ru$(bpy)_2$(**123**)]$^{2+}$, due to their H-bond amidic donor sites, show 1:1 and 1:2 binding with $(H_2PO_4)^-$, respectively, accompanied, in the latter case, by a 5-fold increase in luminescence intensity presumably because of formation of a H-bonded structure in which vibrational relaxation of the triplet MLCT excited state is inhibited [192].

Very recently, Ward and co-workers have prepared, starting from **121**, the heterodinuclear complex **125** (Scheme 46) in which the [Ru$(bpy)_2$(phen)]$^{2+}$ and [Re$(CO)_3$Cl(phen)] lumophores are separated by a saturated crown-ether fragment [193]. As in the case of **120**, the idea was to study any possible way of communication between the two different components of the supramolecular assembly.

Luminescence measurements showed the existence of a Re → Ru photoinduced energy-transfer process in solution of MeCN, at room temperature and at 77 K leading, respectively, to a near-complete and complete quenching of the Re^{+}-based luminescence [193]. Molecular modelling studies indicated the possibility of folded conformers for **125**, having a separation between the two metal centres short enough to make possible energy-transfer processes. Addition of K^+ and Ba^{2+} to **125** did not cause any effect on the photophysical properties of this complex indicating a weak association of these two metal ions to the crown-ether fragment.

Very recently, a phen decorated by a crown ether unit has been used as module to prepare the hybrid metallorganic-polyoxometalate assembly **126** (Scheme 47) *via* an induced dipole interaction [194].

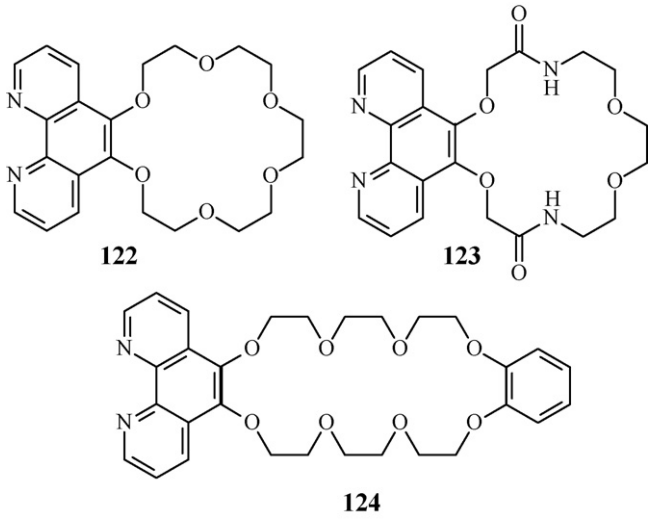

Scheme 45.

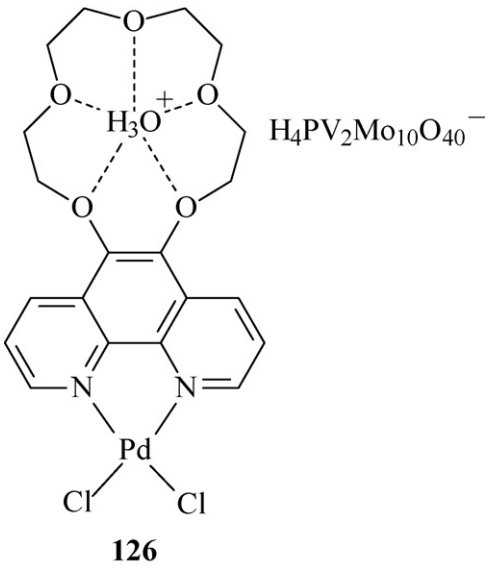

Scheme 47.

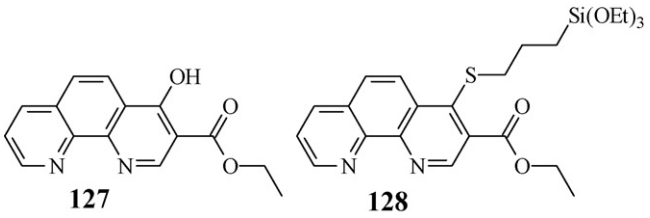

Scheme 48.

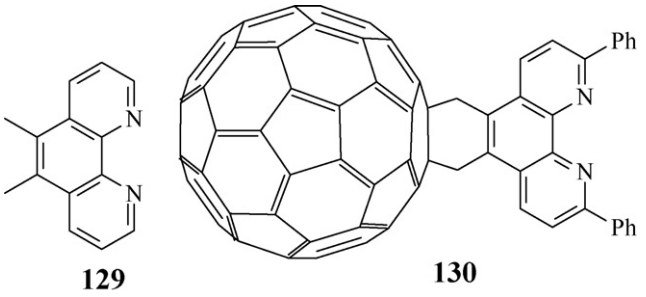

Scheme 49.

Compound **126** catalyzes the Wacker oxidation of alkenes to ketones very efficiently, using the more environmental benign N_2O instead of O_2 as terminal oxidant.

Starting from 4-hydroxy-1,10-phenanthroline-3-carboxylic acid ethyl ester (**127**) [195], Stack and co-workers have recently prepared compound **128** (Scheme 48) [196,197].

128 was immobilized onto the surface of mesoporous SBA-15 silica *via* the propyltrialkoxysilane moiety following two methods: metal templating and random ligand grafting (the purposeful incorporation of the sulfur moiety provides an elemental tag for ligand quantification by inductively coupled plasma (ICP) spectroscopy). The templating method involves the initial formation of the complex $[Cu(\mathbf{128})_2]^+$, covalent attachment of this discrete complex to the silica, and removal of the copper(I) atom template to leave imprinted on the silica surface covalently attached *bis*(phen) coordination environments ready to encapsulate a metal ion. The random ligand grafting method involves covalent attachment of **128** on SBA-15 in the absence of metal template. The templated materials loaded with manganese(II) or iron(II) show enhanced and selective olefin epoxidation catalytic activity with paracetic acid as oxidant, over a wide range of substrate olefin loadings, compared to immobilized catalysts prepared with randomly grafted phen ligands or homogeneous catalysts [196,197].

Finally, by starting from 5,6-dimethyl-1,10-phenanthroline (**129**), which is commercially available, the fullerene-substituted phen derivative **130** has been synthesized (Scheme 49) [198].

The silver (I) complex $[Ag(\mathbf{130})_2]^+$ was also synthesized. However, it was proven to be unstable upon electrochemical reduction, suffering a 3-electron reduction to yield Ag^0, and two $(\mathbf{130})^-$ anions; furthermore, **130** reverts to C_{60} upon a 4-electron reduction [198].

2.2.2. 3-Mono- or 3,8-disubstituted, 4-mono or 4,7-disubstituted 1,10-phenanthroline derivatives

The most common/used starting materials for the functionalization of phen at 3- or 3,8-positions are the corresponding bromo-derivatives **131** and **132** (Scheme 50) which can be prepared in good yields from phen by direct bromination under controlled conditions [199].

131 is the starting material for the preparation of ligands such as **15** (Scheme 6) which have been synthesized by Schmittel and co-workers and magisterially employed for the assembly of supramolecular structures of different topologies (see Section 6).

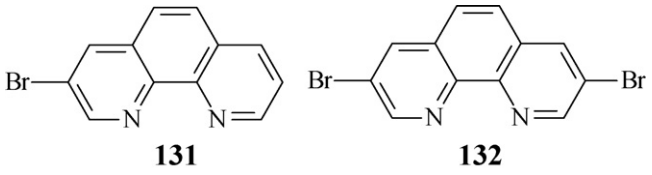

Scheme 50.

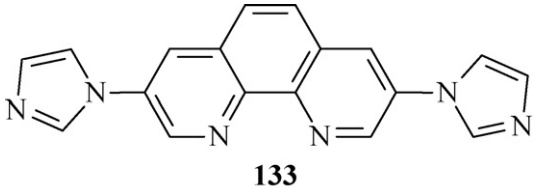

Scheme 51.

132 has recently been employed as starting material for the synthesis of **133** (Scheme 51) *via* a carbon-nitrogen cross-coupling reaction with imidazole using the Ulmann condensation method [200].

This multidentate ligand is able to assume different conformations and can form both coordinative bonds and H-bonds. By exploiting these properties, it has been used in the construction of Cd^{2+} and Zn^{2+} homochiral 2D and 3D coordination polymers involving D-camphoric acid as auxiliary ligand [200].

On the ground of the fact that the most intense electronic transition of the phen skeleton is polarized along the 3–8 positions, also Tor and co-workers thought to increase conjugation along this direction in order to built a new family of highly emissive tunable chromophores based on phen whose emission wavelength could be dictated by the extent of the conjugation, by nature of the substituents at the 3,8-positions and could also be modulated by exogenous additives, such as metal ions. Following a complementary approach based on Sonogashira cross-coupling reactions between **132** and the appropriate substituted phenylacetylenes, Tor and co-workers prepared the conjugated phen derivatives **134**–**137** (Scheme 52) [201,202].

In particular, as compared to the parent phen, **134**–**137** are characterized, in MeCN solution, by a considerable increase in fluorescence quantum efficiency, accompanied by an increasing bathochromic shift of the emission wavelength into the visible region as the electron-donating properties of the R-group increases [λ_{em} = 375 (**134**); 383, 396 (**135**); 441 (**136**), 587 nm (**137**)]. Further modulation of the emission wavelengths was also observed in acetonitrile on adding protons and Zn^{2+} to each chromophore with a considerable bathochromic shifts into the visible region in each case [202].

Following the same convergent synthetic approach used for **134**–**137**, Tor and co-workers have also prepared a series of homonuclear and heteronuclear multimetallic complexes, such as **138**–**140** (Scheme 53), by using direct palladium-mediated cross-

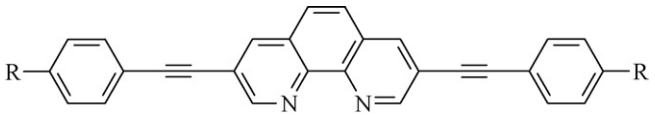

134: R = H
135: R = CH_3
136: R = OCH_3
137: R = $N(CH_3)_2$

Scheme 52.

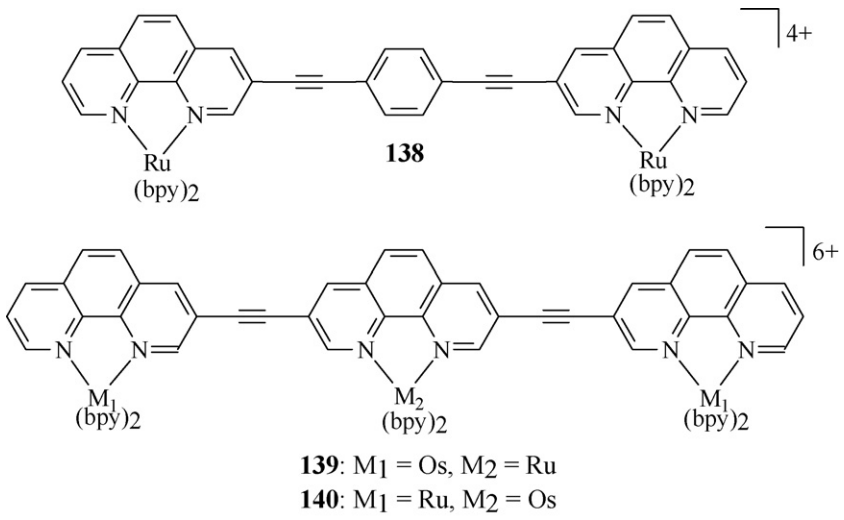

Scheme 53.

coupling reactions between mononuclear metal complexes of **131** and **132**, and mononuclear metal complexes of the corresponding ethynyl-derivatives [203–205].

This kind of multimetallic assemblies of defined architectures are important targets not only for fundamental studies concerning photoinduced energy and electron-transfer, but also for the construction of molecular devices capable for performing light-induced functions.

3-Bromo-1,10-phenanthroline (**131**) has also been used as starting material for the preparation of phen-containing nucleosides as

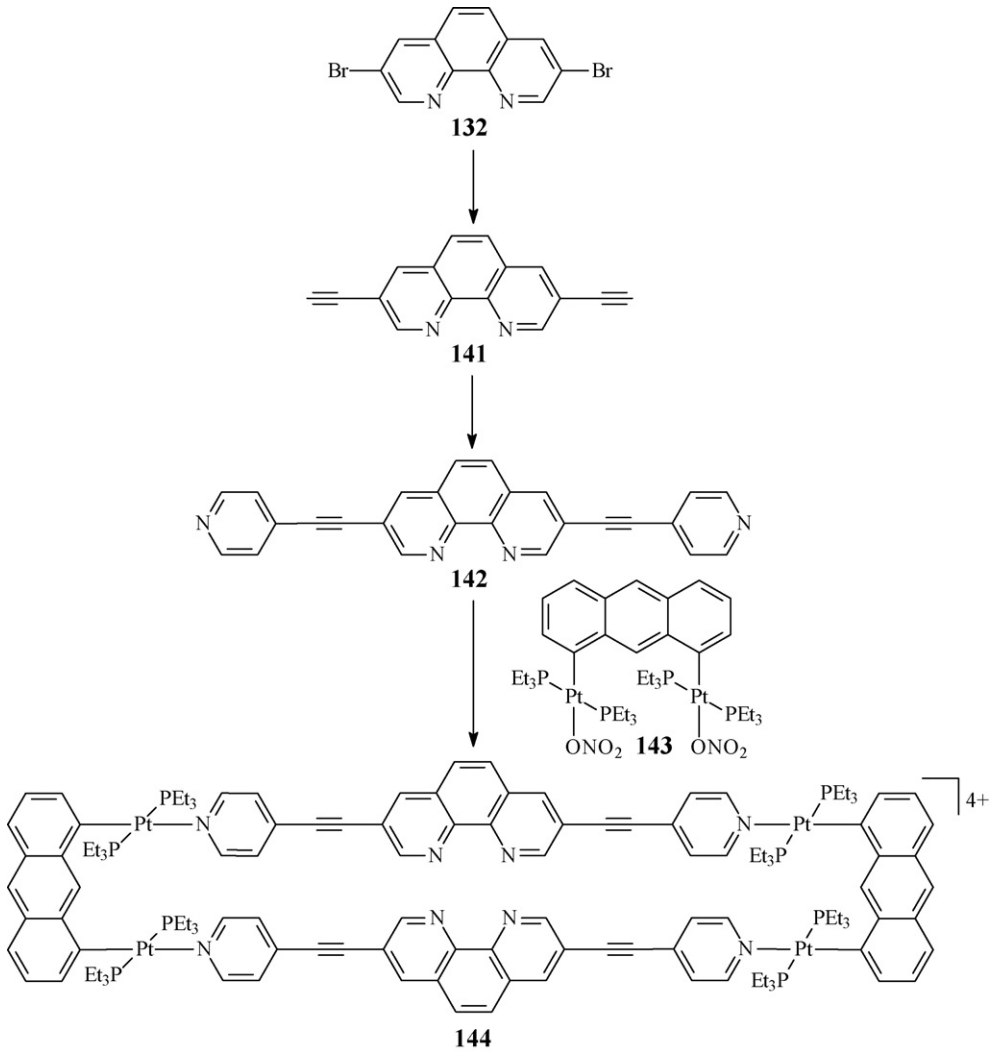

Scheme 54.

"reporter" probes for the local environment of the DNA double helix (see Section 5.2).

Recently, Stang and co-workers, starting from **132** and following the same synthetic approach used by Tor for the synthesis of **134**–**137**, has prepared the ditopic pyridine linker **142** which upon self-assembly with the organometallic anthracene-based "clip" **143** affords the supramolecular phen-containing rectangular metallacyclic macromolecule **144** (Scheme 54) [206].

In this macromolecule, the two juxtaposed phen units define a pre-organized cavity for metal ion binding which can host Ni^{2+}, Cd^{2+} and Cr^{3+} with concomitant dramatic changes in the UV–vis spectrum of the system [206].

Recently, Sauvage and co-workers, starting from **132** synthesized 3,8-*bis*(hydroxyphenyl)-1,10-phenanthroline (**146**) using standard Suzuki cross-coupling conditions to generate first 3,8-dianisyl-1,10-phenanthroline (**145**). The symmetric diphenol **146** was then further reacted in a statistical dissymmetric Williamson reaction with an equimolar mixture of two appropriate alkyl bromides to afford the 3,8-dissymmetrical substituted phen **147** (Scheme 55) [207].

The reaction of **147** with [Ru(tbtpy)Cl_2] (tbtpy = 4′-(3,5-di-*tert*-butylphenyl)-2,2′;6′,2″-terpyridine) afforded after removal of the chloride ion, two scorpionate-type complexes, which are coordination isomers and differ for the tail of **147** occupying the sixth position of the ruthenium(II) coordination sphere. Interestingly, these isomers were characterized by two different MLCT absorption maximum in agreement with a benzonitrile or a sulfoxide monodentate ligand from **147** being coordinated to the metal centre. This allowed selective photoexpulsion of the coordinated tail and opening of the ruthena-macrocycle, followed by the rearrangement of the bidentate phen moiety and coordination of a water molecule

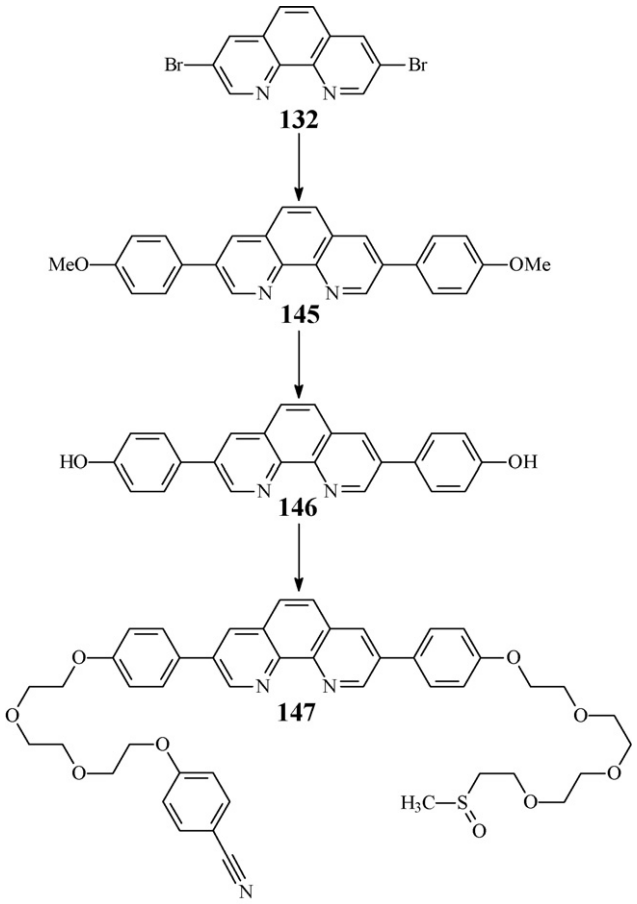

Scheme 55.

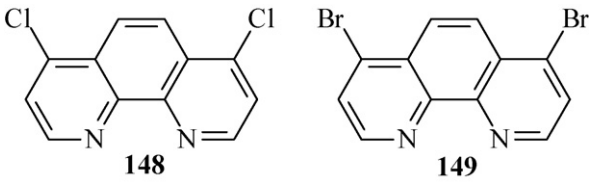

Scheme 56.

or chloride ligand. This rearrangement consisted of a gliding (90°) motion of the phen moiety around the metal centre in the transient pentacoordinated species. While photoinduced opening of the ruthena-macrocycle in acetone was quantitative, the isomerization was a slower process, much less efficient in the presence of Cl^- than in the presence of water; furthermore, thermal back-coordination of the tail resulted quantitative only with chloride as monodentate ligand and it was not followed by further rotation of the bidentate chelate. All this allowed the authors to design a sequence of operations by which a selective irradiation of one isomer in a mixture of the two, resulted in an enrichment of the mixture in the non-irradiated isomer [207].

The best approach to a variety of 4,7-disubstitued phen derivatives is by nucleophilic aromatic substitution of chlorine or bromine atoms in 4,7-dihalo-1,10-phenanthrolines **148** and **149** (Scheme 56) whose synthesis has been optimized by Schmittel and co-workers in the nineties [208,209].

In particular, on heating **149** in a sealed glass tube in the presence of a large excess of *p*-hydroquinone and sodium acetate in dry acetonitrile resulted in the quantitative formation of 4,7-*bis*(4-hydroxyphenoxy)-1,10-phenanthroline **150** (Scheme 57).

This compound was successfully used as building block, according to typical macrocyclization protocols, for the preparation of the first mono- and *bis*(phen) macrocycles with *exo*-coordination sites, like **151** and **152** (Scheme 57) [208,209]. Macrocyclic ligands like **152**, featuring two *exo*-coordinating phen units were subsequently used by Schmittel for the construction of fascinating supramolecular assemblies (see Section 6).

Nucleophilic aromatic substitution of the chlorine or bromine atoms in **148** and **149**, respectively, can also be accomplished with amine and sulfide nucleophiles (see Section 3) [210,211].

The two asymmetrically 4,7-disubstituted phen derivatives **153** and **154** can be easily prepared under Shraup reaction conditions (Scheme 58). The methyl group in 4-position of **153** and **154** can be easily deprotonated with a solution of LDA and reacted with α,α′-

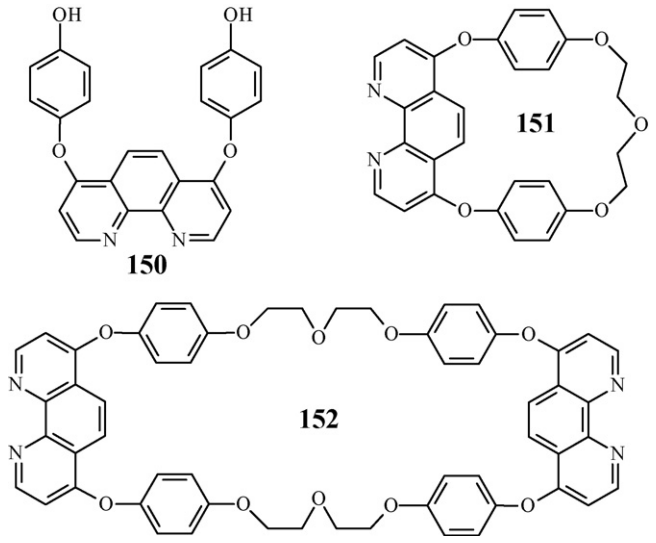

Scheme 57.

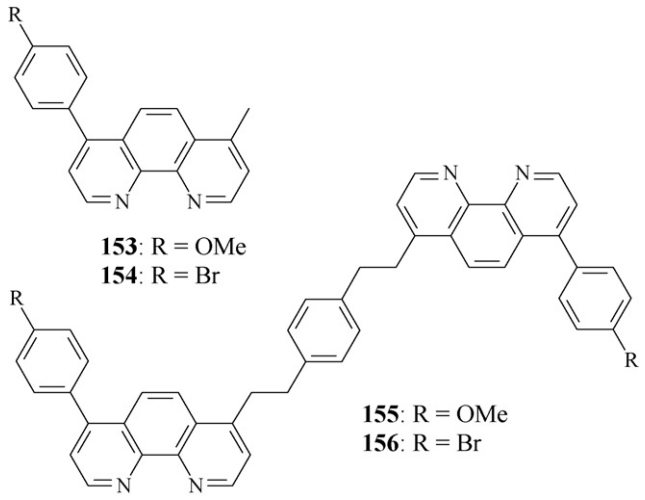

Scheme 58.

dibromo-*p*-xylene to afford helical *bis*-chelating ligands **155** and **156** (Scheme 58) [212,213].

In principle, *bis*-chelating ligands of this type can arrange themselves in three different ways around a metal centre in a *pseudo*-octahedral coordination sphere according to a C_{2v} symmetry (four equatorial positions coordinated by the ligand), C_2 symmetry (two axial and two equatorial sites occupied by the ligand) and C_1 symmetry (three equatorial and one axial position occupied ligand) depending on the length of the spacer linking the two bidentate units. In particular, the complexes [Ru(**155**)(4,4′-dmbp)]$^{2+}$ [212] and [Ru(**156**)(4,7-dpphen)]$^{2+}$ [213] (4,4′-dmbp = 4,4′-dimethyl-2,2′-bipyridine, 4,7-dpphen = 4,7-diphenyl-1,10-phenanthroline) show at the solid state nicely coiling of the *bis*-chelate ligands around the metal centre according to a C_2 symmetry disposition of the two bidentate units of **155** and **156**, respectively. Consequently, an axis running through the terminal aryl substituents of **155** and **156** and the central metal ion in the two complexes is defined by the coordination mode of the two *bis*-chelate ligands (see Fig. 14). Interestingly, for the two ruthenium(II) complexes containing tetradentate ligands **155** and **156**, the luminescence quantum yields and lifetimes are three to ten times larger than those measured for the complex [Ru(bpy)$_3$]$^{2+}$. These unusual properties have been explained in terms of a possible decoupling between the triplet MLCT and MC (metal centred) excited states in the ruthenium(II) complexes with **155** and **156** determined by the geometrically constrained coordination mode of the ligands, which hampers non-radiative processes normally deactivating the MLCT luminescent level in Ru-polypyridine complexes [212,213].

3. Phenanthroline-based receptors for metal ions, recognition and sensing

The development of artificial chemosensors – discrete molecules that selectively recognize and signal to an external operator the presence of a specific analyte in a complex matrix - is one of the main technological applications of supramolecular chemistry, and it is continuing strongly and gaining in momentum [214–220]. The intense interest in this field is driven by the growing demand for extremely sensitive and selective analytical tools for the detection and monitoring of charged and neutral substrates in biological, environmental, and industrial waste effluent samples. Sensing molecules capable of signalling the presence of a target species in a given sample can be generally built attaching a signalling unit (chromogenic, redox-active or fluorescent moieties) to an appropriate binding site (receptor unit). As already pointed out

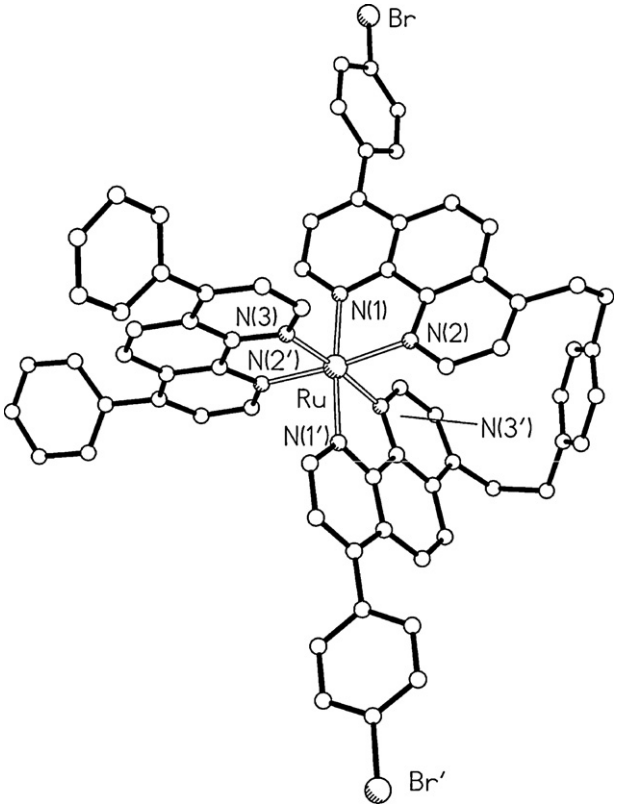

Fig. 14. ORTEP view of the complex cation [Ru(**156**)(4,7-dpphen)]$^{2+}$ [213]. H-atoms are omitted for clarity.

in the previous sections, phen complexes of ruthenium(II) and rhenium(I) are characterized by strong MLCT absorption bands in the visible spectrum and red-shifted fluorescent emissions; they could, therefore represent a good alternative as luminescent signalling units in fluorescent molecular sensors for selective and specific monitoring of metal cations. Furthermore, polypyridyl complexes of redox active metal ions show well defined redox properties and, therefore, they could also be used for the construction of redox-responsive molecular sensors.

The reaction of **148** with excess of aza-crown ethers at relatively high temperatures provided the ligands **157**–**159** (Scheme 59) [210,211]. The 3:1 ligand-to-metal iron(II) complexes of **157**–**159** were studied by cyclic voltammetry in MeCN solution on adding increasing amounts of group Ia and IIa metal cations. All three iron(II) complexes exhibited a clean and reversible oxidation

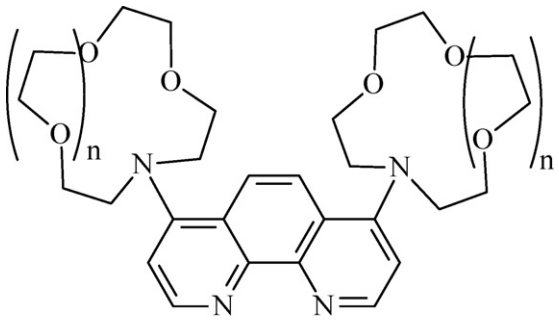

157: n = 1
158: n = 2
159: n = 3

Scheme 59.

wave. However, a large amount of Li^+ for $[Fe(\mathbf{157})_3]^{2+}$, Na^+ for $[Fe(\mathbf{158})_3]^{2+}$, and K^+ for $[Fe(\mathbf{159})_3]^{2+}$ was needed to reach a maximum of about 80 mV for the shift in the $E_{1/2}^{ox}$ potential of the three iron(II) complexes. This is in agreement with a weak binding of the metal ions to the aza-crown ether moieties, presumably caused by the interference of the 5- and 6-protons at the phen backbone with the 4,7-crown ether units, which hamper the cyclic subunit in adopting the best conformation for complexation. Surprisingly, the addition of only 1 equiv. of Ba^{2+} to $[Fe(\mathbf{159})_3]^{2+}$ was responsible for a drastic shift in the $E_{1/2}^{ox}$ potential of about 370 mV. This behaviour was explained considering the Coulombic attraction rather then the ion size as the decisive factor in inducing the aza-crown ether units to assume the right conformation for complexation from a restricted conformational freedom in the uncomplexed state.

In 2007 Schmittel and co-workers implemented **159** in the ruthenium(II) complex $[Ru(phen)_2(\mathbf{159})]^{2+}$ and used it as a sensor molecule that operates on a single type of receptor unit for multi-ion analysis, taking advantage of the different effects exerted by different metal ions on the electronic and photophysical properties of the $[Ru(phen)_3]^{2+}$ signalling core [221]. In fact, the intensity of the strong MLCT charge-transfer absorption band at 429 nm of $[Ru(phen)_2(\mathbf{159})]^{2+}$ in MeCN is drastically reduced only in the presence of Cu^{2+} ions, with Pb^{2+} leading to much minor effects, and all the other metal ions considered (Na^+, K^+, Mg^{2+}, Ca^{2+}, Zn^{2+}, Cd^{2+}, Ag^+, Hg^{2+}) inducing a negligible response. $[Ru(phen)_2(\mathbf{159})]^{2+}$ is characterized by a fully reversible oxidation wave at $E_{1/2}^{ox} = 0.56$ V *vs*. Fc/Fc^+ in MeCN. Upon addition of Pb^{2+} this wave shifts anodically of about 180 mV, whereas only small changes can be noticed upon addition of the other metal ions. Furthermore, the luminescence emission intensity at 672 nm of $[Ru(phen)_2(\mathbf{159})]^{2+}$ in MeCN is affected only by the presence of Pb^{2+} and Cu^{2+}; in particular, addition of Pb^{2+} ions results in a 1.7-fold enhancement in the emission intensity, while addition of Cu^{2+} causes approximately 95% quenching of the emission. Finally, $[Ru(phen)_2(\mathbf{159})]^{2+}$ provides a remarkable electrogenerated chemiluminescence (ECL) at 659 nm in H_2O/MeCN (9:1, v/v) at pH 7.0 in the presence of tri-*n*-propylamine as a co-reactant. Remarkable ECL enhancement (8.2-fold) can be observed only in the presence of Hg^{2+} with minor interference from Ag^+. Fig. 15 summarizes the quadrupole-channel sensing of $[Ru(phen)_2(\mathbf{159})]^{2+}$ which can be used, therefore, as multi-ion sensor [221].

Following the same synthetic strategy adopted for the preparation of **157**–**159**, Schmittel and co-workers have also recently prepared the ligand **160** (Scheme 60), which features N/S/O mixed donor crown ether substituents at the 4,7-positions of the phen nucleus [222].

The complexes $[Ir(ppy)_2(\mathbf{160})]^+$ and $[Ru(phen)_2(\mathbf{160})]^{2+}$ (ppy = 2-phenylpyridine) have been prepared and their optical response to a wide range of metal ions studied in $MeCN/H_2O$ (1:1 v/v) solutions. The iridium(III) complex showed pronounced changes of its luminescence emission intensity only in the presence of Ag^+ and Hg^{2+}. In particular, upon addition of excess of Ag^+ (100 equiv.) to a solution of $[Ir(ppy)_2(\mathbf{160})]^+$, a 3.4-fold enhancement of the luminescence intensity was observed accompanied by a pronounced red-shift (50 nm) of the emission maximum to the value of 595 nm. In contrast, the addition of Hg^{2+} quenched the emission of $[Ir(ppy)_2(\mathbf{160})]^+$, equally showing a red-shift of the emission maximum. Also the optical response of the complex $[Ru(phen)_2(\mathbf{160})]^{2+}$ to the same set of metal ions was investigated. Again significant changes in the luminescent intensity were observed only upon addition of Ag^+ and Hg^{2+}, but the luminescence enhancement factor in the case of Ag^+ was about 10 time lower for $[Ru(phen)_2(\mathbf{160})]^{2+}$ than for $[Ir(ppy)_2(\mathbf{160})]^+$. This different behaviour observed for the two complexes in the presence of silver(I) was attributed to a different origin of their luminescence properties. In particular, a triplet ligand-centred (LC) excited state in the case of $[Ir(ppy)_2(\mathbf{160})]^+$, and a triplet MLCT excited state in the case of $[Ru(phen)_2(\mathbf{160})]^{2+}$. Therefore, binding of Ag^+ to the aza-dioxa-dithia crown ether sites of **160** induces much more influence on the iridium(III) complex than on the ruthenium(II) one [222]. This notwithstanding, the complex $[Ir(ppy)_2(\mathbf{160})]^+$ can be considered as a sensitive and selective luminescent chemosensor for Ag^+ in aqueous solution.

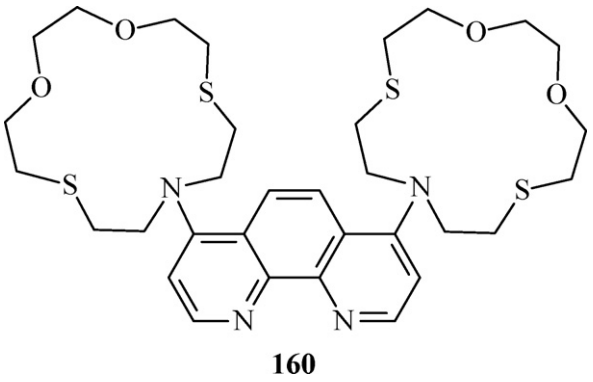

160

Scheme 60.

The ligand **161** (Scheme 61) has been synthesized starting from 4,7-dimethyl-1,10-phenanthroline by oxidation of the methyl groups to carboxylic acids followed by the reaction with the appropriate aza-crown ether [223]. The complexes $[Ru(bpy)_2(\mathbf{161})]^{2+}$ and $[Ru(phen)_2(\mathbf{161})]^{2+}$ exhibit a strong emission in the region 617–633 nm from a MLCL excited states in MeCN solution, which decrease in intensity in the presence of excess of Pb^{2+}, Cu^{2+}, Hg^{2+} and Na^+ in the order $Pb^{2+} > Cu^{2+} > Hg^{2+} > Na^+$ following the formation of 2:1 metal-to-ligand complexes. This quenching effect has been attributed to changes in the orientation and conformation of the two complexed crown moieties with respect to the coordination sphere of Ru^{2+}. These changes in the disposition of the two complexed crown ether units, which serve to minimize steric hindrance in the trinuclear complex, are accompanied by breaking of intramolecular hydrogen-bonding interactions between the amide groups and vicinal 5- and 6-protons at the phen nucleus in the uncomplexed systems, and promote non-radiative decay pro-

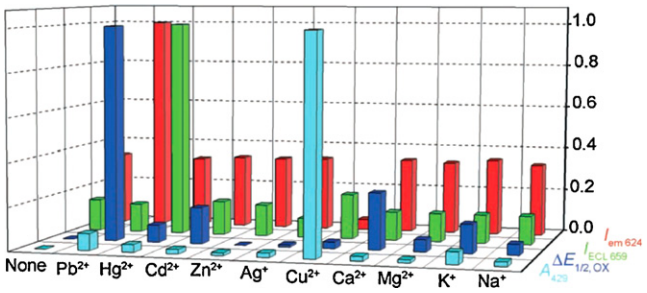

Fig. 15. Plot of relative changes in UV–vis, redox potential, ECL and luminescence of $[Ru(phen)_2(\mathbf{159})]^{2+}$ in the presence of different metal ions. This figure is taken from [221] and reprinted with permission; copyright 2007, by Wiley-VCH.

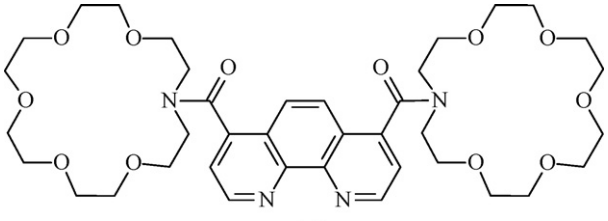

161

Scheme 61.

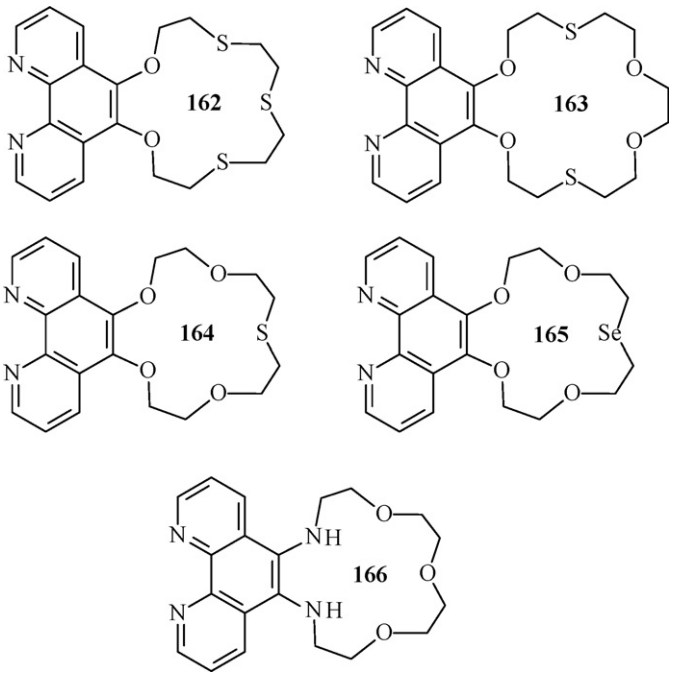

Scheme 62.

cesses for the MLCT excited states [223]. Electrochemical studies in MeCN solution showed also a significant cathodic shift of the oxidation potentials of the Ru^{2+} centres in $[Ru(bpy)_2(\mathbf{161})]^{2+}$ and $[Ru(phen)_2(\mathbf{161})]^{2+}$ in the presence of Na^+ and Pb^{2+}.

Recently, Yam and co-workers have synthesized a series of ruthenium(II) and rhenium(I) diimine complexes of the ligands **162**–**166** (Scheme 62) derived from phen and featuring appended crown ether moieties with one or more of the O-donor atoms replaced by other softer donor atoms such as S, Se, and N [224,225]. The absorption and emission properties of these complexes in the presence of different metal ions were studied in MeCN solutions. In general, the results showed an increased binding affinity for soft metal ions, in particular Hg^{2+}, on replacing O-donor atoms in the crown receptor moiety with softer S-, N- and Se-donors. The luminescence emission intensity at 610 nm of the complex $[Ru(bpy)_2(\mathbf{162})]^{2+}$ was significantly and selectively quenched of *ca.* 40% by the addition of Hg^{2+}, while for the complex $[Ru(bpy)_2(\mathbf{166})]^{2+}$ a selective enhancement by about 8-fold of the luminescence intensity at 620 nm was recorded upon adding the same metal ion (see Fig. 16a).

Such an enhancement in the emission intensity of $[Ru(bpy)_2(\mathbf{166})]^{2+}$ in the presence of Hg^{2+} was explained by

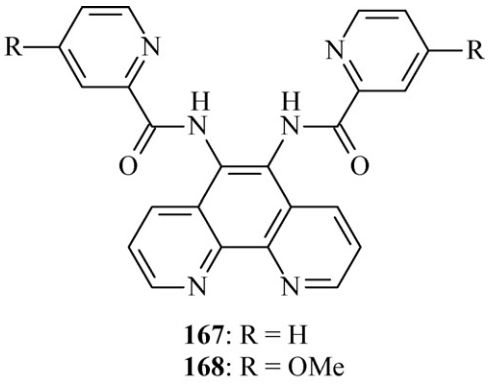

Scheme 63.

considering the direct involvement of the donor atoms in the crown ether moiety, especially the N atoms, in metal coordination, thus reducing the intramolecular reductive electron-transfer quenching mechanism of the emissive triplet MLCT excited state of the ruthenium(II) complexed moiety.

Furthermore, quite interesting is the comparison with the analogous ruthenium(II) complex featuring a pendant 15-crown-5 unit [191,192] for which no significant emission spectroscopic changes were observed even in the presence of alkali and alkaline-earth metal ions. This demonstrates the poor donor ability of the O-atoms directly attached to the phen unit in this complex and the improvement of the binding ability of the crown ether receptor unit by replacement of these O-donors with more electron-rich softer N-atoms.

Enhancement of the triplet MLCT luminescence intensity was also observed for the complexes $[Re(CO)_3(L)(py)]^+$ (L = **162**–**165**, py = pyridine), especially upon adding Hg^{2+}, Pb^{2+} and Ag^+. In particular, a selective enhancement by about 5-fold of the luminescent intensity was observed for $[Re(CO)_3(\mathbf{164})(py)]^+$ upon addition of Pb^{2+} (see Fig. 16b) [225]. Compared to $[Ru(bpy)_2(L)]^{2+}$ (L = **162**–**165**), larger binding constants were observed with $[Re(CO)_3(L)(py)]^+$ (L = **162**–**165**), especially for Hg^{2+} and following the softness of the crown moieties, probably because of smaller charge effects between the Hg^{2+} ions and the monocationic rhenium(I) complexes.

Recently, Comba and co-workers have synthesized the phen-based ditopic ligands **167** and **168** (Scheme 63) from 5,6-diamino-1,10-phenanthroline (**117**, Scheme 42) and picolinic acid or its methoxy derivative [226].

The three complexes $[Ru(bpy)_2(\mathbf{167})]^{2+}$, $[Ru(bpy)(\mathbf{168})]^{2+}$ and $[Ru(\mathbf{167})_3]^{2+}$ show a pH-dependent luminescence emission at 620 nm (λ_{ex} = 450 nm) with a plateau region in the pH range 4.5–9.0. At lower and higher pH values the fluorescence emission

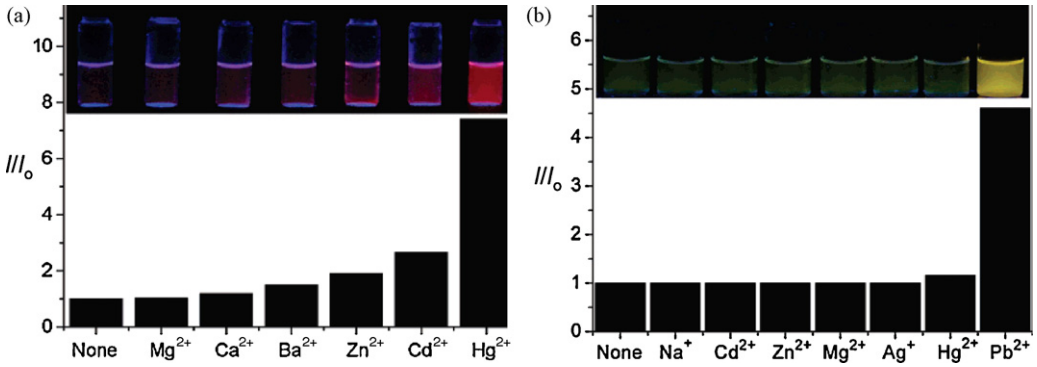

Fig. 16. Photographs showing the selectivity of $[Ru(bpy)_2(\mathbf{166})]^{2+}$ (a) [224], and $[Re(CO)_3(\mathbf{164})(py)]^+$ (py = pyridine) (b) [225], to Hg^{2+} and Pb^{2+}, respectively, and relative enhancement of emission in the presence of 10 equiv. of various metal ions in MeCN solution. These photographs are taken from [224,225] and reprinted with permission; copyright 2007, by The American Chemical Society.

intensity drops sharply to zero. All three complexes show very similar behaviour in aqueous solution on adding increasing amount of different metal ions (Cu^{2+}, Ni^{2+}, Co^{2+}, $Fe^{2+/3+}$, Zn^{2+}, Al^{3+}, Mn^{2+}, Pb^{2+}, alkali and alkaline earth metal ions). In particular, at pH 5.0 (acetate buffer), Cu^{2+} is the only metal ion that leads to an almost complete fluorescence quenching; the addition of an excess of any other metal ion does not have any significant influence on the fluorescence emission of the starting ruthenium(II) complexes. At pH 7.0 (lutidine buffer) other metal ions such as Ni^{2+}, Co^{2+}, $Fe^{2+/3+}$, and Zn^{2+} also cause a significant reduction of the fluorescence emission. At pH 7.0 the quenching efficiency of Cu^{2+} is reduced in the presence of competing citrate and almost destroyed in the presence of EDTA [226].

In principle, phen-containing polyamine macrocycles, such as **78**–**80** and **84**–**87** (Scheme 31) could represent optimal candidates for the development of fluorescence chemosensors for metal cations. In fact, these ligands are versatile receptors for transition and post-transition metal cations and contain a phen moiety as potential signalling units. On the other hand, it was found that coordination of first-row transition or post-transition metals leads to quenching of the fluorescence emission of phen, even in the case of Zn^{2+} and Cd^{2+}, which generally gives fluorescent complexes with polyamine-based chemosensors. This unusual behaviour was ascribed to the presence in their complexes of an amine group, adjacent to phen, not bound to the coordinated metal. This amine group may act as effective quencher of the emission of phen through a PET process to the excited fluorophore [227,228].

However, fluorescent chemosensor for metal cations based on phen-containing macrocycles have also been achieved by appending a second fluorogenic unit on their structure. The first example is represented by ligand **169** (Scheme 64), which contains an anthracene-based pendant arm attached to the central nitrogen of the triamine aliphatic chain of **78** (see Scheme 31).

This ligand was obtained by reaction of **86** (Scheme 31) with anthracene-9-carbaldehyde, followed by reduction *in situ* of the resulting imine [228]. Potentiometric titrations in H_2O/CH_3CN 1:1 (v/v) showed that, by varying pH, **169** forms different stable zinc(II) complexes, *i.e.*, $[Zn(H_2\mathbf{169})]^{4+}$, $[Zn(H\mathbf{169})]^{3+}$, $[Zn(\mathbf{169})]^{2+}$, $[Zn(\mathbf{169})OH]^{+}$ and $[Zn(\mathbf{169})(OH)_2]$. ^{1}H NMR spectra recorded at different pH values showed that deprotonation of the $[Zn(H_2\mathbf{169})]^{4+}$ complex to give $[Zn(H\mathbf{169})]^{3+}$ takes place at the amine groups of the pendant arm and is accompanied by coordination of this donor

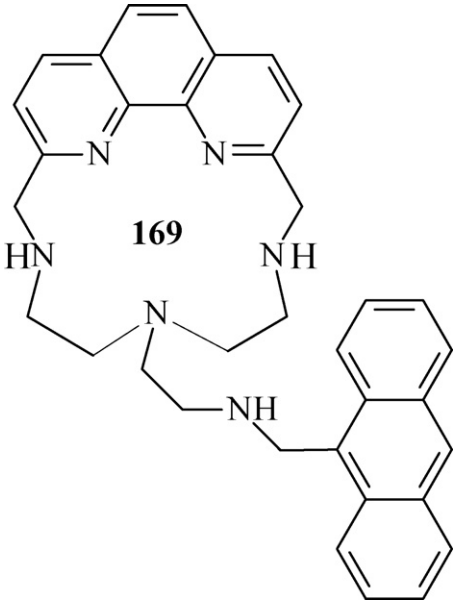

Scheme 64.

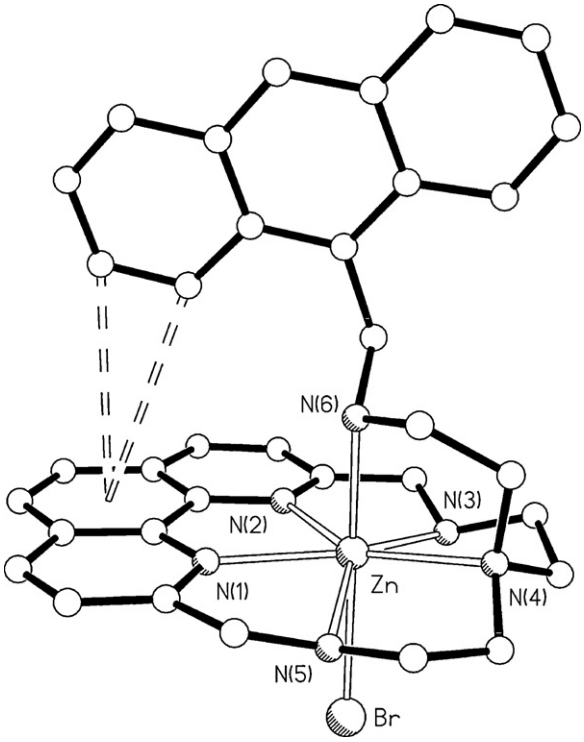

Fig. 17. ORTEP view of the complex cation $[Zn(\mathbf{169})Br]^{+}$ [228]. H-atoms are omitted for clarity.

atom to the metal ion. This enables the two aromatic moieties to interact *via* π-stacking. The interaction between the two aromatic moieties was confirmed by the crystal structure of the $[Zn(\mathbf{169})Br]^{+}$ cation (see Fig. 17), which shows the metal ion bound to the amine group of the pendant arm and a perpendicular disposition of the two aromatic units, which lead two carbon atoms of the anthracene moiety at close distance from the central ring of phen, thus accounting for a edge-to-face π-stacking interaction [228].

Fluorescence emission spectra recorded at different pH values showed that metal complexation leads to quenching of the typical emission band of anthracene and to the formation of a new non-structured and red-shifted emission band (see Fig. 18), occurring for all zinc(II) complexes with the exception of $[Zn(\mathbf{169})(OH)_2]$ [227,228].

This exciplex-type emission was ascribed to an intramolecular π-stacking complex in the excited state, involving phen and anthracene. On the other hand, according to ^{1}H NMR spectra, the π-stacking complex is already formed in the ground state for the species $[Zn(H\mathbf{169})]^{3+}$, $[Zn(\mathbf{169})]^{2+}$, $[Zn(\mathbf{169})OH]^{+}$, but not for $[Zn(H_2\mathbf{169})]^{4+}$ and $[Zn(\mathbf{169})(OH)_2]$. As a consequence, for $[Zn(H_2\mathbf{169})]^{4+}$ the π-stacking exists only during the excited state lifetime. As shown by both ^{1}H NMR and photochemical measurements, the π-stacking interaction disappears at more basic pH values, where detachment of the amine nitrogen of the pendant arm from Zn^{2+} is expected to occur upon metal coordination of a second OH^{-} ion.

Of note, the formation of the exciplex emission depends also on the metal ion used. As a matter of fact, the coordination properties of the ligand toward Cd^{2+} were similar to those observed in the case of Zn^{2+}, and the amine groups of the pendant arm is still coordinated to the metal in the complex $[Cd(\mathbf{169})]^{2+}$ [228]. On the other hand, ^{1}H NMR measurements accounted for a very weak interaction between the two aromatic moieties and no exciplex emission was observed. In fact, the larger dimension of Cd^{2+} does not allow a strong interaction between the two aromatic units upon coordination of the nitrogen donor of the side-arm. Therefore, **169** is able to

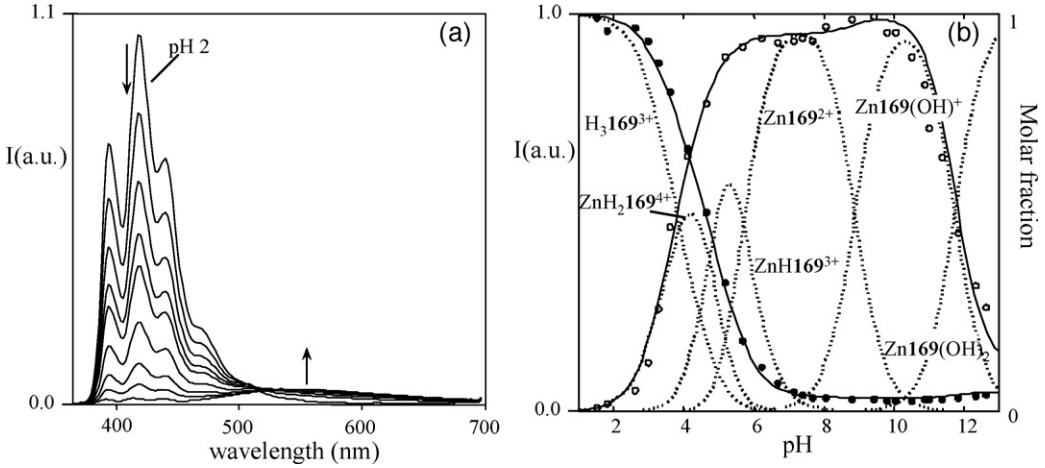

Fig. 18. (a) Fluorescence emission spectra of the Zn^{2+}/**169** system at different pH values: 2.0, 3.73, 4.4, 4.87, 5.1, 5.57, 6.05, 6.55, 10.37. (b) Fluorimetric titrations of the same system (emission followed at 418 nm (○), exciplex emission followed at 600 nm (●) and molar fraction curves of the species formed [227,228]).

perform a selective sensing of Zn^{2+} over Cd^{2+}, forming a complex which behaves as an elementary molecular machine driven by both pH and light.

A phen-containing macrocycle with appended aromatic side arms and capable to give excimer emission in the presence of metal ions has also been reported by García-España, Pina and Seixa de Melo [229]. Ligand **170** (Scheme 65) was synthesized by 2:2 condensation of the tripodal polyamine tren monofunctionalized with a methyl naphthalene group and 2,9-diformyl-1,10-phenanthroline (**28**, Scheme 11), followed by reduction *in situ* of the resulting tetraimide.

Ligand protonation and Zn^{2+} and Cu^{2+} complexation were studied by coupling potentiometric titrations and fluorescence emission spectra recorded at different pH values. The emission spectrum of the ligand is characterized by three bands in aqueous solution, two of which, at 323 and 366 nm attributable to naphthalene and phen moieties, respectively. On the basis of the results deriving from steady state and time-resolved fluorescence measurements, the third band, centred at 460 nm and observable only above pH 4, was attributed to a new intramolecular excimer species resulting from the interaction between one excited phen and one phen in the ground state. Zn^{2+} complexation gives rise to a marked enhancement of the excimer emission, suggesting that the interaction between the two phen units is more efficient upon Zn(II) complexation, probably due to conformational changes favoring the coupling between the two heteroaromatic units. Of note, the most emissive complexes were found the protonated complexes $[Zn(H_4$**170**$)]^{6+}$ and $[Zn(H_3$**170**$)]^{5+}$, where all amine donors are likely to be involved either in proton binding or in metal coordination, thus preventing any suppression of the emission by electron-transfer quenching. Interestingly, the excimer emission is only partially reduced by complexation of Cu^{2+}, a paramagnetic ion well known for its quenching ability.

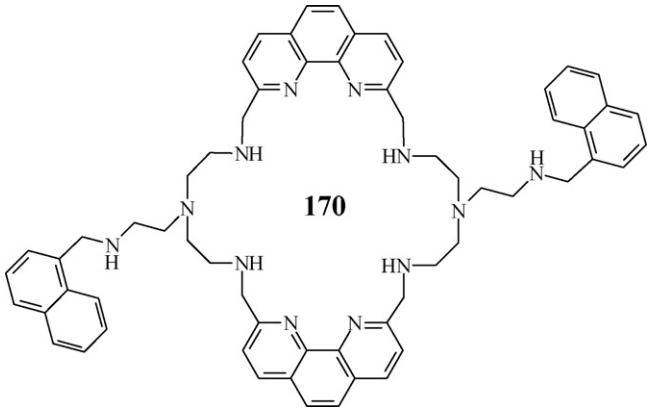

Scheme 65.

4. Phenanthroline-based receptors for anions and neutral molecules, recognition and sensing

The development of synthetic receptors for discriminatory binding and sensing of anions and neutral molecules is also an active area of research as much as it is the development of receptors and sensors for metal ions [230–232]. Anions as metal cations are ubiquitous and play many essential roles in biological systems; they can have deleterious effects on both the environment and the human health, thus justifying the growth in the demand for selective anion receptor and sensor species. Phen has also been largely used as starting material for the construction of elaborated and selective receptors and optical sensors for many anions and neutral molecules.

4.1. Anions

As already discussed for metal cations in the previous section, appropriate functionalizations of the 5,6- and 4,7-positions at the phen scaffold to afford heteroditopic ligands, and subsequent formation of the corresponding ruthenium(II), rhenium(I) or iridium(III) diimine complexes would afford potential optical or redox sensors also for anions or neutral molecules.

Starting from 5-nitro-1,10-phenanthroline (**104**, Scheme 36), in two steps, the urea functionalized phen ligand **171** (Scheme 66) was synthesized by Gunnlaugsson and co-workers who also demonstrated its potential application as fluorescent sensor for Cl^- [233]. In fact, only in the presence of this anion was the fluorescence emis-

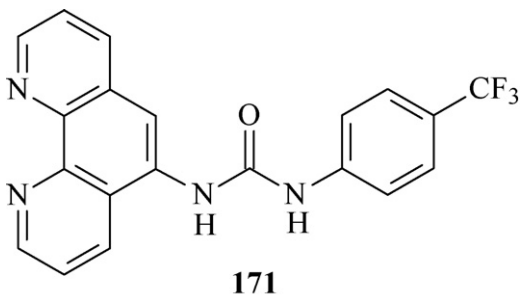

Scheme 66.

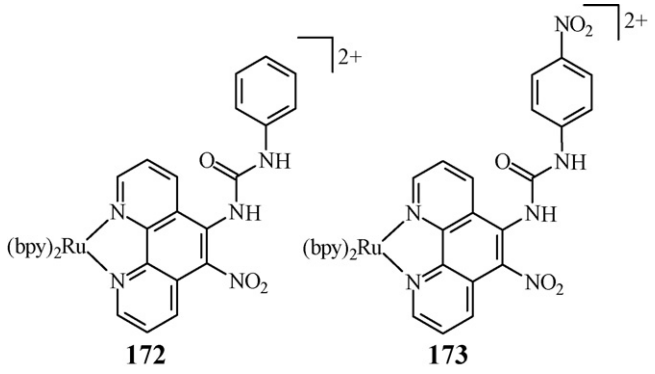

Scheme 67.

sion intensity of **171** enhanced by *ca*. 45% in MeCN solution, while in the presence of other putative anionic guests (F^-, Br^-, $CH_3CO_2^-$ and $H_2PO_4^-$) a considerable quenching was observed. The different effect of Cl^- on the fluorescence emission of **171** was ascribed to inhibition of the photoinduced electron transfer (PET) quenching mechanism from the tolyl group to the phen fluorophore upon formation of a 2:1 **171**/Cl^- adduct, the other anions forming exclusively a 1:1 adduct with the sensor.

Also the $[Eu(\mathbf{171})_3]^{3+}$ complex can interact with anions at the urea moieties in MeCN with significant changes in the Eu(III) emission [234]. In particular, titration of $[Eu(\mathbf{171})_3]^{3+}$ with Cl^-, Br^-, I^-, $CH_3CO_2^-$ and $H_2PO_4^-$ caused a significant quenching of the emission intensity up to a full quenching, in the case of $CH_3CO_2^-$ and $H_2PO_4^-$ within the addition of three equivalents of these anions. In contrast, a titration of $[Eu(\mathbf{171})_3]^{3+}$ with F^- gave rise to initial enhancement in the Eu(III) emission up to one equivalent of F^- added, followed by luminescence quenching. This peculiar behaviour of F^- was ascribed to dual binding modes of this anion to the europium(III) complex involving initial binding at the metal ion centre itself, with concomitant removal of one coordinated solvent molecule, followed by binding of the anion at one or more urea moieties of the $[Eu(\mathbf{171})_3]^{3+}$ complex [234].

Das and co-workers have recently reported the urea-based ruthenium(II)-polypyridyl complexes **172** and **173** (Scheme 67) [235,236].

A change in the absorption spectroscopic pattern along with a naked-eye detectable change in colour was observed only on adding F^-, $CH_3CO_2^-$ or $H_2PO_4^-$ (<2 equiv.) to a MeCN solution of **172** or **173** (see Fig. 19); but, unlike **173**, no further changes could be detected in the absorption spectra of solutions of **172** for further additions of these anions (from 2 to 100 equiv.) [235,236].

In the case of **173**, further colour changes to reddish brown were observed when F^-, $CH_3CO_2^-$ or $H_2PO_4^-$ were added in excess. The origin of this different behaviour of **173** as compared to **172**, was demonstrated to reside in the strong electron-withdrawing effect of the $-NO_2$ functionality on the benzene ring which influences the acidity of the –NH proton in the adjacent urea moiety. In particular, at low concentration of the anions F^-, $CH_3CO_2^-$ or $H_2PO_4^-$ (<2 equiv.) a 1:1 hydrogen-bonded adduct is formed in MeCN with both **172** and **173**. At higher concentrations, classic Brønsted acid–base type reactions prevail, at least in the case of **173** [235,236]. The higher acidity of the H-atoms of the urea groups in **173** can also explain the different changes observed in the emission spectra of **172** and **173** on adding excess (4 equiv.) of F^-, $CH_3CO_2^-$ or $H_2PO_4^-$. In fact an appreciable quenching of the characteristic emission at 616 nm (λ_{ex} = 449 nm) was observed in the case of **172** with all three anions, while a complete quenching was recorded in the case of **173** under identical experimental conditions, presumably determined by deprotonation of the urea functionality [235,236]. No significant changes both in the absorption and emission spectra of **172** and **173** were observed in the presence of other anions (Cl^-, Br^-, I^-, and $H_2SO_4^-$) indicating a relative low binding affinity of these anions for the two receptors [235,236]. Cyclometallated iridium(III) polypyridine complexes containing the ditopic ligands **174**, **175** or **176** (Scheme 68) proved to have a stronger affinity for $CH_3CO_2^-$ than for F^- and $H_2PO_4^-$ in MeCN, independently of the cyclometalating ligands and the substituents of the thiourea moieties [237]. The emission intensities of all the thioureas containing complexes were reduced in the presence of these three anions, about 4-fold in the case of $CH_3CO_2^-$, and about 2-fold in the case of F^- and $H_2PO_4^-$.

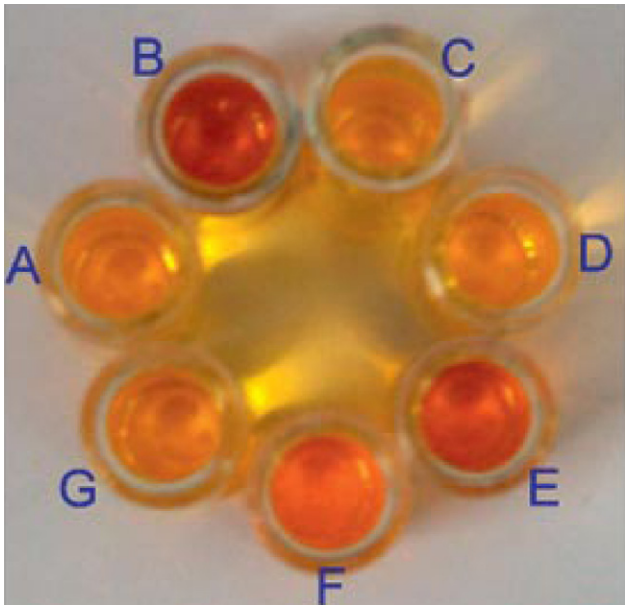

Fig. 19. Colour changes for **172** in the presence of various anions added in excess: free receptor (A), F^- (B), Cl^- (D), Br^- (D), $CH_3CO_2^-$ (E), $H_2PO_4^-$ (F), and HSO_4^- (G). This figure is taken from [235] and reprinted with permission; copyright 2009, by Wiley-VCH.

Recently, Duheme-Klair and co-workers have synthesized and fully characterized two new molecular sensors, **177** and **178** (Scheme 69), featuring the same catechol-based receptor unit, but different lumophores [238].

Both **177** and **178** show an intense emission at about 610 nm in MeCN/H_2O 20:1 (v/v) when excited at 450 and 390 nm, respectively, typical of polypyridyl ruthenium(II) and rhenium(I) complexes which decreases sigmoidally with increasing pH with inflection points located at pH 4.4 (**177**) and 5.4 (**178**). This decrease is ascribed to the deprotonation of the appended phenolic groups.

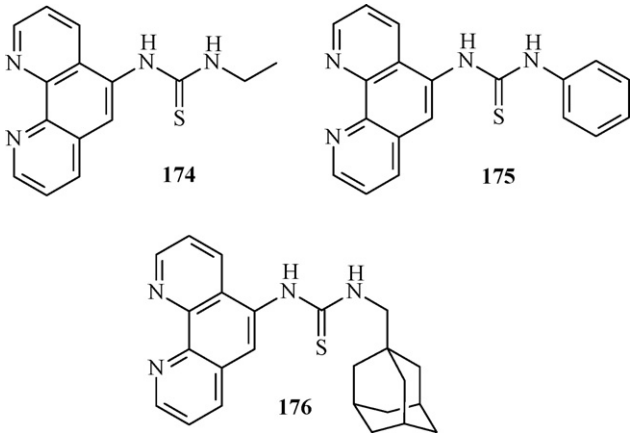

Scheme 68.

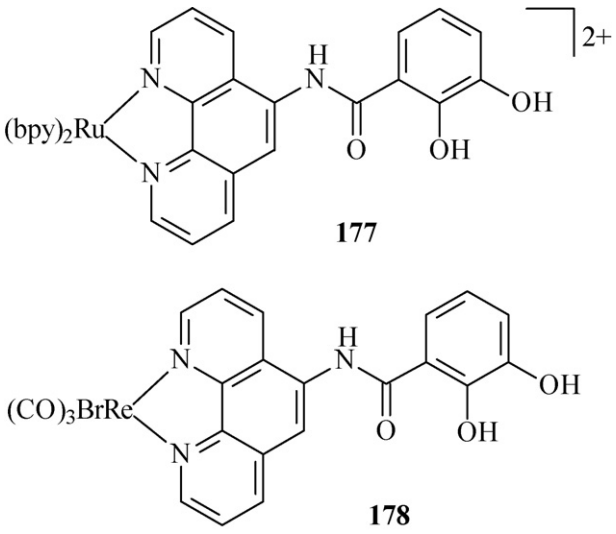

Scheme 69.

Interestingly, both **177** and **178** are able to selectively signal the presence of molybdate and vanadate oxoanions in aqueous acetonitrile in the acidic pH range through a decrease in the luminescence emission intensity. In addition, **178** also detects tungstate, while other oxoanions such as PO_4^{3-}, SO_4^{2-} and ReO_4^- do not interfere in the recognition and signalling processes with both sensors. This selective and sensitive decrease in the emission intensity of **177** and **178** in the presence of the mentioned oxometallates has been attributed to the deprotonation of the cathecol unit upon metal coordination, in agreement with the observation that emission intensity of cathecol methyl-protected derivatives of **177** and **178** is pH-independent and it is not influenced by the presence in solution of oxometallated species [238].

Recently, Lin and co-workers have prepared the hydrazone-based receptors **179** and **180** (Scheme 70) and studied their interaction with different anions [239,240]. In particular, the complex $[Ru(bpy)_2(\mathbf{179})]^{2+}$ proved to be a very selective colorimetric sensor for $CH_3CO_2^-$ in pure aqueous solution changing its colour from purple to green upon the addition of this ion (see Fig. 20). The addition of basic anions such as F^- and $H_2PO_4^-$ triggered similar but much weaker colour changes for $[Ru(bpy)_2(\mathbf{179})]^{2+}$ compared to $CH_3CO_2^-$. Other anions such as Cl^-, Br^- and I^- did not cause appreciable colour changes even in the presence of large excess of them.

A colour change from yellow to purple was instead observed in the case of **180** upon addition of F^-, $CH_3CO_2^-$, $H_2PO_4^-$ or OH^- to a DMSO solution of the receptor. **179**, $[Ru(bpy)_2(\mathbf{179})]^{2+}$ and **180** all formed 1:1 complexes with these anions, but with a marked preference for $CH_3CO_2^-$. ^1H NMR measurements revealed deprotonation of the two –NH groups after the addition of 1 equiv. of acetate ions and potential H-bonds between $CH_3CO_2^-$ and the two N=CH moieties whose spatial disposition, in the deprotonated form of the receptors, would create a host planar cavity perfectly fitting the dimension and geometrical requirements of this trigonal planar anion [239,240].

Host–guest geometrical complementarity has also been invoked to explain the high selectivity for the iodide ion of the carbazole-based anion receptor **181** (Scheme 71) obtained, as in the case of **180**, by starting from 2,9-diformyl-1,10-phenanthroline (**28**, Scheme 11) [241].

Only iodide ion, over the other anions considered (F^-, Cl^-, Br^-, I^- and $CH_3CO_2^-$) was able to induce significant changes in the UV–vis spectrum of **181** in DMF upon formation of a 1:1 complex. ^1H NMR measurements indicated the two –NH hydrogens from the carbazole rings participating in the formation of H-bonds with the I^- ions [241].

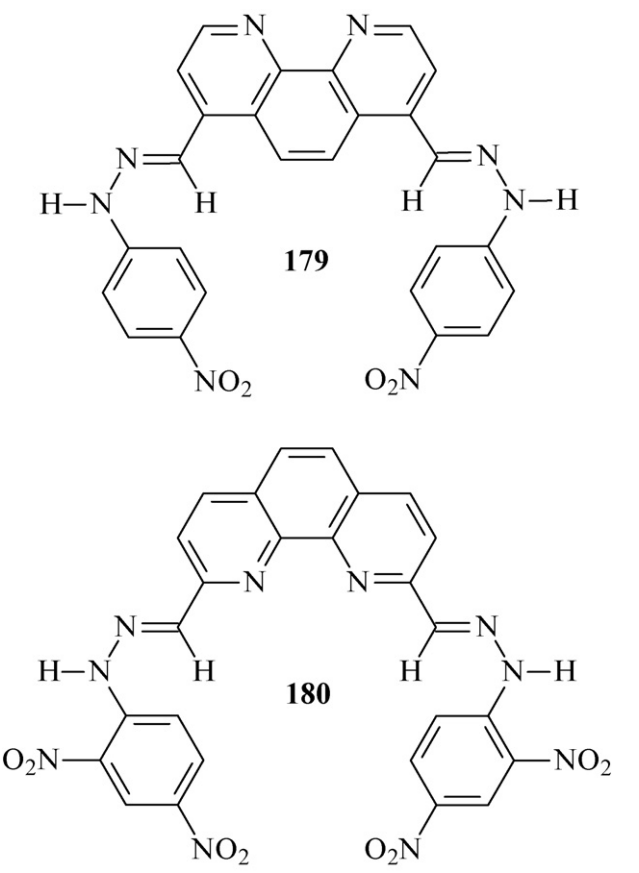

Scheme 70.

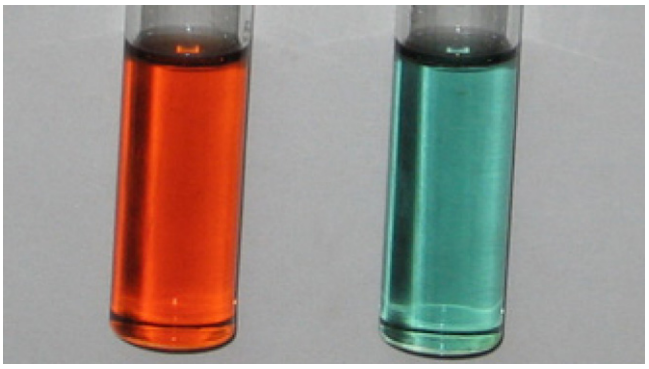

Fig. 20. Colour change of a DMSO solution of $[Ru(bpy)_2(\mathbf{179})]^{2+}$ (red-purple) upon addition of 1 equiv. of acetate (green). This figure is taken from [239] and reprinted with permission; copyright 2007, by Elsevier.

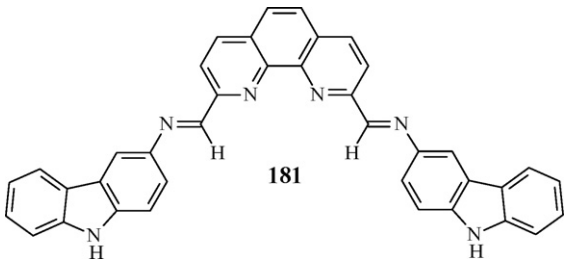

Scheme 71.

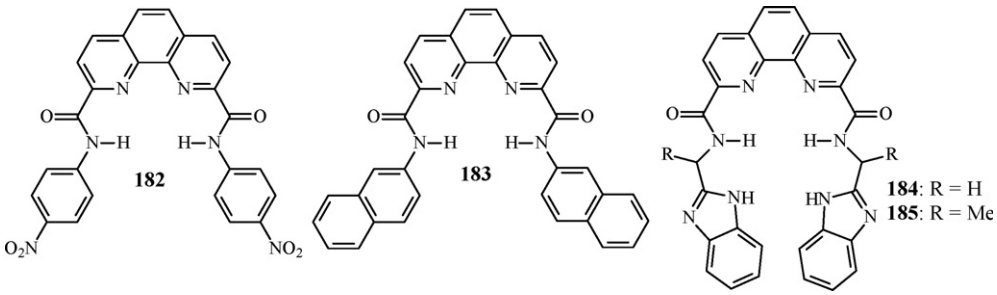

Scheme 72.

Starting from 1,10-phenanthroline-2,9-dicarboxylic acid (**27**, Scheme 11), optical molecular sensors for anions **182**–**185** (Scheme 72) were easily prepared by Lin and co-workers all featuring amide moieties as binding sites [242–244].

In particular, **183** exhibits a marked enhancement in the fluorescent emission intensity at 377 and 397 nm (λ_{ex} = 368 nm) in DMSO upon addition of fluoride or bromide ions [235]. Free **183** is weakly fluorescent in DMSO due to a PET quenching process determined by intramolecular H-bonds between the amidic –NH hydrogen atoms and the nitrogen atoms from the phen unit. In the host–guest complexes with F^- or Br^-, the –NH groups form)N–H···X$^-$···H–N(H-bonds with the anions, thus weakening the PET quenching process and favouring an enhancement in the fluorescence emission of the phen moiety. Furthermore, the complexation process would increase the rigidity of the molecular sensor, thus inhibiting vibrational and rotational relaxation modes (non-radiative decay) of the excited state of the host molecule. No fluorescence response is observed on adding to **183** the anions Cl^-, I^- and $H_2PO_4^-$. Interestingly, upon addition of acetate a new emission band is observed at 450 nm, which was assigned to the formation of an excimer between the two naphthalene units brought together by the coordination of the acetate ion to the amide protons [243].

Surprisingly, the benzimidazole-based sensors **184** and **185** exhibited a turn-OFF fluorescent response at about 460 nm (λ_{ex} = 368 nm) in DMSO in the presence of F^- and $CH_3CO_2^-$, and an enhancement of the fluorescent emission intensity in the presence of Cl^-, Br^- and I^- [244]. The different fluorescent response of both **184** and **185** might be the consequence of a fine interplay between the PET mechanism from the receptor unit to the phen lumophore, and the rigidity change of the host molecules upon host–guest interaction with anions. Interestingly, deprotonation of the –NH groups of the benzimidazole moieties takes place upon addition of increasing amounts of F^- to **184** and **185** [244].

Recently, Yoon and co-workers have reported the new fluorescent and colorimetric chemosensor for anions **186** (Scheme 73) featuring two imidazolium groups as receptors as well as two anthracene groups as signalling moieties implemented at the 2,9-positions of a phen scaffold [245].

This chemosensor displays, in MeCN, a strong and highly selective fluorescent quenching effect of the typical emission anthracene bands only with $H_2PO_4^-$ over other anions considered such as F^-, Cl^-, Br^-, I^-, $CH_3CO_2^-$ and HSO_4^-. Furthermore, a colour change is also observed upon addition of $H_2PO_4^-$ to a solution of **186** (see Fig. 21) due to the formation of an excimer peak at 485 nm. Therefore, hydrogen-bonding between $H_2PO_4^-$ and the imidazolium moieties of **186** (confirmed by ^{1}H NMR measurements) brings the anthracene groups close enough to induce excimer formation, the phen moiety acting as template for introducing binding selectivity [245].

Compound **187** (Scheme 74) is a clear example of the use of phen both as signalling element and as key molecular building block for

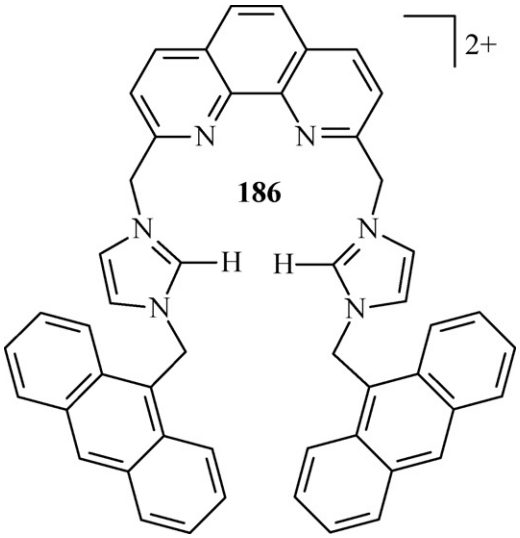

Scheme 73.

the construction of a selective receptor and sensor for a specific anion, in particular citrate [246].

The actual molecular sensor is the complex [Cu(**187**)]$^{4+}$, which is water soluble and forms a suitable cavity for citrate inclusion *via* strong coordination to the metal cation and the guanidinium groups. In the free sensor the copper(II) metal ion quenches a photoexcited state of the phen moiety. The emission of [Cu(**187**)]$^{4+}$ is restored by the addition of increasing amounts of citrate which,

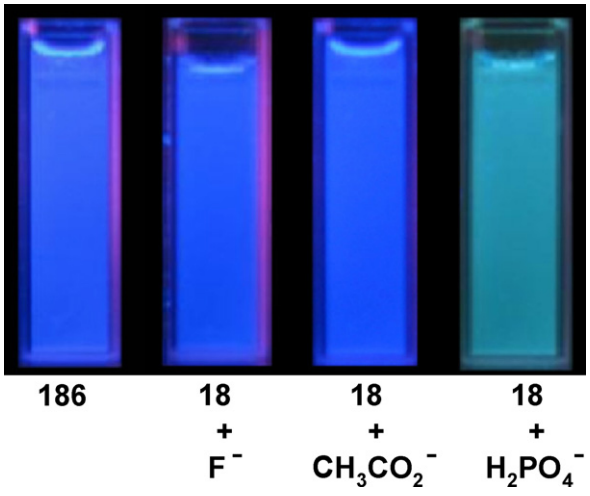

Fig. 21. Colour changes observed on adding F^-, $CH_3CO_2^-$, and $H_2PO_4^-$ to a solution of **186** in MeCN. This photograph is taken from [245] and reprinted with permission; copyright 2007, by Elsevier.

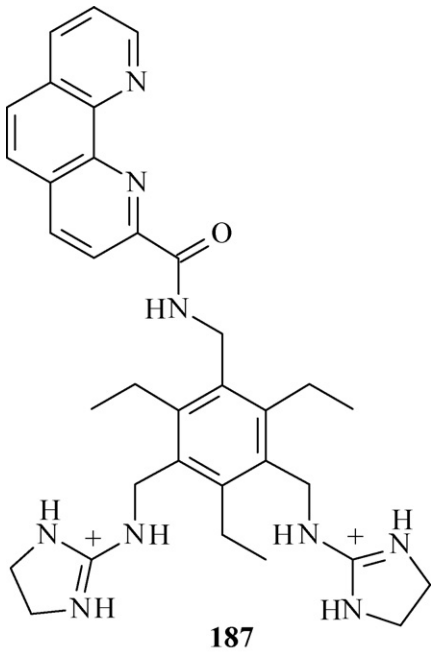

187

Scheme 74.

upon binding to the metal centre, changes the extent of electron charge-transfer from the metal cation to the phen fluorophore, thus modulating the metal quenching effect [246].

Another interesting example of anion recognition and sensing by a phen-based artificial receptor which is designed following the concept of multi-point and cooperative binding interactions, with concomitant fluorescence modulation of an integrated phen metal chelate fragment, is due to Shinkai and co-workers [247,248]. Compound **188** (Scheme 75) can bind to zinc(II) at the phen moiety forming a 1:1 complex at pH 8.0 in H_2O/MeOH (1:2, v/v).

This complex is able to bind, *via* covalent interactions, and sense uronic carboxylates utilizing the cooperative action of the boronic acid and metal chelate moieties to afford **189**, as illustrated in Fig. 22.

As a result of complex formation between $[Zn(\mathbf{188})]^{2+}$ and an uronic carboxylate, in particular D-glucuronate and D-galactouronate, the PET process from the methylamine subunit to the photoexcited phen fluorophore is inhibited, and, therefore, an enhancement in the fluorescence emission intensity is induced at 375 nm (λ_{ex} = 294 nm). Moderate enhancement of the fluorescent emission of $[Zn(\mathbf{188})]^{2+}$ is also observed in the presence of sialate, D-fructose and D-galactose [247,248]. Interestingly, the phen diboronic acid **190** (Scheme 76) can detect a range of saccharides at neutral pH in aqueous solutions [249].

Addition of saccharides (D-glucose, D-galactose) to **190** up to a 2:1 molar ratio causes an enhancement of the fluorescent emission

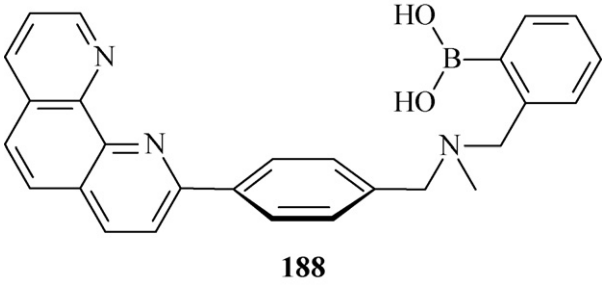

188

Scheme 75.

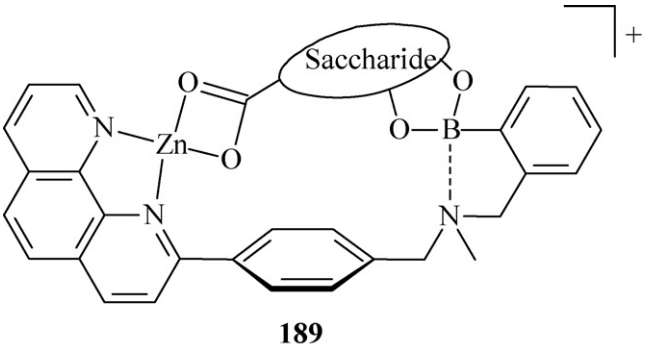

189

Fig. 22. Complexation mode for the binding of $[Zn(\mathbf{188})]^{2+}$ and an uronic carboxylate.

at 365 nm as a consequence of the formation of cyclic boronate esters in which the acid–base interaction between the boronate group and the tertiary amine is strengthened, thus relieving the PET from the methylamine subunit to the excited phen moiety.

Protonated polyamine receptors are known for their ability to bind anionic species in aqueous solutions thanks charge–charge interactions and hydrogen-bonding between the anion and the ammonium functions [250]. From this point of view, the insertion of phen within a polyamine backbone may represent an important added value to this class of receptors. In fact, the heteroaromatic moiety can be used not only to bind substrates containing aromatic portions *via* π-stacking and/or hydrophobic interactions, but also to signal their presence in solution, thanks to quantifiable changes of its emission properties.

With this in mind, Bencini and co-workers have recently paid their attention to phen-based polyamine macrocycles (Scheme 77) with the aim to design new receptors able to bind and signal inorganic anionic species [251,252] and nucleotides [252–254]. Receptors **191**–**193** (Scheme 77) were synthesized by using the same procedure developed for **78**–**80** (see Scheme 31). These macrocycles contain aliphatic chains with different numbers of amine groups separated by propylenic linkers, in order to increase the overall basicity of these receptors with respect to polyazamacrocycles like **78**–**80**, where the amine groups are separated by ethylenic linkages. In fact, propylenic chains exert a larger +I inductive effect on amine groups and confer a higher flexibility to the structure, which allows a better minimization of the electrostatic repulsion between positive charges in the polyprotonated forms of the receptors [255]. As a result, **191**–**193** give highly charged polyammonium cations in aqueous solution at neutral pH. For instance, **193** is present in solution at pH 7 in its penta- and hexa-protonated forms $(H_5\mathbf{193})^{5+}$ and $(H_6\mathbf{193})^{6+}$. ^{1}H NMR mea-

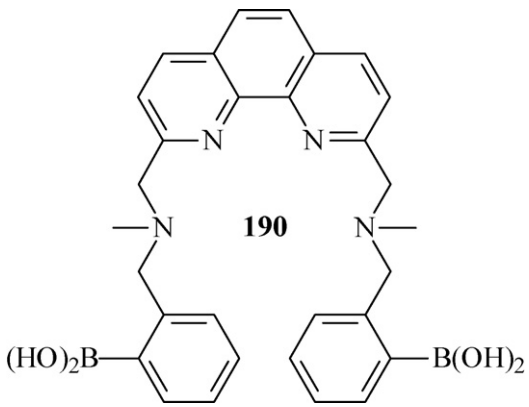

190

Scheme 76.

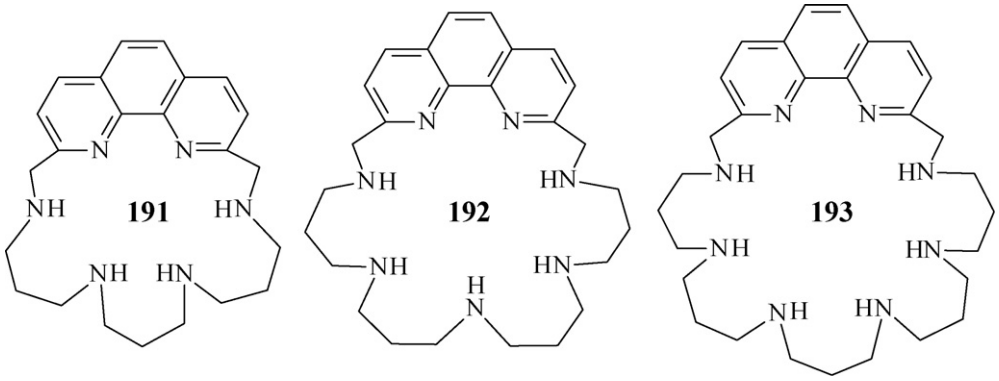

Scheme 77.

surements showed that in all polyammonium cations the acidic protons are bound to the aliphatic amine groups, while phen does not protonate, in agreement with the lower basicity of its nitrogen atoms.

The formation of polyprotonated forms enabled the receptors to form remarkably stable 1:1 complexes with inorganic phosphate anions, such as diphosphate and triphosphate [252] and nucleotides [252–254]. Potentiometric titrations coupled to ^{1}H and ^{31}P NMR measurements showed that the binding ability of **191** towards these anions increases in the order diphosphate < triphosphate < ADP < ATP [252]. While preferential binding of triphosphate over diphosphate and of ATP over ADP was simply attributed to the higher negative charge gathered at a given pH value on triphosphate and ATP with respect to diphosphate and ADP, respectively (for instance at pH 7, ATP and ADP are mainly present in solution in their tetraanionic and trianionic form, ATP^{4-} and ADP^{3-}, respectively), the higher stability of the adducts with ATP and ADP with respect their inorganic counterparts suggested that hydrophobic and stacking interactions take place between the adenine moiety of the nucleotides and phen [256,257]. To better ascertain the role played by the nucleobase in the stabilization of the adducts, Bencini and co-workers analyzed the binding properties of **192** and **193** toward TTP, CTP, GTP and ATP, featured by equal triphosphate chains and sugar moieties, but containing different nucleobases. Both receptors form remarkably stable 1:1 adducts in aqueous solutions with all nucleotides. As generally found with polyammonium receptors, the complexes are stabilized by charge-charge interactions and hydrogen-bonding between the terminal (P_γ) and the central (P_β) phosphate groups of nucleotides and the protonated polyamine chains of the receptors. ^{1}H NMR measurements also showed that phen is indeed strongly involved in the overall anion-receptor interaction. The most interesting finding, however, was the marked selectivity for ATP over the other nucleotides displayed by **193**. As shown in Fig. 23, in a competitive system containing 193, ATP, CTP, TTP and GTP in equimolecular ratio, the formation of ATP adducts with 193 prevails over a wide pH range, *i.e.*, ATP is selectively bound with respect to the other triphosphate nucleotides. Selectivity is completely lost in the case of receptor **192**, to indicate that relatively small changes in the receptor structure can strongly affect its binding ability.

Selectivity is clearly due to the nucleobase and actually ^{1}H NMR measurements pointed out that adenine gives stronger interactions with the receptor than the other nucleobases. On the other hand, ^{31}P spectra showed that, among the four nucleotides, ATP also gives the most robust charge–charge and hydrogen-bonding contacts [253]. Therefore, the strong interaction of the nucleobase also induces an increased involvement of the triphosphate chain in the formation of the adducts. Molecular dynamic calculations pointed out that in all adducts between the hexaprotonated receptor $(H_6\mathbf{193})^{6+}$ and nucleotides the triphosphate chain is enclosed within the cavity of the protonated receptors. Conversely, the nucleobases can interact with the receptor *via* both π-stacking between the heteroaromatic units and hydrogen-bonding between their nitrogen or C=O oxygen heteroatoms. Furthermore, the calculated structures showed that ATP gives the strongest π-stacking pairing between the nucleobase and phen [254]. The adduct between TTP and $(H_6193)^{6+}$ was isolated and its crystal structure solved. Interestingly, the crystal structure showed the assembly in the solid state of the dimeric species $[(H_6\mathbf{193})_2TTP_2]^{4+}$ not observed in aqueous solution. In this dimer, the triphosphate chain of each TTP anion is encapsulated within the macrocyclic cavity of one protonated receptor, to give a network of charge-assisted hydrogen-bonding interactions with the ammonium groups, while its pyrimidine base is sandwiched between the phen unit of the second receptor and the thymine group of the other TTP anion. This leads to the formation of a face-to-face π-stacked array of two thymidine and two phen units (see Fig. 24). Nevertheless, the interaction modes between the nucleotide and the hexaprotonated receptor resemble those suggested by NMR measurements and molecular modeling. In fact, the triphosphate chains of the TTP anions are enclosed within the receptor cavities, affording a network of hydrogen-bonding contact with the ammonium groups. At the same time, each nucleobase interacts *via* π-stacking with one phen unit and, at the same time, displays hydrogen-bonding between its carbonyl oxygen with one protonated amine group.

Receptor **193** was able not only to selectively bind ATP, but also to signal its presence in solution, thanks to quenching of the fluores-

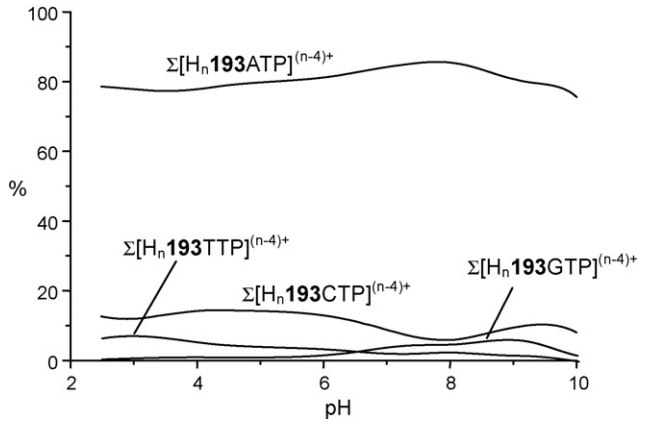

Fig. 23. Overall percentages of **193** complexed species with ATP, CTP, TTP or GTP as a function of pH in a competitive system containing **193**, ATP, CTP, TTP and GTP in equimolecular ratio [253].

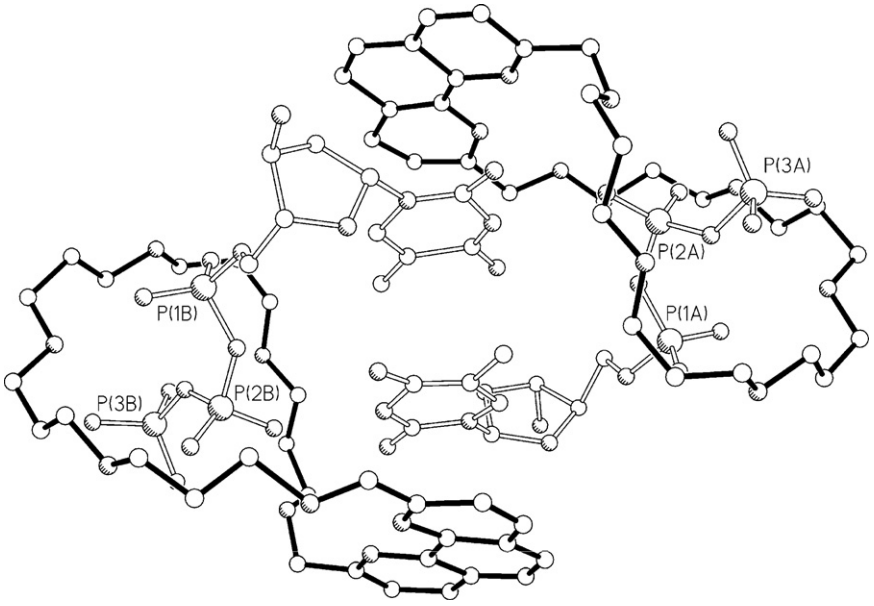

Fig. 24. ORTEP view of the complex cation $[(H_6\mathbf{193})_2TTP_2]^{4+}$ showing the polyphosphate chains enclosed within the receptor cavities, and the π-stacking assembly of nucleobases and phen units [254]. H-atoms are omitted for clarity.

cence emission of the phen upon ATP binding. As shown in Fig. 25, addition of increasing amounts of ATP to a solution of **193** in the pH range 5–7 lead to linear decrease of the fluorescence emission of the receptor, which resulted completely quenched in the presence of 1 equiv. of ATP. Conversely, the other triphosphate nucleotides produced only slight decrease of the fluorescence emission and ratiometric sensing of ATP is almost not affected by the presence in solution of 1 equiv. of CTP, TTP or GTP.

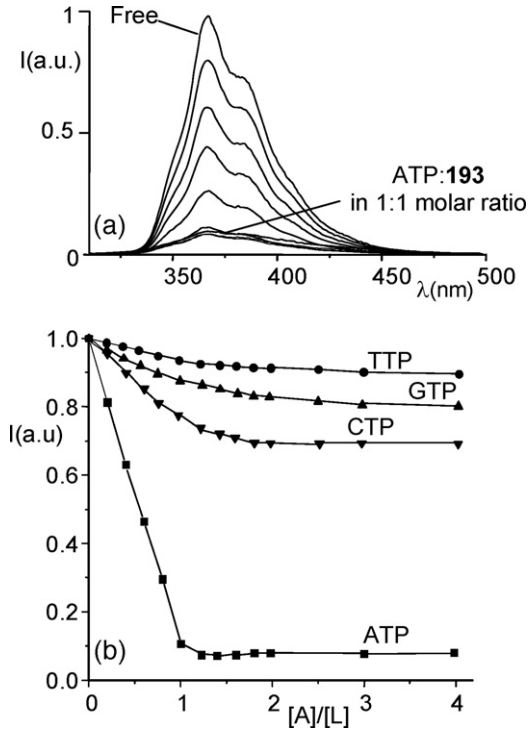

Fig. 25. Fluorescence emission spectra of **193** in the presence of increasing amounts of ATP at pH 6 (a) and fluorescence intensity at 365 nm in the presence of increasing amounts of ATP, TTP, GTP or CTP (b) [253].

The quenching effect was attributed to the strong hydrogen-bonding and charge-interactions between the anionic phosphate moiety and the polyammonium chain of the protonated receptor, which may lead to an intra-complex proton transfer from one ammonium group to a phosphate, thus making an amine lone pair available for a photoinduced electron transfer process to the excited phen.

Metal complex with phen-containing macrocycles can also be used for anion binding. As discussed in Section 2.1.1, the presence of phen leads to a stiffening of the macrocyclic structure and prevents the coordination of all set of donor atoms. As a consequence, the metal often displays a coordination sphere not saturated by the ligand donors and therefore it can be used as anchoring point for anions or ionizable analytes. In this context, the Zn^{2+} complex with ligand **78** (see Section 2.1.1) was used as receptor for amino acids and dipeptides [258]. Potentiometric titrations and ^1H NMR measurements at different pH values showed that these substrates bind to the complex in both their neutral and monoanionic forms. As often observed in metal complexes with amino acids, the neutral forms of the substrates bind to Zn^{2+} through the carboxylate group, while the anionic forms behave as bidentate ligands. More interestingly, the $[Zn(\mathbf{78})]^{2+}$ complex was able to selectively coordinate Trp over the other substrates tested (Gly, Ala, Leu, Phe, Ph-Gly). Furthermore, binding of Trp to $[Zn(\mathbf{78})]^{2+}$ was accompanied by marked downfield shifts of the ^1H NMR signals of its indole moiety. On this basis, it was suggested that stabilizing π-stacking interactions between indole and phen could reasonably account for the observed selective coordination of Trp.

By using the same experimental approach, the Zn^{2+} complex with **191** was tested as receptor for ATP [259]. In fact, it was found that in the complex cation $[Zn(\mathbf{191})]^{2+}$ some amine groups are not bound to the metal and can be easily protonated in aqueous solution affording protonated complexes of the type $[Zn(H_n\mathbf{191})]^{(n+2)+}$ ($n = 1–3$). These complexes present both a metal ion and ammonium groups potentially available to interact with ATP. Furthermore, the crystal structure $[Zn(H\mathbf{191})Br]^{2+}$ showed that the protonated complex assumes a "open" conformation, suitable for ATP coordination through the simultaneous participation of the metal cation and the ammonium groups to the binding of the triphosphate chain of the nucleotide (see Fig. 26a). Actually, poten-

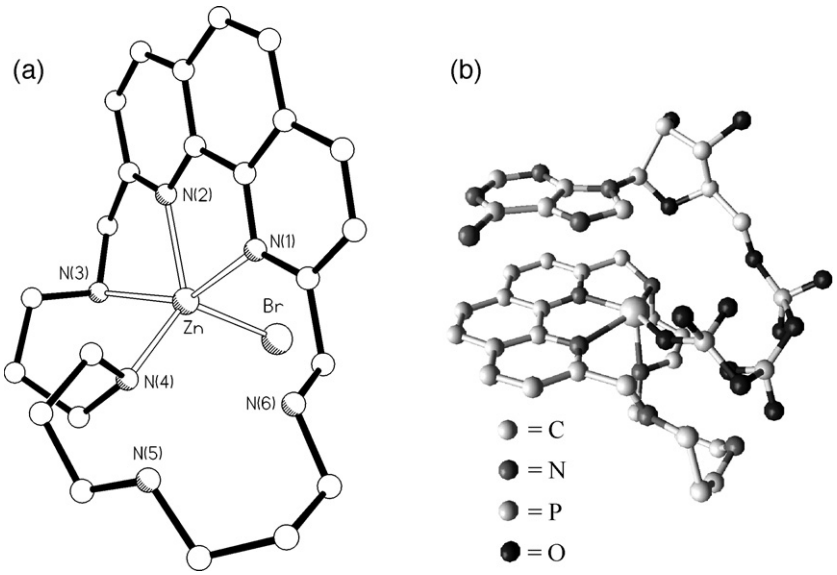

Fig. 26. Crystal structure of the complex cation $[Zn(H\mathbf{191})Br]^{2+}$ (a) [259] and proposed interaction mode between $[Zn(H\mathbf{191})]^{3+}$ and ATP^{4-} (b). H-Atoms are omitted for clarity.

tiometric titrations pointed out that the protonated Zn^{2+} complexes form remarkably stable $[Zn(H_n\mathbf{191})ATP]^{(n-2)+}$ ternary complexes. In particular, the $[Zn(H_n\mathbf{191})]^{(n+2)+}$ protonated complexes possess a higher binding ability for ATP than the protonated forms of **191** with the same charge, indicating that Zn^{2+} exerts a beneficial effect on the stability of the complexes. ^{31}P NMR measurements suggested that in the ternary complexes ATP binds to Zn^{2+} using the terminal phosphate group P_γ, while the central phosphate P_β is involved in charge-charge interactions and hydrogen-bonding with the ammonium function of the metal-based receptor. At the same time, ^1H NMR measurements showed that π-stacking interactions between adenine and phen are at work to further stabilize the complexes.

Fig. 26b shows a proposed model for the interaction of $[Zn(H\mathbf{191})]^{3+}$ with ATP, based on the crystal structure of the $[Zn(H\mathbf{191})Br]^{2+}$ complex and on the evidence derived from the NMR study of the system.

With the aim to develop new receptors able to recognize aromatic carboxylate anions, Delgado and Felix have recently reported the synthesis of a series of macrocyclic polyamines containing two phen moieties linked by two aliphatic chains (Scheme 78) [260,261]. These ligands were synthesized by condensation of 2,9-diformyl-1,10-phenanthroline (**28**) (Scheme 11) with the appropriated diamine derivative, followed by reduction of the resulting diimine.

These receptors protonate in aqueous solutions affording polyammonium cations able to interact with anionic species *via* charge-charge and hydrogen-bonding interactions. A preliminary study carried out on the binding ability of receptor **194** toward aromatic and aliphatic carboxylate anions (**198**–**209** in Scheme 79) showed that the receptor forms stable 1:1 adducts with these anionic substrates [260]. The adducts with aromatic substrates were generally more stable than those with aliphatic carboxylate. Among aromatic carboxylates, the authors observed higher binding ability of **194** toward **202**, the most charged substrate and **204**, which presents the most extended aromatic system. These data suggested that the stability of the adducts is not only determined by the formation of charge-charge and hydrogen-bonding contacts, but also by π-stacking interactions between the phen units and the aromatic rings of the host species [260]. This suggestion was corroborated by the crystal structure of the cation $[(H_5\mathbf{194})]^{5+}$ as chloride and bromide salts. In fact, these structures showed that the protonated receptor assumes a "horseshoe" conformation delimiting a cavity where condensed aromatic systems can be conveniently inserted. NOESY NMR experiments gave fur-

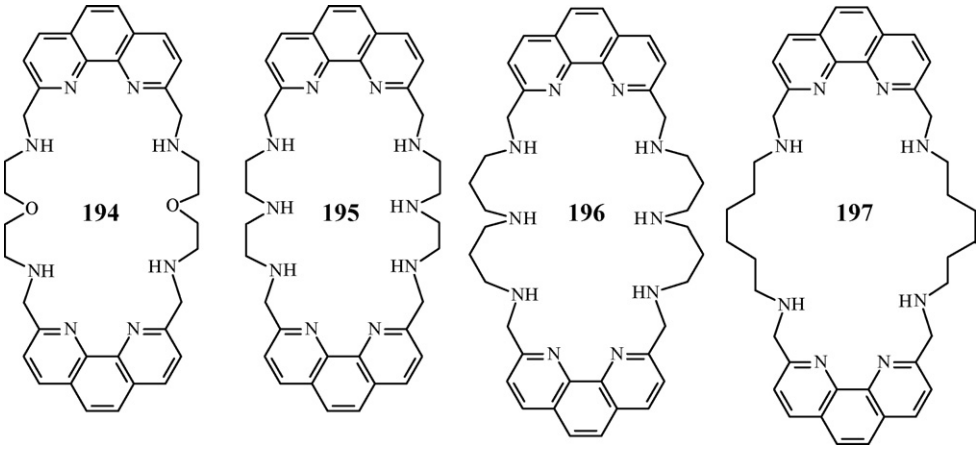

Scheme 78.

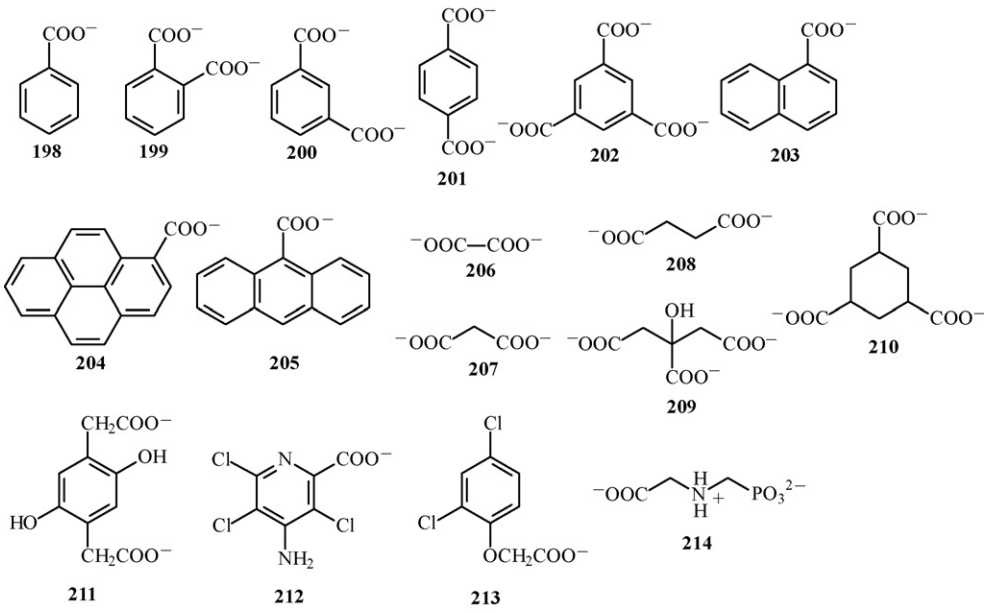

Scheme 79.

ther evidence for the presence of π-stacking interactions between phen and the aromatic systems of **202** and **204**.

Molecular dynamic simulations, carried out on the pentaprotonated form of the receptor **194** in solution using an explicit model for water molecules, confirmed that **202** and **204**, as well as **200** and **203**, are encapsulated within the receptor cavity, interacting *via* π-stacking with phen and *via* charge-assisted hydrogen-bonding with the protonated amine groups of **194**, as sketched in Fig. 27.

By using the same approach, the authors analyzed the interaction of receptors **195**–**197** toward aromatic carboxylate anions (**198**–**205** in Scheme 79) and some anionic herbicides (**210**–**214**) [261]. **195**–**197** displayed binding properties similar to those previously found in the case of **194**. The three receptors displayed higher binding ability toward **202**, the most charged carboxylate anion, and **204** and **205**, which present the most extended aromatic structure.

More interestingly, receptor **195** formed more stable adducts than **196** and **197** with most of the anions under investigation and also formed stable adducts with herbicides **210**–**213**. This result appeared rather surprising considering that **195** is less protonated, and therefore less charged, than **196** at a given pH value, due to the lower basicity of its amine groups. At the same time, **195** displays selective binding of **202** over **204** and **205** in the pH range 4.5–8, while **204** is preferentially bound below pH 4.5, as expected considering that protonation of the carboxylate groups at acidic pH values can reduce charge–charge and hydrogen-bonding interactions, but has probably minor effect on π-stacking interactions. The observed higher binding ability displayed by **195** with respect to **196** and **197** was explained on the light of molecular dynamic calculations, which pointed out that structure of the 30-membered macrocycle **195** is more suitable for accommodating the anionic substrates within the receptor cleft upon the formation of the host–guest adducts.

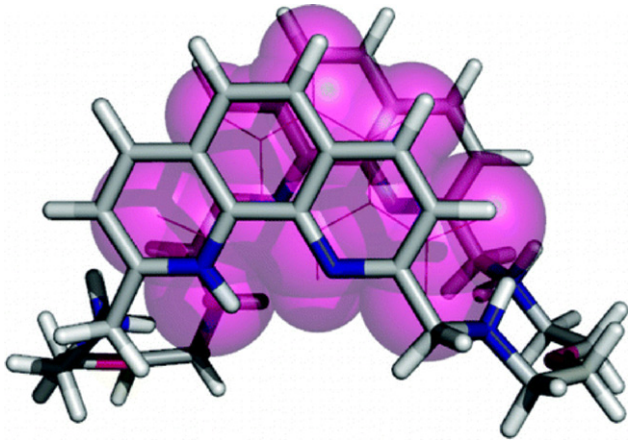

Fig. 27. Sketch of the adduct between the pentapronated receptor **194** and the anionic guest **200**. This figure is taken from [260] and reprinted with permission; copyright 2007, by The American Chemical Society.

Lin and co-workers analyzed the binding ability of a series of phen-based open-chain polyamine receptors (**215**–**218**, Scheme 80) toward ATP and ADP in the absence and in the presence of metal cations with different hard-soft characteristics, *i.e.*, Zn^{2+}, Mg^{2+}, Ca^{2+} and, in the case of **217**, also in the presence of Ln^{3+} [262,263].

These ligands were synthesized starting from 2,9-diformyl-1,10-phenanthroline (**28**) (Scheme 11) following a procedure similar to that described for **194**–**197**. Receptors **215**–**218** formed 1:1 complexes with ATP and ADP in water with interaction modes similar to that previously discussed for **191**–**193**. The ternary complexes obtained in the presence of metal cations displayed different structural features, depending on the metal cation used. In fact, Zn^{2+} was coordinated by the polyamine ligand, while Ca^{2+} and Mg^{2+} and La^{3+} (in the case of **217**) interact preferentially with the phosphate chain of ATP. The authors then investigated the ability of receptors to promote ATP hydrolysis in aqueous solution at 70 °C at different pH values in the absence and in the presence of the above cited metal cations [262,263]. As generally found in ATP hydrolysis promoted by polyamines [264], the hydrolytic reaction in the presence of the ligands with or without metal cations basically occurred *via* nucleophilic attack of an amine group to the terminal phosphate of ATP to give ADP and a *N*-phosphoramidate intermediate, which is then fast hydrolyzed to produce inorganic phosphate. It was found that the overall rate constants for ATP cleavage are enhanced by the simultaneous presence in solution of ligands and metal cations with respect to the rate constants measured in the presence of the

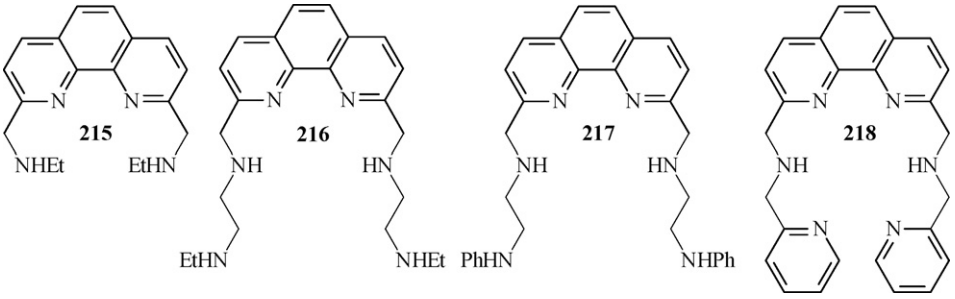

Scheme 80.

ligands alone. This effect resulted more consistent with the hard Ca^{2+}, Mg^{2+} and La^{3+} cations than with Zn^{2+}. This experimental finding was reasonably ascribed to the stronger interaction of Ca^{2+}, Mg^{2+} and La^{3+} with the phosphate chain of ATP, which favours the nucleophilic attack of amine groups to the terminal phosphate of ATP.

4.2. Neutral molecules

The design and development of synthetic selective receptors for neutral molecules is an area of active research and a much more difficult task as compared to the development of receptors for metal cations and anionic species. In fact, the synthetic chemist needs to properly assembly the binding groups in the final host so to complement those of the intended guest in order to maximize the various forces involved in the binding process, which generally are weak forces such as hydrophobic interactions, π–π stacking and hydrogen-bonding. Frequently, subtle design changes can dramatically affect substrate binding affinity and selectivity. The potential of phen-based receptors in the recognition of neutral molecules *via* non-covalent interactions has also been considered, and some very interesting examples of receptors for neutral molecules containing the phen unit have been proposed in the last 15 years.

Anslyn and co-workers described in 1995 the coordination properties of receptors **219**–**221** (Scheme 81) towards cyclohexane diols (cyclitols) [265].

In fact, the phen moiety and the adjacent amide group can be used for cooperative binding of an alcoholic function. An alcoholic group can behave simultaneously as hydrogen-bonding donor to the nitrogen atom of phen in 10-position and as hydrogen-bonding acceptor from the amide group adjacent to phen. According to this two-point hydrogen bond approach, **220** and **221** were designed to be complementary to *cis*-1,3- and *trans*-1,4-cyclohexanediols, respectively. **220** and **221** behave as ditopic receptors for these diols, each hydroxyl binding site (the phen moiety and the adjacent amide group) interacting simultaneously with one of the two alcoholic functions of the diol [265]. Analogously, the development of synthetic binding agents for carbohydrates of which cyclitols can be considered simplified models, requires the presence of several appropriately positioned hydrogen-bonding points in the final host, as well as their cooperation in the recognition process. This problem has been tackled by Mazik and co-workers who developed, following molecular modelling studies, the hydrogen-bonding phen- and aminopyridine-based carbohydrate receptors **222** and **223** (Scheme 82) [266,267].

The recognition properties of **222** and **223** were analyzed on the base of ^{1}H NMR spectroscopic titrations in competitive and non-

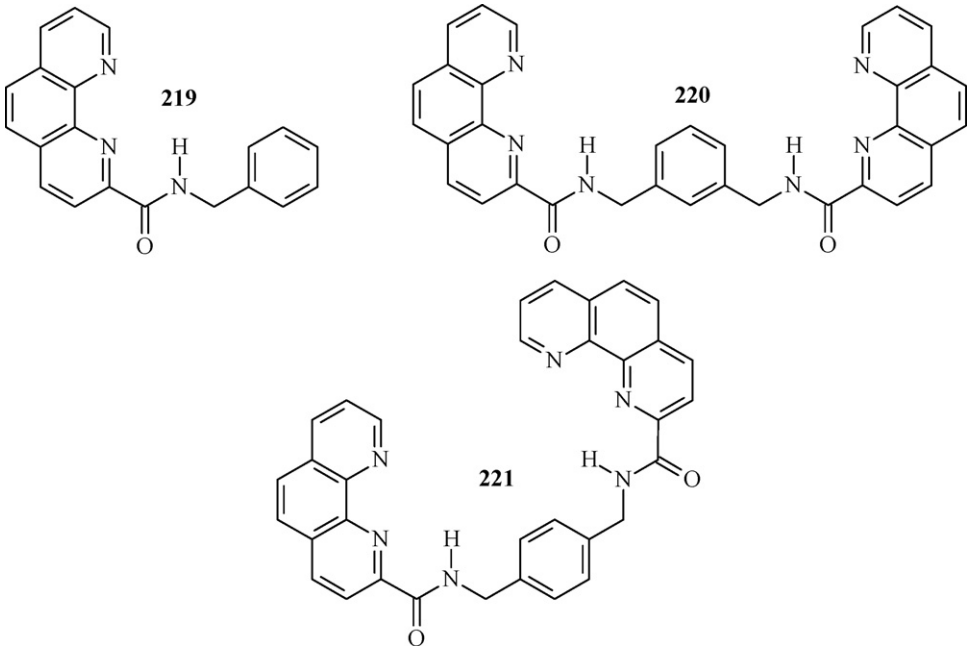

Scheme 81.

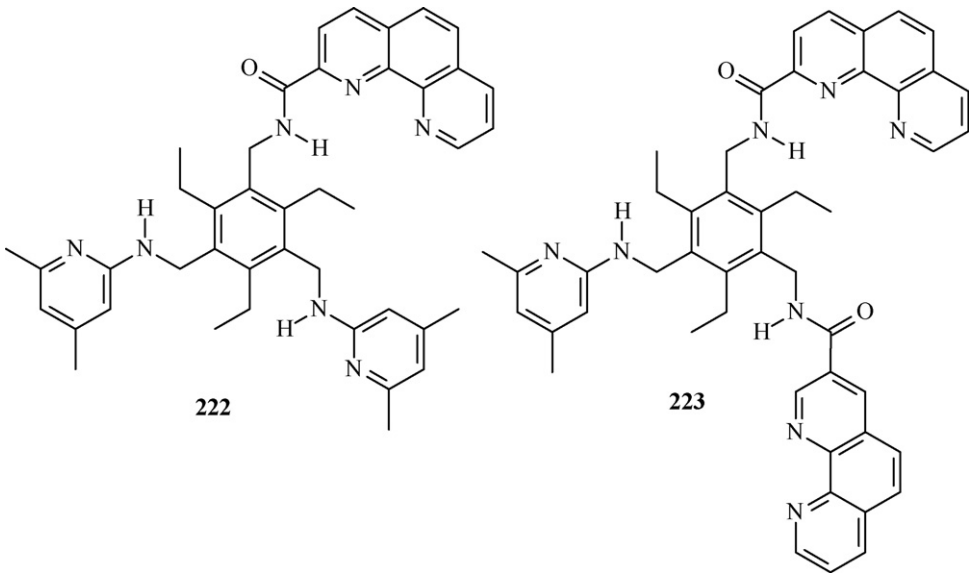

Scheme 82.

competitive media, as well as in two-phase systems (phase transfer of carbohydrates from aqueous into organic solvents, and dissolution of solid carbohydrates directly into apolar solvents). Both receptors were established to perform effective and selective recognition of neutral carbohydrates through multiple non-covalent interactions. In particular, both **222** and **223** displayed interesting α- vs. β-anomer binding preference in the recognition of glycosides with binding affinity higher for **223** than for **222** and decreasing in the sequence α-glucoside > β-glucoside ∼ α-galactoside > β-galactoside in DMSO/$CDCl_3$ mixtures. This notable α- vs. β-anomer selectivity in homogeneous solutions in the recognition of glucosides and galactosides was confirmed, respectively, in extraction experiments from the solid state into a $CDCl_3$ solution, and liquid–liquid extraction experiments from water to a chloroform solution [266,267].

The association of phen units and amido groups in the construction of receptors and sensors for neutral molecules has also been exploited by Gozin and co-workers, who designed compounds **224** and **225** (Scheme 83) for the detection and sensing of ureas and uronium salts [268]. Receptor **224** is composed of two phen fluorophores which also function as hydrogen bond acceptors. Two phen units are linked by an aromatic bridge containing two amide groups as potential hydrogen bond donor; the polyoxa chain is for improving the solubility of the receptor in solvents that are better suited to ureas and uronium salts (MeCN). Compound **225** represents a truncated version of **224** with a single phen arm. Compound **224** can form very stable 1:1 complexes with several ureas (urea, thiourea, imidazolidin-2-one, tetrahydropyrimidin-2(*1H*)-one); this process is followed by substantial changes (quenching) in the fluorescence spectrum of the receptor on exciting at 396 nm. In particular, thiourea has a higher binding constant for **224** than urea by a factor of 2, due to its more acid protons that can give stronger hydrogen bonds with the nitrogen atoms of the phen moieties. On the other hand, the higher basicity of urea's oxygen relative to thiourea's sulfur allows the urea to form stronger hydrogen bonds with protons of the adjacent amide functional groups. Overall, these hydrogen-bonding interactions with the ureas are considered responsible of the stabilization of the poorly emissive $n\pi^*$ state with respect to the strongly emissive $\pi\pi^*$ state of the phen moieties and consequently of the observed decrease in the fluorescence emission intensity of **224** upon the host–guest interaction.

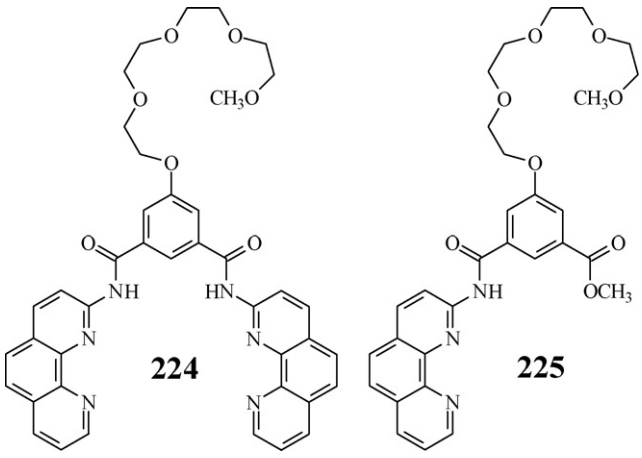

Scheme 83.

Interestingly, no changes are observed in the fluorescence spectrum of **225** upon addition of neutral ureas, thus confirming the fundamental role of the two phen moieties and their disposition in the binding of the various ureas by **224** [268]. Exposure of **224** and **225** to uronium cations produces an optical response completely different than that observed upon exposure to neutral ureas. Firstly, in contrast to the addition of neutral ureas, the addition of uronium salts to **224** and **225** results in a substantial change in their UV–vis absorption spectra in MeCN, which show a gradual shift in λ_{max} from 286 to 297 nm. Furthermore, a fluorescence quenching is observed at 426 nm on exciting at 396 nm, while an enhancement of the fluorescence emission intensity is observed at 478 nm on exciting at 297 nm. Similar behaviours are observed on adding trifluoroacetic acid to **224** and **225** indicating that uronium cations act as an acid and prefer to protonate rather than to bind the phen moieties of the two receptors. The two different interaction mechanisms make **224** and **225** capable of distinguishing between neutral ureas and their salts by producing a different optical response for each type of compounds [268].

Particularly interesting is the macrocyclic fluorescent receptor **226** (Scheme 84) designed and synthesized for the recognition of urea [269].

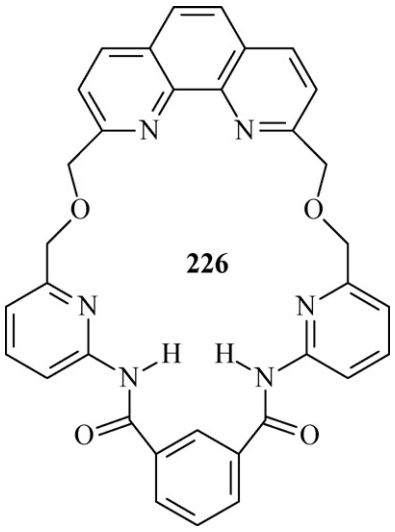

Scheme 84.

As in **224**, the fluorescent chromophore phen is used to form hydrogen-bonding interactions with two hydrogens of urea, while the pyridine nitrogen atoms can act as hydrogen bond acceptors for the remaining two hydrogens of urea. Finally, the two amido groups act as hydrogen bond donors to carbonyl oxygen of urea. The perfect complementarity of **226** and urea in the corresponding 1:1 complex **227** (see Fig. 28) is responsible for the solubilization of urea in chloroform in the presence of **226**, furthermore the complexation process is accompanied by a significant quenching of the fluorescence emission of the receptor when excited at 272 nm [269].

Interestingly, though **226** displays a stronger binding ability for urea than for thiourea, the quenching effect by thiourea on the fluorescence emission of **226** is greater than that determined by urea. This behaviour can be explained, as in the case of **224**, by a stronger interaction of thiourea with the fluorophore moiety, due to the more acidic character of thiourea NHs than urea ones, despite thiourea makes weaker hydrogen bond with the sulfur at the amido groups as compared to the oxygen of urea [268,269].

Examples of receptors and sensors for neutral molecules based on the photophysical properties of metal-phen derivative com-

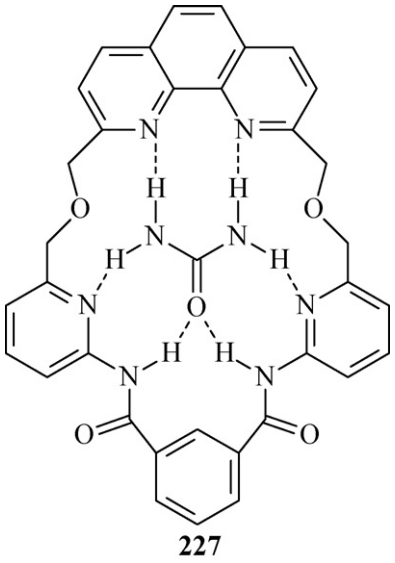

Fig. 28. Proposed structure of the 1:1 complex between **226** and urea [269].

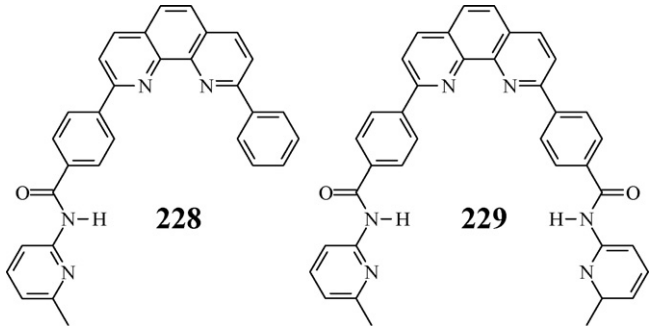

Scheme 85.

plexes are much less numerous and somehow rare. In 1995, Weiss and co-workers reported the synthesis of compounds **228** and **229** (Scheme 85) bearing one or two acylaminopyridine binding sites at the 2- and 2,9-positions, respectively, of a phen nucleus [270].

Compound **228** forms a quite stable 1:1 complex with glutaric acid in chloroform, with an association constant ($2.7 \times 10^3\ M^{-1}$) higher than that expected for one carboxylic acid–aminopyridine interaction, thus suggesting a bidentate interaction mode also involving the weaker phen binding site to give complex **230** (see Fig. 29). Receptor **229** binds to glutaric acid in chloroform with an association constant of $3.6 \times 10^4\ M^{-1}$ to form a 1:1 complex **231** (see Fig. 29), in which, according to ^{1}H NMR measurements, the dicarboxylic acid is hydrogen-bonded to both acylaminopyridines groups, while the phen moiety is not involved in the binding process [270]. Both **228** and **229** can assemble on a copper(I) template, forming the complex cations $[Cu(\mathbf{228})_2]^+$ and $[Cu(\mathbf{229})_2]^+$ in which the metal centre is coordinated to the phen moieties in a *pseudo*-tetrahedral environments and leaves the acylamidopyridine arms free to interact with dicarboxylic acids [270].

Both $[Cu(\mathbf{228})_2]^+$ and $[Cu(\mathbf{229})_2]^+$ bind to a variety of dicarboxylic acids in chloroform, with a slight preference for C_5-dicarboxylic, glutaric acid and *N*-Cbz-glutamic acid (Cbz = benzyloxycarbonyl), over shorter and longer analogues. Spectroscopic data indicate the formation of 1:1 complexes for $[Cu(\mathbf{228})_2]^+$ and 2:1 complexes for $[Cu(\mathbf{229})_2]^+$ with the dicarboxylic acid hydrogen-bonding simultaneously to juxtaposed acylaminopyridine binding sites from each receptor unit. For $[Cu(\mathbf{229})_2]^+$ the complexation process results in a large shift in the visible absorption bands and a consequent colour change from orange to red [270].

Finally, quite recently, Sleiman and co-workers have reported the synthesis of ligand **232** (Scheme 86) featuring a phen unit functionalized at the 5-position with a biotin ending pendant arm [271].

The complexes $[Ru(bpy)_2\mathbf{232}]^{2+}$ and $[Ru(phen)_2\mathbf{232}]^{2+}$ bind to the protein avidin through their biotin moieties with high affinity

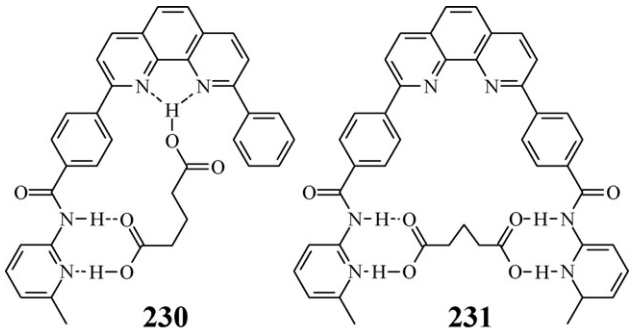

Fig. 29. Proposed structure of the 1:1 complexes between **228** and **229** with glutaric acid [270].

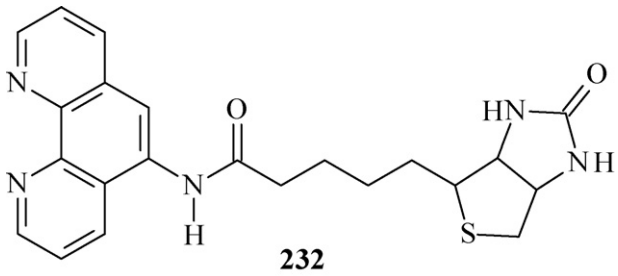

232

Scheme 86.

in a 4:1 molar ratio. The binding of avidin to the two complexes results in a marked enhancement in luminescence intensity with respect to the unbound biotinylated ruthenium(II) complexes.

In the last ten years, Weiss and co-workers have developed very interesting phen-strapped zinc(II)-porphyrins such as **233** (Scheme 87) as selective receptors for imidazoles [272].

Systems like **233** strongly and selectively bind *N*-unsubstituted imidazoles by establishing a Zn–$N_{imidazole}$ bond and bifurcated hydrogen bonds at the nitrogen acceptor atoms of the phen strap. Secondary interactions such as π–π stacking, C–H···π, or hydrophobic interactions further contribute to strengthen the final assemblies. The phen-strapped receptors display "induced fit" related distortions to accommodate bulky imidazole-substrates on the hindered face of the zinc(II)-porphyrin moiety within the phen pocket. These distortions, which include porphyrin ring distortions, longitudinal cavity distortions, the strap tilting above the plane of the porphyrin moiety, and deviation of the Zn–$N_{imidazole}$ bond vs. the normal of porphyrin mean plane, depend on the nature of the substituent at the imidazole-guests and demonstrate the ability of the rigid host to adapt itself to the need of the guest in order to produce energetically optimized supramolecular complexes [272]. Weiss and co-workers have magisterially exploited the binding affinity of these phen-strapped zinc(II)-porphyrins for *N*-unsubstituted imidazoles to built more elaborated superstructured systems as models of cytochrome *c* oxidase [273], hemoproteins [274], and as photochemical dyads such as **234** (Scheme 88) [275,276].

In **234**, a very efficient energy transfer process takes place between the zinc(II)-porphyrin moiety as energy donor and the free base porphyrin moiety as energy acceptor [275,276]. Weiss and co-workers have further applied the affinity of phen-strapped zinc(II)-porphyrins for *N*-unsubstituted imidazoles to the construction *via* self-assembly of multiporphyrin photonic wires such as **235** (see Fig. 30) [277]. **235** can be considered a photochemical triad, in which the 4,4-difluoro-4-bora-3a,4a-diaza-s-indacene unit (BODIPY) functions as energy donor (input element), the zinc porphyrin moiety as primary energy acceptor (transmission element), with

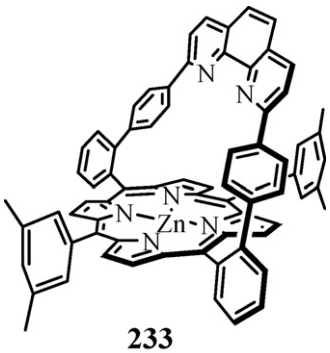

233

Scheme 87.

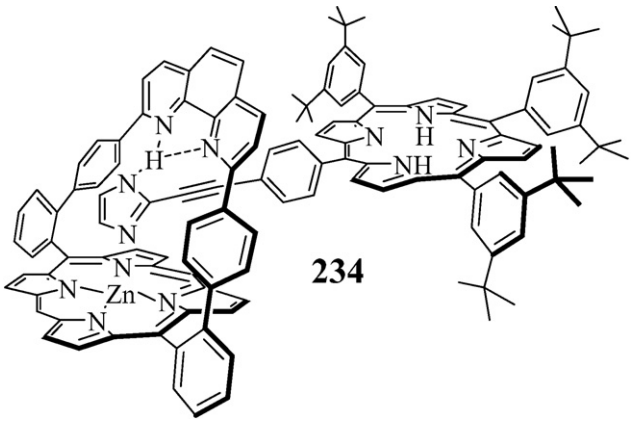

234

Scheme 88.

the free base porphyrin unit working as secondary energy acceptor (output element).

On exciting the BODIPY residue at 495 nm a concomitant increase of the emission arising from the optical output (free base porphyrin) is observed at about 730 nm with a global energy transfer efficiency of about ~0.80 ± 0.08% along the non-covalent assembly.

5. Phenanthroline-based ligands and corresponding metal complexes for DNA and polynucleotides binding and cleavage

Complexes of phen with a variety of metal ions, including Cu^{2+}, Co^{2+}, Zn^{2+}, Mn^{2+}, Ln^{3+}, Ru^{2+}, Rh^{3+} and Os^{2+} [278–287], are known for their ability to interact with DNA, often inducing cleavage of polynucleotide chains. As in the case of most planar heteroaromatic compounds, the mode of interaction depends on the form of DNA as well as on the structural characteristics of the complexes. In fact, complexes with phen can interact with DNA in an intercalative fashion with the A and B forms of DNA, while show a scarce tendency to give intercalation between base pairs of the Z form of DNA, due to the less ordered alignment of base pairs, which does not allow insertion of the heteroaromatic units without causing a strongly distortion of the polynucleotide chains. Alternatively, metal complexes with phen can interact with DNA simply by insertion into either the minor or major groove without intercalating [278–284]. In these cases, adducts are stabilized by hydrophobic effects occurring between the phen moiety and the DNA backbone, as well as by C–H···π interactions involving the heteroaromatic unit of the complexes.

Interaction of phen metal complex with DNA may be followed by cleavage of the DNA strand, which generally occurs *via* either a hydrolytic mechanism involving interaction of the metal centre with a phosphate group and cleavage of the phosphate ester bond [288–291], or an oxidative pathway. In the latter case abstraction of a hydrogen atom from a ribose or a deoxyribose unit produces a carbon-based sugar radical that can rearrange, culminating in the scission of the DNA strand [287]. The cleavage mechanism is strongly influenced by the metal cation bound to the phen unit. While complexes with Cu^{+} or Fe^{2+} can give oxidative cleavage of the DNA strand [278–287], Zn^{2+} or lanthanide complexes act essentially as hydrolytic agents of the phosphate ester bonds [288–291]. In the former case, the oxidant activity can be due to the formation of hydroxyl radicals, produced *via* Fenton chemistry or can involve the formation of strongly M–O oxidant species. Finally, rhodium(III) or ruthenium(II) metal complexes with polypyridyl ligands induce photocleavage of DNA [281,282,285,286].

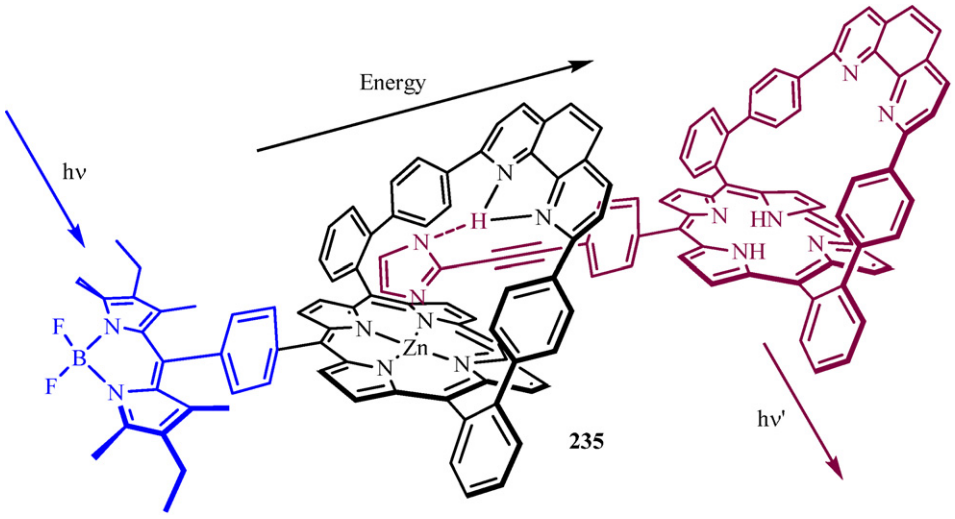

Fig. 30. Schematic of a photochemical triad non-covalently assembled at at phen-strapped zinc(II)-porphyrin [277].

The binding and cleavage properties of complexes with phen can be modulated by functionalization of the phen unit, in order to simply increase the DNA cleavage and binding ability of the complexes or to obtain selective binding to specific DNA sequences. In this section we will try to elucidate these concepts by using selected examples of metal complexes with phen derivatives. To allow the reader to make comparisons, the DNA binding and/or cleavage characteristics of the corresponding complexes with unfunctionalized phen will also be shortly presented.

5.1. Copper complexes with 1,10-phenanthroline derivatives

The system copper/phen represents the most studied example of a metal complex with phen able to interact and cleave the DNA/RNA backbone. In 1979 Sigman discovered that the complex $[Cu(phen)_2]^+$, obtained from the corresponding Cu^{2+} complex by reduction with 3-mercaptothiol acid, cleaves the DNA backbone [292]. The reaction only proceeds in the presence of H_2O_2 [293] and occurs *via* oxidation of a deoxyribose unit to a resonance-stabilized furan derivative [294]. The one-electron reduction of the starting complex $[Cu(phen)_2]^{2+}$ can also be accomplished by using different reducing agents such as ascorbate [295], thiols like 3-mercaptopropionic acid [293,295–297], and 2-mercaptoethanol [295], or by using superoxide generators (for instance, xanthine/xanthine oxidase [294]), while H_2O_2 can be either added exogenously, or generated *in situ* by the spontaneous dismutation of the superoxide anion produced during the oxidation of the Cu^+ complex by molecular oxygen [293].

The nature of the oxidant species has not been completely clarified yet. Although some researchers have proposed, as oxidant species, the hydroxyl radical generated by Cu^+ *via* the Fenton chemistry [298,299], the most commonly accepted mechanism considers the involvement of $[CuO]^+$ or $[CuOH]^{2+}$ species (Scheme 89) [300–302].

The first step in the cleavage mechanism involves the reversible binding of the $[Cu(phen)_2]^+$ complex within the minor groove of DNA to form an essential non-covalent intermediate. UV–vis measurements, viscometric experiments and DFT calculations suggested that binding within the minor groove is accompanied by partial intercalation of one phen moiety between base pairs. Then, reaction of Cu^+ with H_2O_2 produces an oxo-copper species, probably $[CuO]^+$ or $[CuOH]^{2+}$ [303,304], which is the reactive species directly responsible for initiating the cleavage process. Detailed analysis of the reaction products showed that the initial site of attack was mainly the H-1′ hydrogen, buried in the minor groove, confirming the hypothesis that the cleavage is operated by a $[Cu(phen)_2]^+$ complex inserted within the less accessible DNA minor groove [294,305,306]. The abstraction of the H-1′ hydrogen gives the radical compound **237**. The final scission products include free base, equal amounts of DNA fragments with 3′-phosphate (**242**) and 5′-phosphate (**238**) termini and 5-methylene-2-furanone (**241**) (Scheme 89). Oxygen-labelling studies carried out using H_2O^{18} showed that the carbonyl oxygen of 5-methylene-2-furanone originates from solvent [301,302]. This evidence leads one to propose that the initial 1′-deoxyribosyl radical, **237**, is converted to a carbocation, probably by copper-mediated oxidation. Nucleophilic attack by water at C-1′ of **237** produces the intermediate **239**, which decomposes to afford the final scission products.

Although abstraction of H-1′ is considered the major cleavage mechanism, the copper complex can also cleave DNA by a minor pathway that begins with abstraction of H-4′. The H-4′ hydrogen is easily accessible from the minor groove, in agreement with the proposed interaction mode of the $[Cu(phen)_2]^+$ complex with DNA [307,308]. Some authors have recently proposed that the cleavage can also begin with abstraction of H-5′ [309].

Key features of $[Cu(phen)_2]^+$ as DNA cleaving agent are specificity for different secondary structures of DNA and for primary sequences within the B-DNA form. B-DNA is the secondary structure most susceptible to the cleaving action of $[Cu(phen)_2]^+$. The complex cleaves A-DNA less efficiently than B-DNA (A-DNA is 14–17% as reactive as B-DNA, depending on the polynucleotides used) presumably because of fewer favourable contacts between the copper(I) complex and the widened minor groove of the A-form double helix [293,296,310]. Z-DNA, a conformation in which the DNA has little or no minor groove, is almost not cleaved. Furthermore, the complex cleaves double-stranded DNA more efficiently than single-stranded DNA. The opposite behaviour was found in the case of RNA. In fact, single-stranded RNA was cleaved more efficiently than duplex RNA by $[Cu(phen)_2]^+$ [310]. Specificity for a particular DNA secondary structure seems to rule out possible oxidation of the sugar moiety by Fenton-generated hydroxyl radicals, since reactions which proceeds *via* freely diffusible reactive species, such as hydroxyl radicals, would not be expected to possess conformational specificity, assuming that oxidatively sensitive bonds are readily accessible through the solvent. Conversely, the specificity displayed by the complex $[Cu(phen)_2]^+$ suggested that this complex plays a central role in the oxidative mechanism. It was

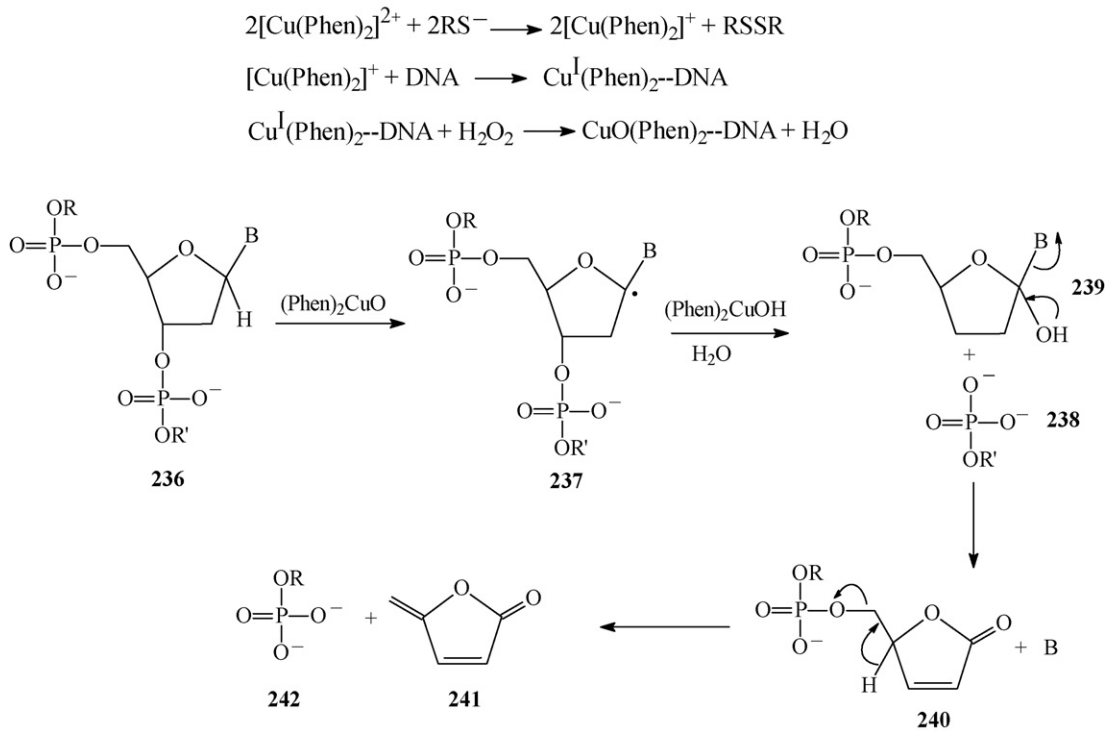

Scheme 89.

proposed that the complex directly participates in the cleavage pathway thanks to its insertion in the minor groove in an orientation in which the metal is accessible to the H-1′ hydrogen of deoxyribose.

$[Cu(phen)_2]^+$ does not display a marked specificity for primary sequences, although it does not cleave DNA at all sequence positions at the same rate. In particular, the most sensitive sequence to scission was the deoxyribose of adenosine in TAT triplet, while related sequences TGT, TAAT, TAG an CGAT were moderately preferred [311,312]. All these characteristics make $[Cu(phen)_2]^+$ an useful tool in molecular biology, in particular as footprinting agent or conformational probe. However, the complex $[Cu(phen)_2]^+$ presents also some drawbacks that limit its applicability. First, the value of the addition constant of phen to the 1:1 complex $[Cu(phen)]^+$ is only 5.5 log units. Therefore, in the concentrations generally used in DNA cleavage experiments, a large excess of phen (often 10 equiv.) is usually necessary to increase the amount of $[Cu(phen)_2]^+$ formed. However, free phen can exert a competitive inhibiting effect on the DNA binding process of $[Cu(phen)_2]^+$. At the same time, $[Cu(phen)]^+$ has a lower cleavage activity than $[Cu(phen)_2]^+$ and its sequence preference is different from that of $[Cu(phen)_2]^+$. Furthermore, thiols added in large excess to reduce $[Cu(phen)_2]^{2+}$ to the corresponding Cu^+ complex can compete with phen in coordinating the metal centre, thus reducing the quantity of $[Cu(phen)_2]^+$ available as cleaving agent.

This problem can be overcome by the use of appropriately designed ligands containing two phen units linked by a single flexible bridge, connecting the 2- or 3-positions of the heterocyclic skeleton. The bridge must have the appropriate length and flexibility to assure coordination of both phen units to the same metal cation and to allow the ligand to easily change conformation during the reduction of Cu^{2+} to Cu^+. With this in mind, Meunier and co-workers synthesized ligands **243** and **244** (often named ClipPhen, Scheme 90) by reaction of 2-chloro-1,10-phenanthroline or 3-bromo-1,10-phenanthroline (**131**) with serinol in the presence of a base [313,314]. It is important to underline that in **243** and **244** the 9-position and 2,9-positions, respectively, of the phen units remain unfunctionalized. In fact, phen ligands functionalized at both 2- and 9-positions most often do not form redox-active Cu^{2+} complexes [300,315], due to steric interactions which inhibit the redox cycle to pass through a square planar copper complex. Of note, in **243** and **244** the aliphatic bridge also contains an amine group which can facilitate a further functionalization of the ligands.

Both **243** and **244** form stable 1:1 complexes with Cu^{2+}, where both the phen moieties are bound to the metal centre. The EPR spectrum of the complexes $[Cu(\mathbf{243})]^{2+}$ suggested a trigonal bipyramidal coordination geometry of the complex [316]. In analogy with other Cu^{2+} complexes with phen derivatives [317], the authors suggested that each phen unit provides an equatorial and an axial nitrogen atom to Cu^{2+}, the fifth position of the trigonal bipyramid being probably occupied by a water molecule.

The EPR spectrum of $[Cu(\mathbf{244})]^{2+}$ was in agreement with classical 5- or 6-coordinate Cu^{2+} complexes in a distorted square-

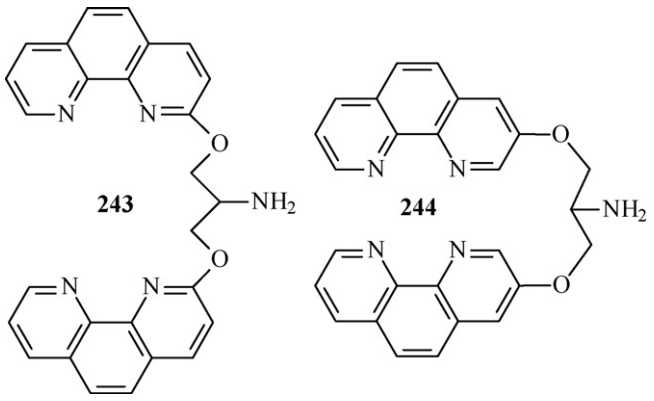

Scheme 90.

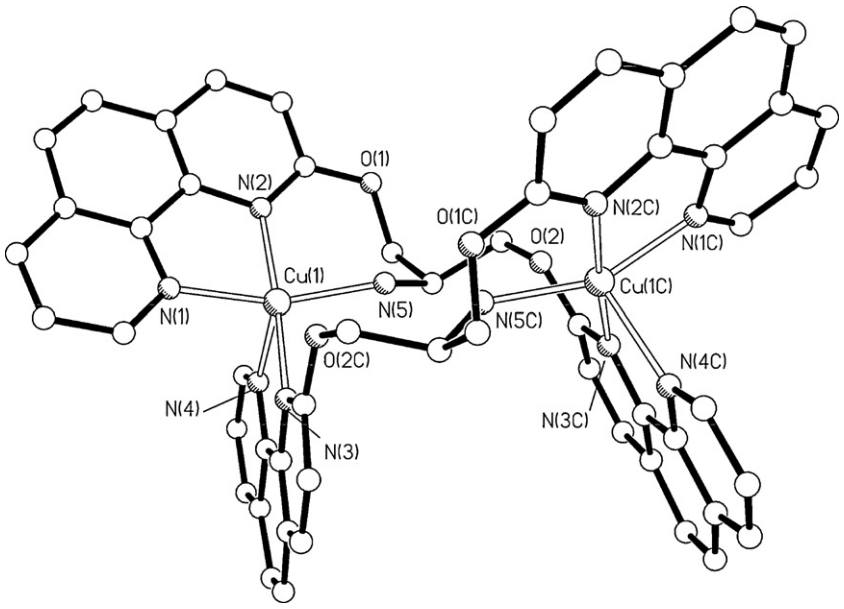

Fig. 31. ORTEP view of the complex cation $[Cu(\mathbf{243})]_2^{4+}$ [316]. H-atoms are omitted for clarity.

pyramidal or octahedral geometry. Interestingly, the crystal structure of the Cu^{2+} complexes with **243** revealed the assembly of the dimeric complex $[Cu(\mathbf{243})]_2(BF_4)_4$. Each Cu^{2+} ion is bound to two phen moieties belonging to two different ligand units, affording an overall double-helical structures (see Fig. 31) [316].

However, ESI mass spectra and electrochemical measurements indicated that the dimeric structure is not retained in aqueous solution, where only 1:1 complex species are formed [316]. Electrochemical measurements accounted for a quasi-reversible mono-electronic metal centred process, with a reduction potential slightly higher than that measured for $[Cu(phen)_2]^{2+}$, indicating that the presence of a bridge linking the 2-positions of the phen moieties facilitates the reduction of the metal centre, probably thanks to the stabilization of the copper(I) oxidation state in the complexes with **243** [316]. Conversely, the Cu^{2+} complex with **244** displayed a more strongly negative potential than $[Cu(phen)_2]^{2+}$, reflecting a greater stabilization of the copper(II) oxidation state.

Cleavage experiments were carried out on the ΦX174 plasmidic DNA monitoring the relaxation of supercoiled circular form I into the nicked circular and linear forms II and III. The two copper complexes with Clip-Phen ligands **243** and **244** gave significant increase of the DNA cleavage activity with respect to the complexes with unfunctionalized phen in the same experimental conditions. In fact, the amounts of single-strand breaks, expressed as μ values (μ = −ln(fraction of form I)), were 1.4 and 34 for the copper complexes with **243** and **244**, while μ values of 0.55 and 0.88 were measured for Cu^{2+} in the presence of 1 and 2 equiv. of phen, respectively. These results indicated that binding of two phen units to the metal, as with Clip-Phen, has a beneficial effect on the DNA cleaving activity of the corresponding copper(II) complexes. The dramatic enhancement in the cleaving activity observed in the case of the copper complex with **244** with respect to the complex with **243** can be ascribed to the different position of functionalization of phen in **243** and **244**, in agreement with the general observation that functionalization at 2-position of phen tends to deactivate the cleavage activity of the copper(II) complexes [300,315]. Furthermore, recent DFT studies have shown that the different position of phen functionalization in **243** and **244** strongly affects the geometry of their complexes. For instance, while the calculated structure of the Cu^{+} complex with **243** strongly resembles that of complex $[Cu(phen)_2]^{+}$, with a dihedral angle of 70° between the phen planes, the corresponding complex with **244** is calculated to be fairly planar, favouring minor groove DNA binding and intercalation [318]. The consequent tight association of the copper complex with **244** with DNA could justify its higher activity in DNA cleavage.

Meunier and co-workers also synthesized several ligands with bridges of different lengths linking the 2- or 3-positions of two phen moieties (**245**–**250** in Scheme 91) [316].

An electrochemical and EPR study of their copper(II) complexes revealed that the coordination properties of compounds **245**, **246** and **247**–**250** are similar to those found for **243** and **244**, respectively. For instance, the complexes with **245** and **246** showed a reduction potential higher than that measured for $[Cu(phen)_2]^{2+}$, while those with **247**–**250** displayed a lower reduction potential than $[Cu(phen)_2]^{2+}$. Furthermore, the crystal structure of the complex $[Cu(\mathbf{245})Cl]_2Cl_2$ (see Fig. 32) revealed the formation of an assembly with a 2:2 metal-to-ligand stoichiometry in the solid state, with structural features similar to that observed in the case of the complex $[Cu(\mathbf{243})]_2(BF_4)_4$.

All copper(II) complexes with **245**–**250** showed a remarkably lower DNA cleavage activity than the complex with **244**. However, this study pointed out a higher cleaving ability for the copper(II) complexes with the Clip-Phen ligands featuring a bridge linking the 3-positions of the two coordinated phen moieties with respect

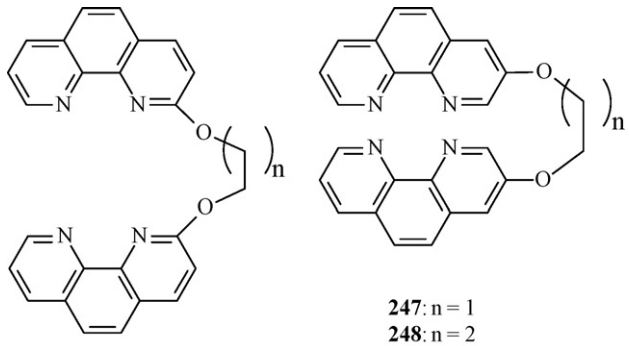

245: n = 1
246: n = 2
247: n = 1
248: n = 2
249: n = 3
250: n = 4

Scheme 91.

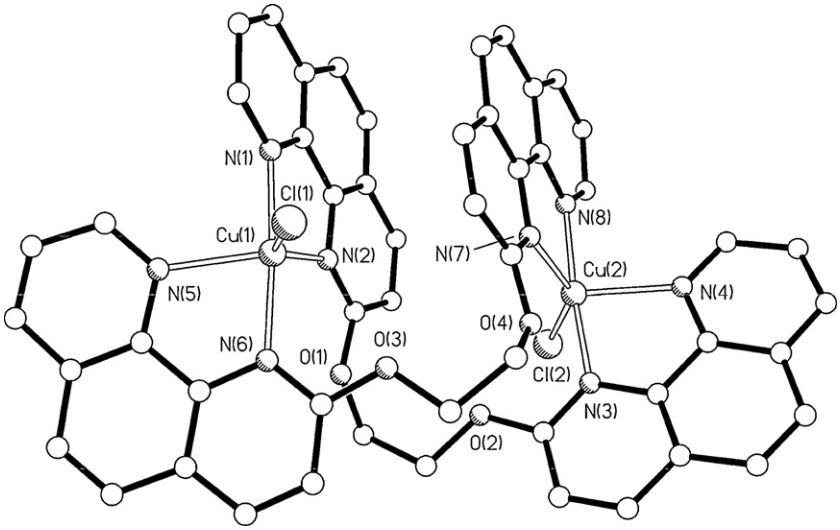

Fig. 32. ORTEP view of the complex cation $[Cu(\mathbf{245})Cl]_2^{2+}$ [316]. H-atoms are omitted for clarity.

to the complexes with the ligands featuring a bridge connecting the 2-positions. Furthermore, the primary amine group on the aliphatic bridge of **243** and **244** was demonstrated to be very important in determining the different DNA cleaving ability of the corresponding copper(II) complexes. In fact, while the complex with **243** is less active than the complex with the Clip-Phen ligand featuring a bridge of the same length as **243** but without the amine group (**246**), the complex with **244** is more active than that with **248**. To explain this surprising feature, it was hypothesized that in **243** the amine group could be bound to the metal cation, thus reducing the activity of the complex. Geometrical constraints would not allow this type of coordination in the case of **244** and the primary amine group could be protonated at physiological pH, thus favouring the interaction of the copper(II) complex with the polyanionic structure of DNA. The most interesting finding, however, was the observation that there is no correlation between the redox properties of the copper(II) complexes with **243**–**250** and their DNA cleavage ability. Conversely, it was generally observed that the cleavage ability depends on the length of the linker bridging the two phen moieties in the Clip-Phen ligands, the most active complexes being those with the ligands having shorter linkers. Therefore, the nuclease properties of the complexes with Clip-Phen ligands is probably determined by the different coordination geometry of the complexes imposed by the bridge, rather than by the Cu^{2+}/Cu^{+} redox potential [316].

These suggestions have been recently corroborated by Reedijk and Meunier with a DFT study carried out on the Cu^{+} and Cu^{2+} complexes with 3-substituted Clip-Phen **244** and **247**–**250**. It was substantially found that a shorter linker between the two phen units leads to an increase of the planarity of the corresponding Cu^{+} complexes, thus enhancing their affinity for DNA. At the same time, the structural changes occurring upon oxidation or reduction are less dramatic for complexes with a short linker. Both these effects can be beneficial on the DNA cleavage pathway, thus increasing the cleavage properties of the complexes with short linkers between the two binding phen units [319].

The primary amino group in the Clip-Phen ligands **243** and **244** allows further functionalization of these systems. In this respect, different approaches have been used to synthesize new copper(II) Clip-Phen complexes with increased DNA binding ability and/or DNA cleavage activity: (a) attachment to the $-NH_2$ group of a side arm containing an intercalating unit, such as acridine, (b) attachment to the primary amine of a minor groove binding agent, and (c) attachment of a Pt(II)-containing nucleobases binding moiety.

Following approach (a), a 9-aminoacridine or a 9-amino-6-chloro-2-methoxyaminoacridine moieties were appended to Clip-Phen **243** and **244**, through aliphatic linkers with variable length (Scheme 92), in order to obtain copper(II) complexes with enhanced DNA binding ability and cleaving efficiency [320,321]. Acridine and 6-chloro-2-methoxyacridine are well known DNA intercalating moieties and represent the intercalating units of the antitumor drug amsacrine and the antimalarian quinacrine, respectively.

Different synthetic approaches were followed to prepare compounds **251**–**260**. **251** and **252** were obtained from the reaction of compound **243** with BOC-protected 6-aminohexanoic acid followed by removal of BOC to afford the intermediate **261**. Reaction of this compound with 9-phenoxyacridine (**262**) and 6-chloro-2-methoxy-9-phenoxyacridine (**263**) gave the desiderate ligands **251** and **252**, respectively (Scheme 93). Their mononuclear Cu^{2+} complexes were then isolated as hexafluorophosphate salts $[Cu(H\mathbf{251})](PF_6)_3$ and $[Cu(H\mathbf{252})](PF_6)_3$, containing the acridine moieties in their protonated forms [320].

Compounds **253**–**260** were obtained either by using the synthetic procedure described for **251** and **252** (compounds **253**–**256** and **260**) or by the two-step procedure depicted in Scheme 94 (compounds **257**–**259**). In the first step, reaction of 6-chloro-2-methoxy-9-phenoxyacridine (**263**) with the appropriate amino acids produces the acridine derivatives **264**–**266**. Activation of the carboxylic groups by ethyl chloroformate and coupling with **244** afforded ligands **257**–**259** [321].

The DNA cleaving activity of the copper(II) complexes with these ligands was generally higher than that observed for the copper complexes with simple **243** or **244**, in agreement with an enhanced affinity of these complexes with DNA due to intercalation of the acridine moieties. Only the copper complex with **253**, featured by the shortest aliphatic chain ($n = 1$), displayed a DNA cleaving ability almost equal to that of complex with **244**. In the case of complexes with **251** and **252**, UV–vis spectra performed on the free ligands and on their copper(II) complexes showed, in the presence of DNA, a bathochromic and hypsochromic shifts of the acridine bands in the visible region, in agreement with the expected intercalative binding mode of acridine [320]. The most interesting finding of this study, however, was the dependence of the DNA cleavage ability on the length of the aliphatic chain in the ligands [321]. In fact, among copper(II) complexes with **251**–**260**, the cleaving ability increases with the length of the aliphatic chain up to $n = 5$. The DNA cleavage ability then decreases in the complexes with $n > 5$ (n = number of

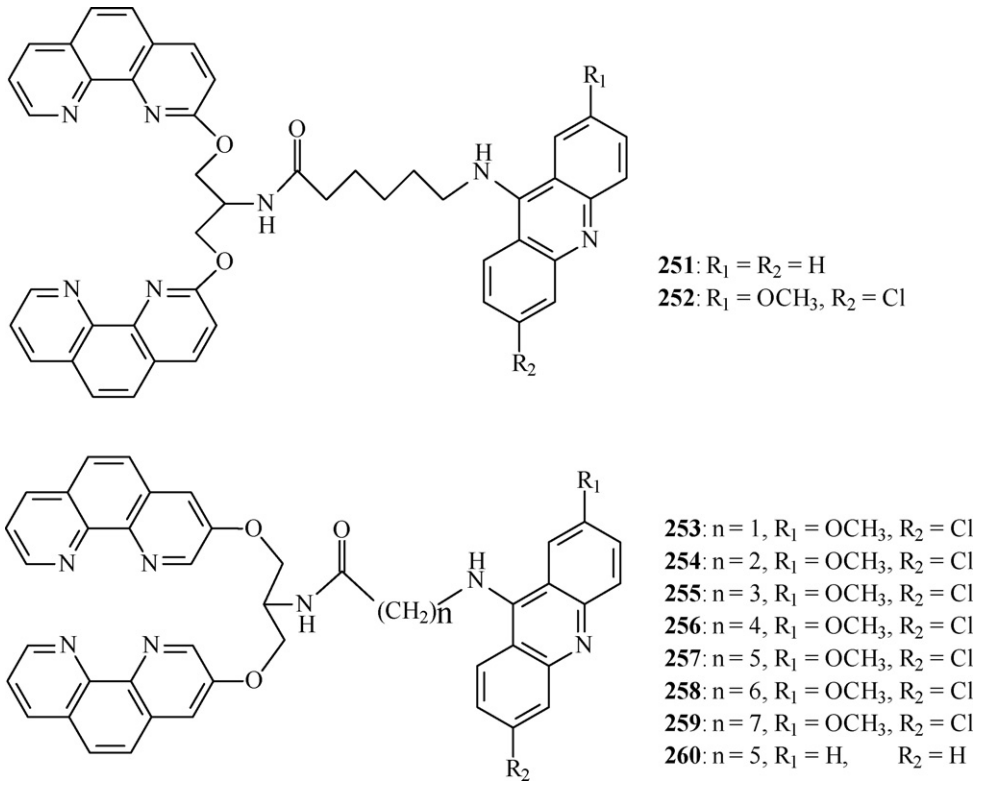

Scheme 92.

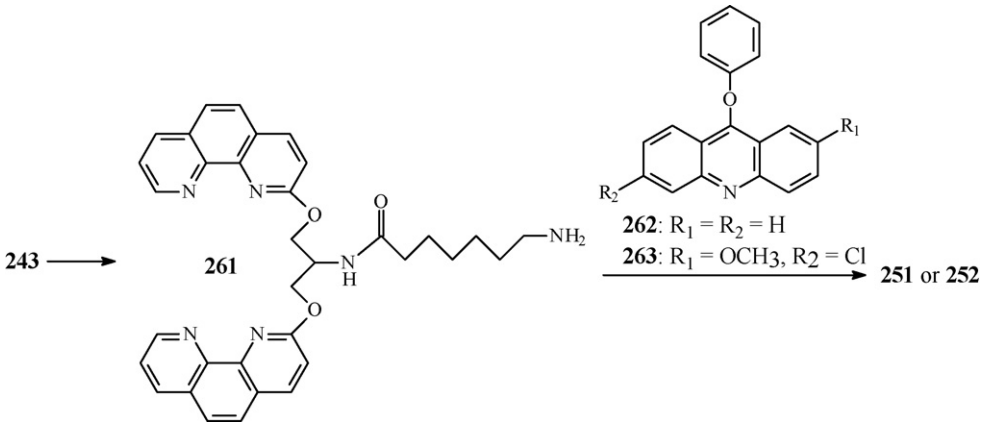

Scheme 93.

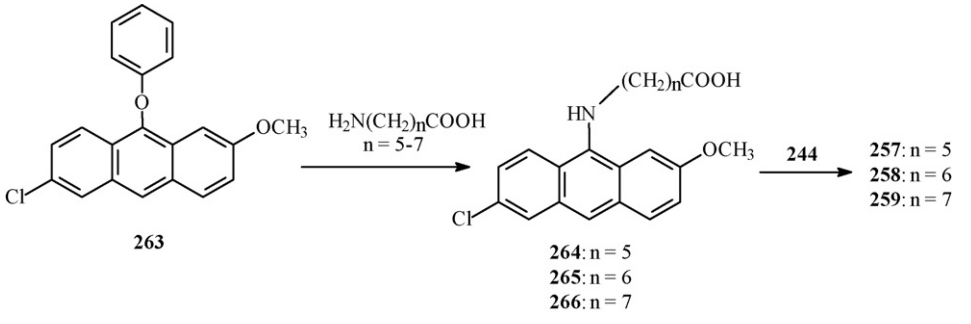

Scheme 94.

methylene groups). The reason of this behaviour could not be clarified on the basis of the experimental data available, although the authors reasonably supposed that the complexes with ligands having shorter aliphatic linkers are sterically constrained and therefore less efficient. Of note, complex with **257** was more active than that with **252**, in agreement with the observed higher DNA cleaving ability of the copper(II) complex with "3-functionalized" Clip-Phen **244** with respect to the complex with "2-functionalized" Clip-Phen **243**.

The attachment onto ligands **243** or **244** of appropriately minor groove binders (approach (b)) can lead to copper(II) complexes having not only an increased efficiency in DNA cleavage but also a cleavage activity targeted to specific sequences of polynucleotides. A necessary condition to obtain the latter result is the use of a minor groove binder able to interact with a specific section of DNA. From this point of view functionalization of **243** and **244** with spermine, a non-specific minor groove binder [322,323], lead to ligands whose copper(II) complexes showed a marked increase in the DNA cleavage efficiency, but no sequence specificity was observed [324]. This goal was achieved by using distamycin derivatives of **243** and **244**. Distamycin is a tri-*N*-methylpyrrole system that tightly binds to the minor groove thanks to a combination of electrostatic, hydrogen bonds and van der Waals contacts, with a marked preference for sequences of five successive AT base pairs [325]. The attachment of a tri-*N*-methylpyrrole moiety to Clip-Phen ligands **243** and **244** at their primary amino group allowed the preparation of ligands **267**–**269** (Scheme 95) [326].

These compounds were obtained by means of a synthetic method on a solid support, starting from appropriate derivatives of Clip-Phen **243** or **244** containing a carboxyalkyl chain linked to the primary amino group *via* an amidic bond. These compounds were coupled with the required poly-*N*-methylpyrrole portion functionalized with a H_2N-terminal amine group at one end, and covalently linked to Boc-β-Pam resin at the second end. The anchored poly-*N*-methylpyrrole fragment was prepared from Boc-β-Pam resin by means of successive reactions of condensation with Boc-*N*-methyl-pyrrole-O-benzotriazole ester and deprotection with trifluoroacetic acid, according to Dervan methodology [327]. The final product was then detached from the resin by common means. The synthesis on solid support provided facile purification of the products (excess of reagents was easily removed by filtration) and, overall, avoided isolation of the poly-*N*-methyl-pyrrole unit before reaction with Clip-Phen derivatives. In fact, it is known that poly-*N*-methyl-pyrroles are unstable when their terminal amine function is not protected.

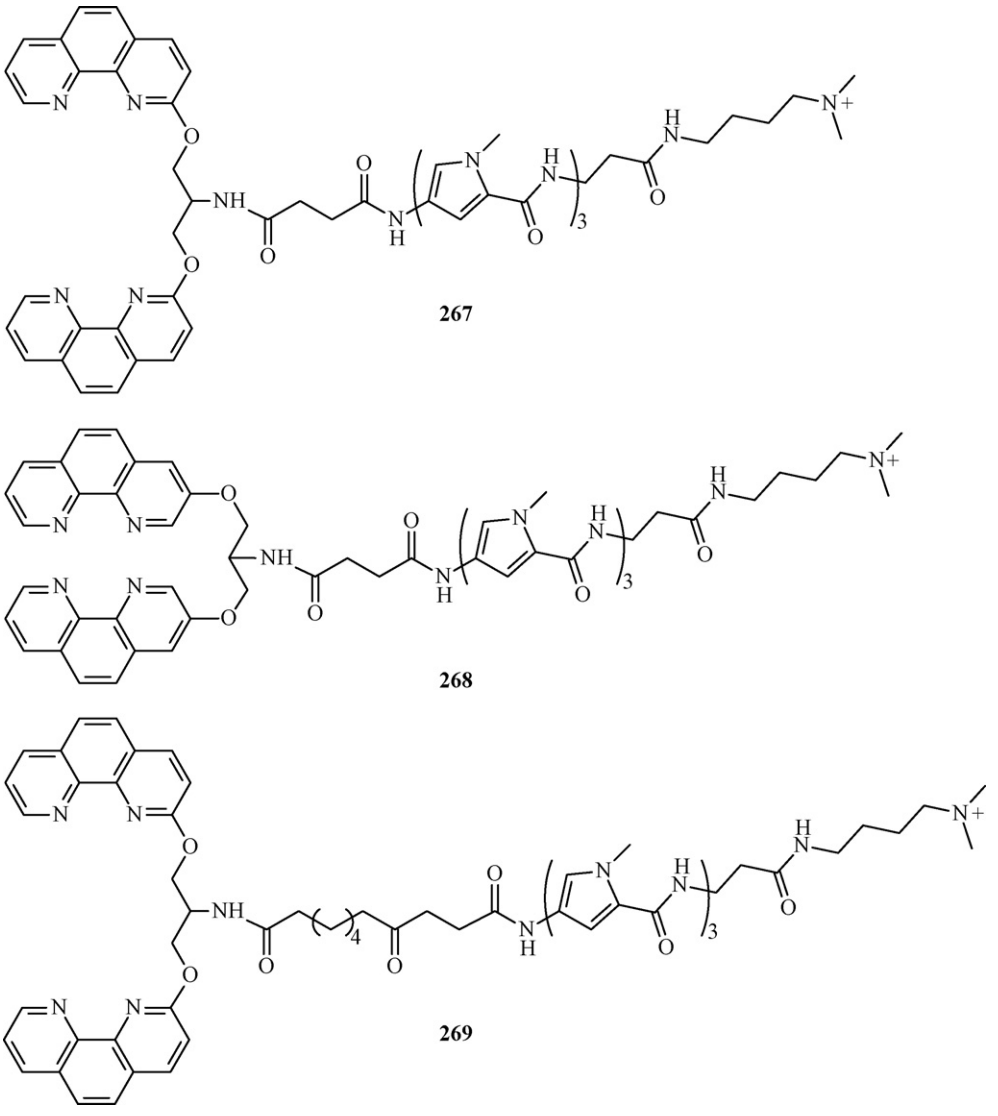

Scheme 95.

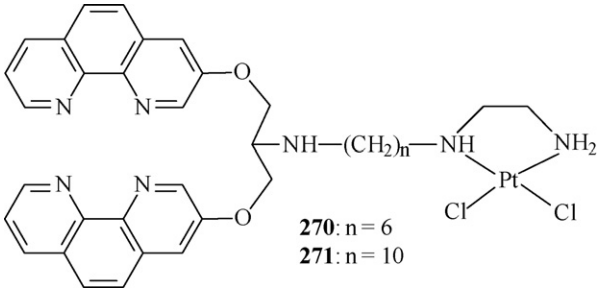

Scheme 96.

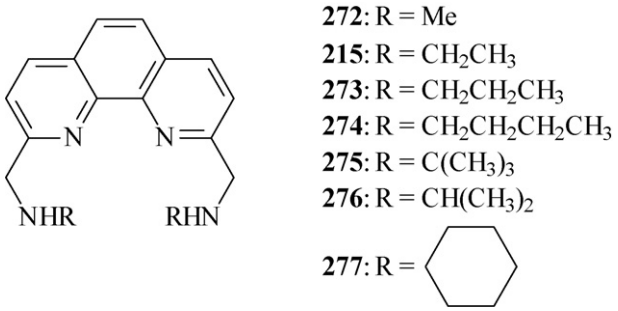

Scheme 97.

DNA cleavage experiments were carried out on a restriction fragment containing three sites for potential binding of the distamycin analogues, with 5, 6, and 7 successive AT base pairs, respectively. Indeed, the copper complexes with ligands **267**–**269** induced a specific cleavage pattern. In fact, cleavages were limited to localized sites around the three regions containing the three sequences of AT base pairs [326]. A secondary binding site was also observed at another AT rich sequence, where 10 out of 12 base pairs are AT. The copper(II) complex with **268** was the most active in targeting the three AT sequences, as expected considering the high cleaving ability of complexes with "3-functionalized" Clip-Phen ligands with respect to the corresponding complexes with "2-functionalized" ones. The other complexes were generally less active, and, at the same time, displayed somewhat different cleavage pattern. For instance, complex with **268** cleaved always at the 5′- and 3′-sides of the fragment containing 7 AT base pairs, whereas the preferential cleavage site for the copper complex with **267** was inside this seven AT base pairs fragment. Conversely, complex with **269** showed less cleavage specificity, displaying more diffuse strand breaks around the three AT sequences considered. These characteristics were attributed to the increased length of the chain linking the Cu^+ binding site and the tri-*N*-methylpyrrole unit of **269**, which allows the $[Cu(phen)_2]^{2+}$ moiety to oxidize a larger number of nucleotides around the binding site. Therefore, site-specific DNA cleavage depends not only on the characteristics of the minor groove binder, but also on the structural characteristics of complexes and on the length of the linker joining the two functional parts of these DNA cleavers [326].

Detailed analysis of the reaction products allowed to determine more precisely the scission sites of complexes with **244** and **268** and revealed that these complexes produces abstraction of H-1′ (see Scheme 89), and at a less extent, of H-4′ and H-5′, essentially confirming the scission mechanism proposed by Sigman. Of note, in the case of complex with **268**, the abstraction of H-1′ appeared to be less predominant, suggesting that steric constraints resulting from conjugation of the distamycin analogue limits the accessibility of the copper Clip-Phen complex to the deoxyribose H-1′ hydrogen, that is embedded within the minor groove [328].

The third approach used to increase the DNA cleavage activity was the attachment to Clip-Phen **244** of a $[Pt(en)Cl_2]$ complex unit through an aliphatic chain of 6 or 10 methylene groups (Scheme 96) [329]. Copper(II) complex with **271**, containing the $-(CH_2)_{10}-$ linker, was designed with a bridge longer enough to allow DNA interaction of both metal centres at their preferential binding sites, *i.e.*, the minor groove for the $[Cu(phen)_2]^{2+}$ and the major groove for the $[Pt(en)Cl_2]$ one, while the shorter bridge of **270** forces the two metal cations to sit in the same groove.

The analysis of relaxation of supercoiled ΦX174 DNA in the presence of the copper(II) complexes with **270** and **271** revealed that the dinuclear complexes are more potent DNA cleavers than the copper complex with the parent ligand **244**. At the same time, the cleavage experiments showed that the DNA linear form III already appears when the supercoiled form I is still present. Conversely, in same experimental conditions the copper(II) complex with **244** affords only the DNA form II. These results indicated that the heterodinuclear complexes are able to perform direct double strand cuts, whereas the mononuclear copper(II) complex with **244** is able only to carry out two successive single-strand cuts. On the other hand, the cleavage reaction induced by the heterodinuclear complexes and by the mononuclear Pt^{2+} complexes **270** and **271** on a 36 bp (base pairs) fragment gave smearing of the electrophoretic bands, suggesting that these complexes are less specific than *cis*-platin, which is known to cleave DNA at the GG sites and, at a less extent, at the AG ones. Nevertheless, these complexes display a high cytotoxicity in several tumoral cell lines, in some cases even higher than *cis*-platin. For instance, the mononuclear complex **271** is *ca.* 10 times more active than *cis*-platin for the breast cancer cell line MCF-7.

The study of the DNA cleaving properties of the simple $[Cu(phen)_2]^{2+}$ system and of the Clip-Phen complexes outlined that phen represents an optimal building blocks to construct new Cu^{2+} complexes able to interact with DNA and to cleave its strain(s). To this purpose, a number of phen-based ligands have been recently developed, by synthesizing new phen derivatives containing either additional metal binding sites, to increase the binding ability of the ligand toward Cu^{2+}, or functional groups capable to interact with DNA to enhance the affinity and/or specificity of the resulting copper(II) complex toward polynucleotides.

Lin and co-workers synthesized a series of 1,10-phenanthroline-2,9-dimethylenediamine dialkyl derivatives by reaction of 2,9-diformyl-1,10-phenanthroline (**28**) (Scheme 11) with the corresponding aliphatic amine, followed by reduction of the resulting Schiff bases, ligands **215** (Scheme 80), and **272**–**277** (Scheme 97) [330]. These ligands contain a tetradentate binding site which can host transition metal cations, such as Pd^{2+} [319] and Cu^{2+} [331], and form stable metal chelates in aqueous solutions.

UV–vis and EPR studies carried out by Chikira [332] suggested that Cu^{2+} is coordinated by the two heteroaromatic nitrogen atoms, a single amine donor and two exogenous chloride anions or water molecules, with coordination geometries spanning from square-based pyramidal to trigonal bipyramidal. Therefore, binding of the small Cu^{2+} ion does not allow the simultaneous involvement of both secondary amine groups in metal coordination to the metal cation.

The analyses of the interaction between the Cu^{2+} complexes with **215**, **272**–**277** and calf thymus DNA was carried out by Lin and co-workers by means of melting, circular dichroism (CD) and fluorescence emission measurements in the presence of ethydium bromide (EtB) as fluorescence probe. It was suggested that the complexes bind to DNA by simultaneous covalent and intercalative binding modes [331]. The binding process was also kinetically studied by monitoring the changes in the fluorescence emission of EtB in the presence of the complexes with **215** and **272**–**276**. In fact, the fluorescence emission of EtB is greatly increased upon its intercalation within base pairs and eventual time-course quench-

ing of its fluorescence can be used to monitor the kinetic aspects of binding [333]. Lin and co-workers found successive time-separated steps in the DNA binding process of the complexes. In the fast first step the complexes give essentially electrostatic interactions with the phosphate groups of DNA, perturbing its structure and squeezing out EtB from the DNA helix, leading to a marked decrease of the fluorescence emission intensity. A second decrease of the fluorescence emission is also observed in a longer time, in agreement with the occurrence of a second slow step, due to interaction of the complexes with nucleobases *via* intercalation and/or coordination of the metal centre to the heteroatoms of the nucleobases [331].

Successive analysis of the binding mode toward DNA of the complexes with **272**–**275** was also carried out by Chikira, by coupling spectroscopic, viscometric and electrochemical techniques [332]. This study confirmed partial intercalation of the phen unit, but ruled out covalent binding of the metal to DNA, due to the presence of the sterically hindered alkyl groups. Among the different complexes, the one with **275** featuring the most hindered *N*-*tert*-butyl-substituent displayed the lower affinity for DNA, but was the most active in the process of oxidative cleavage of the pBR 322 plasmid DNA. Its efficiency was just somewhat lower than that of $[Cu(phen)_2]^{2+}$. The authors suggested that this higher activity is related to the redox potential of the Cu^{2+}/Cu^{+} couple in the complex with **275**, which is the highest among the copper(II) complexes with these type of ligands, thus favouring the $Cu^{2+} \rightarrow Cu^{+}$ reduction necessary to induce the cleavage process.

Cu^{2+} complexes with polyamine macrocycles incorporating a phen unit have also been used as artificial nucleases. This class of ligands offers the advantage to form remarkable stable Cu^{2+} chelates, due to metal encapsulation within their cavities, avoiding possible dissociation of the complexes in the course of the cleavage reaction. Furthermore, polyazamacrocycles containing a sufficiently high number of donor atoms (generally seven or more) can form polynuclear complexes. The metals are kept at short distances by the cyclic structure of ligands, making it possible the study of the effect of closely positioned Cu^{2+} metal cations on the DNA binding and cleavage properties of the complexes. On this ground, Schneider and co-workers analyzed the binding and cleaving properties of ligands **78**–**80** and **192** (see Schemes 31 and 77) and their Cu^{2+} complexes [136]. Polyazamacrocycles **78**, **79** and **192** form only mononuclear complexes with Cu^{2+} in aqueous solutions, while the larger **80** can give both mono- and dinuclear complexes. Melting measurements showed that both ligands and their complexes have higher binding affinity for DNA than their linear amine counterparts, *i.e.*, diethylenetriamine, triethylenetetraamine and tetraethylenepentaamine, which are protonated at neutral pH value and bind to DNA thanks to electrostatic interactions. This result suggested that the phen unit of **78**–**80** and **192** is indeed intercalating. More interestingly, the Cu^{2+} complexes efficiently cleave the pBR322 plasmid DNA as well as the DNA model BNPP. Although the cleavage mechanisms are likely to be extremely different (BNPP is generally cleaved *via* a hydrolytic pathway), the dinuclear complex with **80** and the mononuclear complex with **192** were the most efficient in both DNA and BNPP cleavage. While in the case of $[Cu_2(\mathbf{80})]^{4+}$ the presence of two metal ions in close proximity and the high charge can favour the cleavage thanks to a stronger interaction with DNA, in the case of the complex with **192** the high activity in the cleaving process was attributed to the fact that the complex is present in aqueous solution mainly in a protonated form $[Cu(H\mathbf{192})]^{3+}$. In fact, the presence of a protonated amine group can strengthen the interaction with substrates *via* hydrogen-bonding and charge-charge contacts with the phosphate groups [136].

The interaction between calf-thymus DNA and the mononuclear Cu^{2+} complex with **79** and the mono- and dinuclear complexes with **80** was analyzed in details by means of UV–vis and fluorescence emission measurements [334–336]. Fluorescence emission titrations, carried out by adding the complexes to DNA previously saturated with EtB, showed that the complexes are able to displace the intercalated EtB from DNA, supporting the hypothesis that the interaction of the Cu^{2+} complexes with phen-containing polyamine macrocycles implies intercalation of the heteroaromatic units between DNA base pairs [334–336]. Interestingly, the dinuclear complex with **80** was able to displace EtB more efficiently than the corresponding mononuclear complex, in agreement with a greater affinity of the former for DNA, due to the beneficial effect of the presence of two Cu^{2+} cations on the overall complex–DNA interaction [336]. Conversely, the addition of EtB to DNA previously treated with the Cu^{2+} complexes with **80** does not lead to the fluorescence emission expected for EtB intercalation [335,336]. This suggested the DNA structure is modified upon binding of the complexes to such a level that ordinary intercalation of EtB could not take place, probably due to cleavage of the DNA strands. Cleavage experiments confirmed this hypothesis. Interestingly, it was found that the complex with **79** efficiently cleaves Poly(dC-dT)·Poly(dC-dT), but not Poly(dA-dT)·Poly(dA-dT), indicating that DNA cleavage takes place in proximity of the CG base pairs [335]. The DNA binding process of the complexes with **79** and **80** was also analyzed from a kinetic point of view. This study revealed that the process is composed by two distinct steps. The first step, diffusion controlled, is very fast and lead to an external interaction between the copper complexes and DNA. The second step consists in a monomolecular migration of the Cu^{2+} complexes from the outside to inside DNA to intercalate between base pairs [335,336].

Cu^{2+} complexes have also been designed to specifically cleave particular DNA structures. Zain and co-workers synthesized new ligands capable, in the presence of Cu^{2+}, to selectively cleave triple helical structures of DNA [337,338]. Triple helix structures can be formed upon intermolecular sequence specific recognition of an oligopyrimidine–oligopurine sequence of double stranded DNA by an oligonucleotide. The third-strand binds to the major grove of the double helix, *via* hydrogen-bonding with the purine bases [339]. These structures constitute the basis of the antigen strategy aimed at controlling gene expression and at targeting specific DNA modifications [340]. On the other hand, triple helical structures can also be formed *via* an intramolecular process involving rearrangements of double stranded oligopyrimidine-oligopurine sequences subjected to physical constraints and/or acidic conditions [341]. However, the cellular role of these structures (H-DNA) is still scarcely known. Zain and co-workers coupled within the same ligands a benzoquinoxaline unit, a well known heteroaromatic unit capable to recognize and stabilize triple helix sequences and a phen moiety, capable, when complexed with Cu^{2+}, to cleave the DNA strands. Conjugates **281** and **282** were obtained by reaction of **278** with 5-formyl-1,10-phenanthroline (**279**) and 4-formyl-1,10-phenanthroline (**280**), respectively (Scheme 98) [337].

Both **281** and **282** in the presence of Cu^{2+} and reducing agents were indeed able *in vitro* to bind and selectively cleave double stranded DNA specifically at the site where a triple helix was formed *via* an inter- or intra molecular process [337,338]. Their cleaving ability was also successfully tested in Escherichia coli cells [338] and has been recently also used in the study of gene modifications inducing the Friedreich' ataxia disease, which is known to be caused by hyperexpansion of $(GAA)_n$-repeat sequences in the frataxin gene ($n < 40$ in normal genes, $n = 90$–1700 in Friedreich' ataxia patients genes) [342]. In particular, **282** has been used to demonstrate the formation of triple helix H-DNA by a hyper-expanded $(GAA)_n$-repeat sequence ($n = 115$) in the human frataxin gene [343].

Cu^{2+} complexes with phen-based ligands have also been used to cleave DNA upon photoreduction of Cu^{2+} to Cu^{+}. Lorente

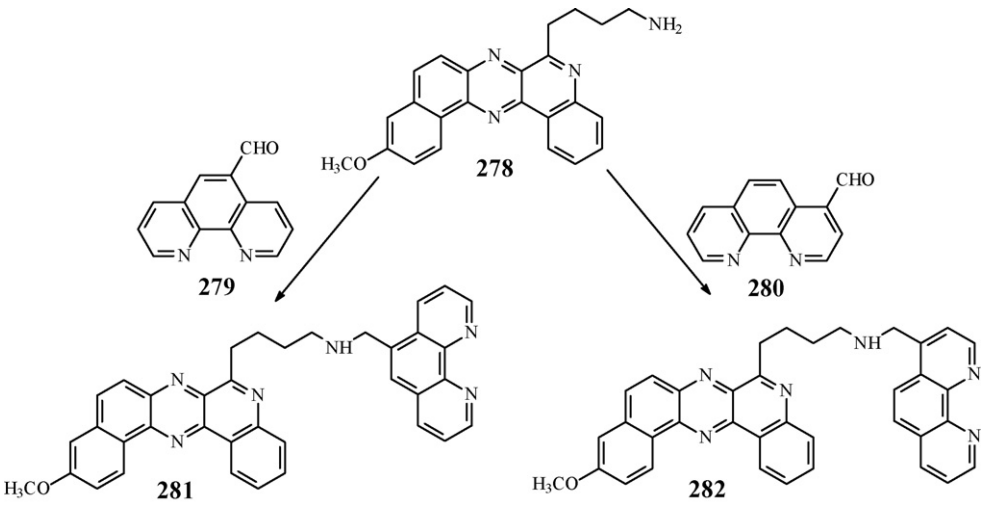

Scheme 98.

and Grant developed a series of phen-based conjugate systems containing two benzene, naphthalene, anthracene or acridine moieties to analyze their DNA cleaving properties in the presence and in the absence of Cu^{2+} [344]. As sketched in Scheme 99, 1,10-phenanthroline-2,9-dicarboxylic acid (**27**, Scheme 11) was first reacted with an excess of 1,1′-carbonyldiimidazole and then with *N,N*′-dimethylethylenediamine. This procedure afforded the precursor **284** in a facile one-pot procedure, *via* the unstable imidazolide intermediate **283** (not isolated). Reaction of **284** with the alkylating reagents 9-bromomethylanthracene or 9-bromomethylacridine gave conjugates **285** and **286**. Compound **287** was obtained by reaction of 2,9-*bis*(hydroxymethyl)-1,10-phenanthroline (**29**, Scheme 11) with 9-bromomethylanthracene by using the methodology described by Chandler [67].

Compounds **285**–**287** were able to cleave the pUC19 plasmid DNA upon photoactivation in the absence of Cu^{2+} added. However, the photocleavage levels markedly increase upon addition of Cu^{2+}, the most active being the anthracene derivative **287**. It was proposed that the cleavage process involves photoreduction of Cu^{2+} to Cu^{+}, the formation of which being confirmed by a colorimetric assay using 4,7-dpphen as indicator.

The cleavage activity of the copper complexes with phen suggested that conjugation of oligonucleotides or DNA binding proteins to this heteroaromatic unit could provide opportunities to combine together the sequence recognition properties of these

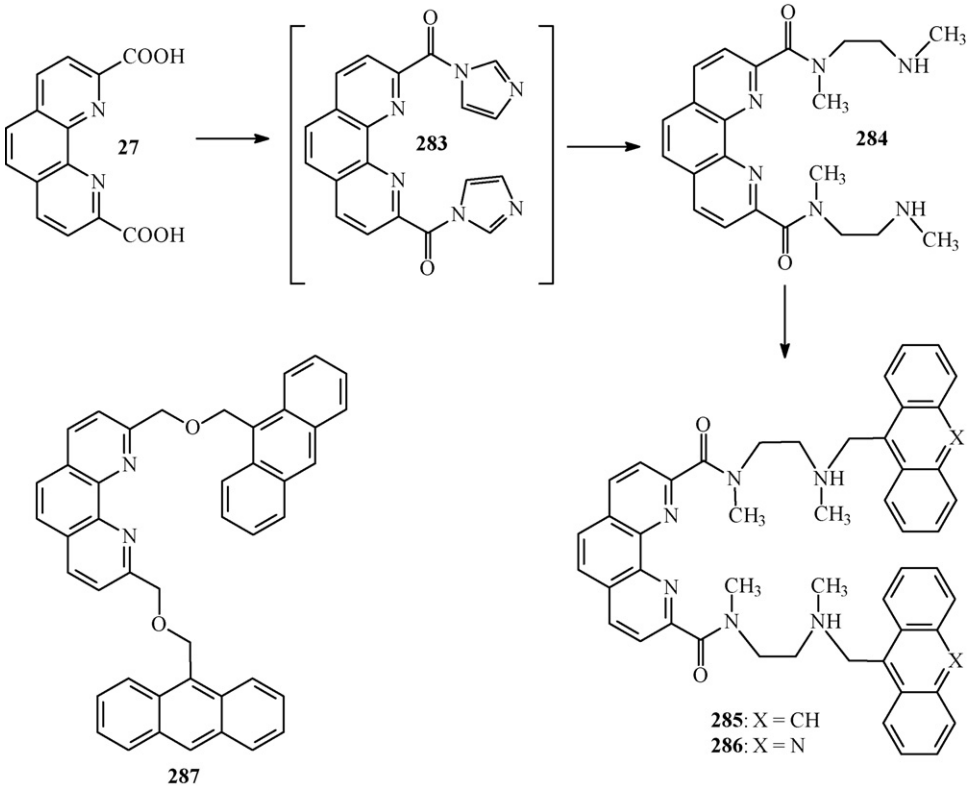

Scheme 99.

macromolecules with the cleavage properties of phen upon copper binding.

In the eighties and nineties, phen has been tethered to a variety of oligonucleotides [278–280]. In most cases, phen was attached to DNA/RNA strand through the 5′ end of oligonucleotides, using various synthetic pathway, the most common being reaction of 5′-phosporothioate with 5-iodoacetamido-1,10-phenanthroline [345,346]. However, examples of phen derivatives linked to the nucleobases, such as guanine [347] or uridine [348,349], have also been reported. It was found that the length of the linker and the position of linkage may play an important role in the efficiency and accuracy of the target cleavage [350–353]. Similarly, phen has also been covalently bound to DNA binding proteins, tethering phen to a native cysteine within a DNA binding protein, or to a cysteine introduced within the protein structure. This procedure generally involves the covalent linking of a 5-acetoamido-1,10-phenanthroline or a 5-acetylglycylamido-1,10-phenanthroline to the sulfur atom of a cysteine residue [280,354]. The protein or oligonucleotide conjugates were used not only to achieve specific cleavage of DNA sequences [350,354–358], but also to investigate the ribosomal machinery [345,346,349,359–361], to elucidate DNA structures [362], to develop antisense oligonucleotides [363,364] or to achieve structural information on the protein–DNA complexes [365–371].

This work has been reported in several reviews [278–280,345,358,372] and will not be further discussed.

5.2. Ruthenium, osmium and rhodium complexes with phenanthroline derivatives

The binding features of the octahedral *tris*(phen) complexes with transition metal ions, such as Ru^{2+}, Zn^{2+} and Co^{3+}, toward DNA were substantially elucidated by Barton [373–379]; her work will only be briefly discussed here. These complexes can bind DNA either *via* hydrophobic and van der Waals interactions within the minor groove or through partial intercalation of a phen unit into the helix in the major groove. More interestingly, these chiral complexes display enantiomeric preferences for one of these binding modes [380]. For instance, in the case of the complex $[Ru(phen)_3]^{2+}$ (**288**) the right-handed Δ-isomer, preferentially binds to DNA *via* intercalation into the right-handed B-DNA, while DNA binding within the minor groove is preferred by the Λ-isomer (Scheme 100).

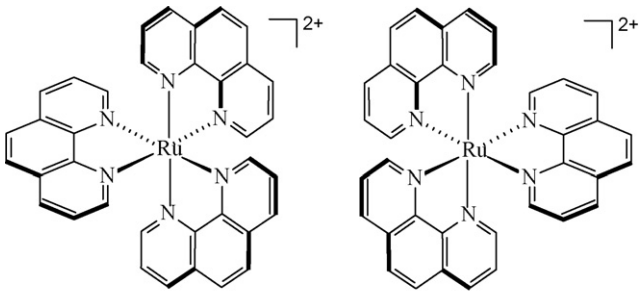

Scheme 100.

Metal centres coordinated to more sterically demanding phen-based ligands, such as 4,7-dpphen, display more marked chiral discrimination [381]. In fact, while Δ-$[Ru(4,7\text{-dpphen})_3]^{2+}$ (Δ-**289**) (Scheme 101) binds enantiospecifically to right-handed B-DNA, the Λ-enantiomer of this complex binds only to the left-handed Z-DNA. Chiral discrimination of this type clearly depends on matching the symmetry of the metal complex with that of the DNA double helix. Considering the peculiar photophysical and redox properties of *tris*(phen) complexes with several metal cations, such as Ru^{2+} or Rh^{3+}, these complexes appeared promising tools to develop new probes for DNA. Nevertheless, their binding affinity for DNA was not impressive and the possibility of different binding modes resulted problematic for their use as DNA probes. These problems were overcome by Barton and co-workers by using new metal complexes bearing at least one strongly intercalating ligand, *i.e.*, metallointercalators containing an expanded aromatic heterocyclic ligand, which can readily allow π-stacking interactions within the DNA double helix. Two well-known examples are dipyrido[3,2-*a*:2′,3′-*c*]phenazine (dppz, see complex **290** in Scheme 101) [382–388], and 9,10-phenanthrenequinone diimine (phi, see complex **291** in Scheme 101) [389–396]. These ligands behave as stable anchors for the corresponding metal complexes with respect to the DNA duplex, and direct the orientation of the other ancillary ligands with respect to the DNA duplex. Different ancillary ligands were used, including bpy [382–384], phen [385–388], NH_3 [391] and aliphatic di- and tetraamines [390,392–396]. Our discussion will be limited to metallointercalators containing phen and its derivatives as ancillary ligands.

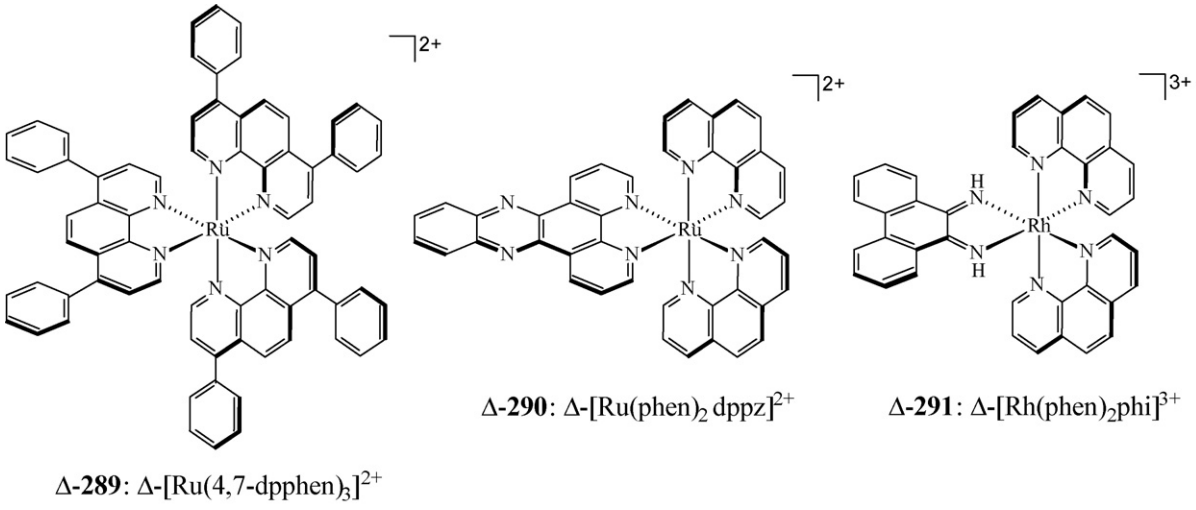

Scheme 101.

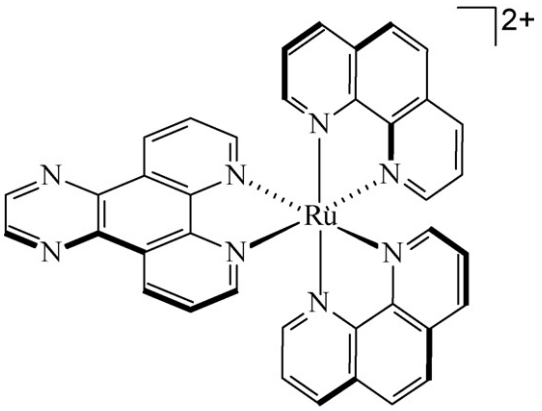

Δ-**292**: Δ-[Ru(phen)$_2$dpq]$^{2+}$

Scheme 102.

Taking advantage from their peculiar photophysical properties, the Ru^{2+} complexes were advantageously used to probe their interaction with DNA. The most studied example is probably the molecular light switch complex $[Ru(phen)_2(dppz)]^{2+}$ (**290**) [385–388]. This complex shows solvatochromic luminescence in organic solutions. In aqueous solutions, however, it does not show luminescence emission because of deactivation of the excited state by water through hydrogen-bonding with the endocyclic nitrogen atoms of the intercalating ligand or quenching by molecular oxygen. Renewal of the fluorescence emission takes place upon the addition of double stranded DNA. In fact, the metal complex intercalates into the DNA, and the surrounding duplex prevents water from gaining access to the intercalated ligand. In this condition, the metal complex can display again its characteristic luminescence emission band centred at 620 nm [382,397,398]. A similar behaviour was also found for the corresponding Os^{2+} complex $[Os(phen)_2(dppz)]^{2+}$, which gives rise to a band at 738 nm upon binding to DNA, behaving as a red-emitting luminescent reporter for the presence of DNA [399].

Like $[Ru(phen)_3]^{2+}$, $[Ru(phen)_2(dppz)]^{2+}$ is chiral. The binding mode of the two enantiomers has been subject of discussion. On the basis of both photophysical studies and NMR data, Barton and co-workers proposed that Δ- and Λ-$[Ru(phen)_2(dppz)]^{2+}$ enantiomers intercalate within the DNA major groove [388,400,401]. Nordén and co-workers, on the basis of the similarity of the binding geometry to that of actinomycin D and photophysical studies using T4-DNA, proposed that both Δ- and Λ-$[Ru(phen)_2(dppz)]^{2+}$ intercalate within the minor groove [385,402]. Similarly, Aldrich-Wright suggested that the metal complex Δ-$[Ru(phen)_2dpq]^{2+}$ (Δ-**292**) (dpq = dipyrido[3,2-f:2′,3′-h]quinoxaline, Scheme 102), which is closely related to Δ-$[Ru(phen)_2(dppz)]^{2+}$ (Δ-**290**) intercalates within the minor groove of a hexanucleotide [403,404].

While Ru^{2+} complexes with dppz behave as molecular light switches for the detection of DNA, Rh^{3+} complexes with phi, such as $[Rh(phen)_2(phi)]^{3+}$ (**291**), can be efficient agents for photoactivated DNA strand cleavage [405]. It was proposed that UV irradiation of $[Rh(phen)_2(phi)]^{3+}$ leads to the generation of a radical on the phi ligand *via* ligand-to-metal charge-transfer. The ligand radical then can abstract a deoxyribose hydrogen atom easily accessible from the major groove (H-3′ or H-2′). As a result, the sugar radical would degrade, leading to DNA strand cleavage. Detailed analysis of the degradation products obtained both in the absence and in the presence of O_2 lead initially to propose abstraction of the H-3′ hydrogen. However, successive ^{1}H NMR and crystallographic studies indicated a close association between the phi ligand and the C-2′ position, rather than the H-3′ one. It was suggested, therefore, that the initial reaction of the photoexcited intercalator occurs *via* abstraction of the H-2′ hydrogen followed by H-migration to form the C-3′ radical with subsequent degradation [405].

Of note, photocleavage of the DNA strands enables to individuate directly the site of intercalation and to characterize the recognition properties of the intercalating agent. For instance, it was found that **291** cleaves preferentially the 5′-Py-Py-Pu-3′ sites (Py = pyrimidine base, Pu = purine base) and, at to a less extent, the 5′-Pu-Py-Pu-3′ sequences, but never the 5′-Pu-Pu-Py-3′ ones. The complex $[Rh(bpy)_2(phi)]^{3+}$, bearing two less hindered bpy units cleaves DNA with lower selectivity. Barton and co-workers attributed these recognition properties to the overall shape of the complex $[Rh(phen)_2(phi)]^{3+}$ (**291**). In fact, this complex preferentially intercalates at sites with high propeller twisting toward the major groove [405,406], which possess a shape that is complementary to that of the host complex. Opening of the major groove in correspondence of the 5′-Py-Py-Pu-3′ sequence reduces the steric hindrance between the ancillary phen ligands and the major groove, thus enabling deeper intercalation of the metal complex. The Δ isomer of $[Rh(phen)_2(phi)]^{3+}$ (Δ-**291**) was more reactive at the 5′-Py-Py-Pu-3′ site, due to its better fitting within this interaction site. Conversely, in the case of the 5′-Pu-Pu-Py-3′ sequence, the reduced propeller twisting at this site creates a more sterically confining major groove. As a consequence, the increased steric hindrance between the phen units and the groove pushes the intercalating phi ligand farther away from the DNA helical axis, reducing the overall binding affinity of the complex.

5.2.1. Ru^{2+} complexes with functionalized phenanthroline ligands for DNA binding and/or fluorescence sensing

The ability of $[Ru(phen)_2dppz]^{2+}$ (**290**) to act as fluorescent probe has lead to the synthesis of a number of ruthenium(II) complexes containing different intercalating units, mostly dppz-analogues. The analysis of their binding and luminescence properties, recently overviewed by Liu and co-workers [407], are outside the purposes of the present review. Our attention will be devoted to Ru^{2+} complexes with ligands containing the phen unit developed for DNA binding and/or sensing.

One of the strategy to increase the binding ability of polypyridyl-Ru^{2+} complexes is the derivatization of one of the Ru^{2+}-bound heteroaromatic ligands with a pendant arm containing a second binding moiety with high affinity for DNA. Kirsch-De Mesmaeker and co-workers synthesized a $[Ru(bpy)_2phen]^{2+}$ complex tethered through an aliphatic chain to 4-aminomethyl-7-chloroquinoline, a note DNA groove binder [408].

Ligand **295** was synthesized by reaction of the thiol derivative **294** with 5-iodoacetamidophenanthroline **293** (Scheme 103). **294** was obtained starting from **297**, according to a well established procedure [409]. Reaction of $[Ru(bpy)_2]Cl_2$ with **295** and **297** afforded the functionalized complex **296** and **298**, respectively [410].

The binding ability toward calf thymus DNA of the difunctional complex **296** was analyzed by means of UV–vis, steady-state and time-resolved fluorescence emission measurements and compared with that of the monofunctional analogues, $[Ru(bpy)_2phen]^{2+}$, complex **298** and 7-chloro-4-[*N*-(2-hydroxyethyl)-*N*-methylamino]quinoline (**299** in Scheme 103) [411]. The authors found that the difunctional complex **296** displays a binding affinity for DNA one order of magnitude higher than that of $[Ru(bpy)_2phen]^{2+}$, **298** or **299**, to indicate that both metal complex and quinoline play a cooperative role in DNA binding. The photophysical study of the adduct between **296** and DNA accounted for an "internal" binding mode of quinoline, involving interaction of the heteroaromatic rings with the nucleobases. The available data, however, were not conclusive on the exact nature of this interaction, which could take place either *via* simple groove binding or intercalation (or both). More interestingly, it

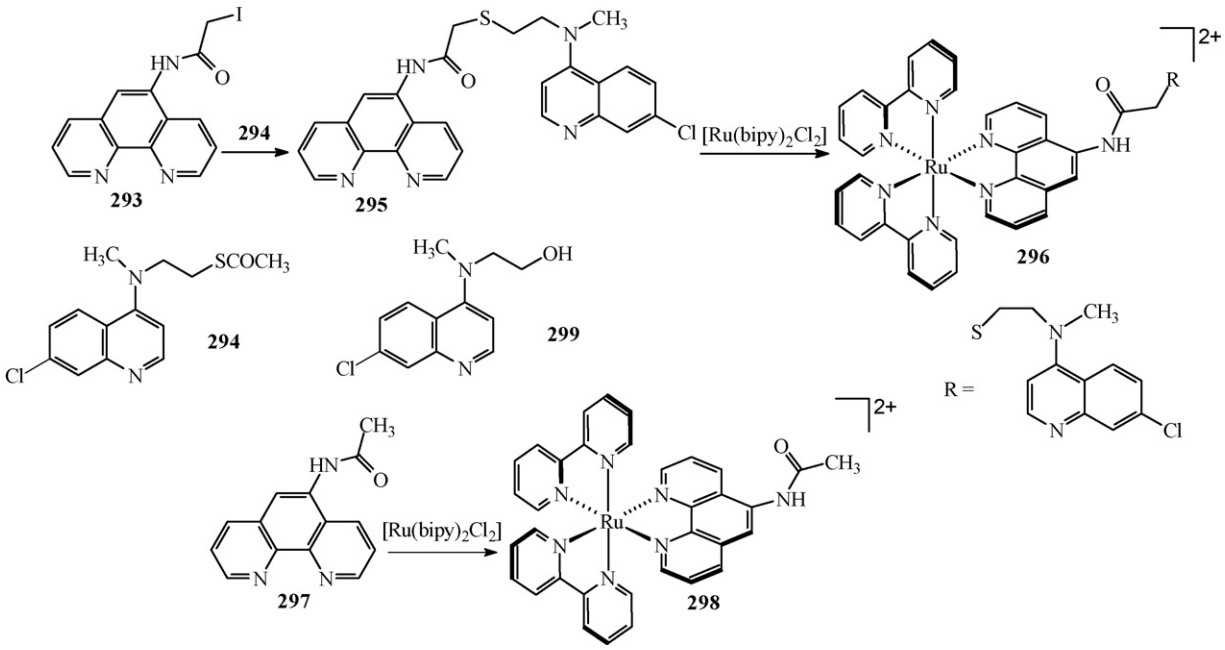

Scheme 103.

was observed the amine group in 4-position of the quinoline unit protonates at neutral pH, thus reinforcing the overall **296**–DNA interaction, although the pK_a value for the protonation process is only 6.1. The authors suggested that the observed protonation would occur upon DNA binding, thanks to the presence of acidic domains, *i.e.*, local increases in H^+ concentrations, in nucleic acids. Conversely, the metal complex moiety of **296** binds to DNA in an "external" mode, *i.e.*, essentially *via* electrostatic interactions with the negatively charged double helix.

$[Ru(bpy)_2(phen)]^{2+}$ complexes coupled to an adenine unit *via* an ethynyl or a phenyl bridge have also been synthesized as potential model compounds for electrochemical DNA labelling. Although their binding features toward DNA/RNA were not tested, they displayed cytotoxic activity against the hepatitis C virus [412].

Several dinuclear ruthenium(II) complexes containing two $[Ru(phen)_x(a)_y]^{2+}$ (a = dppz or dppz analogue, $x = 1$ or 2, $y = 1$ or 2) linked by flexible or rigid spacers have also been synthesized. In most cases the two complex units were linked through flexible or rigid bridges connecting two dppz units [413–426]. Conversely, Aldrich-Wright and co-workers reported the synthesis of symmetrical homometallic Ru^{2+} dinuclear complexes containing two $[Ru(phen)(dpq)_2]^{2+}$ units with a flexible 2-mercaptoethyl ether linker connecting the 3-, 4- or 5-position of two ancillary phen ligands (see Scheme 104 for the dinuclear complex **300** bridged at the 5-position of two phen units) [427,428].

To achieve these complexes, the mononuclear complexes $[Ru(L)(dpq)_2]Cl_2$ (L = 3-bromo-1,10-phenanthroline, 4-chloro-1,10-phenanthroline or 5-chloro-1,10-phenanthroline) were first synthesized by reaction of $[Ru(dpq)_2Cl_2]$ with the appropriate phen derivative. The resulting racemic mixtures were resolved by selective extraction of the diastereisomer salts of the Δ- and Λ-$[Ru(L)(dpq)_2]^{2+}$ enantiomers with the Λ- and Δ-[(*tris*(tetrachlorocatecholato)phosphate(V))]$^-$ anion, according to the technique of Lacour and co-workers [429]. Reaction of the Δ- and Λ- $[Ru(L)(dpq)_2]^{2+}$ enantiomers with *bis*(2-mercaptoethyl) ether in the presence of NaH afforded a mixture consisting of 25% of each of the two homochiral enantiomers, ΔΔ and ΛΛ, and of 50% of the meso (ΔΛ/ΛΔ) diastereoisomer, which were separated with the same method used for the mononuclear complexes [428]. Preliminary results on the binding affinity of racemic mixtures of the three dinuclear complexes showed that all complexes display a binding affinity for calf thymus DNA higher than the mononuclear

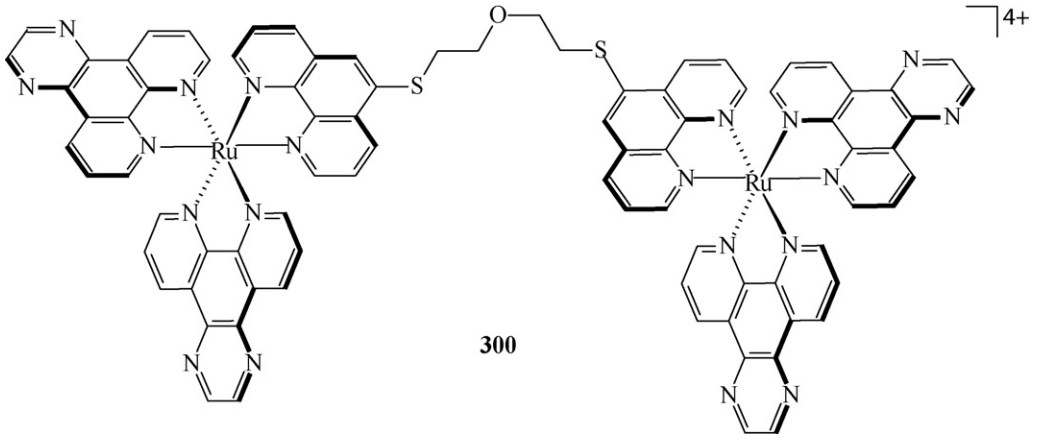

Scheme 104.

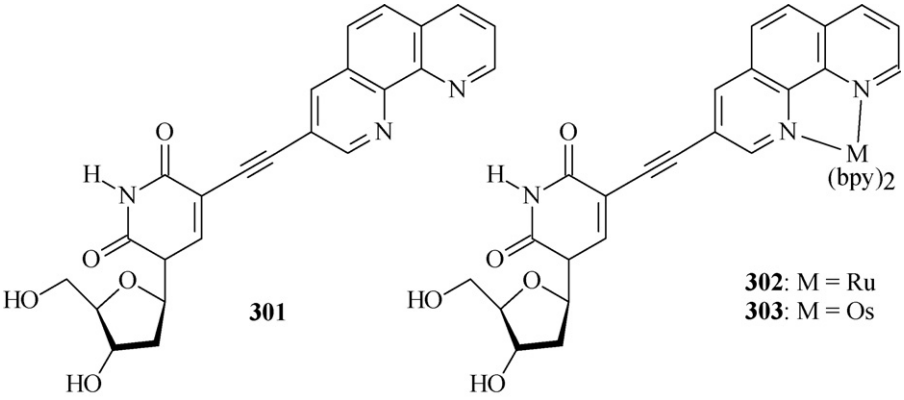

Scheme 105.

complex $[Ru(phen)(dpq)_2]^{2+}$, thanks to the beneficial effect of two metallo-intercalating units. Among the three dinuclear complexes, the dimer **300** gave the strongest interaction [427].

The phen-containing nucleosides **301**–**303** (Scheme 105) as "reporter" probes for the local environment of the DNA double helix have been prepared by Tor and co-workers following a convergent approach whose key step is the Sonogashira cross-coupling reaction between 5-ethynyldeoxy-uridine and **131** (Scheme 50) and $[(bpy)_2M(\mathbf{131})]^{2+}$ (M = Ru, Os), respectively, in the presence of $[(dppf)PdCl_2]\cdot CH_2Cl_2$, CuI, and DMF/$Et_3N$ [430–432].

301–**303** have been engineered into modified single-stranded oligonucleotides and DNA double helices whose thermal stability is dependent on the number and position of the modified deoxy-uridine bases as well as on the sequence composition of the oligonucleotides [430–432]. In particular, the fluorescent emission of free **301** and of single-stranded oligonucleotides containing **301** [$\lambda_{em} \cong 407$ nm] is different from that observed when **301** is incorporated into DNA duplex [$\lambda_{em} \cong 385$ nm] in agreement with a different environment experienced by the fluorescent nucleoside within the single- and double-stranded systems. Furthermore, the I_{407}/I_{305} fluorescence intensity ratio monitored during thermal denaturation of DNA duplexes internally modified with **301**, resulted dependent on the nature of the nucleotide opposite to the fluorescent base, thus allowing to recognize mismatched complementary oligonucleotides [430]. Differences were also observed between Ru^{2+} and Os^{2+} single-stranded oligonucleotides and complementary DNA duplexes. In particular, when compared to single strand oligonucleotides, an 8–15% decrease was observed in the steady-state emission intensity upon hybridization of ruthenium(II)- and osmium(II)-containing oligonucleotides to a complementary strand. This lower luminescence intensity depends on the sequence and position of the emitting nucleotide within the duplex and it has been attributed to an increased electronic coupling of the metallated base with the complementary guanine residue within the base pair stack, and consequent quenching of the excited state [432].

Ihara and co-workers anchored $[Ru(phen)_3]^{2+}$ and $[Ru(phen)_2dppz]^{2+}$ to the oligonucleotide 5′-CCCTAA-3′ (Scheme 106) [433]. This sequence is complementary to one unit of the repetitive sequence of human telomere (5′-TTAGGG-3′). The tethering of the complexes was carried out by reaction of the 5′-aminohexyl-linked oligonucleotide with the corresponding *N*-hydroxy-succinimide ester of 5-carboxy-1,10-phenanthroline (**113** in Scheme 41) to afford equimolecular mixtures of the Δ and Λ isomers, which were separated by HPLC using a chiral column. The authors found that the two conjugates Δ-**304** or Δ-**305** cooperatively recognize the oligomer **307**, containing two complementary sequences of bases, affording the assemblies (Δ-**304**)$_2$**307** or (Δ-**305**)$_2$**307**, respectively. The "tandem duplexes" (Δ-**305**)$_2$**307** and, to a lesser extent, (Δ-**304**)$_2$**307** were more stable than the corresponding single duplexes (Δ-**305**)**306** and (Δ-**304**)**306**. Conversely, the two isomers Λ-**304** or Λ-**305** afforded "tandem duplexes" with stabilities comparable to those of the corresponding single duplexes.

The higher stability of the (Δ-**305**)$_2$**307** "tandem duplex" was explained considering that in the (Δ-**305**)$_2$**307** assembly the $[Ru(phen)_2(dppz)]^{2+}$ complex unit of one **305** conjugate, located at the centre of the "tandem duplex", can either intercalate within the TT/AA base pairs located at the end of the duplex formed by the second **305** conjugate or intercalate between the GG/CC base pairs belonging to its own tethered hexanucleotide unit. The former binding mode is preferred because of the higher tendency of the $[Ru(phen)_2(dppz)]^{2+}$ complex to intercalate within A/T base pairs, rather than within G/C base pairs [400]. Conversely, in (Λ-**305**)$_2$**307** the Ru^{2+} complex would bend backward to intercalate within the GG/CC base pairs belonging to its own hexanucleotide unit. Therefore, Δ-**305** stabilizes the "tandem duplex" thanks to dppz intercalation within the nucleobases of the adjacent duplex [433].

5.2.2. Rh^{3+} and Ru^{2+} complexes with functionalized phenanthroline ligands for binding and cleavage of specific DNA sequences

Beside the shape of the cleaving metal complex, functionalization of the ancillary ligands with appropriate DNA binding moieties has often been used to achieve selective recognition of different specific sequences. The first example is offered by the complex $[Rh(gmp)_2phi]^{5+}$ (**308**) (Scheme 107), where gmp = 4-(guanidylmethyl)-1,10-phenanthroline [434–436]. The guanidium moieties were introduced to recognize more complex specific base sequences than $[Rh(phen)_2(phi)]^{3+}$ (**291**), in particular sequences containing flanking guanines. In fact, these nucleobases can use their O6 and N7 atoms, located within the major groove, to form hydrogen bonds contacts with the guanidinium units. 4-(Guanidylmethyl)-1,10-phenanthroline was obtained by reaction of 2-methyl-2-thiouronium hydrogen sulfate with 4-aminomethyl-1,10-phenanthroline, prepared from 4-methyl-1,10-phenanthroline using the procedure developed by Chandler [67]. The complex $[Rh(gmp)_2phi]^{5+}$ (**308**) was then obtained in a one-pot synthesis by treatment of rhodium trinitrate with gmp and phi [434]. As expected, the reaction afforded three different geometrical isomers (Scheme 107), differing in the relative positions of the two guanidylmethyl arms, which were separated by reverse phase HPLC. Each isomer exists as an equal mixture of two enantiomers. Their separation was achieved initially by using a reverse phase chiral

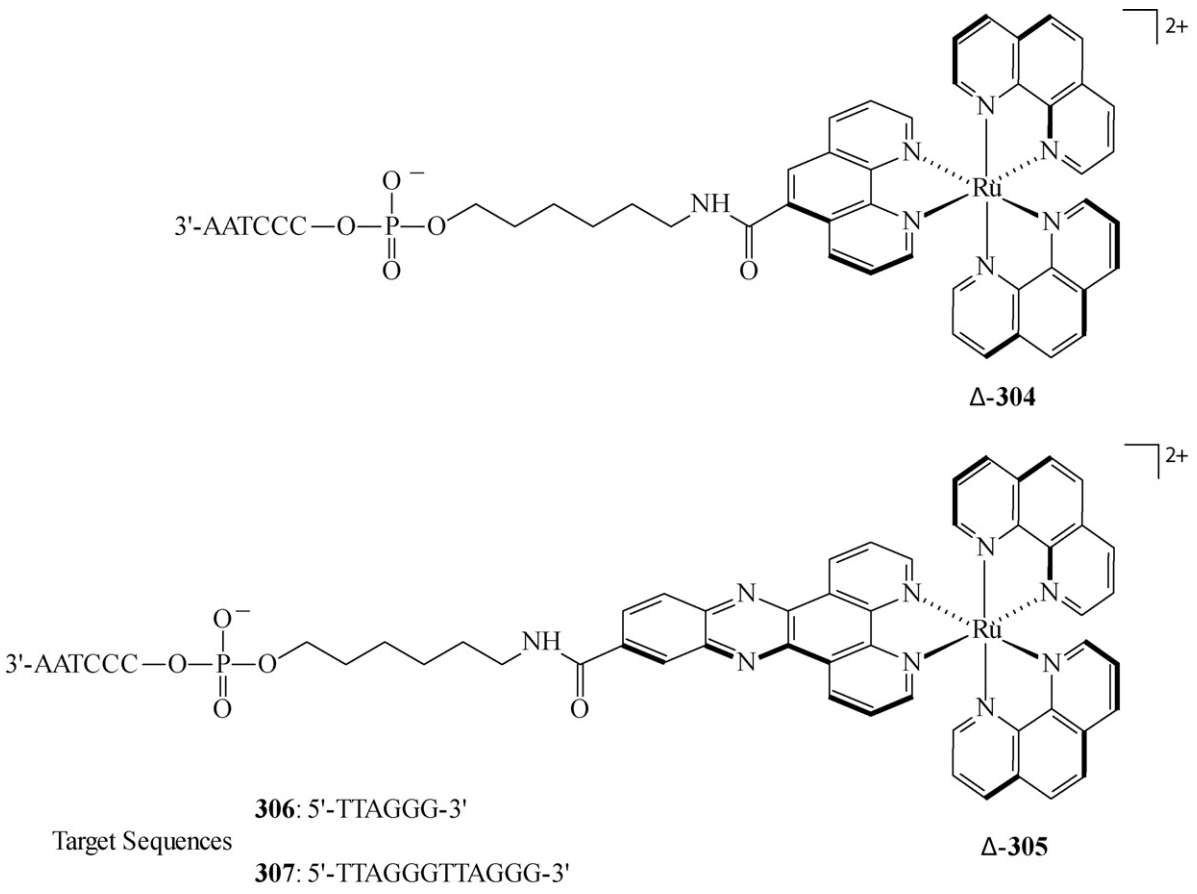

Scheme 106.

HPLC column. Interestingly, the authors were also able to separate the initial mixture of six isomers (3 geometrical isomers, each with 2 enantiomers) by cation exchange chromatography using a chiral eluant ((+)-potassium antimonyl tartrate) [434].

Among the geometrical isomers, only complex 1-**308** contains two guanidinium moieties directed above and below the intercalating units or, when intercalated, oriented towards DNA. Actually, the right-handed Δ-1-**308** isomer specifically binds and cleaves the sequence 5′-CATCTG-3′ (cleavage at the C base); this site represents one of the family of sites targeted by Δ-[Rh(phen)$_2$phi]$^{3+}$ (Δ-**291**), and, at the same time, contains flanking G bases. The recognition is accomplished not only by complementing the shape of the major groove, like with Δ-[Rh(phen)$_2$phi]$^{3+}$ (Δ-**291**), but also by hydrogen-bonding with the flanking 3′-G base. ^{1}H and 2D-NOESY experiments by using the decamer 5′-CGCATCTGAC-3′ → 3′-CAGTCTACGC-5′ showed that the Δ-1-**308** complex binds to its 6-bp recognition site in two different conformations, slowly exchanging on the NMR time scale (Fig. 33), each of which allows one guanidinium-guanine hydrogen bond at time and brings the other guanidinium side arm close to the anionic phosphate backbone [434,435].

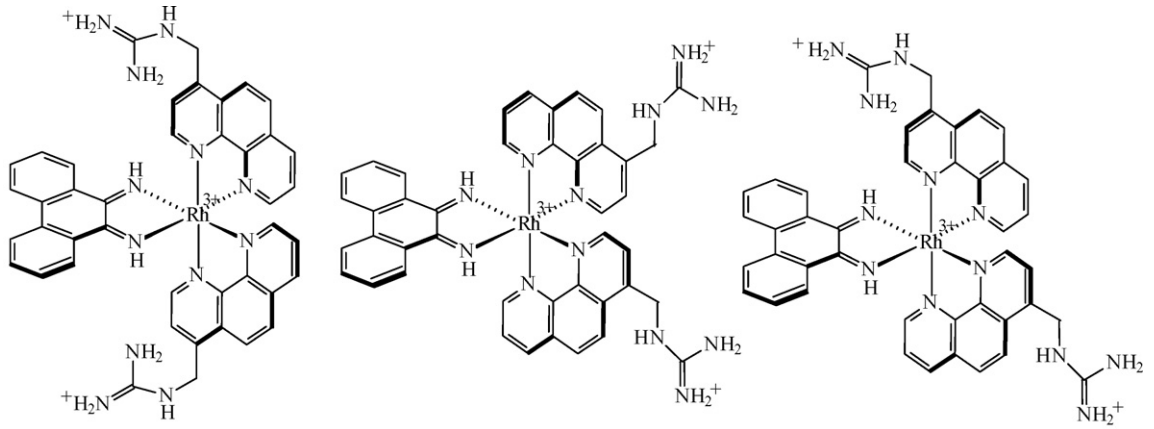

Scheme 107.

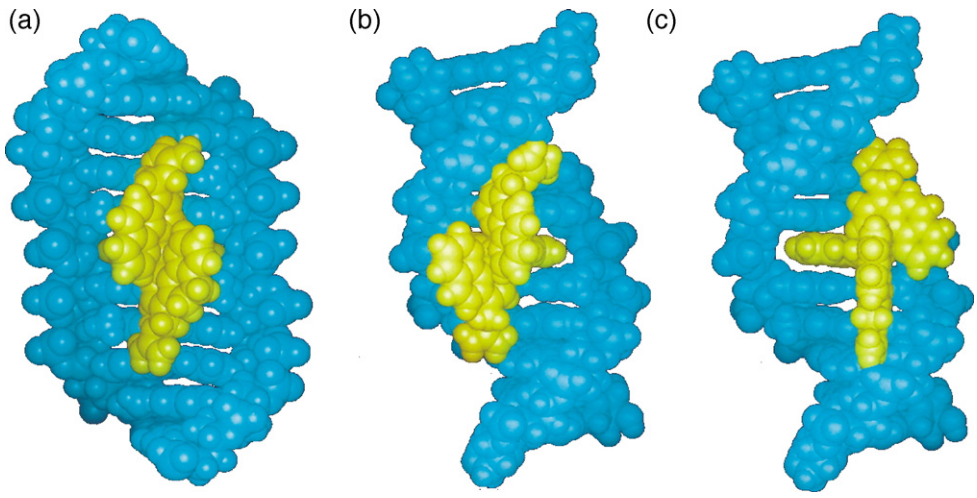

Fig. 33. Models of Λ-1-**308** (a) and Δ-1-**308** (b and c) intercalated into their respective recognition DNA sites (from Ref. [422]). Δ-1-**308** is shown in its two possible conformations (b and c). This figure is taken from [435] and adapted with permission; copyright 1998, by The American Chemical Society.

Conversely, the Λ-1-**308** isomer was able to specifically bind and cleave a slight different DNA sequence (5′-CATATG-3′) at remarkably lower concentration than the other isomers and than $[Rh(phen)_2(phi)]^{3+}$ [436]. However, the left-handed Λ-1-**308** complex cannot passively enter the major groove of the right-handed B-DNA. Actually, binding of Λ-1-**308** implies unwinding of B-DNA up to 70°, making the 5′-CATATG-3′ sequence accessible to the complex. Considering the interaction mode of Λ-1-**308**, the complex can simultaneously intercalate at the centre of the 5′-CATATG-3′ sequence and interact *via* hydrogen-bonding with the flanking G base at the first and six positions of the sequence (Fig. 33) [435,436].

With the aim to explore whether the side-chain functionalities of small peptides may be used to enhance metal complex recognition, Barton and co-workers also attached to the $[Rh(phi)_2phen]^{3+}$ complex two families of oligopeptides (13 and 14 residues, respectively) [437–439], in order to investigate the recognition properties of selected sequences of amino acids. It is known that DNA binding proteins generally use a significant percentage of their amino acids to provide a scaffold with high affinity, but scarce specificity, for DNA. Conversely, only a limited number of amino acids contact the base pairs directly and ensures site-specificity. Therefore, the oligopeptide sequences chosen were derived from the region of a DNA binding protein that directly contacts the DNA base pairs. In particular, Barton and co-workers chose to investigate the recognition ability of the small α_3 helix (eight residues) belonging to phage 434 repressor protein, known for its ability to bind to DNA, and therefore synthesized a series of conjugate complexes containing oligonucleotides derived from this binding moiety of the protein. The complex-oligonucleotide conjugates (see Fig. 34) were prepared individually on a solid support (Pam resin) either by coupling of the complex $[Rh(phi)_2(5\text{-}(amidoglutaryl)\text{-}1,10\text{-}phenanthroline)]^{3+}$ with the terminal amine group of oligonucleotides or by coordination of the precoupled phen derivative with $[Rh(phi)_2(DMF)_2]^{3+}$ [437].

It was found that the conjugates bind and cleave DNA upon photoactivation, and partially confer to the $[Rh(phi)_2phen]^{3+}$ complex the sequence selectivity of the parent protein [435,436]. In fact, some of the oligopeptides, when tethered to the metal complex, displayed highly selective recognition of the 5′-CCA-3′ sequences. Actually, the highest site specificity was observed with

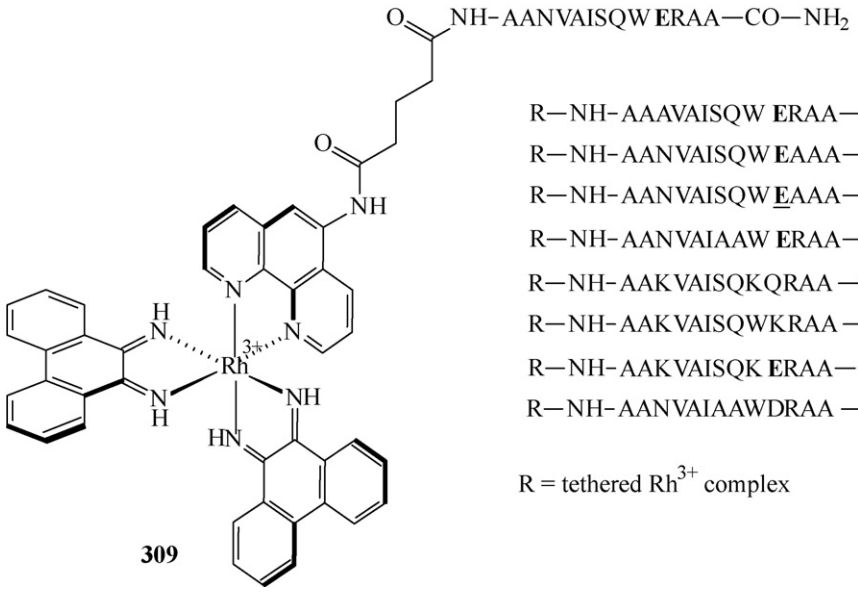

309

R—NH-AAAVAISQW **E**RAA—CO—NH_2 **310**
R—NH-AANVAISQW **E**AAA—CO—NH_2 **311**
R—NH-AANVAISQW **E**AAA—CO—NH_2 **312**
R—NH-AANVAIAAW **E**RAA—CO—NH_2 **313**
R—NH-AAK VAISQK QRAA —CO —NH_2 **314**
R—NH-AAK VAISQWK RAA —CO —NH_2 **315**
R—NH-AAK VAISQK **E**RAA—CO—NH_2 **316**
R—NH-AANVAIAAWDRAA —CO —NH_2 **317**

R = tethered Rh^{3+} complex

Fig. 34. Examples of conjugate complexes, with glutamate in 10-position in boldface. The underlined glutamate in **312** contains the carboxylate group derivatized as methyl ester [437].

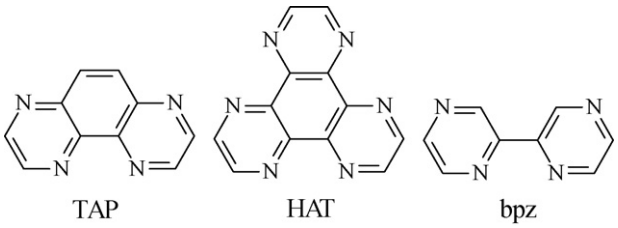

Scheme 108.

the conjugate $[Rh(phi)_2phen]^{3+}$-AANVAIAAWERAA-$CONH_2$ (**313**). Interestingly, the presence of a glutamate residue E at the 10-position is necessary to direct DNA site recognition to the sequence 5′-CCA-3′ [437]. Selectivity is lost upon derivatization of glutamate in 10-position to its methyl ester (complex **312** in Fig. 34) as well as when glutamate is replaced by isostere glutamine or by aspartate (the amino acid with a side chain shortened by one methylene), whereas systematic mutation of amino acid residues other than glutamate in 10-position did not significantly alter the sequence selectivity of the conjugates (complexes **310**, **311**, **313** and **316** in Fig. 34). Conversely, diminished specificity was observed with mutations that reduce the helical content of the peptide. From these results, it was suggested a "glutamate switch" model for 5′-CCA-3′ recognition by these conjugates [437,438]. In fact, it was suggested that glutamate in 10-position confers high helical content on the peptide and establishes specific interactions with DNA, in particular a hydrogen-bonding contact with the 4-amino group of cytosine.

Interestingly, a photocleavage study carried out moving the glutamate from the 10-position to other positions of the 13-membered oligonucleotide showed that selectivity for a determined DNA sequence is also achieved when glutamate is located in the 6-position. In fact, the $[Rh(phi)_2phen]^{3+}$-AANVAEAAWARAA-$CONH_2$ conjugate targets the 5′-ACA-3′ DNA sequence, thanks to the still present helical character of the conjugate and to hydrogen-bonding between glutamate and cytosine. Conversely, different localization of glutamate within the oligopeptide chain lead to cleavage patterns similar to that of the simple $[Rh(phi)_2phen]^{3+}$ complex [439].

Beside Rh^{3+}, Ru^{2+} complexes have also been used to induce photocleavage of DNA. The most famous examples are Ru^{2+} complexes with strongly electron-deficient heteroaromatic ligands such as TAP (1,4,5,8-tetraazaphenanthrene), HAT (1,4,5,8,9,12-hexaazatriphenylene) or bpz (2,2′-bipyrazine) (Scheme 108).

Like in $[Ru(phen)_3]^{2+}$, irradiation of $[Ru(TAP)_3]^{2+}$ or $[Ru(HAT)_3]^{2+}$ produces a metal-to-ligand charge-transfer, giving rise initially to a MLCT singlet excited state, which rapidly deactivate to the lower energy MLCT triplet state [440–442]. Like

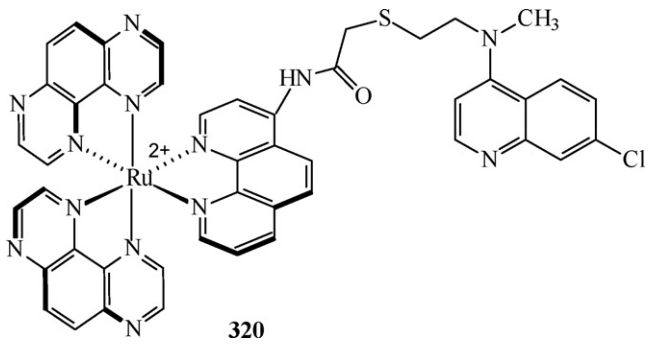

Scheme 110.

in $[Ru(phen)_3]^{2+}$, the fluorescence of the complex $[Ru(TAP)_3]^{2+}$ is renewed in the presence of $[poly(dA\text{-}dT)]_2$, due to the protective effect of the DNA environment on the excited state of the complex. Conversely, the fluorescence emission of $[Ru(TAP)_3]^{2+}$ is efficiently quenched in the presence of $[poly(dC\text{-}dG)]_2$ [443].

The origin of this effect was clarified by the extensive work of Kirsh-De Mesmaeker and co-workers on Ru^{2+} complexes with electron-poor heteroaromatic ligands [444]. The quenching effect in the presence of G-containing polynucleotides was attributed to a photoelectron transfer from G bases to the excited state of the complex. This process generates a G radical cation and is generally followed by a back electron transfer from the complex to the G radical [444]. The process occurs mainly with G moieties of polynucleotides (the most reducing base) and the complexes containing at least 2 π-deficient ligands, such as 2 TAP, 2 HAT or 3 bpz ligands. However, other events can compete with the back electron transfer from guanine. As observed with DNA plasmids [444,445], the guanine radical cation generated by electron transfer can react with a sugar moiety, leading to its demolition and generating single-strand breaks followed by double strand breaks. Alternatively, the G base can react upon photoirradiation directly with the heteroaromatic units of the complex, with the formation of a covalent bond between the amine group of the nucleobase and a carbon atom of the ligand (complex **319** in Scheme 109) [446]. In fact, the formation of covalently linked photoadducts has been observed in the case of complexes containing TAP, HAT or bpz ligands [447–449] upon photoirradiation in the presence either of mononucleotide 5′-GMP or of G-containing polynucleotides [450].

These properties make this type of complexes promising probes for the study of the DNA structure, and for their potential effects on DNA functions, such as gene transcription and replication. Complex $[Ru(TAP)_2$**295**$]^{2+}$ (**320**) (Scheme 110) represents an example of photocleaving agent used as DNA probe.

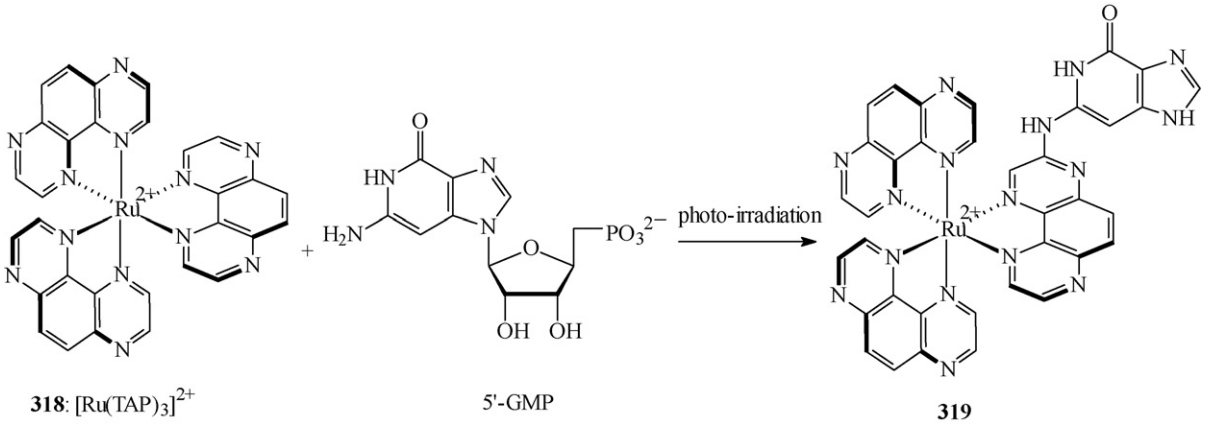

318: $[Ru(TAP)_3]^{2+}$ 5'-GMP **319**

Scheme 109.

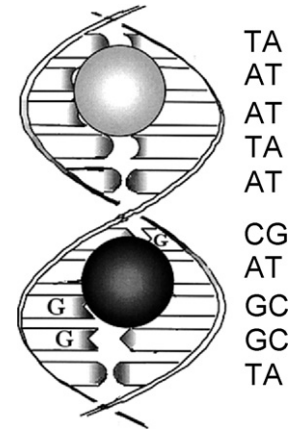

Fig. 35. Luminescence properties of complex **320** in the presence of different base sequences (dark sphere: quenched complex; bright sphere: emissive complex) [451].

The complex was prepared by using the same procedure used for the preparation of **296** (see Scheme 103) [410] and its binding mode and luminescence properties were analyzed in the presence of calf thymus DNA, Poly(dC-dT)·Poly(dC-dT) and Poly(dA-dT)·Poly(dA-dT). The interaction mode with DNA was similar to that reported for the analogous dipyridine complex **296** [411]. In fact, the quinoline pendant arm protonates upon DNA binding and interacts with DNA *via* groove binding or intercalation. Conversely, a fraction of the Ru^{2+}-based moieties interacts externally to the groove, while a second fraction is inserted into the groove. More interestingly, the complex displayed different luminescence properties in the presence of Poly(dC-dT)·Poly(dC-dT) and Poly(dA-dT)·Poly(dA-dT). In fact, while an intense emission with long emission lifetime was observed in the presence of Poly(dA-dT)·Poly(dA-dT), a very weak emission with short lifetime was found with Poly(dC-dT)·Poly(dC-dT), in agreement with an electron transfer process from guanine to the metal centre, which quenches the emission of the fluorophore [451]. Therefore, this complex represents a case of a "light switch" with selective luminescence emission in the presence of AT sequence, as sketched in Fig. 35.

The complexes $[Ru(TAP)_2phen]^{2+}$ and **320** were also tested as "*in vitro*" inhibitor of gene expression of a target plasmid vector transcribed by a bacteriophage RNA polymerase [452]. The two complexes display similar photooxidizing power but different DNA binding ability. In fact, **320** is a stronger DNA binder, thanks to the beneficial effect of the appended quinoline, an additional binding site for DNA. The inhibition activity of the complex $[Ru(bpy)_2phen]^{2+}$, which is unable to give photoadducts with G bases, was also tested for comparison. It was found that $[Ru(TAP)_2phen]^{2+}$ and **320** significantly reduce the transcription rate of a RNA polymerase activity to around 50% upon irradiation, while no inhibition effect was observed in the dark. In the same conditions, the complex $[Ru(bpy)_2phen]^{2+}$ reduced the activity to only 20%. This slight, but not negligible, inhibitory activity of $[Ru(bpy)_2phen]^{2+}$ was reasonably attributed to DNA damage *via* the formation of the $^1O_2$ oxidant species, a normal pathway observed for DNA cleavage in the presence of dioxygen photosensitizing complexes, like $[Ru(bpy)_3]^{2+}$ or $[Ru(phen)_3]^{2+}$ [453,454]. Conversely, the higher inhibition activity displayed by the two TAP-containing complexes, poor dioxygen photosensitizers, was attributed to their ability to give photoinduced electron transfer and formation of photoadducts with guanine.

A photoactive Ru^{2+} complex with TAP was also conjugated to various oligoribonucleotides, which would give, upon irradiation, photoadducts with the G bases present in the complementary DNA strand, leading to the formation of crosslinking between the two strands. The formation of adducts between the complex and G bases involves initially an electron transfer process from guanine to the complex and then the reaction between the radical guanine and the complex. Therefore, it was expected crosslinking to be dependent on different factors, in particular the ionization potential of stacked guanine units and the relative position and orientation of the guanine units and the tethered metal complex. With this in mind, Kirsh-De Mesmaeker and co-workers synthesized a number of 17-mer oligonucleotides containing only A and T nucleobases, with attached the $[Ru(TAP)_2(4,7\text{-dpphen})]^{2+}$ complex on a T base in the middle of the probe sequence. These oligonucleotides were then coupled with the complementary oligonucleotides containing GG doublets, a donor site with high electron transfer yields, located up to six base pairs away from the central anchoring site of the Ru^{2+} complex (see Fig. 36a) [455–457]. The synthetic procedure to achieve the functionalized oligonucleotides is depicted in Scheme 111 [455]. The Ru-labeled oligodeoxyribonucleotides were prepared from amino-modified oligomers containing a propylamine linker arm at the 5 position of a central uracil residue. These amino-oligonucleotides were synthesized by standard automated solid-phase procedures using the phosphoramidite method, starting from the modified phosphoramidite precursor **322**, which was obtained from **321** *via* protection of the 5′-OH with 4,4′-dimethoxytrityl

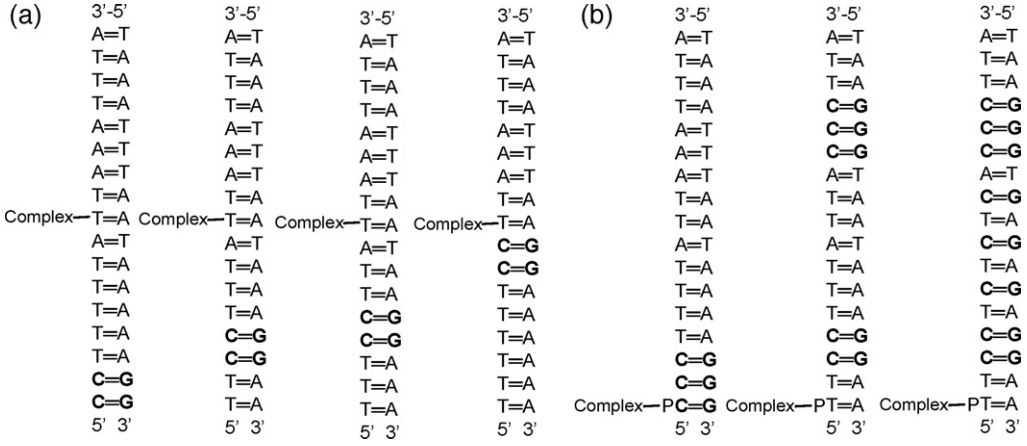

Fig. 36. Examples of [Ru^{2+} complex]-oligonucleotide conjugates with the Ru^{2+} complex linked to a thymine at middle of the sequence (a) or to the terminal (b) 5′-phosphate of the sequence [457].

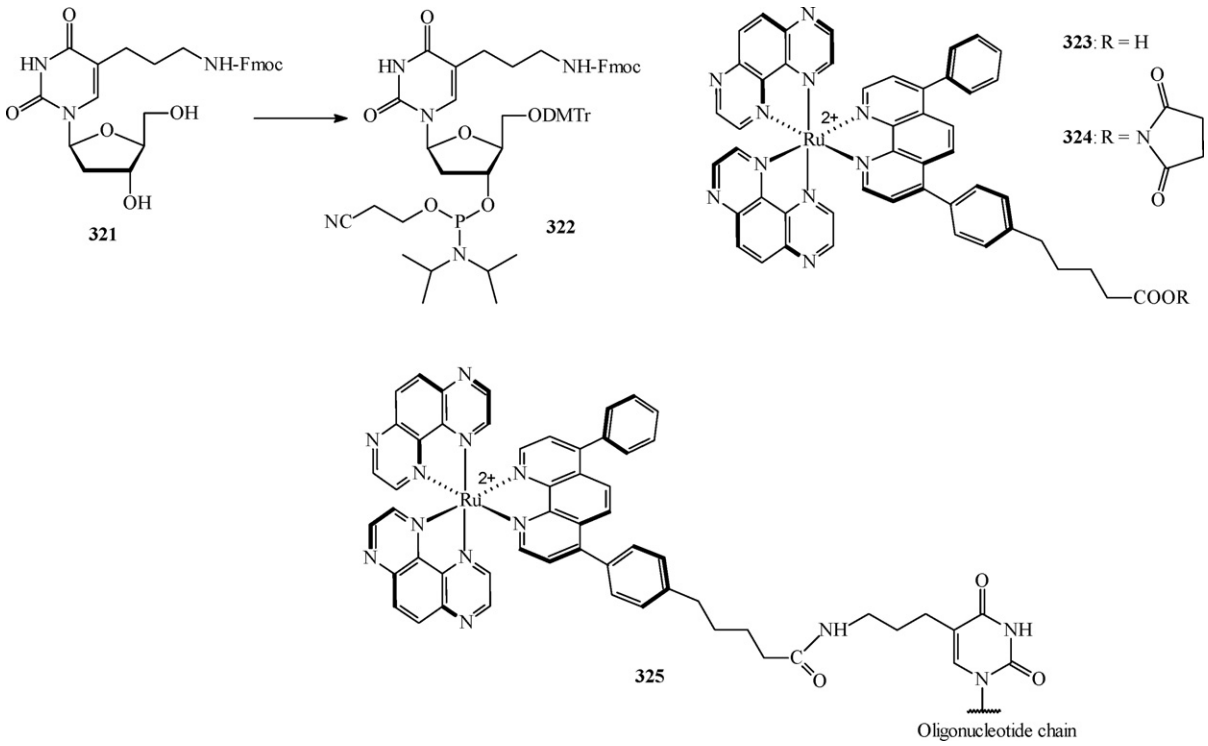

Scheme 111.

(DMTr), followed by phosphitylation carried out by conventional means.

The protected nucleoside **321** was prepared from 5-iodo-2′-deoxyuridine with the coupling procedure described by Hobbs [458]. The Ru^{2+} complex **323** was prepared by reaction of 5-[*p*-(7-phenyl-1,10-phenanthroline-4-yl)phenyl]pentanoic acid with $[Ru(TAP)_2Cl_2]$. The carboxylic group was then activated *via* esterification with TSU (TSU = *N*,*N*,*N*′,*N*′-tetramethyl(succinimido) uronium tetrafluoroborate) and the resulting complex **324** was coupled with the deprotected amino-oligonucleotides to afford the final conjugates **325** (Scheme 111).

Quenching of the fluorescence emission intensity upon the electron transfer process from guanine to the complex and analysis of the products formed *via* electrophoresis were then used to determine the electronic and geometrical parameters that regulate the electron transfer process and the successive formation of photoadducts. Indeed, irradiation of the G-containing duplexes produces the formation of adducts between guanine and the Ru^{2+} complex, as sketched in Fig. 37 [459,460].

Photophysical studies by means of steady state fluorescence and lifetimes measurements showed that the luminescence quenching can be correlated in first approximation to the ionization potential, theoretically calculated [459], of the stacked guanine residues, in agreement with the hypothesis that the first step of the formation of the photoadducts implies an electron transfer process from a G base to the complex [456,459,460]. On the other hand, it was found that the possibility of formation of the adducts also depends on the distance between guanine and the anchoring point of the complex on the duplexes. Only GG doublets separated by a maximum of three (in the 3′-direction) or four bases (in the 5′-direction) from the anchoring point produced photoadducts. Therefore, it was concluded that the formation of photoadducts does not only depend on the ionization potential of G bases, but also on geometrical and conformational factors, such as the distances between the nucleobases and the anchored complex.

Finally, to explore the possibility that a "hole" (the one-electron deficit present in guanine radicals generated upon photoirradiation) can migrate within a stack of alternating GC and AT base pairs, the authors synthesized oligonucleotides with the Ru^{2+} complex linked to the terminal 5′-phosphate of the sequence and containing a GG doublet one base pair away from the anchoring site (Fig. 36b). A GGG site, which can act as a "trap" for the migrating hole, thanks to its lower ionization potential, was located seven bases away from the GG doublets. Oxidation of guanines in the GGG triplets could be used to detect the possible migration of the hole within the duplexes. It was found that oxidation at GGG site was very scarce, to suggest that hole migration does not compete with the formation of the adducts between guanine and the Ru^{2+} complex, which remains the most efficient process [457].

Kirsh-De Mesmaeker and co-workers have recently reported an alternative method for the conjugation of complexes with phen or TAP to oligonucleotides or peptides through the formation of an oxime linkage [461].

As shown in Scheme 112, reaction of *cis*-$[Ru(TAP)_2Cl_2]$ with oxyamino derivatives of TAP or phen, obtained by an established method [462], lead to complexes **326** or **327**. Then, reaction of **326** or **327** with oligonucleotides functionalized in 5′- or 3′-position with reactive aldehyde groups (**328** or **329**), accordingly to the recent procedure developed by Defrancq and co-workers [463,464], afforded the desired 5′ or 3′ [Ru^{2+} complex]-oligonucleotide conjugates **330**–**333**. The same procedure can be used to synthesize [Ru^{2+} complex]-peptides conjugates, using aldehyde-functionalized peptides [461].

By using this method, the authors synthesized 17-mer oligonucleotides containing a strand functionalized with a $[Ru(TAP)_2(phen)]^{2+}$ or a $[Ru(TAP)_3]^{2+}$ complex at the terminal 3′- or 5′-phosphate groups, in order to investigate the effects of the tethered ligand as well as of the site of attachment (3′ *vs.* 5′) on the formation of crosslinking with G bases upon irradiation [462]. The Ru^{2+}-functionalized oligonucleotides were then coupled with complementary strand containing a single GG doublet

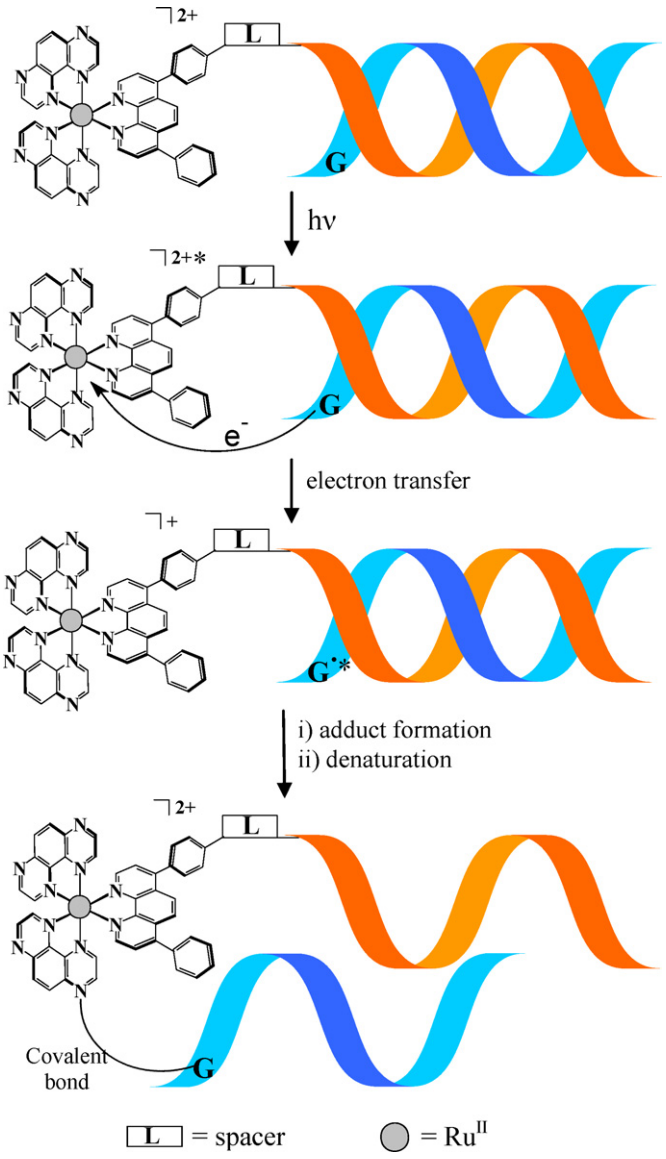

Fig. 37. Schematic representation of the formation of interstrand adducts upon irradiation of [Ru^{2+} complex]-oligonucleotide conjugates shown in Fig. 36 [459].

located a single base away from the anchoring site of the Ru^{2+} complex.

Photophysical and electrophoresis measurements showed that attachment of the complexes to the terminal 5′-phosphate produces a scarce number of photoadducts, due to the long distance between the Ru^{2+} complex and the G bases. Furthermore, in the case of $[Ru(TAP)_3]^{2+}$, a light induced dechelation effect, *i.e.*, the detachment of one TAP ligand, competed efficiently with the formation of photoadducts, which in consequence decreased. Conversely, an increased formation of adducts was observed in the case of the 3′-functionalized oligonucleotides, where the complex is close enough to allow a better interaction with the duplexes. Furthermore, the formation of photoadducts is higher in the case of oligonucleotides 3′-functionalized with $[Ru(TAP)_3]^{2+}$ than in the case of those containing the $[Ru(TAP)_2phen]^{2+}$ complex, due to the stronger oxidizing power of $[Ru(TAP)_3]^{2+}$.

Interestingly, the attachment of $[Ru(TAP)_3]^{2+}$ to the 3′-phosphate lead also to the formation of adducts with adenine, despite the lower tendency of this base to give an electron transfer process to the Ru^{2+} complex with respect to guanine [465].

The synthetic procedure in Scheme 112 was also used to attach the $[Ru(TAP)_2(phen)]^{2+}$ and $[Ru(TAP)_3]^{2+}$ complex units to a soluble 6 or 80 kDa poly-[*N*-(2-hydroxyethyl)-L-glutamine] polymer, with purpose to obtain polymer conjugates as vectorizing agents of the complexes inside cells [466]. The authors found that the complex-polymer conjugates show photophysical properties comparable with those of the free complexes. Furthermore, the 6 kDa functionalized polymer was able to form photoadducts with a 17-mer oligonucleotide containing a GG doublet. However, its ability to form adducts with the oligonucleotide was much lower than the free complex, probably due steric hindrance between the polymer chain and the oligonucleotide that could prevent the attached Ru^{2+} complex from assuming the correct orientation to react with guanine [466].

5.3. Other metal complexes with functionalized phenanthroline ligands for DNA binding and/or cleavage

Although Cu^{+}, Ru^{2+} and Rh^{3+} complexes with polypyridyl ligands have mainly attracted the attention of several authors thanks to their luminescence and DNA cleaving or photocleaving properties, the DNA binding ability of complexes of phen-based ligands with other metal cations have also been investigated and will be here discussed.

Ln^{3+} complexes with phen derivatives have been recently used either as DNA binders in view of their possible use as novel antitumor agents or as luminescent probes for DNA, exploiting their luminescence in the visible region.

Lin and co-workers have recently synthesized a variety of ligands containing a phen unit(s) functionalized at the 2- or 2,9-positions with amine or amino-carboxylate groups as additional binding site for the La^{3+} ions, with the purpose to investigate their interaction with DNA in view of their use as cytotoxic agents with anticancer activity.

The simplest example is constituted by ligands **336**–**338** (Scheme 113), which contain a phen moiety with an *N*-alkyl or *N*-benzyl aminomethylene side arm in 2-position [467]. These compounds were obtained by condensation of 2-carboxyaldehyde-1,10-phenanthroline with the appropriate amine, followed by reduction of the resulting Schiff bases. On the basis of spectroscopic, thermal gravimetric and conductivity measurements, the authors proposed the formation of La^{3+} complexes with 1:2 metal-to-ligand stoichiometry, where the metal centre is 10-coordinate by two tridentate ligands and four water molecules.

The analysis of the interaction of the La^{3+} complexes with calf thymus DNA, carried out by means of fluorescence, UV–vis, CD, melting and viscosity measurements, suggested that the binding process probably involve both partial intercalation of the phen moiety and coordination of the metal cation to a phosphate group. The interaction *via* intercalation decreased with the length of the aliphatic chain, whereas the coordinative binding mode was more relevant in the complexes with the longer chains.

A similar study was also carried out on ligands **339** and **340** (Scheme 113), which were prepared using an analogue procedure to that reported for **334**–**338** [468]. Both ligands were form 1:1 complexes with La^{3+}, as expected considering the larger number of nitrogen donors available for metal coordination. Both complexes interact with DNA in a similar fashion to that found for the complexes with **334**–**338**. In fact, partial intercalation of one phen is accompanied by other interactions, most likely coordination of the metal ion to phosphate or hydrogen-bonding. Interestingly, both complexes displayed high cytotoxic activity in cancer cell lines, being in some cases more potent cytotoxic agents than *cis*-platin.

Lin and co-workers extended their study also to phen-based ligands containing amino acid side arms (see Scheme 114) [469,470]. These groups deprotonate upon metal coordination, leading to an

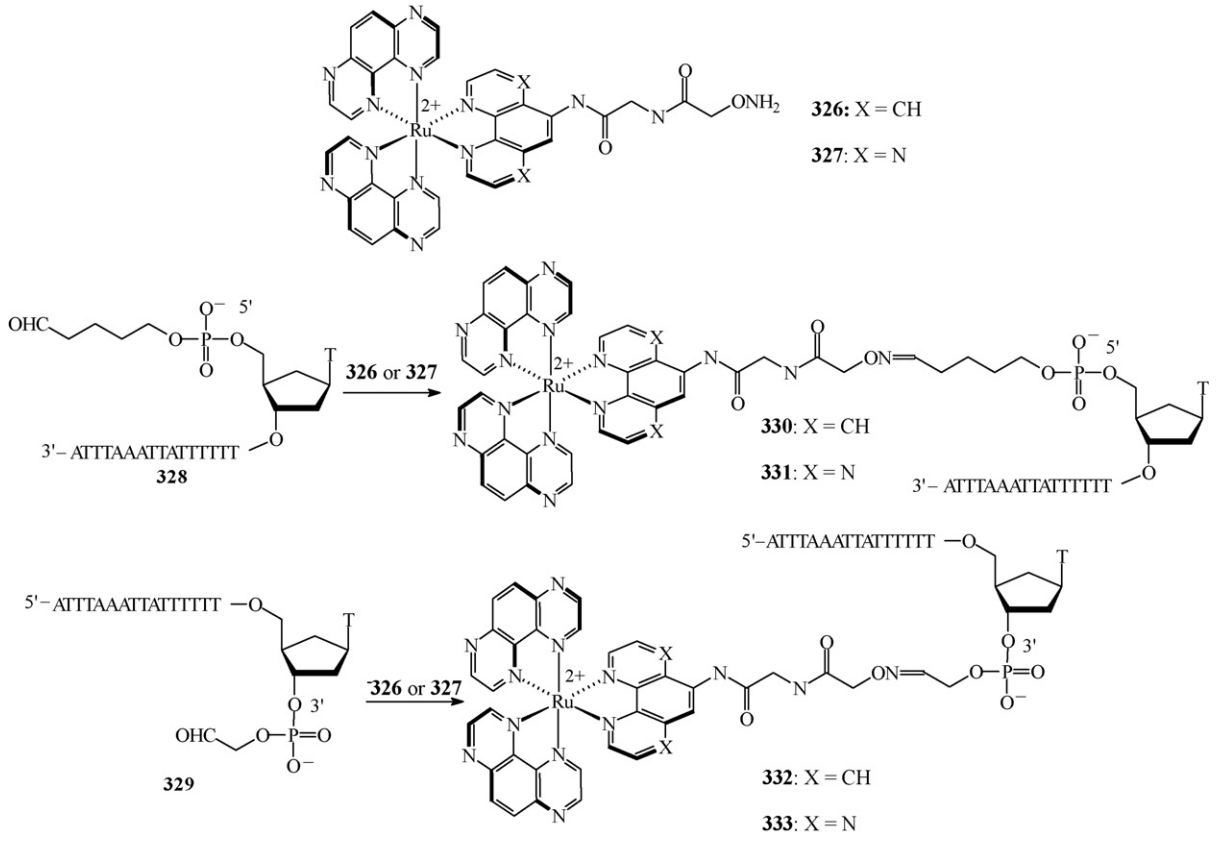

Scheme 112.

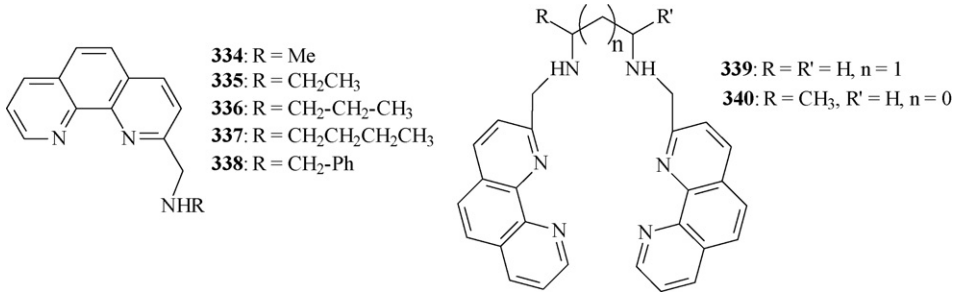

Scheme 113.

increased stability of the complexes, thanks to coordination of the anionic carboxylate functions to the hard La^{3+} cation (Scheme 114). Actually, a potentiometric study on the coordination properties of **341** toward La^{3+} showed that this ligand, in its dianionic form (**341**-2H)$^{2-}$ has a discrete binding ability for La^{3+} in aqueous solution

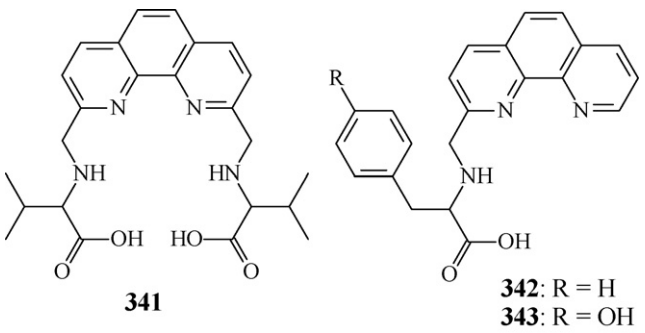

Scheme 114.

(log K = 9.5 for the equilibrium (**341**-2H)$^{2-}$ + Ln^{3+} = [Ln(**341**-2H)]$^{+}$). Protonation of the amino groups can also occur in solution to give the protonated complexes species [Ln(**341**-H)]$^{2+}$ and [Ln(**341**)]$^{3+}$, the former being predominant in aqueous solution at neutral pH [469]. Conversely, ligands **342** and **343** form, in solution, complexes with both 1:1 and 1:2 metal-to-ligand stoichiometry, which were also isolated in the solid state [470].

All La^{3+} complexes with **341**–**343** interact with DNA in a similar fashion to that found in the case of complexes with ligands **334**–**340**. In fact, partial intercalation of phen is accompanied by interaction of the metal cation with phosphate and/or by hydrogen-bonding between the complex and the DNA backbone. The binding process of the La^{3+} complexes with **341** to DNA was also analyzed from a kinetic point of view by monitoring the changes in fluorescence of EtB in the presence of the complexes [469]. It was found that the binding process occurs *via* two successive time-separated steps, analogous to those observed by the same authors in the case of the Cu^{2+} complexes with ligands **215**, **272**–**277**. Finally, the cytoxicity of the 1:1 La^{3+} complexes with **341** and of the 1:1 and 1:2 complexes with **342** and **343** was tested in several tumor cell

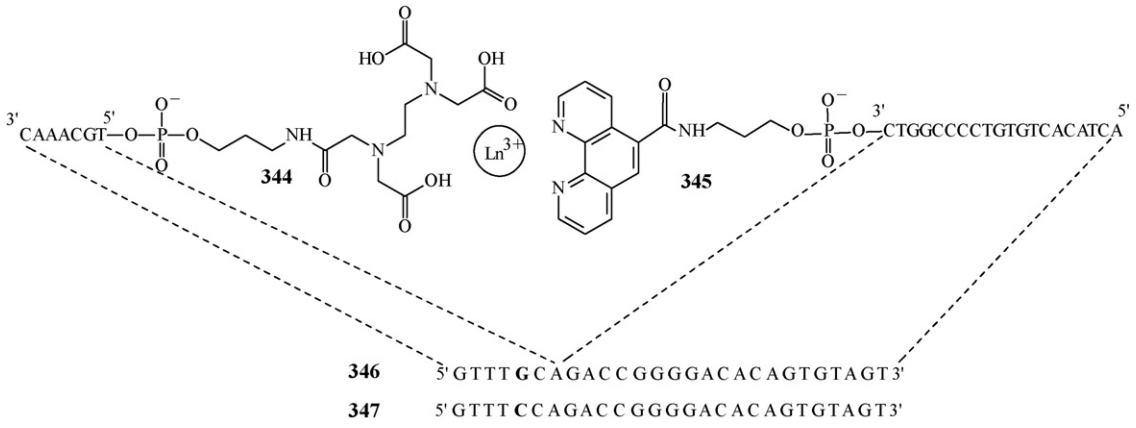

Scheme 115.

lines [469,470]. The most efficient cytotoxic agents were the complexes with **342**. In particular, the 1:2 complexes with **342** resulted to have higher cytotoxic activity than *cis*-platin in all tested cell lines. This was attributed by the authors to the higher lipophilic character of ligand **342** with respect to **341** and **343**, due to the presence of the benzyl group in **342**, whereas in **343** the presence of the phenol moiety could reduce the overall lipophilicity of the complexes [470].

An interesting perspective in the chemistry of lanthanide complexes, especially Tb^{3+} or Eu^{3+}, with phen-containing ligands is the use of their peculiar luminescence properties [108] to detect particular DNA sequences. A recent example has been reported by Ihara and co-workers [471–473] who used the assembly of a Tb^{3+} or Eu^{3+} complex with two oligonucleotides functionalized with two different chelating agents, to detect colorimetrically single nucleotide polymorphisms (SNP), one of the most frequent type of variation in the human genome consisting in the variation of a single nucleobase. Ihara and co-workers showed that two oligonucleotides, functionalized at their terminal phosphate group (Scheme 115) with different chelating units, EDTA and phen, respectively, cooperatively hybridize to target sequences in the presence of Tb^{3+} or Eu^{3+}, which act as promoting centre for the assembly of the two functionalized oligonucleotides.

The formation of the ternary duplex, composed by the target sequence and the two metal-linked conjugates, can produce a colorimetric response, the characteristics of which depended on the nature of the target sequence. This approach was used in the analysis of the thiopurine S-methyl transferase gene. **346** and **347** were the synthetic 27-mer sequences of the gene containing one of the "hot spots", *i.e.*, a tract of the gene with high frequency of mutation. The former is the sequence of the wild-type gene and the latter is that of the mutant one, in which a single G → C mutation occurred. The functionalized sequences were respectively the 7-mer oligonucleotide **344**, complementary to a part of **346** and carrying an EDTA unit at the 5′ terminal phosphate, and a 20-oligonucleotide **345** bearing a phen unit at the terminal 3′-phosphate and complementary to the remaining part of **346**. Solutions containing the target sequence **346**, the two functionalized nucleotides **344** and **345**, and Eu^{3+} or Tb^{3+} produced the typical emission spectra of the phen-based metal complexes with these metal cations. As a result, the solutions appeared naked-eye red or green coloured. In contrast, the emission intensities were strongly reduced when **346** is replaced by **347**. This method enable the selective detection of the sequence **346** over the **347** one through the assembling of three different oligonucleotides and Eu^{3+} or Tb^{3+} (see Fig. 38) [473]. Of note, the emission intensities were also remarkably less intense (less than 1/15) in the absence of the target sequence **346**. This suggested that the complex is scarcely formed in the absence of **346**, due to the poor binding ability of phen toward Eu^{3+} or Tb^{3+}. On this basis, the authors suggested that the target sequence, by gathering together the two functionalized oligonucleotides, one of which containing the strongly chelating agent EDTA, can increase the local concentration of the Eu^{3+} or Tb^{3+}, thus favouring their coordination to the phen derivative.

The ability of planar Pt^{2+} complexes with phen to bind to DNA in an intercalative fashion is known since seventies. Lippard and co-workers showed that the $[Pt(phen)en]^{2+}$ complex interacts with DNA in a way similar to that of the classical intercalator ethydium bromide [474]. More recently, Aldrich-Wrigth reported

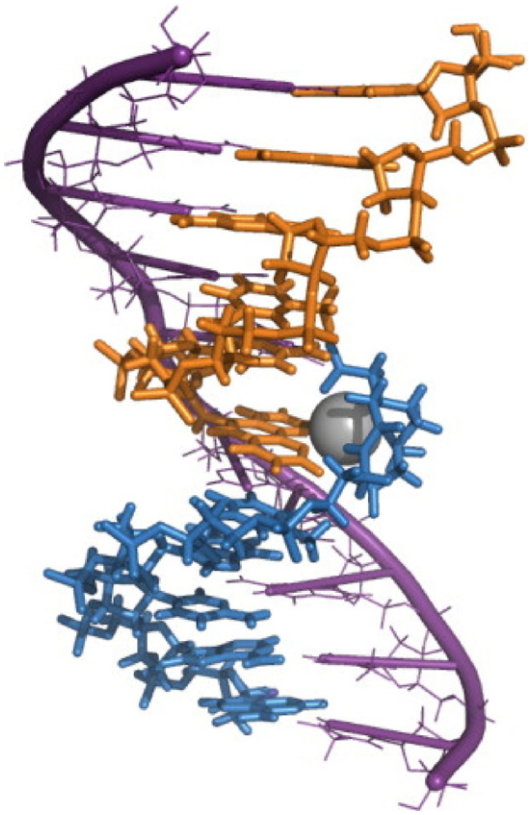

Fig. 38. Proposed structure for the ternary adducts **346**/**344**-Ln^{3+}-**345** (violet: target sequence, **346**; blue: EDTA-containing oligonucleotides, **344**; orange: phen-containing oligonucleotides, **345**). This figure is taken from [473] and reprinted with permission; copyright 2008, by Elsevier.

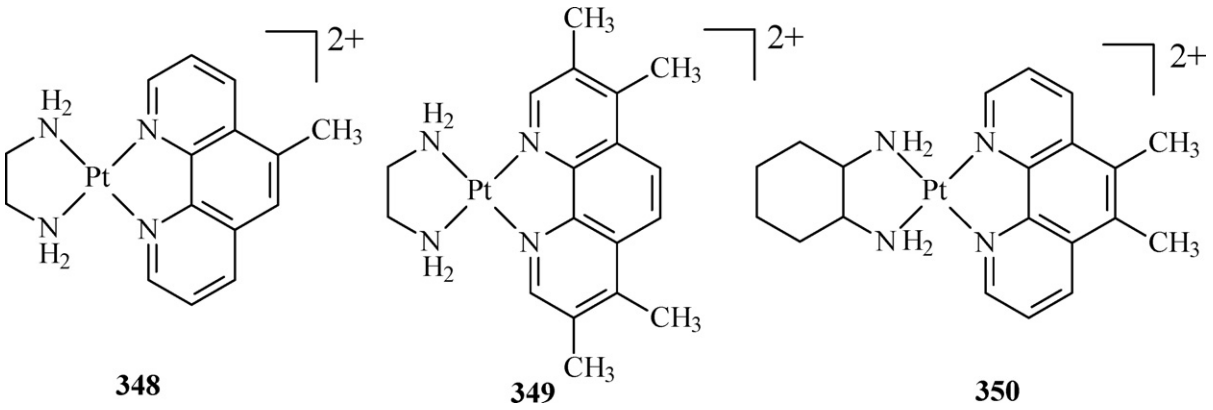

Scheme 116.

that $[Pt(phen)en]^{2+}$ intercalates within the hexamer $d(GTCGAC)_2$ from the minor groove at the C_3–G_4 site [475]. With the aim to develop new Pt-based intercalating agents with anticancer activity [476–483], in the last few years Aldrich-Wright and co-workers have extensively analyzed the DNA binding and cytotoxic properties of a number of Pt^{2+} complexes with mono- or di- and even tetramethylated phen derivatives as intercalating agents and different ancillary ligands, including en [476], the diastereoisomers of 1,2-diaminocyclohexane [478–482], 1,3-diamino-1,2,2-trymethylciclopentane [477], and other chiral diamines [479,483] (see Scheme 116 for a few examples). Viscometric, circular and linear dichroism and NMR measurements suggested intercalation or partial intercalation of the phen moiety within the DNA base pairs [476,477]. The complexes often displayed high cytotoxicity in cancer cell lines, in some cases higher than that of *cis*-platin [478–480]. The authors demonstrated that the ancillary ligand chirality and functionalization of the phen moiety are important factors in determining the cytotoxic characteristics of the resulting Pt^{2+} complexes. Methylation in the 5-, or 5,6-positions of phen and the use as ancillary ligand of 1,2-diaminocyclohexane in an S,S-conformation, confer the highest cytotoxicity, the S, S isomer of complex **350** (Scheme 116) being *ca.* 100-fold more cytotoxic than of *cis*-platin in L2110 murine leukemia cell lines [480]. However, the cytotoxic activity was found not to be strictly related to the intercalating ability of the complexes, suggesting that DNA binding is not the sole mechanism that determines the cytoxicity of these complexes [478]. The authors suggested that differing cellular uptake levels or intracellular transport may influence the amount of each complex that reaches DNA intact, thus affecting the overall cytotoxicity. A recent study has also shown that these complexes can be partially degraded by glutathione, which can displace the ancillary ligands to give dinuclear complexes where each Pt^{2+} cation is bound by one phen unit and by two bridging thiolate groups belonging to two glutathione moieties [482]. Interestingly, this degradation can be inhibited by complexes encapsulation, or partial encapsulation in cucurbit[n]urils [482], carboxylated-β-cyclodextrin [481] or *p*-sulfonatocalix[4]arene [481].

A different approach to the development of new Pt^{2+} complexes with potential anticancer ability was used by Vilar and co-workers [484,485]. In fact, the ability of Pt^{2+} to give planar complexes can be used to assembly charged phen-containing planar complexes able to stabilize guanine quadruplexes (see Section 5.4 for a short discussion on G-quadruplex stabilization). With this in mind, ligands **351**–**354** (Scheme 117) and their Pt^{2+} complexes were designed with appropriate structural features to favour the formation of π-stacking interactions with G quadruplexes. The ligands were synthesized starting from 1,10-phenanthroline-2-carbonyl chloride using a well established procedure [486] and used to prepare the corresponding Pt^{2+} complexes. Interestingly, it was found that ligands **351** and **352** form in the solid state complexes with a 2:2 metal-to-ligand stoichiometry [485]. In particular, the crystal structure of the dimeric complex with **352** showed that each ligand coordinates to one Pt^{2+} centre *via* the phen and the adjacent deprotonated amide nitrogen, and to the second one *via* the pyridine nitrogen of the same ligand. The dimer assumes a distorted boat-like conformation, not suitable for G-quadruplex stabilization, due to the lack of planarity.

However, these complexes partially dissociate in aqueous solution, affording also 1:1 species. Conversely, ligands **353** and **354**

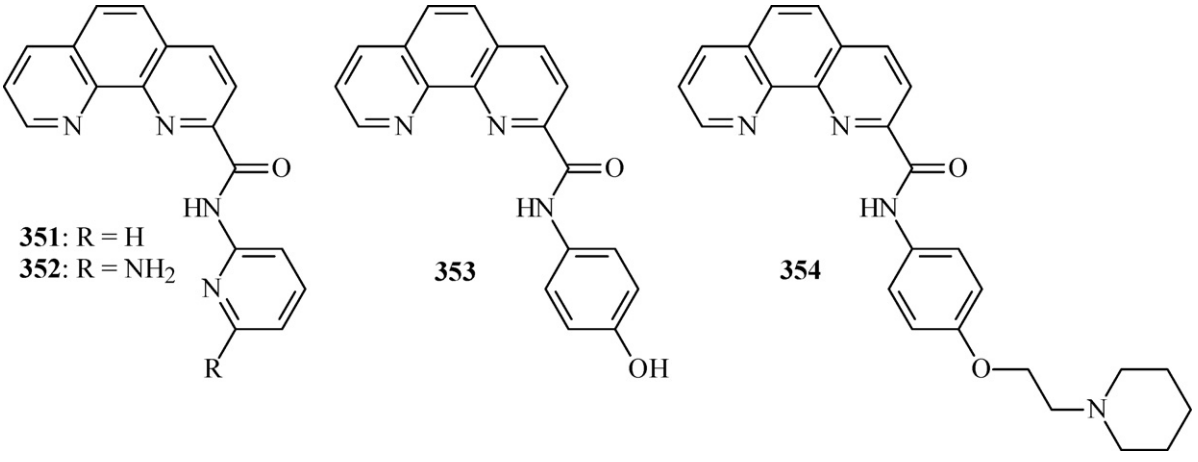

Scheme 117.

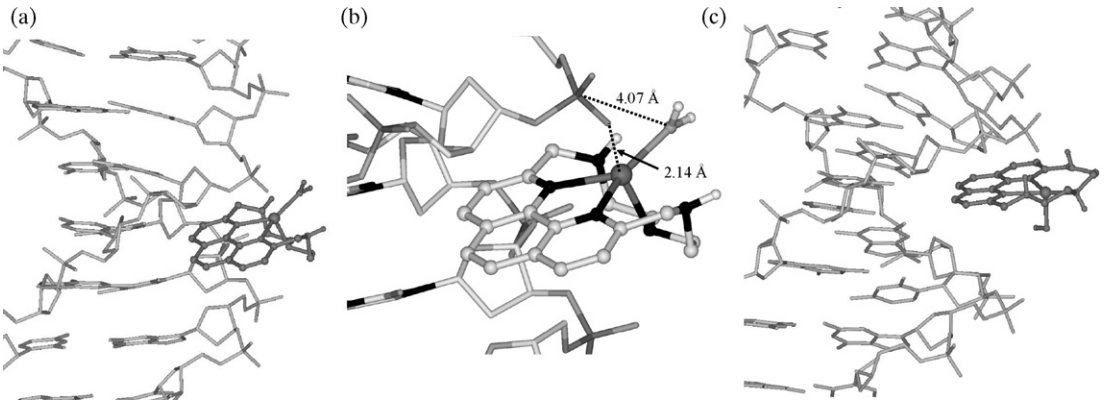

Fig. 39. Minimized structures of the $[Zn(\mathbf{78})(H_2O)]^{2+}$/DNA adduct (a) with enlarged view showing the interaction mode (b) and of $[Zn(\mathbf{78})(OH)]^{+}$/DNA adduct (c). This figure is taken from [487] and adapted with permission; copyright 2008, by The American Chemical Society.

gave only mononuclear complexes, due to the replacement of the coordinating pyridine moiety with a benzene unit. The ligands and their Pt^{2+} complexes were then tested as stabilizing agents for the human telomeric G-quadruplex by a FRET (fluorescence resonance energy transfer) quadruplex-DNA melting assay. The Pt^{2+} complex with **354** displayed the highest activity in G-quadruplex stabilization and selectivity in quadruplex- vs. duplex-DNA stabilization (the complex with **353** was not tested due to its scarce solubility). Surprisingly, also the dimeric complexes with **351** and **352** showed a certain degree of stabilization of G-quadruplexes, probably thanks to interactions with the TTA loops of the telomeric DNA sequence or π-stacking with one of the phen moieties of the complexes. Preliminary results showed that the complex with **354** and at to a less extent, ligands **353** and **354** are also active as inhibitors for telomerase [484].

Recently, examples of Zn^{2+} complexes with phen derivatives with cleavage ability toward DNA have also been reported. The interest toward this metal cation is mainly due to its presence in several hydrolytic metallo-enzyme, including those able to cleave the DNA backbone. Clearly, complexes with the Zn^{2+} ion cannot "cut" DNA *via* an oxidative pathway and their cleavage activity involves hydrolysis of the phosphate ester bond. The role of the zinc(II) ion is generally ascribed to binding and activation of the substrates, while a Zn^{2+}-OH function acts as intramolecular general base catalyst or a Zn^{2+}-H_2O group behaves as intramolecular general acid catalyst [288–290].

Like in the case of the copper complexes, the ability of phen to insert within the grooves can be used to design complexes able to act as carriers of the active Zn^{2+} ion in close proximity of the phosphate-sugar backbone.

On this ground, the simple mononuclear Zn^{2+} complex with ligand **78** (Scheme 31) was tested as potential DNA cleaving agents. Its hydrolytic ability was first analyzed by using BNPP as DNA model compound [487]. Depending on pH, the complex exists in solution in two different species, $[Zn(\mathbf{78})]^{2+}$ from acidic to neutral pH values and $[Zn(\mathbf{78})(OH)]^{+}$ in the alkaline pH region, the latter species being formed upon deprotonation of a Zn^{2+}-bound water molecule present in $[Zn(\mathbf{78})]^{2+}$. Only $[Zn(\mathbf{78})(OH)]^{+}$ was able to cleave the phosphate ester bond of BNPP, in agreement with a hydrolytic mechanism involving a nucleophilic attack of a Zn^{2+}-bound hydroxide anion, a more powerful nucleophile than Zn^{2+}-bound water molecules, to the phosphorous atom of BNPP. As a consequence, BNPP cleavage occurred only in the alkaline pH region, with increasing rate constants as the pH increases from 7 to 10.

The complex interacts with DNA in a non-intercalative mode. More interestingly, it efficiently cleaved the supercoiled plasmidic DNA pBR 322 to its nicked form II. Surprisingly, it was found the opposite pH dependence of the hydrolytic ability with respect to BNPP. In fact, the cleaving activity was higher at slightly acidic or neutral pH values and lower in the alkaline pH region. This unexpected behaviour was explained on the light of quantum mechanics/molecular mechanics calculations [487]. In fact, the modelling study showed that the complex $[Zn(\mathbf{78})(H_2O)]^{2+}$ is placed within the minor groove of DNA, with the phen moiety close to the more hydrophobic zone of the nucleobases. Such a disposition enables the formation of a strong interaction between the Zn^{2+} ion and an oxygen atom of the phosphate group and allows the Zn^{2+}-bound water molecule to stay at close distance from phosphate (see Fig. 39). It was suggested that both activation of the phosphate group, due to its interaction with zinc, and presence of a metal-bound water molecule, a potential acid catalyst, at a close distance from phosphate, favour the cleavage process.

The hydroxo-complex $[Zn(\mathbf{78})(OH)]^{+}$ is still inserted within the minor groove. On the other hand, the $[Zn(\mathbf{78})(OH)]^{+}$/DNA adduct is featured by a weak interaction between phosphate and Zn^{2+} and, overall, the potential nucleophilic hydroxide group is located far from the phosphate group, on the opposite side of the macrocyclic ring of the complex, and thereby cannot act as a nucleophile.

Yu and co-workers have tested the DNA cleavage ability of the dinuclear Zn^{2+} complex with ligand **355**, composed by two 1,4,7,10-tetraazacyclododecane (cyclen) units linked by a phen bridge (Scheme 118) [488]. The ligand was obtained by reaction of 2,9-*bis*(bromomethyl)-1-10-phenanthroline (**33**) (Scheme 11) with cyclen containing three Boc-protected amine groups, followed by deprotection with standard methods.

The dinuclear Zn^{2+} complex was able to cleave efficiently the supercoiled plasmid DNA pUC18 at pH 7.5 affording the nicked form II. Although no comparison with the activity of the corresponding mononuclear Zn^{2+} complex was reported, the authors suggested

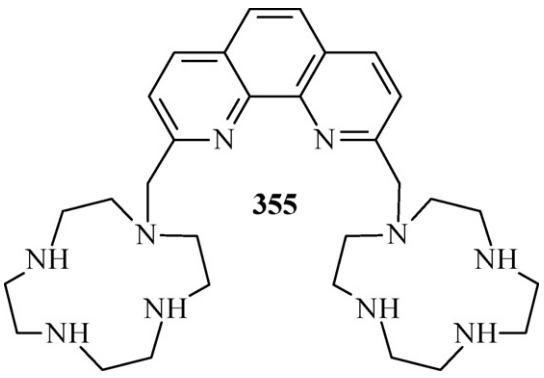

Scheme 118.

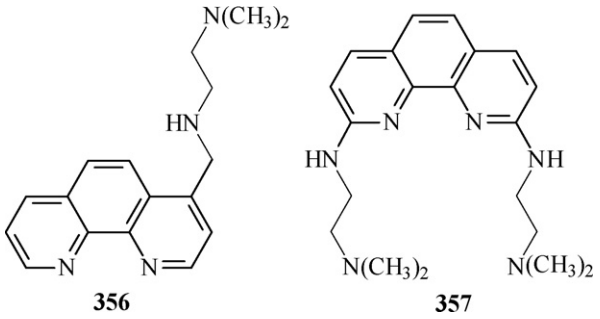

Scheme 119.

that the two Zn^{2+} ion play a cooperative role in the hydrolytic mechanism, thanks to a bridging interaction of the DNA phosphate groups with the two metal centres. A metal-bound hydroxide anion would act as nucleophile.

Sissi and co-workers analyzed the ability of Cu^{2+} and Ni^{2+} complexes with the ligands **356** and **357** (Scheme 119) to stabilize G-quadruplex DNA arrangements (see Section 5.4 for a short discussion on G-quadruplex stabilization) [489].

Ligands **356** and **357** were obtained by condensation of *N*,*N*′-dimethylethylenediamine with 4-formyl-1,10-phenanthroline or 2,9-diformyl-1,10-phenanthroline, respectively, followed by reduction of the resulting imine derivatives. Both ligands form stable 1:1 complexes with Cu^{2+} and Ni^{2+}, with the only exception of the Ni^{2+} complex with **356**, which featured a metal-to-ligand 1:2 stoichiometry. It was reasonably assumed that in this complex Ni^{2+} is bound to the two phen moieties to achieve an overall square planar geometry. Actually, melting measurements and CD spectra, performed on an oligonucleotide formed by four repeats of the human telomerase, showed that only the 1:2 Ni^{2+} complex with **356** gives a remarkable stabilization of the G-quadruplex structure, as a result of efficient π-stacking interactions between the phen units assembled in a planar complex and the terminal guanine quartet. Therefore, it was concluded that G-quadruplex recognition and stabilization can be modulated not only by the organic ligands used but also by the stoichiometry of their complexes and by the stereochemical characteristics of the coordinated metal cations [489].

Bailly and co-workers carried out a comparison of the binding and cleavage properties of the Cu^{2+}, Mn^{3+}, Co^{2+} and Ni^{2+} complexes with 2,9-*bis*(2-hydroxyphenyl)-1,10-phenanthroline **11** (see Scheme 5) [490]. Melting measurements showed that the Co^{2+} complex and, at to a less extent, the Ni^{2+} complex tend to stabilize the DNA double helix, suggesting a stronger interaction of these complexes with DNA. Conversely, Mn^{3+} and Cu^{2+} complexes gave a very weak stabilization. More interestingly, the authors found that the Co^{2+} and Mn^{3+} complexes, in the presence of a reducing agent (2-mercaptopropionic acid or ascorbic acid), cleave the supercoiled form of plasmid DNA pUC12 to the nicked form II and, at high complex concentrations, also to the linear form III. No cleavage was observed for the Cu^{2+} complex, probably due to the scarce binding ability of this complex to DNA, and for the Ni^{2+} one. EPR measurements showed that in these experimental condition Mn^{3+} is reduced to Mn^{2+}, suggesting that DNA cleavage is induced by hydroxyl radicals formed upon ascorbate-induced manganese reduction. Conversely, in the case of the Co^{2+} complex DNA cleavage is probably due to the formation of an oxidizing cobalt–oxygen adduct.

The cleaving ability of the Mn^{3+} and Ni^{2+} complexes was also tested in oxidative conditions (in the presence of peroxysulfate). In these conditions the manganese complex still cleaved DNA, probably thanks to the formation of an oxidant Mn^{V}–O species, while the nickel(II) complex remained inactive.

Recently Sleiman and co-workers have shown that oligonucleotides can be used as building blocks to assemble bi- and three-dimensional nanostructures with precisely programmed features, following a template approach that uses polypyridyl ligands, such as tpy [491–494] or phen [494–496], as junctions between the oligonucleotides. This approach allowed for the incorporation of normally labile metal cations, such as Cu^{+} or Ag^{+}, within the junctions linking the building blocks of the nanostructures. We will report here only on the phen-based DNA nanostructures. 2D triangular nanostructures were engineered using three building blocks (**358**, **359** and **360**), each containing three oligonucleotides separated by 2,9-diphenyl-1,10-phenanthroline (2,9-dpphen) moieties, linked to the 3′- or 5′-end of the DNA single strands *via* flexible diethylen-glycol bridges. The two outer 10-mer strands of each building block are complementary to one of the outer strand of the other two building blocks (see Fig. 40) [495]. Thereby, the outer 10-mer DNA sequences work as template regions to mediate the assembly of the DNA triangle **361** and to direct Cu^{+} binding by the three $(2,9\text{-dpphen})_2$ coordination moieties.

Actually, self-assembly of the desired metal-containing triangle resulted to be highly efficient. Gel electrophoresis pointed out that sequential hybridization of **358** with **359** gave quantitative forma-

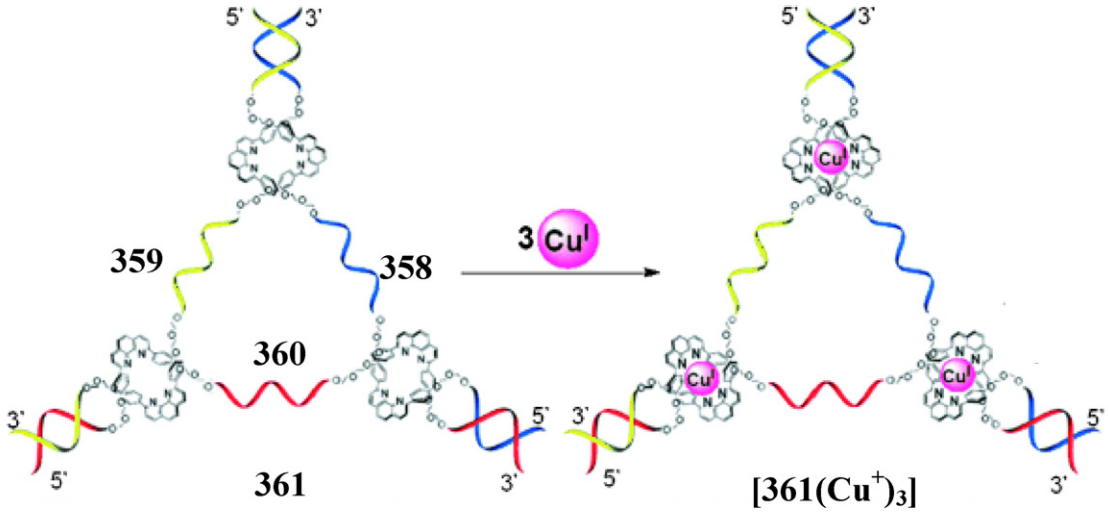

Fig. 40. Schematic representations of the structures of **361** and [**361**$(Cu^{+})_3$]. This figure is taken from [495] and adapted with permission; copyright 2008, by Wiley-VCH.

tion of the dimer **358**:**359** and afforded triangle **361** upon addition of **360**. Addition of Cu^+ showed near quantitative product formation to give [**361**$(Cu^+)_3$].

Of note, highly stable triangular assemblies were also obtained by using other metal cations, such as Ag^+, instead of Cu^+. Interestingly, both the Cu^+ and Ag^+ triangular assemblies resist conditions (4 M urea) that normally denature double-stranded DNA. Conversely, the corresponding not metal containing triangles completely disassembled into its component strands [496]. This pointed out that metal coordination plays a fundamental role in the stabilization of these triangular structures.

The three internal 15-mer sequences served not only as single-stranded sides in the triangle but also as anchoring point to construct more elaborated structures, including 3D assemblies featuring trigonal prisms [496]. In fact, addition of three strands, each containing outer sequences complementary to a single internal side of two different triangles, lead to the formation of the 3D product **362**, composed by the two initial triangular compounds linked by three flexible single strands (see Fig. 41). Subsequent addition of three rigidifying strands produced a more rigid trigonal prismatic capsule **363**, with inner volume dimensions of approximately 25–30 nm^3 (based on a modelling study). Finally, addition of Ag^+ or Cu^+ lead to their complexation by two adjacent phen moieties, to form stable hexanuclear metal assemblies (**364** in Fig. 41). Once again, metal complexation increases the stability of the 3D assembly. In fact, the authors found that the melting temperature increases remarkably upon Ag^+ complexation. Interestingly, the hexanuclear Cu^+ complex displayed two distinct transitions (both at higher temperature than the uncomplexed cage), one of which at the same temperature of the starting 1D triangular complex. Of note, it was also found that the cage compound is able to bind not only Ag^+ and Cu^+, but also other metal cations, including Zn^+, Cd^{2+} and Au^+, affording in all cases hexanuclear complexes with structural features similar to those of the Ag^+ and Cu^+ complexes.

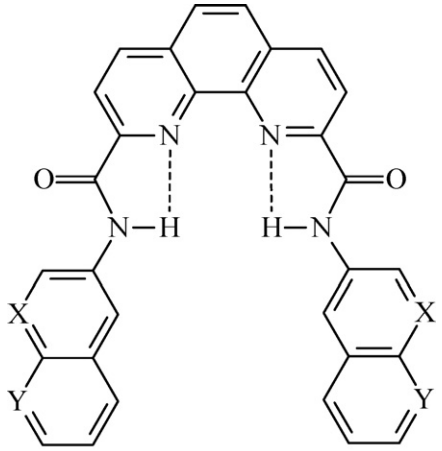

365: X = CH Y = NCH_3^+

366: X = NCH_3^+ Y = CH

Scheme 120.

5.4. Phenanthroline-based organic compounds for DNA binding

As reported above, most of the compounds used for DNA binding and/or cleavage are metal complexes. While phen is an appropriate ligand for DNA binding, due to its heteroaromatic planar and hydrophobic structure, the coordinated metal cation confers to the resulting complexes peculiar binding or reactivity properties, affording cleaving or photocleaving agents, DNA binders able to recognize specific base sequences or luminescent probes. However, phen has also been used to design non-metal-based compounds able to interact with DNA and to perform specific functions, from simple DNA damage to stabilization of particular DNA structures.

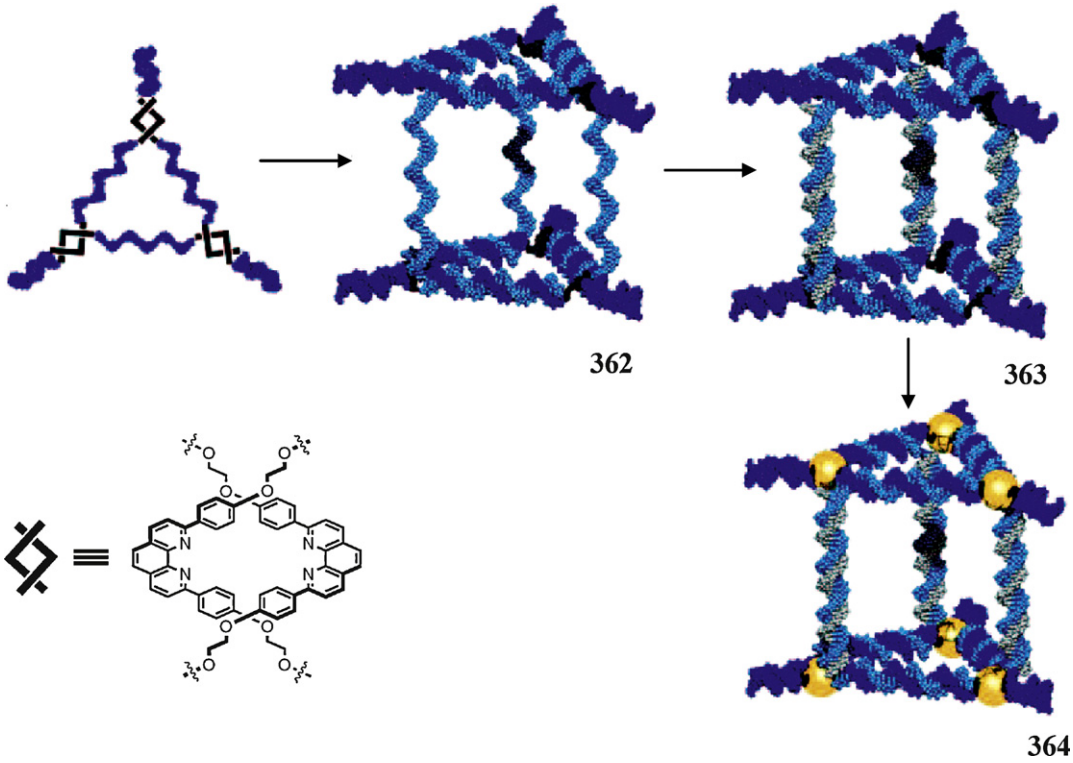

Fig. 41. Sketch of the assembly of a DNA-based trigonal-prismatic architecture. This figure is taken from [496] and adapted with permission; copyright 2009, by Nature Chemistry.

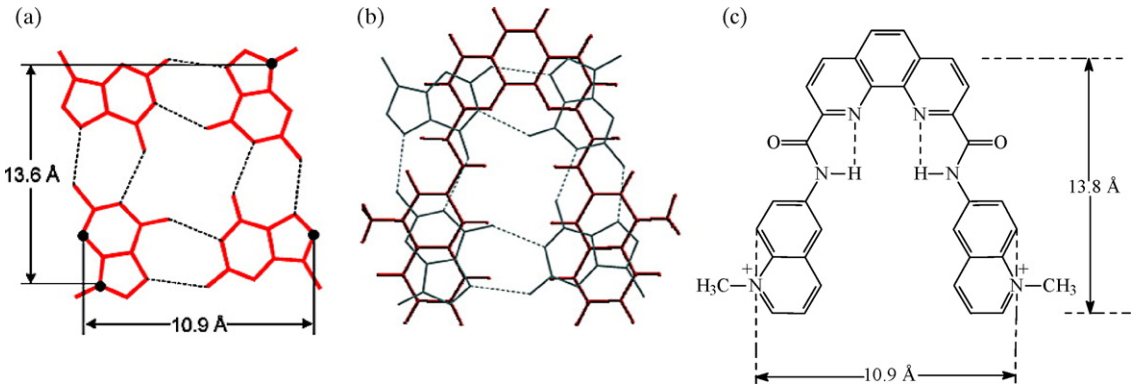

Fig. 42. Selected dimension of a G-quartet (from X-ray analysis) (a), and proposed interaction mode (b) and calculated dimension of compound **365** (from MM2 calculations) (c). This figure is taken from [500] and adapted with permission; copyright 2007, by The American Chemical Society.

One of the most recent examples is the use of phen-based compounds to stabilize guanine quadruplexes [497,498]. These structures arise from the assembly of four G bases into a planar structure *via* hydrogen-bonding interactions involving the Watson-Crick edge of one guanine and the Hoogsteen edge of its neighbour.

G-rich sequences, which can potentially form quadruplex DNA structures, are thoroughly distributed along the human genome. In particular, human telomeric DNA consists of the tandem repeat sequence TTAGGG. Folding telomeric DNA (the end of which is singly-stranded) into a quadruplex structure inhibits the activity of telomerase. This enzyme maintains telomere integrity preventing the shortening of telomeric DNA. However, it is often over-expressed in cancer cells and plays an important role in cancer cell immortalisation. In fact, the proliferative potential of cancer cells depends on telomere maintenance. Since the substrate of telomerase is the 3′-single-stranded overhang of telomeric DNA, molecules that stabilise quadruplex structures in the telomere can lead to inhibition of telomerase. Therefore, the development of new molecules able to stabilize G-quadruplexes can open up new perspectives for the discovery of anticancer agents.

Large and flat aromatic moieties are promising G-quadruplex stabilizing agents, since they can interact *via* hydrophobic and π-stacking interactions with the planar G-quartet. Positive charges gathered on the ligands or complexed metal cations may also stabilize the adducts, thanks to electrostatic interactions with the electron-rich G-quartets. Therefore, phen derivatives can represent promising ligands for telomerase inhibition, due to its planar structure and hydrophobic characteristics. In this context, phen-based ligands have been recently developed by Teulade-Fichou with the aim to bind and stabilize G-quadruplexes [499–504]. Ligands **365** and **366** (Scheme 120) were prepared by condensation of 1,10-phenanthroline-2,9-dicarboxylic acid (**27**, Scheme 11) with 3- or 6-aminoquinoline, followed by methylation of quinoline nitrogen atoms [500]. In these compounds, the 2,9-phenanthroline-dicarboxyamide unit produced an internally organized hydrogen-bonded *syn-syn* configuration (Scheme 120), which locks the ligand in a planar conformation suitable for G-quadruplex binding.

Indeed, both **365** and **366** appeared to be strong quadruplex stabilizers and, at the same time, they displayed selective stabilization of G-quartet with respect to duplex DNA. These properties were attributed to an optimal dimensional and geometrical complementarity with the G-quadruplex assembly, as sketched in Fig. 42. Of note, structural rigidity generated by the internal hydrogen-bonding organization of **365** and **366** was a key parameter for G-quadruplex stabilization. In fact, replacement of phen with 2,2′-

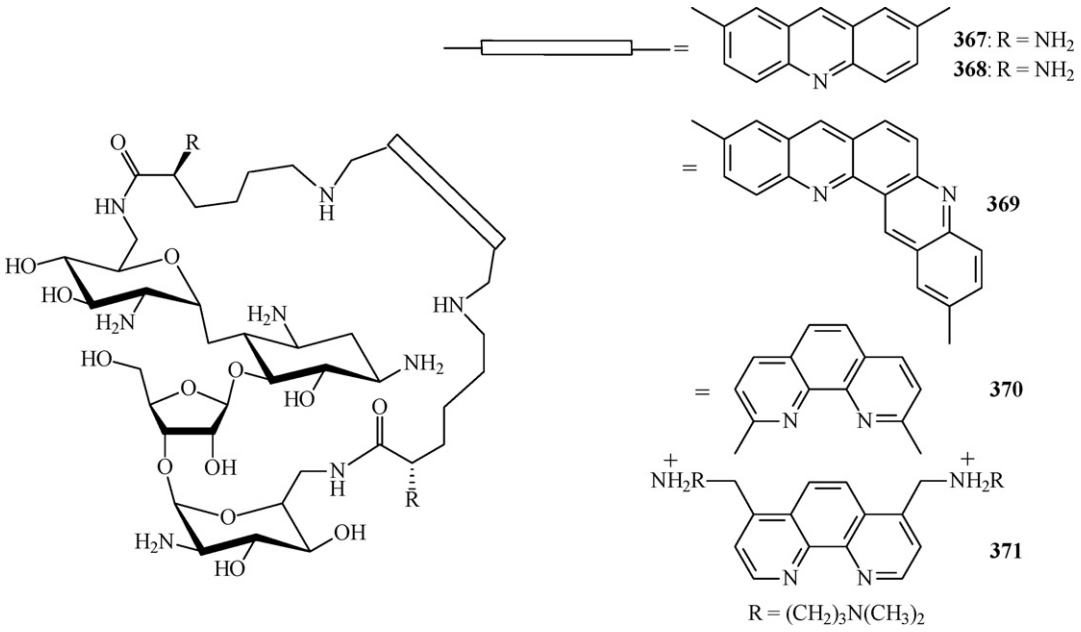

Scheme 121.

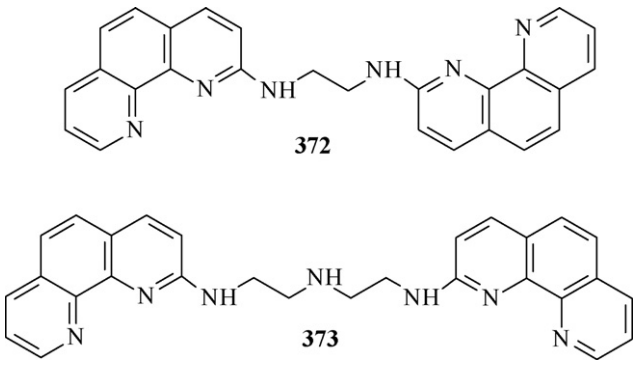

Scheme 122.

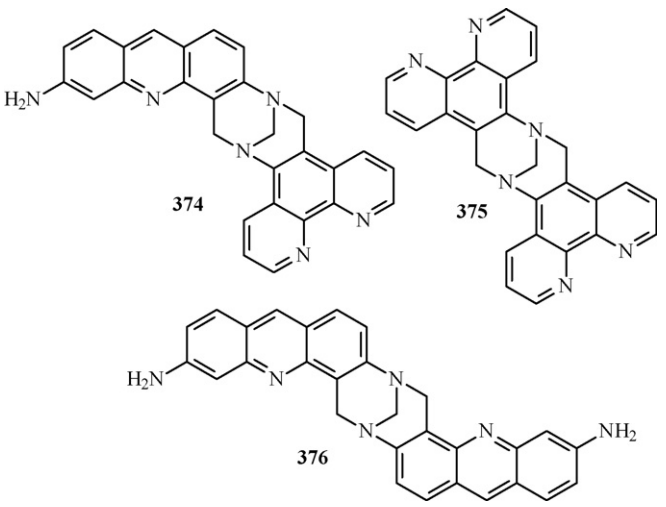

Scheme 123.

bipyridine in the structure of **365** and **366** lead to poorly efficient G-quadruplex stabilizing agents, due to the rotation around the biaryl axis which can disrupt the internal hydrogen-bonding motif [500].

To obtain efficient G-quadruplex binders, the authors also coupled within the same ligand different fused polycyclic heteroaromatic compounds, 1,10-phenantholine, acridine and quinacridine and an amino-glycoside fragment derived from the natural anti biotic neomicyn (**367**–**370** in Scheme 121) [504]. In fact, amino-glycosides contain amine groups, that, upon protonation, can give charge-charge and hydrogen-bonding interactions with nucleic acids and actually neomicyn exhibits a high selectivity for DNA triplexes. Furthermore, the 1,3 hydroxyl-amine motif present in amino-glycosides is known as recognition site for the complexation of phosphate and of the Hoogsteen face of guanine. Therefore ligands containing both an amino-glycoside unit and a heteroaromatic moiety could display high affinity for quadruplexes, targeting simultaneously the G quartet surface and phosphate groups.

Ligands **367**–**370** were synthesized by condensation of the appropriate dicarboxyaldheyde (2,9-diformyl-1,10-phenanthroline (**28**) in the case of the phen derivative) with neomycin functionalized with two alkyl-amino side-arms linked to its amino-methyl groups.

It was found that G-quadruplex stabilization increases with the size of the aromatic moiety, the quinacridine-containing macrocycle **369** being the most active. At the same time, however, the phen derivative **371**, not containing the neomycin moiety, was almost ineffective in inhibiting the telomerase activity, thus suggesting that in **370** the heteroaromatic units and the neomycin moiety play a cooperative role in the stabilizing effect. All compounds showed also selective stabilization of G-quadruplexes with respect to duplexes. Finally, all macrocycles were active in telomerase inhibition. Only **369**, however was active in the submicromolar range of concentrations.

Conjugates containing two heteroaromatic units linked by flexible or rigid linkers have been recently developed with the aim the generate molecule capable to give multiple interactions with DNA.

The simplest examples are the *bis*(phen) ligands **372** and **373**, recently reported by Sawai and co-workers (Scheme 122). **372** and **373** were obtained by reaction of 2-chloro-1,10-phenanthroline with en and diethylenetriammine, respectively. The latter being protected on the central amine group with BOC, which was subsequently removed [505]. A fluorimetric study showed that the typical emission of **372** and **373** at 400 nm is quenched in the presence of calf thymus DNA, indicating that both ligands bind to DNA. Surprisingly, **372**, but not **373**, gave rise to a new broad band at 528 nm, which was attributed to an exciplex emission produced by an intramolecular interaction between the two phen rings. Viscometric titrations showed that the viscosity of DNA increases in the presence of **373** in a manner similar to that observed for DNA intercalating agents. Conversely, **372** did not affect DNA viscosity. On this basis, the authors proposed that **373** binds to DNA in an intercalative mode, thereby preventing any interaction between the two phen units, whereas **372** behaves as a groove binder, making it possible the interaction between the two heteroaromatic units to produce the exciplex emission. Interestingly, the exciplex emission of **372** is enhanced upon interaction with $[poly(dA\text{-}dT)]_2$ and depressed in the presence of $[poly(dC\text{-}dG)]_2$, probably due to an energy or electron transfer process involving the G bases.

Bailly and co-workers have recently reported the synthesis of the Tröger base **374**, containing proflavine and phen linked by a rigid diaza-bridge (Scheme 123) [506]. **374** was synthesized from mono-protected proflavine and 5-amino-1,10-phenanthroline (**105**, Scheme 36) in the presence of formaldehyde. Spectroscopic (UV–vis, linear and circular dichroism) measurements and the assay of topoisomerase I inhibition provided evidence for DNA intercalation of the acridine moiety of **374**, while phen is probably hosted within a DNA groove. More interestingly, a footprinting study carried out on compounds **374**–**376** (Scheme 123) using a 117 bp (base pairs) restriction fragment and

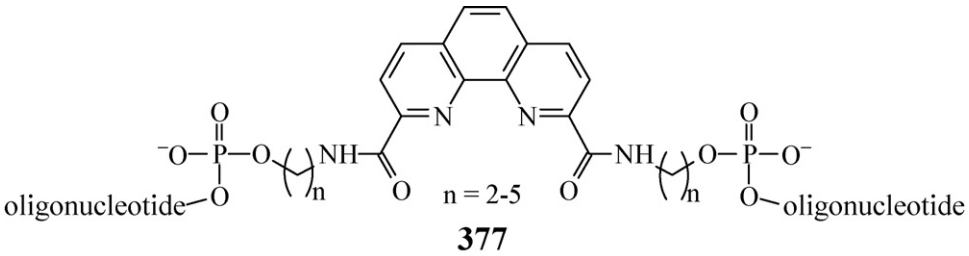

377

Scheme 124.

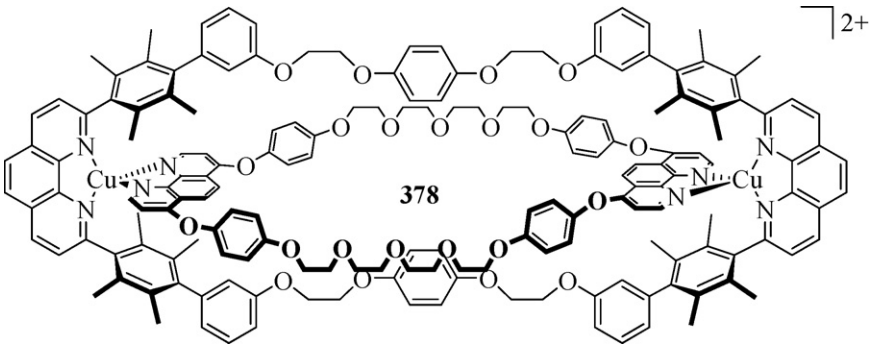

Fig. 43. Metallosupramolecular ring-in-ring structures [50].

the bovine pancreatic DNAase showed that **374** and **375** binds preferentially to sequences containing the triplets 5′-GTC and 5′-GAC. Conversely, **376** binds preferentially 5′-GTT·AAC or 5′-ATGA·TCAT motifs. This suggested that the footprinting pathway observed in the presence of **374** is mainly due to the phen moiety located in the DNA groove.

Phen has also been conjugated to oligonucleotides with the aim to stabilize DNA duplex containing an abasic site [507,508] or for the synthesis of oligonucleotides able to stabilize triplex structures [509].

Häner and co-workers have recently synthesized phen derivatives of general formula **377** (Scheme 124) conjugated to two oligonucleotides through linkers of different length, with the aim to stabilize duplexes containing an abasic site [507,508]. The phen-containing oligonucleotides, when coupled with the complementary strand containing the abasic site, due to a lacking thymine, lead to the assembly of stable duplexes. In these duplexes, the phen is positioned between the base pairs adjacent to the abasic site. This arrangement allows the maintenance of the stacking interactions within the helix even in the absence of a nucleobase. It was also found that the stability of the duplexes depends of the length of linker, the most stable being formed by the linker with $n = 4$.

Randazzo and co-workers have recently developed a protocol for the synthesis of 16 bp oligonuleotides, containing a phen moiety in the 3′-3′ inversion site of polarity, capable to induce the formation of triplex structures when coupled with the appropriate double-strand oligonucleotides [509]. Interestingly, the authors found that the presence of phen does not have negative effects on the stability of the triplexes and, in some cases, can give a stabilizing effect, probably due to the formation of energetically favorable interactions with groups in the major groove of the target duplex and/or to its intercalation between base pairs.

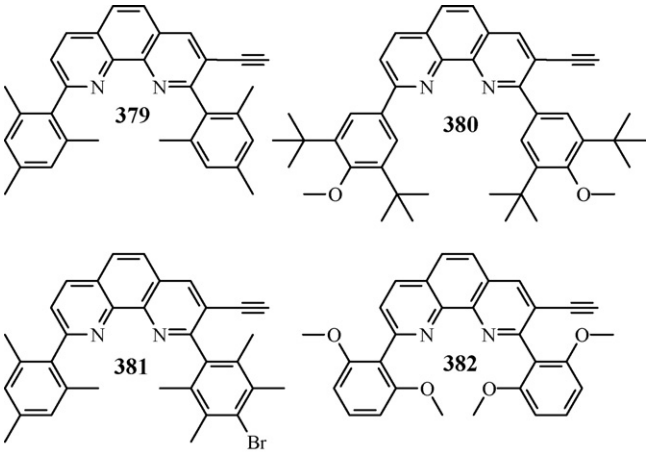

Scheme 125.

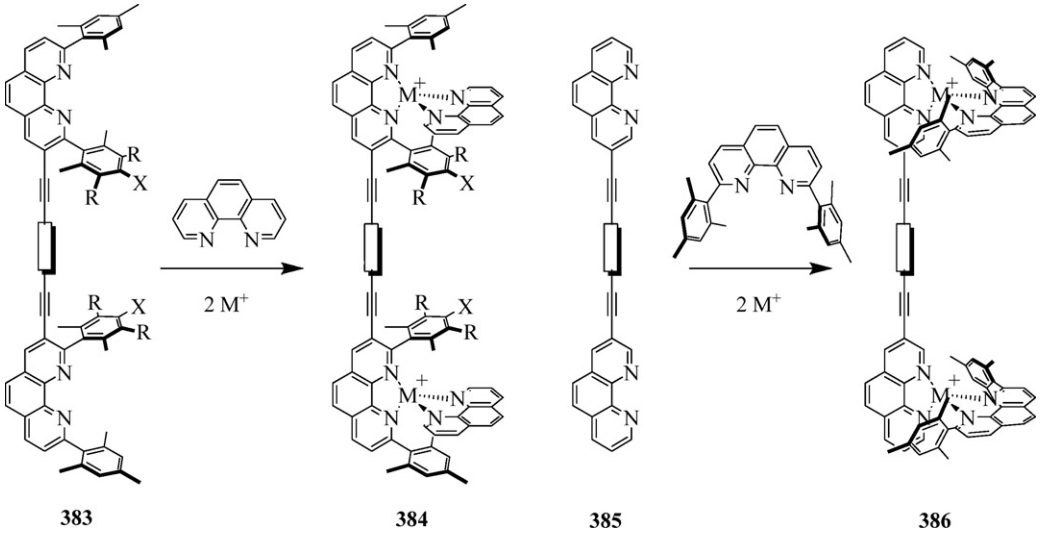

Fig. 44. Approaches for the constructions of dynamic rack-type motifs along with the HETPHEN concept [512].

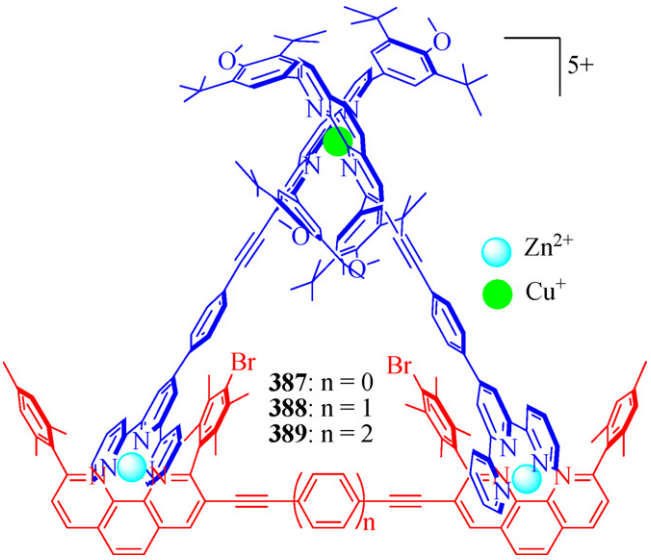

Fig. 45. Hereometallic isosceles triangles featuring tetrahedral and trigonal bipyramidal metal centres [514].

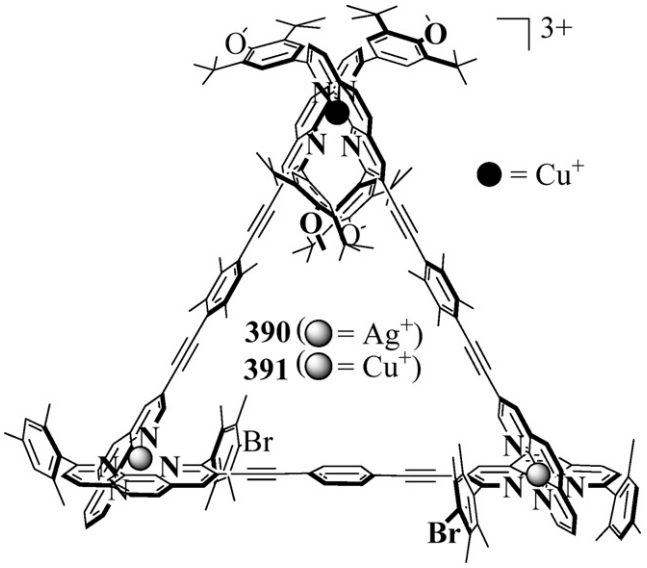

Fig. 46. Heterometallic isosceles triangles featuring tetrahedral only metal centres [513].

6. Phenanthroline in self-assembly processes and building of new materials

The appearance in the literature of threaded and interlocked macromolecules like rotaxanes, catenanes and knots officially determined the launch of phen in the world of supramolecular chemistry as key protagonist. From the previous sections, we hope it is clear the message that starting from phen as fiduciary binding site many molecular scaffolds can be developed for a great variety of usages. In this last section we want to consider the work it has been done in the last decade or so in developing supramolecular architectures *via* self-assembly and new materials starting from phen. We will not consider the wide field of catenanes and rotaxanes for which many reviews have been written [21,129–134].

6.1. Heteroleptic bis(phenanthroline) complexes and the HETPHEN and HETTAP approaches to self-assembly of supramolecular structures: racks, triangles, grids, prisms, tweezers

Schmittel and co-workers, in the late nineties developed for the first time a general procedure to prepare heteroleptic *bis*(phen) complexes of tetrahedrically coordinated metal ions such as copper(I) and zinc(II). They discovered that sterically hindered 2,9-diarylphenanthrolines cannot generally form the thermodynamically favoured homoleptic 2:1 ligand-to-metal complexes because of steric reasons. Therefore, only 1:1 complexes are obtained with such ligands, which can readily be treated with less hindered ligands such as phen and tpy to afford heteroleptic compounds in high yields according to the HETPHEN (Heterolopetic Phenanthroline Metal Complexes) and HETTAP concepts (Heteroleptic Terpyridine And Phenanthroline Metal Complexes) [43–45]. Schmittel and co-workers recognised immediately the possibility to use these concepts for the self-assembly of supramolecular structures and published in 2002 the synthesis of metallosupramolecular ring-in-ring structures such as **378** (see Fig. 43) obtained by self-assembly at copper(I) centres of two macrocyclic ligands, one having two endotopic phen units with binding sites shielded by functionalization at the 2,9-positions, and the other in which the two 4,7-disubstituted phen moieties are characterised by unshielded coordination sites [50].

In order to apply the HETPHEN and HETTAP concepts to the synthesis by dynamic self-assembly of nanostructured multicomponent structures of defined architectures and regular geometrical shapes, the first step was the preparation of 3-ethynyl-2,9-diaryl-1,10-phenanthrolines such as **379**–**382** (Scheme 125).

This was accomplished starting from 3-bromo-1,10-phenanthroline (**131**, Scheme 50) *via* sequential arylation reactions according to Sauvage method, and Sonogashira cross-couplings (see above) [49,510]. Starting from **379** to **382** and similar systems, a whole library of rigid oligo(2,9-diaryl-1,10-phenanthrolines) were synthesised, which, therefore, were encoded with the required control features to prevent any homoleptic combination with themselves, in agreement with the HETPHEN and HETTAP concepts [511]. The appropriate combination of such ligands with sterically innocent mono- or oligophenanthrolines and/or mono or oligoterpyridines, and tetrahedrically coordinated metal ions, mainly Cu^+ and Zn^{2+}, allows heteroleptic self-assemblies under thermodynamic control of multicomponent aggregates of well defined and programmed shapes.

For example, multitopic dymanic rack-type aggregates have been prepared following the two synthetic possible approaches along the HETPHEN concept as outlined in Fig. 44 [51,512].

Accordingly, ligands bearing shielded phen moieties bind strongly to Cu^+ ions but do not undergo self-association to homoleptic complexes. In combination with unshielded ligands give in a stepwise manner rack-type aggregates. The nature of these aggregates is dynamic in solution as, on mixing two of them, a ligand exchange equilibrium takes place [512].

The simplest and smallest of the two-dimensional architecture family is the supramolecular triangle. Matallosupramolecular triangles have been assembled by mixing a ditopic ligand with a metal ion using homoleptic binding motif, but the outcome of this procedure is generally a mixture of homometallic and equilateral (both geometrically and chemically) triangle and square assemblies [513]. Using the PHENLOCK concept (preparation of a kinetically locked homoleptic copper(I) *bis*(phen) complex [54]) in combination with dynamic heteroleptic aggregation of phen and tpy ligands at a single metal centre along the HETPHEN and HETTAP concepts, Schmittel and co-workers have been able to prepare the first supramolecular triangles, **387**–**389**, which are heterometallic and isosceles, both geometrically and chemically (see Fig. 45) [513,514].

Interestingly, these isosceles triangles were obtained in exclusive manner by reacting either the preformed homoleptic copper(I) hinge module with the *bis*(phen) module and Zn^{2+} (see Fig. 45) or by

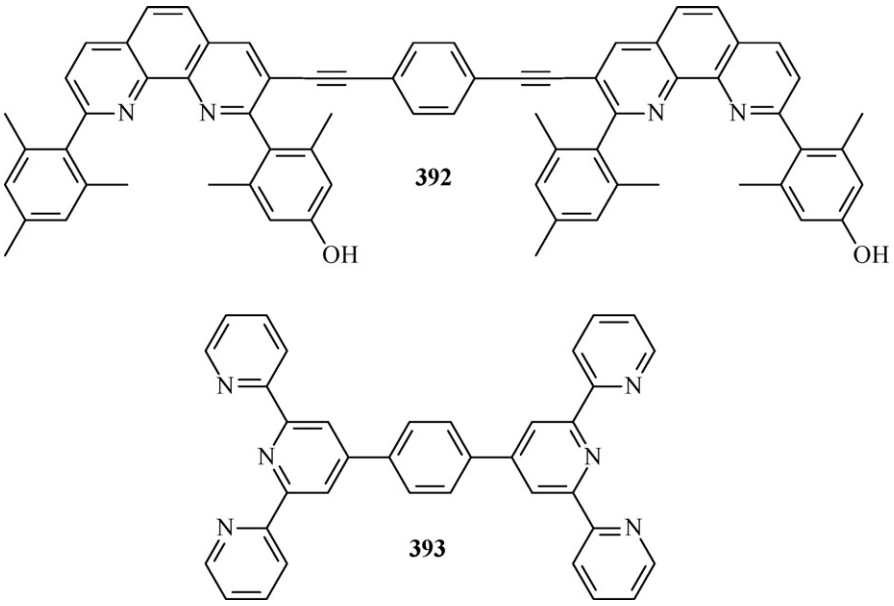

Scheme 126.

reacting all single components in MeCN in a one pot procedure. The same kind of supramolecular triangles can be dynamically assembled by using a kinetically stable copper(I) complex as angular unit equipped with phen terminals and all tetrahedral metal centres (see Fig. 46) [513].

If polytopic phen ligands with steric stoppers at the 2,9-positions of the *bis*-imine units are combined with ditopic innocent *bis*(terpyridines), *bis*(phenanthrolines) or mixed ligands in the presence of appropriate metal ions, nanoscale ladders- and grid-motifs, respectively can dymanically self-form and self-recognize under thermodynamic control along the HETPHEN and HETTAP concepts and consequent self-sorting processes [46,53,515]. For example upon reaction of **392** and **393** (Scheme 126) with $Zn(OTf)_2$ in 1:1:2 molar ratio, the clean formation of the ladder-like assembly $[Zn_4(\mathbf{392})_2(\mathbf{393})_2]^{8+}$ is observed in basically quantitative yield (see Fig. 47) [53]. Interestingly, the ladder-like assembly $[Zn_4(\mathbf{392})_2(\mathbf{393})_2]^{8+}$ exhibits distinct fluorescence emissions in MeCN solution as contrary to the corresponding ladder-like

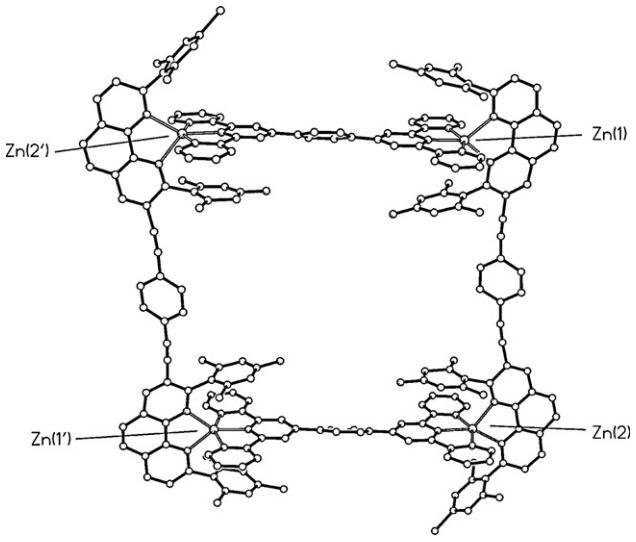

Fig. 47. ORTEP view of the ladder-like complex cation $[Zn_4(\mathbf{392})_2(\mathbf{393})_2]^{8+}$ [53]. H-atoms are omitted for clarity.

multicomponent assemblies featuring Cu^+ or Hg^{2+} at the four corners of the structure, which do not fluoresce. On the basis of the dynamic nature of these supramolecular systems, the authors conceived a two-step double-transmetallation OFF-ON-OFF system: indeed, upon addition of Zn^{2+} to a solution of the non-fluorescent (OFF) $[Cu_4(\mathbf{392})_2(\mathbf{393})_2]^{4+}$ system, the fluorescent (ON) $[Zn_4(\mathbf{392})_2(\mathbf{393})_2]^{8+}$ system is formed that can be further transformed into $[Hg_4(\mathbf{392})_2(\mathbf{393})_2]^{8+}$ (non-fluorescent, OFF) upon addition of Hg^{2+} following the binding constants for the three heteroleptic multicomponent structures which increase in the order $Cu^+ < Zn^{2+} < Hg^{2+}$ [53].

At this stage, it should be clear the power of the HETPHEN and HETTAP approaches to dynamic self-assembly of supramolecular structures once the proper components have been designed and engineered. For example to prepare sufficiently the large (nanoscale) and stable double and triple deckers with large internal voids **394** and **395** (see Fig. 48), a rigid macrocycle with two exotopic phen binding sites was combined with linear *bis*- or *tris*(phen) derivatives bearing bulky groups at the 2,9-positions in the presence of tetrahedral coordinated metal cations (Cu^+, Ag^+), thus calling in action the thermodynamic control along the HETPHEN concept [516,517].

Following this powerful and effective synthetic approach to heterometallic and heteroleptic multimetallic assemblies, remarkable supramolecular multicomponent structures have been produced such as void and filled nanoprisms [49,518], spoked wheels [519], nanobaskets [520], dubbell-shaped supramolecules [52] and tweezers [521]. The last type of supramolecular assembly, for example **396**, was the exclusive product of a three-component assembly, namely a phen-appended zinc(II)-porphyrin, Cu^+ and an unshielded *bis*(phen) ligands (see Fig. 49).

On adding *bis*-N-donor spacers to **396** to set up an additional orthogonal binding motif between the tweezers arms, different and still dynamic assemblies such as a bridged mono-tweezers, a double bridged double-tweezers and a triple bridged double-tweezers (**397**) were formed, depending on the length of the spacer [521]. Notably, the multimolecular aggregate **397** (see Fig. 50) is formed either following a stepwise approach by adding 1,4-diazabicyclo[2.2.2]octane (DABCO) to the preformed **396**, or *via* a one-pot reaction, where all components were mixed as solids using the correct stoichiometry and then brought in solution upon

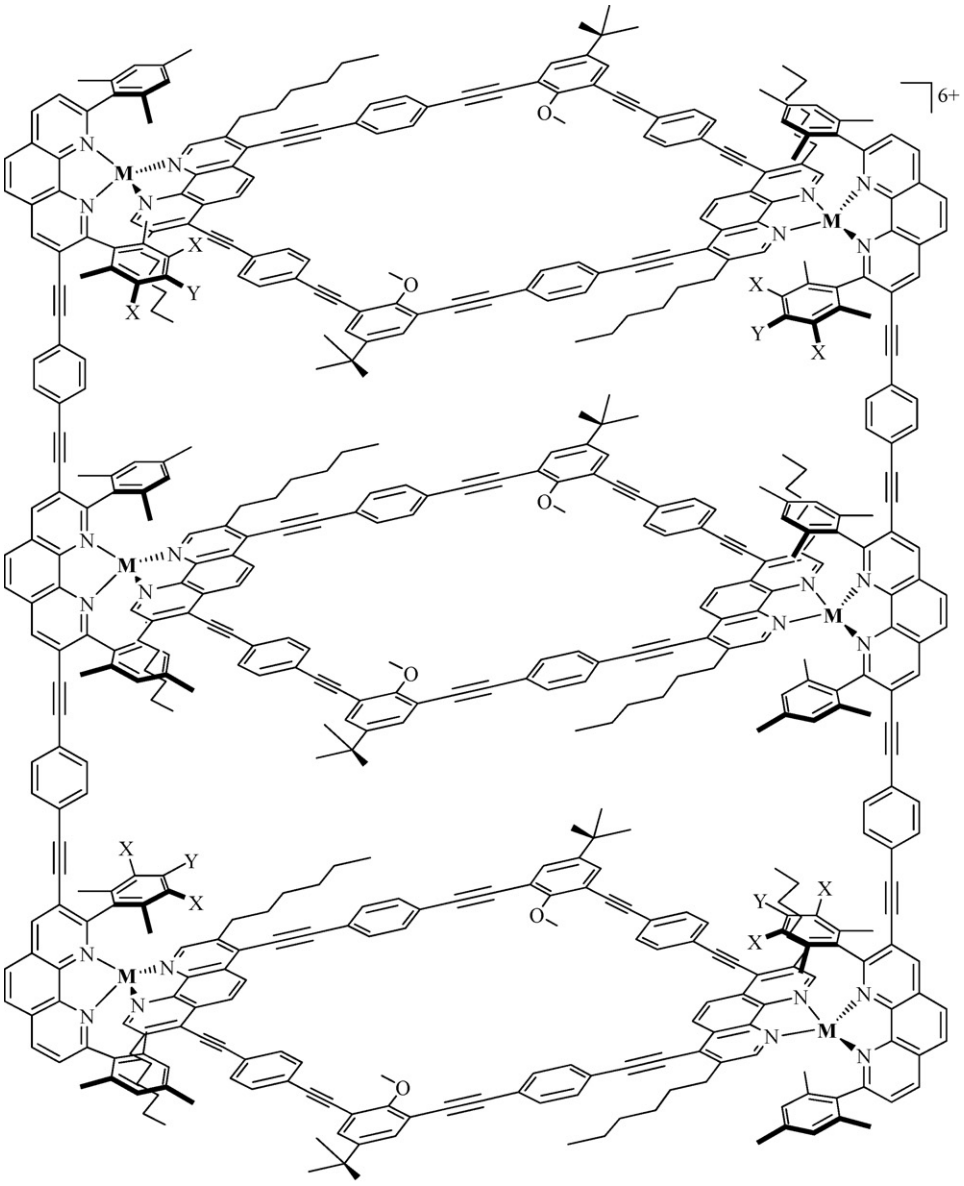

394: X = H, Y = Me, M = Cu^+
395: X = Me, Y = Br, M = Cu^+

Fig. 48. Nanotubular structures assembled along the HETPHEN concept [517].

addition of dichloromethane, as proved by monodimensional ^{1}H NMR, UV–vis spectroscopies and DOSY experiments [521].

Following a more classic synthetic approach Sauvage and co-workers developed in the late nineties another type of porphyrin tweezers, **398** (Scheme 127), that features two oblique zinc(II)-(*tris*-*t*butylphenyl)porphyrins connected covalently through a phen moiety functionalised at the 2,9-positions [522,523].

Systems like **398** were initially conceived to investigate intramolecular energy-transfer processes between the two porphyrinic units (one containing a zinc(II) centre and the other empty) on changing the relative distance and orientation. Subsequently, **398** proved to be a perfect host, acting as bifunctional receptor for *meso*-5,10-*bis*(4′-pyridyl)-15,20-diphenylporphyrin to give quantitatively a *tris*-porphyrin macrocyclic supramolecular assembly [524]. X-ray diffraction analysis (see Fig. 51) confirmed the perfect geometrical match between the two interacting components. Photophysical measurements indicated that the free-base porphyrin guest behaves as an energy sink by collecting almost quantitatively the light energy absorbed on irradiation by the two zinc(II)-porphyrin chromophore units [524].

6.2. Double stranded Helicates and foldamers

Helices are the key structural features of many biological macromolecules and for this reason many efforts have been devoted to the synthesis of either helical complexes *via* self-assembly of properly designed organic poly-bidentate ligands and metal cations preferring four-coordination and tetrahedral geometry, or oligomers that can fold into stable helical secondary structures. In this game, phen has also been considered due to its denticity and binding properties.

Starting from **29**, **33**, **38** (Scheme 11) and the corresponding bpy analogues, Cohen and co-workers prepared the ligands **399**–**402** (Scheme 128) [525]. **399** and **400** were proven to self-assembly in solution into trinuclear double-stranded $[(L)_2M_3]^{3+}$-type helicates

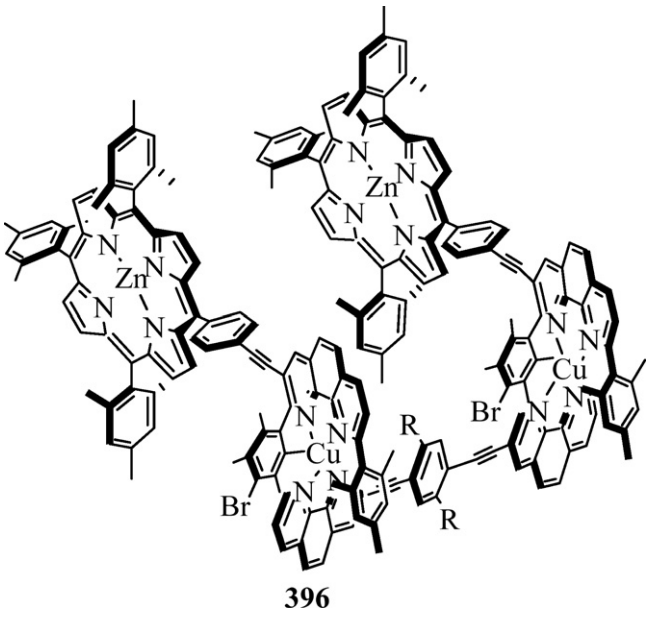

Fig. 49. Supramolecular porphyrin tweezer [521].

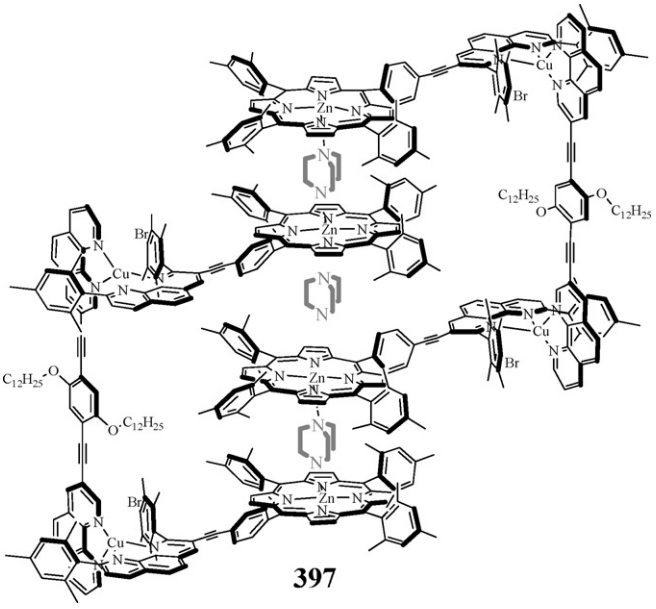

Fig. 50. Triple bridged double-tweezers [521].

upon reaction with copper(I) and silver(I). Interestingly, a statistical mixture of homoleptic and heteroleptic trinuclear double-stranded helicates was formed on treating a mixture of the above ligands with copper(I), thus confirming the absence of self-recognition during the course of self-assembly process [525].

Following a multistep procedures based on sequential Suzuki coupling reactions between aromatic nuclei and nucleophilic addition of aryllithium derivatives onto a phen fragment, Sauvage and co-workers synthesised the two multi-site ligands **403** and **404** (Scheme 129) containing four and five phen moieties in line, respectively, connected by 1,3-phenylene linkers, and ending with two olefinic chains.

403 and **404** afforded almost quantitatively the four- and five-lithium double-stranded complex helicates $[Li_4(\mathbf{403})_2]^{4+}$ and $[Li_5(\mathbf{404})_2]^{5+}$, respectively. Interestingly, metal-exchange reactions on $[Li_5(\mathbf{404})_2]^{5+}$ showed selective replacement of the terminal lithium(I) cations by copper(I) to form a mixed pentanuclear helical complex featuring a Cu^+–Li^+–Li^+–Li^+–Cu^+ sequence [526].

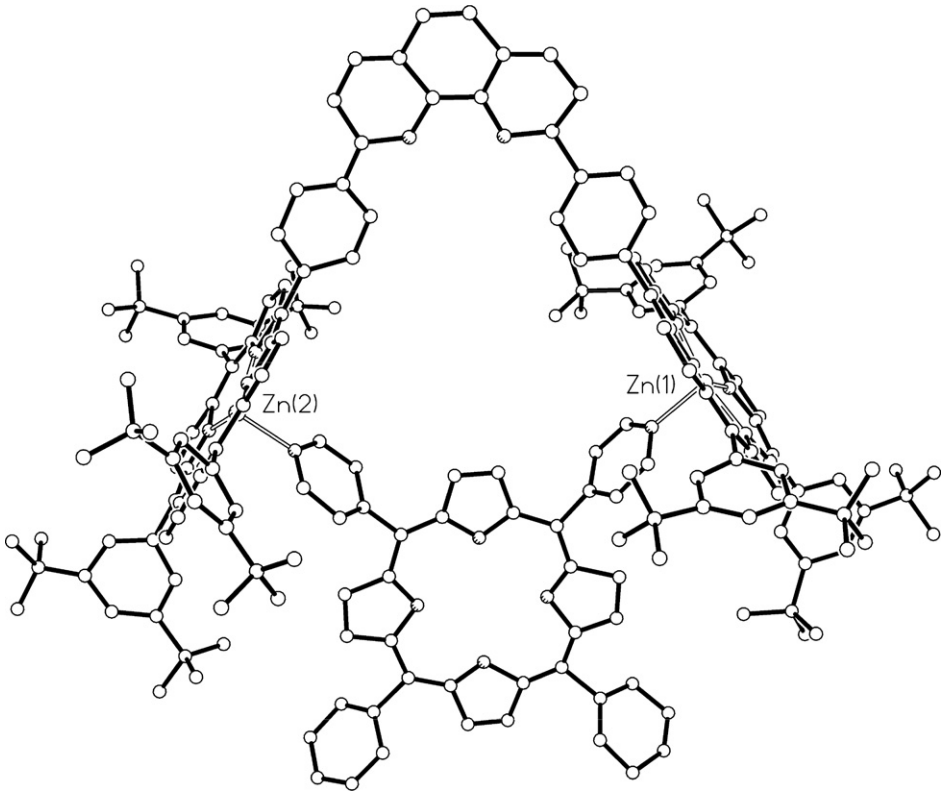

Fig. 51. ORTEP view of *tris*-porphyrin macrocyclic supramolecular assembly based on the porphyrin tweezers **398** [524].

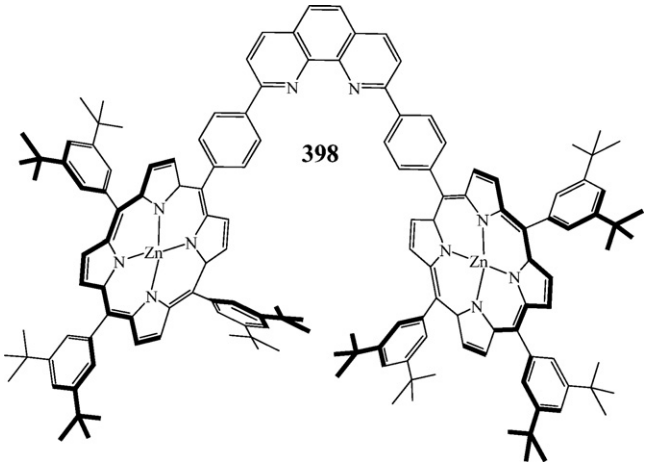

Scheme 127.

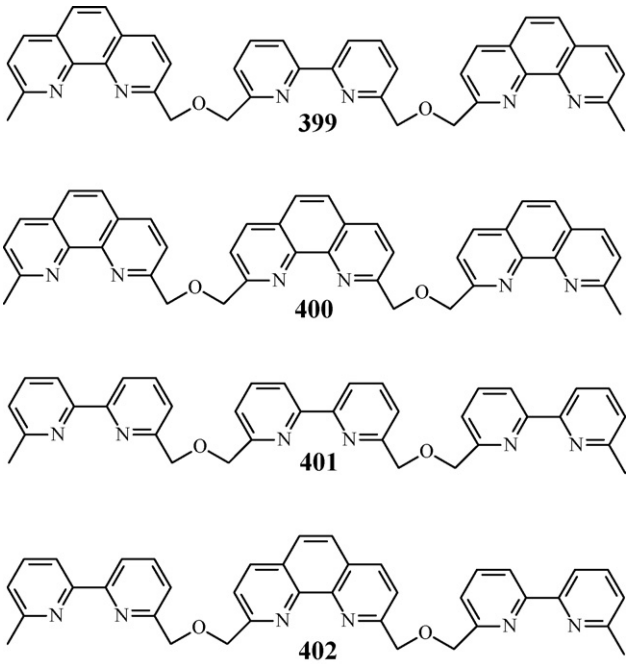

Scheme 128.

Recently, Nitschke and co-workers have established dynamic subcomponent self-sorting and self-assembly into copper(I) double helicates [527]. In particular, the reaction of copper(I) (3 equiv.), 8-aminoquinoline (4 equiv.) and 2,9-diformyl-1,10-phenanthroline (**28**, Scheme 11) (2 equiv.) in DMSO or acetonitrile afforded the tricopper double helicate **405** (Scheme 130).

If 4-chloroaniline was used in place of 8-aminoquinoline, the structure generated in the presence of copper(I) was the dicopper helicate **406**. Interestingly, the addition of 8-aminoquinoline (4 equiv.) and copper(I) (1 equiv.) to **406** resulted in quantitative subcomponent substitution and formation of **405**. Furthermore, on mixing of 4-chloroaniline, 8-aminoquinoline and **28** (4 equiv. each) a dynamic library of imine condensation products formed in equilibrium with the starting materials, on adding copper(I) (5 equiv.) this mixture collapsed within about four days to give **405** and **406** as uniquely templated products.

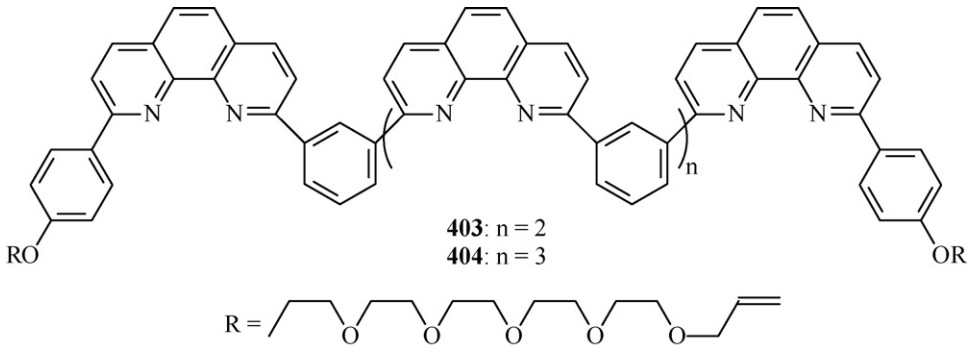

Scheme 129.

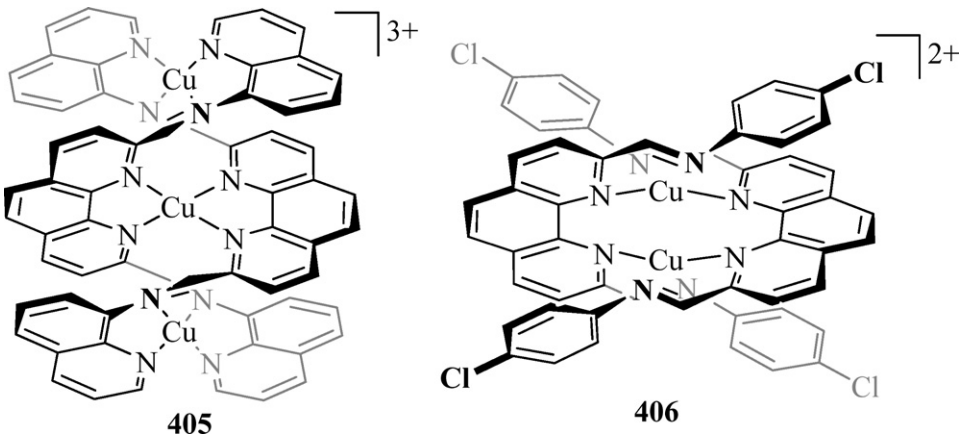

Scheme 130.

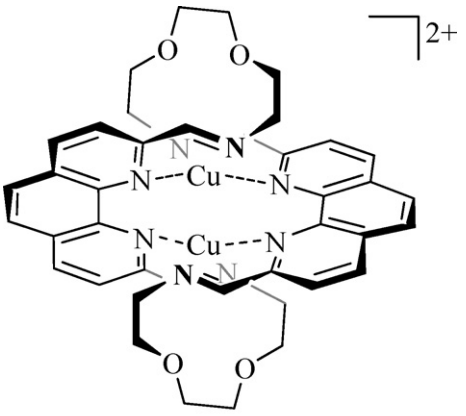

407

Scheme 131.

If **28** is reacted with an equimolar amount of the aliphatic diamine 2-(2-(2-aminoethoxy)ethoxy)ethanamine in the presence of copper(I) (2 equiv.) the dimeric helical macrocycle **407** (Scheme 131) is formed quantitatively [528]. The ring closure responsible of the formation of **407** could also occur on adding stoichiometrically the aliphatic diamine to an acyclic helicate similar to **406** containing four mono-imine residues; this would agree with the chelate effect being the driving force of the transformation. Interestingly, if the acyclic helicate contains mono-imines derived from aniline (sulfanilic acid) it is possible by changing the pH, to switch dynamically between the acyclic helicate and **407**, with the closed topology of **407** being favoured at basic pH values [528]. Further dynamic topological control over subcomponent self-assembly reaction was achieved by using longer diamines as starting material; in particular, the use of a diamine incorporating two rigid phenylene moieties between the flexible chain and the amino group resulted in the formation of catenate instead of closed helicate, the imine bonds formation and ring closure process taking place, therefore, at the 2,9-positions of the same phen moiety [528].

The possibility of controlling thermodynamically the subcomponent self-assembly of helicate structures through dynamic covalent imine bonds formation has recently been exploited by Nitschke and co-workers in helicate extension reactions performed by adding to preformed dicopper(I) or tricopper(I) helicates appropriate building blocks and leaving the "programming instructions" (electronic, steric and entropic effects, the conformational preferences of organic building blocks, the coordinative preferences of the metal ion, pH and solvent nature) to operate [529–531]. For example, the reaction between the dicopper(I) double-helicate **408** and 1,2-diaminobenzene gave the double-helicate **409** featuring four closed spaced copper(I) ions (Scheme 132), whose nature was also ascertained by X-ray diffraction analysis [530]. Although in lower yield, **408** could also be obtained starting from a mixture of each subcomponent by self-assembly. This result is quite remarkable being known that diamines and dialdehydes usually react with each other to form metal-templated macrocycles. This cannot happen on mixing 1,2-diaminobenzene and 2,9-diformyl-1,10-phenanthroline (**28**) as an entirely flat, conjugated macrocyclic product would be characterised by excessive straining in bond angles [530].

The pre-formed *bis*-tridentate imino-phenanthroline ligand **410** (Scheme 133) has also been used in the formation of low-spin dinuclear iron(II) double helical complex $[Fe_2(\mathbf{410})_2]^{2+}$ [532], while phen cyclophanes **411** and **412** (Scheme 133), prepared start-

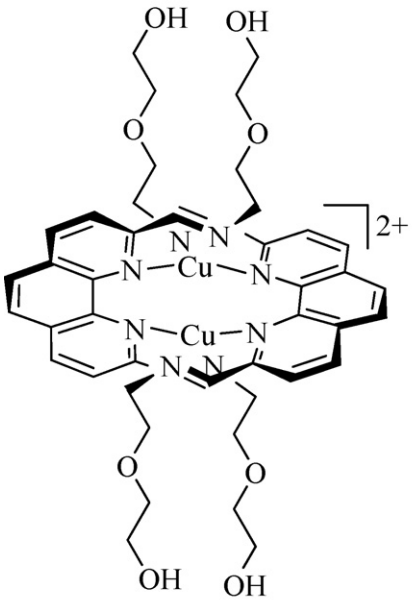

408

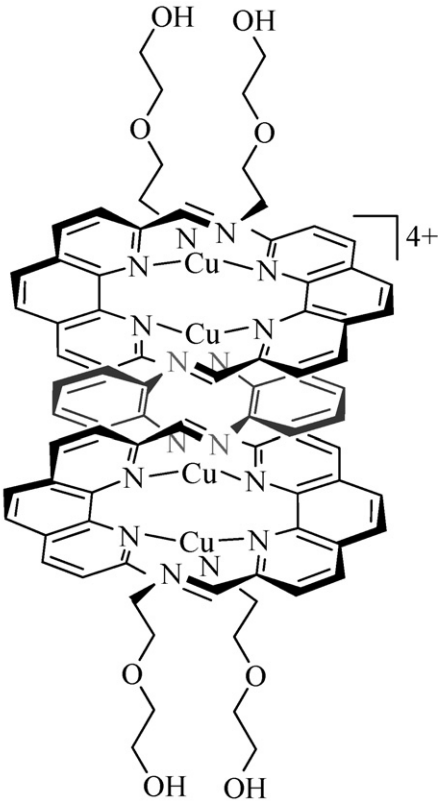

409

Scheme 132.

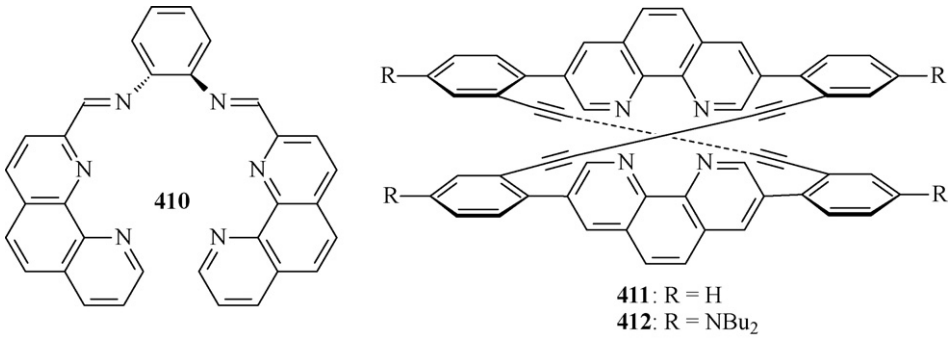

Scheme 133.

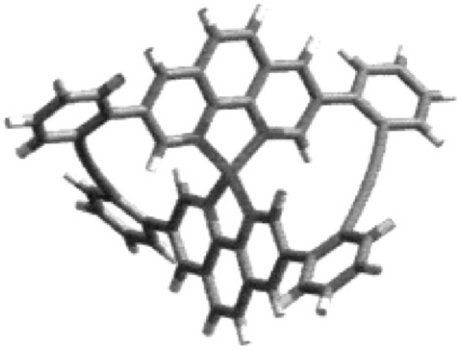

Fig. 52. Molecular model of [Cu(**411**)]$^+$. This figure is taken from [533] and reprinted with permission; copyright 2002, by Wiley-VCH.

ing from 3,8-dibromo-1,10-phenanthroline (**132**, Scheme 50) by Pd^{2+}- and Cu^{2+}-mediated cross-coupling reactions [533], displayed a clear helical nature in their mononuclear copper(I) complexes.

Fig. 52 shows the calculated structures of [Cu(**411**)]$^+$ mononuclear helicate, the metal centre fits nicely in the *pseudo*-tetrahedral coordination site created by the mutual perpendicular phen moieties of **411**.

Beside helical complexes (helicates) prepared *via* self-assembly of properly designed organic poly-bidentate ligands and metal cations, oligomers that could fold on their own into stable, well-defined helical secondary structures (synthetic foldamers) are also receiving increasing attention [534]. In this context, aromatic oligoamides based on phen dicarboxyamides such as **413** (Scheme 134), obtainable from the 2,9-dicarboxylic acid-1,10-phenanthrolines, are very interesting [535–537].

In oligoamides like **413**, the *o*-phenylenediamide moieties can assume s-*cis* and s-*trans* conformations as a consequence of the rotation about the CONH-aryl bond (see Fig. 53). Generally, such s-*cis* conformations for the *o*-phenylenediamide bonds are favoured and this causes the oligomers to assume secondary helical structures in solution and in the solid state.

An s-*cis*/s-*trans* conformational transition in one of the *o*-phenylenediamide subunits would cause the formation of a supersecondary helix-turn structure. Clearly, solvent effects together with intramolecular hydrogen-bonding and π–π staking interactions play a key role in stabilizing and therefore determining

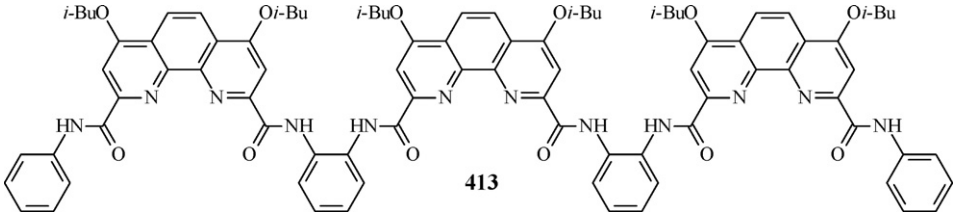

Scheme 134.

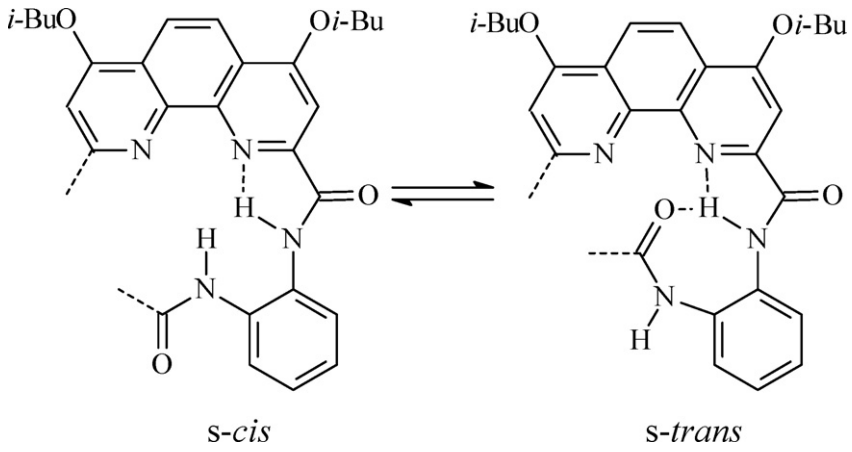

Fig. 53. s-*cis*/s-*trans* isomerization in oligo(phenanthroline dicarboxamide)s.

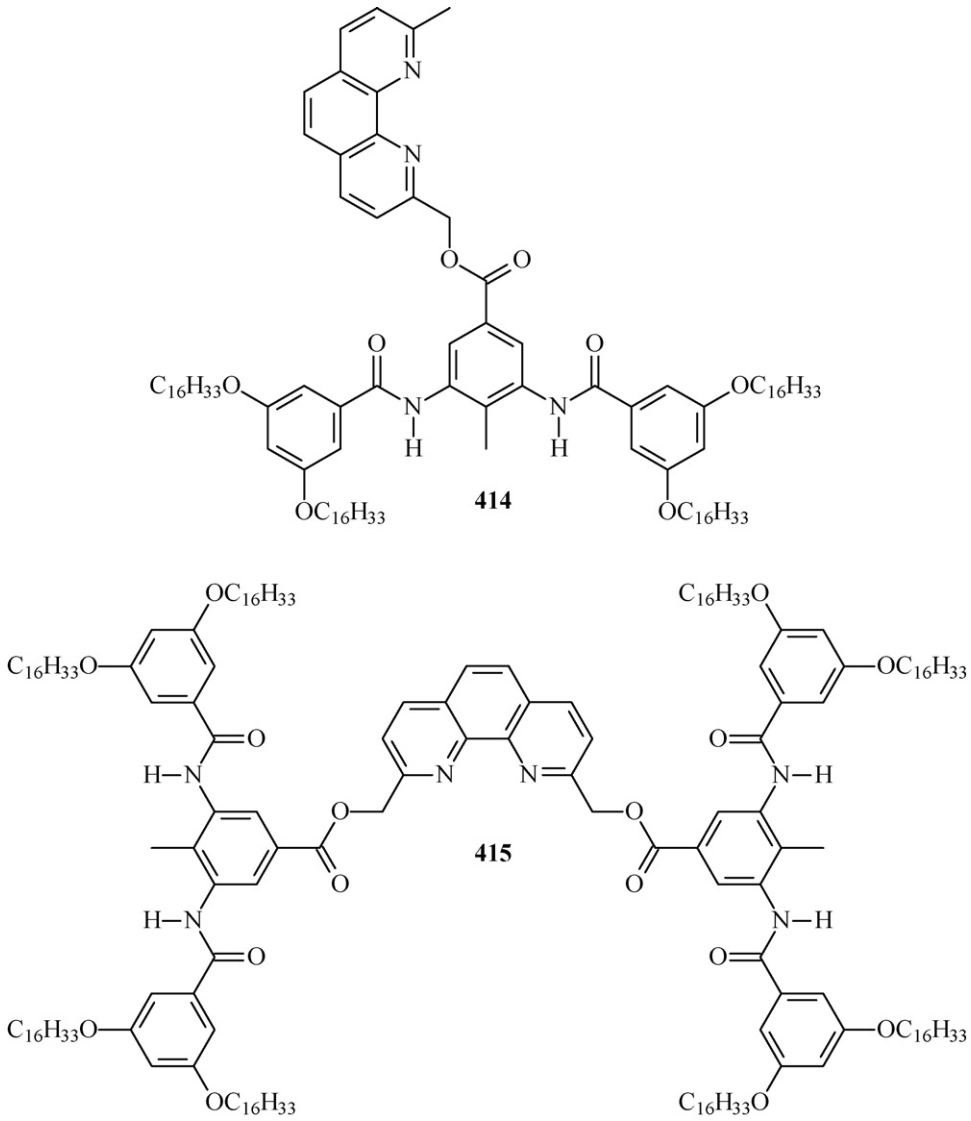

Scheme 135.

both the secondary helical and supersecondary helix-turn structures [536]. In order to built foldamers with encoded instructions for a helix-turn-helix supersecondary structure, composed by two helices connected by a turn, a binaphthyldiamine moiety has been inserted into the chains of the oligo(phenanthroline dicarboxamide)s so to impart a turn to the normal secondary helical structure determined by the s-*cis* conformation of the *o*-phenylenediamide bonds [537].

6.3. Dendrimers

Phen-based dendritic ligands are of great interest especially for the development of luminescent and redox-active metallodendrimers featuring in general $[Ru(phen)_3]^{2+}$ and $[Cu(phen)_2]^{+}$-type cores. In this respect, in order to have dendrimers exhibiting a regular branched architecture, due to steric reasons, the attachment of highly branched units (dendrons) at the phen nucleus is only possible at the 2,9-, 3,8- and 4,7-positions.

1,3,5-Phenylene-, carbazole- and benzylether-based Fréchet-type dendrons have been implemented at the above mentioned positions of a phen unit to give dentritic ligands and the corresponding ruthenium(II) [538–541] and copper(I) complexes [542–545]. Some of these metallodendrimers can be regarded as efficient light-harvesting antenna systems as the light absorbed by the dendritic branches is transferred with high efficiency to the luminescent MLCT states of the ruthenium(II) chromophoric core [540,541].

Cascade or functional dendrimers containing various electro- and photoactive chromophores that can influence the properties of the phen-based-core moiety are of great interest. Recently, Nierengarten and co-workers have prepared fascinating dendrimers in which a $[Cu(phen)_2]^{+}$-type core is surrounded by up to 16 C_{60} terminal units [544,545]. In the smaller members of this family of dendrimers, the surrounding fullerene-functionalised dendritic branches are able to isolate the central copper(I) complex. In fact, as contrary to the dendrimers mentioned above and having $[Ru(phen)_3]^{2+}$-type cores, upon excitation of MLCT absorption bands of the $[Cu(phen)_2]^{+}$-type core, no luminescence is detected due to an energy transfer quenching process to the peripheral C_{60} units. Furthermore, for the larger dendrimers belonging to this family, the core is inaccessible to external stimulus (molecules, electron and photons) and it is as buried in a sort of "black box" made up of fullerene units.

Ziessel and co-workers have recently reported the synthesis of the two phen-based ligands **414** and **415** (Scheme 135) bearing one or two 4-methyl-3,5-diacylaminophenyl modules

equipped with two lateral dialkoxyphenyl groups, respectively [546,547].

These two ligands were prepared starting from 3,5-dinitro-*p*-toluic acid and **38** and **29** (Scheme 11), respectively, *via* an esterification reaction in the final coupling step [546,547]. Compound **414** aggregates through non-covalent interactions (intermolecular H-bonds involving amide groups and π–π staking interactions of the phenyl subunits) in hydrocarbon solvents, thus causing their gelation, and it has a liquid crystalline behaviour exhibiting thermotropic cubic mesophases [546,548]. This high tendency to supramolecular organization and self-organization does not take place in diluted solutions. Interestingly, the corresponding 2:1 metal-to ligand copper(I) complex of **414** is not an organogelators, but analogously to the free ligand exhibits liquid-crystalline mesomorphism giving rise to a columnar mesophase. Furthermore, for the copper(I) complex intermolecular H-bonds persist even in diluted solutions. This represents a rare case of production of mesomorphic materials with both ligands and corresponding complexes, and of ligands highly ordered either at the solid state or in solution, which behave as organogelators and as thermotropic liquid crystals. The combination of non-covalent intermolecular interactions can be considered at the origin of these properties.

7. Conclusions and perspectives

In this work we have reviewed the most recent (10–15 years) developments in the synthetic and coordination chemistry of phen-based ligands. In particular, with this work we wanted to bring at the attention of chemists working in different fields of research, the extraordinary versatility of phen: an old ligand that has passed the age of "coordination chemistry" to enter the era of "supramolecular chemistry" as protagonist. We believe that this overview of the different uses that can be made of this ligand will be inspirational for further fascinating compounds with interesting applications.

References

[1] L.A. Summers, Adv. Heterocycl. Chem. 22 (1978) 1.
[2] P.G. Sammes, G. Yahioglu, Chem. Soc. Rev. 23 (1994) 327.
[3] C.R. Luman, F.N. Castellano, in: J.A. McCleverty, T.J. Meyer, A.B.P. Lever (Eds.), Comprehensive Coordination Chemistry, vol. 1, Elsevier, Oxford, UK, 2004, p. 25.
[4] G. Anderegg, Helv. Chim. Acta 46 (1963) 2397.
[5] G. Anderegg, Helv. Chim. Acta 46 (1963) 2813.
[6] P. Paoletti, Pure Appl. Chem. 56 (1984) 491.
[7] S.F. Ashcroft, C.T. Mortimer, Thermochemistry of Transition Metal Complexes, Academic Press, NY, USA, 1970.
[8] K.E. Erkkila, D.T. Odom, J.K. Barton, Chem. Rev. 99 (1999) 2777.
[9] D.S. Sigman, R. Landgraf, D.M. Perrin, L. Pearson, in: A. Sigel, H. Sigel (Eds.), Metal Ions in Biological Systems, vol. 33 (Probing of Nucleic Acids by Metal Ion Complexes of Small Molecules), Marcel Dekker, NY, USA, 1996, p. 485.
[10] N. Armaroli, L. De Cola, V. Balzani, J.-P. Sauvage, C.O. Dietrich-Buchecker, J.-M. Kern, J. Chem. Soc., Faraday Trans. 88 (1992) 553.
[11] M.S. Henry, M.Z. Hoffman, J. Phys. Chem. 83 (1979) 618.
[12] G. Accorsi, A. Listorti, K. Yoosaf, N. Armaroli, Chem. Soc. Rev. 38 (2009) 1690.
[13] A. Juris, V. Balzani, F. Barigelletti, S. Campagna, P. Belser, A. Von Zelewsky, Coord. Chem. Rev. 84 (1988) 85.
[14] N. Armaroli, Chem. Soc. Rev. 30 (2001) 113.
[15] D.V. Scaltrito, D.W. Thompson, J.A. O'Callaghan, G.J. Meyer, Coord. Chem. Rev. 208 (1) (2000) 243.
[16] J. Bossert, C. Daniel, Coord. Chem. Rev. 252 (23–24) (2008) 2493.
[17] A. Lavie-Cambot, M. Cantuel, Y. Leydet, G. Jonusauskas, D.M. Bassani, N.D. McClenaghan, Coord. Chem. Rev. 252 (23–24) (2008) 2572.
[18] Y.-N. Chen, Y. Fan, J. Ni, Dalton Trans. (2008) 573.
[19] V. Balzani, A. Credi, M. Venturi, Molecular Devices and Machines. Concepts and Perspectives for the Nanoworld, 2nd ed., Wiley-VCH, Weinheim, Germany, 2008.
[20] H. Sugihara, K. Hiratani, Coord. Chem. Rev. 148 (1996) 285.
[21] J.-P. Sauvage, C.O. Dietrich-Buchecker, Molecular Catenanes. Rotaxanes and Knots. A Journey through the Wolrls of Molecular Topology, Wiley-VCH, Weinheim, Germany, 1999.
[22] E.C. Riesgo, X. Jin, R.P. Thummel, J. Org. Chem. 61 (1996) 3017.
[23] R. Zong, D. Wang, R. Hammitt, R.P. Thummel, J. Org. Chem. 71 (2006) 167.
[24] A. Juris, L. Prodi, A. Harriman, R. Ziessel, M. Hissler, A. El-ghayoury, F. Wu, E.C. Riesgo, R.P. Thummel, Inorg. Chem. 39 (2000) 3590.
[25] Y.-Z. Hu, Q. Xiang, R.P. Thummel, Inorg. Chem. 41 (2002) 3423.
[26] L. Chouai, F. Wu, Y. Jang, R.P. Thummel, Eur. J. Inorg. Chem. (2003) 2774.
[27] D. Brown, R. Zong, R.P. Thummel, Eur. J. Inorg. Chem. (2004) 3269.
[28] T. Bark, R.P. Thummel, Inorg. Chem. 44 (2005) 8733.
[29] R. Zong, R.P. Thummel, Inorg. Chem. 44 (2005) 5984.
[30] A.N. Singh, R.P. Thummel, Inorg. Chem. 48 (2009) 6459.
[31] Y. Jahng, R.P. Thummel, S.G. Bott, Inorg. Chem. 36 (1997) 3133.
[32] M. Abrahamsson, H.-C. Becker, L. Hammarström, C. Bonnefous, C. Chamchoumis, R.P. Thummel, Inorg. Chem. 46 (2007) 10354.
[33] Y.-Z. Hu, M.H. Wilson, R. Zong, C. Bonnefous, D.R. McMillin, R.P. Thummel, Dalton Trans. (2005) 354.
[34] J.J. Moore, J.J. Nash, F.E. Fanwick, D.R. McMillin, Inorg. Chem. 41 (2002) 6387.
[35] D.R. McMillin, J.J. Moore, Coord. Chem. Rev. 229 (2002) 113.
[36] C.O. Dietrich-Buchecker, P.A. Marnot, J.-P. Sauvage, Tetrahedron Lett. 23 (1982) 5291.
[37] S.-N. Pun, W.-H. Chung, K.-M. Lam, P. Guo, P.-H. Chan, K.-Y. Wong, C.-M. Che, T.-Y. Chen, S.-M. Peng, Dalton Trans. (2002) 575.
[38] M. Feng, K.-S. Chan, Organometallics 21 (2002) 2743.
[39] Y.-Y. Lin, S.-C. Chan, M.C.W. Chan, Y.-J. Hou, N. Zhu, C.-M. Che, Y. Liu, Y. Wang, Chem. Eur. J. 9 (2003) 1264.
[40] R.J.M. Klein Gebbink, M. Watanabe, R.C. Pratt, T.D. Stack, Chem. Commun. (2003) 630.
[41] D.A. Bardwell, J.G. Crossley, J.C. Jeffery, A.G. Orpen, E. Psillakis, E.E.M. Tilley, M.D. Ward, Polyhedron 13 (1994) 2291.
[42] D.A. Bardwell, A.M.W. Cargill Thompson, J.C. Jeffery, E.E.M. Tilley, M.D. Ward, J. Chem. Soc., Dalton Trans. (1995) 835.
[43] M. Schmittel, A. Ganz, Chem. Commun. (1997) 999.
[44] M. Schmittel, A. Ganz, D. Fenske, M. Herderich, Dalton Trans. (2000) 353.
[45] M. Schmittel, C. Michel, S.-X. Liu, D. Schildback, D. Fensje, Eur. J. Inorg. Chem. (2001) 1155.
[46] K. Mahata, M. Schmittel, J. Am. Chem. Soc. 131 (2009) 16544.
[47] M. Schmittel, B. He, J. fan, J.W. Bats, M. Engeser, M. Schlosser, H.-J. Deiseroth, Inorg. Chem. 48 (2009) 8192.
[48] M. Schmittel, R.S.K. Kishore, Org. Lett. 6 (2004) 1923.
[49] M. Schmittel, B. He, P. Mal, Org. Lett. 10 (2008) 2513.
[50] M. Schmittel, A. Ganz, D. Fenske, Org. Lett. 4 (2002) 2289.
[51] M. Schmittel, V. Kalsani, J.W. Bats, Inorg. Chem. 44 (2005) 4115.
[52] M. Schmittel, V. Kalsani, P. Mal, J.W. Bats, Inorg. Chem. 45 (2006) 6370.
[53] M. Schmittel, V. Kalsani, R.S.K. Kishore, H. Cölfen, J.W. Bats, J. Am. Chem. Soc. 127 (2005) 11544.
[54] V. Kalsani, M. Schmittel, A. Listorti, G. Accorsi, N. Armaroli, Inorg. Chem. 45 (2006) 2061.
[55] M.T. Miller, P.K. Gantzel, T.B. Karpishin, Inorg. Chem. 37 (1998) 2285.
[56] M.T. Miller, P.K. Gantzel, T.B. Karpishin, Inorg. Chem. 38 (1999) 3414.
[57] J. Cody, J. Dennisson, J. Gilmore, D.G. VanDerveer, M.M. Henary, A. Gabrielli, C.D. Sherrill, Y. Zhang, C.-P. Pan, C. Burda, C.J. Fahrni, Inorg. Chem. 42 (2003) 4918.
[58] M. Yamada, Y. Nakamura, S. Kuroda, I. Shimao, Bull. Chem. Soc. Jpn. 63 (1990) 2710.
[59] A.C.S. Samia, J. Cody, C.J. Fahrni, C. Burna, J. Phys. Chem. B 108 (2004) 563.
[60] R. Zong, R.P. Thummel, J. Am. Chem. Soc. 126 (2004) 10800.
[61] E.C. Constable, C.J. Cathey, M.J. Hannon, D.A. Tocher, J.V. Walker, M.D. Ward, Polyhedron 18 (1999) 159.
[62] G.M. Cockrell, G. Zhang, D.G. VanDerveer, R.P. Thummel, R.D. Hancoch, Inorg. Chem. 130 (2008) 1420.
[63] R.D. Hancock, A.E. Martell, Chem. Rev. 89 (1989) 1875.
[64] J.C. Loren, J.S. Siegel, Angew. Chem., Int. Ed. Engl. 40 (2001) 754.
[65] J.K. Klosterman, A. Linden, J.S. Siegel, Org. Biomol. Chem. 6 (2008) 2755.
[66] J.K. Klosterman, K.K. Baldridge, J.S. Siegel, Phys. Chem. Chem. Phys. 11 (2009) 5408.
[67] C.J. Chandler, L.W. Deady, A. Reiss, J. Heterocycl. Chem. 18 (1981) 599.
[68] G.R. Newkome, K.J. Theriot, V.K. Gupta, F.R. Fronczek, G.R. Baker, J. Org. Chem. 54 (1989) 1766.
[69] R.H. Beer, J. Jimenez, R.S. Drago, J. Org. Chem. 58 (1993) 1746.
[70] D.L. Melton, D.G. VanDerveer, R.D. Hancok, Inorg. Chem. 45 (2006) 9306.
[71] N.E. Dean, R.D. Hancock, C.L. Cahill, M. Frisch, Inorg. Chem. 47 (2008) 2000.
[72] N.J. Williams, N.E. Dean, D.G. VanDerveer, R.C. Luckay, R.D. Hancock, Inorg. Chem. 48 (2009) 7853.
[73] L.-L. Fan, C.-J. Li, Z.-S. Meng, M.-L. Tong, Eur. J. Inorg. Chem. (2008) 3905.
[74] A. Moghimi, R. Alizadeh, A. Shokrollahi, H. Aghabozorg, M. Shamsipur, A. Shockravi, Inorg. Chem. 42 (2003) 1616.
[75] A. Moghimi, R. Alizadeh, H. Aghabozorg, A. Shockravi, M.C. Aragoni, F. Demartin, F. Isaia, V. Lippolis, A. Harrison, A. Shokrollahi, M. Shamsipur, J. Mol. Struct. 750 (2005) 166.
[76] A. Moghimi, R. Alizadeh, M.C. Aragoni, V. Lippolis, H. Aghabozorg, P. Norouzi, F. Isaia, S. Sheshmani, Z. Anorg, Allg. Chem. 631 (2005) 1941.
[77] J. Coates, P.G. Sammes, R.M. West, J. Chem. Soc., Perkin Trans. 2 (1996) 1275.
[78] J. Coates, P.G. Sammes, R.M. West, J. Chem. Soc., Perkin Trans. 2 (1996) 1283.
[79] T. Steinkamp, H. Hayen, J. Huskens, U. Karst, Inorg. Chim. Acta 362 (2009) 421.
[80] R.T. Gephart III, N.J. Williams, J.H. Reibenspies, A.S. De Sousa, R.D. Hancock, Inorg. Chem. 47 (2008) 10342.
[81] R.T. Gephart III, N.J. Williams, J.H. Reibenspies, A.S. De Sousa, R.D. Hancock, Inorg. Chem. 48 (2009) 8201.

[82] J.M. Plummer, J.A. Weitgenant, B.C. Noll, J.W. Lauther, O. Wiest, P. Helquist, J. Org. Chem. 73 (2008) 3911.
[83] F. Loiseau, C. Di Pietro, S. Serroni, S. Campagna, A. Licciardello, A. Manfredi, G. Pozzi, S. Quici, Inorg. Chem. 40 (2001) 6901.
[84] E.J. Corey, A.L. Borror, T. Foglia, J. Org. Chem. 30 (1965) 288.
[85] Y. Bretonnière, R. Wietzke, C. Lebrun, M. Mazzanti, J. Pécaut, Inorg. Chem. 39 (2000) 3499.
[86] W.-H. Sun, S. Jie, S. Zhang, W. Zhang, Y. Song, H. Ma, Organometallics 25 (2006) 666.
[87] W.-H. Sun, S. Zhang, S. Jie, W. Zhang, Y. Li, H. Ma, J. Chen, K. Wedeking, R. Frölich, J. Organomet. Chem. 691 (2006) 4196.
[88] J.D.A. Pelletier, Y.D.M. Champouret, J. Cadarso, L. Clowes, M. Gañete, K. Singh, V. Thanarajasingham, G.A. Solan, J. Organomet. Chem. 691 (2006) 4114.
[89] M. Zhang, S. Zhang, P. Hao, S. Jie, W.-H. Sun, P. Li, X. Lu, Eur. J. Inorg. Chem. (2007) 3816.
[90] M. Carcelli, G. Corazzari, S. Ianelli, G. Pelizzi, C. Solinas, Inorg. Chim. Acta 353 (2003) 310.
[91] M. Carcelli, S. Ianelli, P. Pelagatti, G. Pelizzi, D. Rogolino, C. Solinas, M. Tegoni, Inorg. Chim. Acta 358 (2005) 903.
[92] A.M.S. Garas, R.S. Vagg, J. Heterocycl. Chem. 37 (2000) 151.
[93] Z.P. Demko, K.B. Sharpless, J. Org. Chem. 66 (2001) 7945.
[94] W. Zhang, T. Liu, M. Yuan, Z.-M. Wang, S. Gao, Inorg. Chem. 46 (2007) 2541.
[95] F.H. Case, J. Heterocycl. Chem. 7 (1970) 1001.
[96] G.R. Pabst, O.C. Pfüller, J. Sauer, Tetrahedron Lett. 39 (1998) 8825.
[97] G.R. Pabst, O.C. Pfüller, J. Sauer, Tetrahedron 55 (1999) 8045.
[98] H. Chao, G. Yang, G.-Q. Xue, H. Li, H. Zang, I.D. Williams, L.-N. Ji, X.-M. Chen, X.-Y. Li, Dalton Trans. (2001) 1326.
[99] Md.A. Masood, D.J. Hodgson, Inorg. Chem. 32 (1993) 4839.
[100] Md.A. Masood, T. Storr, T.D.P. Stack, Inorg. Chim. Acta 361 (2008) 1142.
[101] Y.B. Lei, F.C. Anson, Inorg. Chem. 34 (1995) 1083.
[102] C. Bazzicalupi, A. Bencini, S. Ciattini, C. Giorgi, A. Masotti, P. Paoletti, B. Valtancoli, N. Navon, J. Chem. Soc., Dalton Trans. (2000) 2383.
[103] C. Bazzicalupi, A. Bencini, E. Berni, A. Bianchi, P. Fornasari, C. Giorgi, A. Masotti, P. Paoletti, B. Valtancoli, N. Navon, J. Phys. Org. Chem. 14 (2001) 432.
[104] G. Ambrosi, M. Formica, V. Fusi, L. Giorgi, A. Guerri, M. Micheloni, P. Paoli, R. Pontellini, P. Rossi, Inorg. Chem. 46 (2007) 4737.
[105] M. Arca, A. Bencini, E. Berni, C. Caltagirone, F.A. Devillanova, F. Isaia, A. Garau, C. Giorgi, V. Lippolis, A. Perra, L. Tei, B. Valtancoli, Inorg. Chem. 42 (2003) 6929.
[106] O. Iranzo, T. Elmer, J.P. Richard, J.R. Morrow, Inorg. Chem. 42 (2003) 7737.
[107] S. Quici, M. Cavazzini, G. Marzanni, G. Accorsi, N. Armaroli, B. Ventura, F. Barigelletti, Inorg. Chem. 44 (2005) 529.
[108] S. Quici, G. Marzanni, M. Cavazzini, P.L. Anelli, M. Botta, E. Gianolino, G. Accorsi, N. Armaroli, F. Barigelletti, Inorg. Chem. 41 (2002) 2777.
[109] S. Quici, G. Marzanni, A. Forni, G. Accorsi, F. Barigelletti, Inorg. Chem. 43 (2004) 1294.
[110] S. Quici, C. Scalera, M. Cavazzini, G. Accorsi, M. Bolognesi, L. Armelao, G. Botaro, Chem. Mater. 21 (2009) 2941.
[111] S. Bernhard, K. Takada, D. Jenkins, H.D. Abruña, Inorg. Chem. 41 (2001) 765.
[112] A. Listorti, G. Accorsi, Y. Rio, N. Armaroli, O. Moudam, A. Gégout, B. Delavoux-Nicot, M. Holler, J.-F. Nierengarten, Inorg. Chem. 47 (2008) 6254.
[113] V.J. Catalano, B.L. Bennett, B.C. Noll, Chem. Commun. (2000) 1413.
[114] V.J. Catalano, M.A. Malwitz, B.C. Noll, Chem. Commun. (2001) 581.
[115] V.J. Catalano, M.A. Malwitz, Inorg. Chem. 41 (2002) 6553.
[116] V.J. Catalano, B.L. Bennett, R. Yson, B.C. Noll, J. Am. Chem. Soc. 122 (2000) 10056.
[117] V.J. Catalano, B.L. Bennett, H.M. Kar, B.C. Noll, J. Am. Chem. Soc. 121 (1999) 10236.
[118] V.J. Catalano, M.A. Malwitz, J. Am. Chem. Soc. 126 (2004) 6560.
[119] E. Buhleier, F. Vögtle, Justus Liebigs Ann. Chem. (1977) 1080.
[120] A. Caron, J. Guilhelm, C. Riche, C. Pascard, B. Alpha, J.-M. Lehn, J.-C. Rodriguez-Ubis, Helv. Chim. Acta 68 (1985) 1577.
[121] C.J. Chandler, L.W. Deady, J.A. Reiss, J. Heterocycl. Chem. 23 (1986) 1327.
[122] C.J. Chandler, L.W. Deady, J.A. Reiss, Aust. J. Chem. 41 (1988) 1051.
[123] U. Luning, M. Muller, Liebigs Ann. Chem. (1989) 367.
[124] T. Wang, J.S. Bradshaw, P. Huszihy, X. Kou, N.K. Dalley, R.M. Izatt, J. Heterocycl. Chem. 31 (1993) 1.
[125] Y.-H. Lai, L. Ma, K.F. Mok, Tetrahedron 52 (1996) 4673.
[126] J.K. Judice, S.J. Keipert, C.B. Knobler, D.J. Cram, J. Chem. Soc., Chem. Commun. (1993) 1325.
[127] H. Ross, U. Luning, Tetrahedron Lett. 38 (1997) 4539.
[128] F. Loffler, U. Luning, G. Gohar, New J. Chem. (2000) 935.
[129] D.B. Amabilino, J.F. Stoddart, Chem. Rev. 95 (1995) 2725.
[130] J.-M. Kern, J.-P. Sauvage, J.-L. Weidmann, N. Armaroli, L. Flamigni, P. Ceroni, V. Balzani, Inorg. Chem. 36 (1997) 5329.
[131] F.M. Raymo, J.F. Stoddart, Chem. Rev. 99 (1999) 1643.
[132] C. Dietrich-Buchecker, G. Rapenne, J.-P. Sauvage, Coord. Chem. Rev. 185–186 (1999) 167.
[133] T.J. Hubin, D.H. Busch, Coord. Chem. Rev. 200–202 (2000) 5.
[134] Z. Niu, H.W. Gibson, Chem. Rev. 109 (2009) 6024.
[135] C. Bazzicalupi, A. Bencini, V. Fusi, C. Giorgi, P. Paoletti, B. Valtancoli, Inorg. Chem. 37 (1998) 941.
[136] D.K. Chand, H.-J. Schneider, A. Bencini, A. Bianchi, C. Giorgi, S. Ciattini, B. Valtancoli, Chem. Eur. J. 6 (2000) 4001.
[137] C. Bazzicalupi, A. Bencini, A. Bianchi, C. Giorgi, S. Ciattini, P. Paoletti, B. Valtancoli, F. Secco, M.R. Tinè, M. Venturini, Phys. Chem. Chem. Phys. 2 (2000) 4864.
[138] C. Bazzicalupi, A. Bencini, A. Bianchi, C. Giorgi, V. Fusi, B. Valtancoli, M.A. Bernardo, F. Pina, Inorg. Chem. 38 (1999) 3806.
[139] A. Bencini, M.A. Bernardo, A. Bianchi, V. Fusi, C. Giorgi, F. Pina, B. Valtancoli, Eur. J. Eur. J. Inorg. Chem. (1999) 1911.
[140] A. Bencini, A. Bianchi, P. Fornasari, C. Giorgi, P. Paoletti, B. Valtancoli, Polyhedron 21 (2002) 1329.
[141] C. Bazzicalupi, A. Bencini, V. Fusi, C. Giorgi, P. Paoletti, B. Valtancoli, J. Chem. Soc., Dalton Trans. (1999) 393.
[142] C. Bazzicalupi, A. Bencini, A. Bianchi, L. Borsari, A. Danesi, C. Giorgi, C. Lodeiro, P. Mariani, F. Pina, S. Santarelli, A. Tamayo, B. Valtancoli, Dalton Trans. (2006) 4000.
[143] C. Bazzicalupi, A. Bencini, E. Berni, A. Bianchi, L. Borsari, C. Giorgi, B. Valtancoli, C. Lodeiro, J.C. Lima, A.J. Parola, F. Pina, S. Santarelli, Dalton Trans. (2004) 591.
[144] A. Bencini, A. Bianchi, P. Paoletti, P. Paoli, Coord. Chem. Rev. 120 (1992) 51.
[145] C. Bazzicalupi, A. Bencini, S. Biagini, A. Bianchi, E. Faggi, C. Giorgi, M. Marchetta, F. Totti, B. Valtancoli, Chem. Eur. J. 15 (2009) 8049.
[146] A. Mendoza, J. Aguilar, M.G. Basallote, L. Gil, J.C. Hernández, M.A. Mañez, E. García-España, L. Ruiz-Ramírez, C. Soriano, B. Verdejo, Chem. Commun. (2003) 3032.
[147] J. Aguilar, A. Bencini, E. Berni, A. Bianchi, E. García-España, L. Gil, A. Mendoza, L. Ruiz-Ramírez, C. Soriano, Eur. J. Inorg. Chem. (2004) 4061.
[148] H. Keypour, H. Goudarziafshar, A.K. Bridson, R.G. Pritchard, Inorg. Chim. Acta 360 (2007) 2298.
[149] H. Keypour, H. Goudarziafshar, A.K. Bridson, R.B. Pritchard, M. Rezaeivala, Inorg. Chim. Acta 361 (2008) 1415.
[150] A.J. Blake, F. Demartin, F.A. Devillanova, A. Garau, F. Isaia, V. Lippolis, M. Schröder, G. Verani, J. Chem. Soc., Dalton Trans. (1996) 3705.
[151] M. Arca, A.J. Blake, J. Casabò, F. Demartin, F.A. Devillanova, A. Garau, F. Isaia, V. Lippolis, R. Kivekas, V. Muns, M. Schröder, G. Verani, J. Chem. Soc., Dalton Trans. (2001) 1180.
[152] M. Shamsipur, M. Hosseini, K. Alizadeh, M.F. Mousavi, A. Garau, V. Lippolis, A. Yari, Anal. Chem. 77 (2005) 276.
[153] M.C. Aragoni, M. Arca, F. Demartin, F.A. Devillanova, F. Isaia, A. Garau, V. Lippolis, F. Jalali, U. Papke, M. Shamsipur, L. Tei, A. Yari, G. Verani, Inorg. Chem. 41 (2002) 6623.
[154] G. De Filippo, F. Demartin, A. Garau, V. Lippolis, A. Yari, A. Shokrollahi, M. Shamsipur, Inorg. Chim. Acta 358 (2005) 801.
[155] M. Arca, G. Azimi, F. Demartin, F.A. Devillanova, L. Escriche, A. Garau, F. Isaia, R. Kivekas, V. Lippolis, V. Muns, A. Perra, M. Shamsipur, L. Sportelli, A. Yari, Inorg. Chim. Acta 238 (2005) 2403.
[156] M.C. Aragoni, M. Arca, A. Bencini, S. Biagini, A.J. Blake, C. Caltagirone, F. Demartin, G. De Filippo, F.A. Devillanova, A. Garau, K. Gloe, F. Isaia, V. Lippolis, B. Valtancoli, M. Wenzel, Inorg. Chem. 47 (2008) 8391.
[157] A.J. Blake, J. Casabò, F.A. Devillanova, L. Escriche, A. Garau, F. Isaia, V. Lippolis, R. Kivekas, V. Muns, M. Schröder, R. Sillanpää, G. Verani, J. Chem. Soc., Dalton Trans. (1999) 1085.
[158] A.J. Blake, F.A. Devillanova, A. Garau, A. Harrison, F. Isaia, V. Lippolis, S.K. Tiwary, M. Schröder, G. Verani, G. Whittaker, J. Chem. Soc., Dalton Trans. (2002) 4389.
[159] M.C. Aragoni, M. Arca, F. Demartin, F.A. Devillanova, A. Garau, F. Isaia, V. Lippolis, S. Rizzato, G. Verani, Inorg. Chim. Acta 357 (2004) 3803.
[160] F. Contu, F. Demartin, F.A. Devillanova, A. Garau, F. Isaia, V. Lippolis, A. Salis, G. Verani, J. Chem. Soc., Dalton Trans. (1997) 4401.
[161] A.J. Blake, M.H.M. Caçote, F.A. Devillanova, A. Garau, F. Isaia, V. Lippolis, C.M. Pereira, F. Silva, L. Tei, Eur. J. Inorg. Chem. (2002) 1816.
[162] V. Lippolis, M. Shamsipur, J. Iranian Chem. Soc. 3 (2006) 105.
[163] H. Tsukube, S. Shinoda, Y. Mizutani, M. Okano, K. Takagi, K. Hori, Tetrahedron 53 (1997) 3487.
[164] M. Shamsipur, M. Javanbakht, M.F. Mousavi, M.R. Ganjali, V. Lippolis, A. Garau, L. Tei, Talanta 55 (2001) 1047.
[165] M. Shamsipur, M. Javanbakht, V. Lippolis, A. Garau, G. De Filippo, M.R. Ganjali, A. Yari, Anal. Chim. Acta 462 (2002) 225.
[166] M. Shamsipur, M. Javanbakht, M.R. Ganjali, M.F. Mousavi, V. Lippolis, A. Garau, Electroanalysis 14 (2002) 1691.
[167] M. Shamsipur, S.Y. Kazemi, G. Azimi, S.S. Madaeni, V. Lippolis, A. Garau, F. Isaia, J. Membr. Sci. 215 (2003) 87.
[168] M. Shamsipur, O.R. Hashemi, V. Lippolis, J. Membr. Sci. 282 (2006) 322.
[169] M. Shamsipur, F. Mizani, K. Alizadeh, M.F. Mousavi, V. Lippolis, A. Garau, C. Caltagirone, Sens. Actuators B 130 (2008) 300.
[170] Y. Shen, B.P. Sullivan, Inorg. Chem. 34 (1995) 6235.
[171] K. Binnemans, P. Lenaerts, K. Driesen, C. Görller-Walrand, J. Mater. Chem. 14 (2004) 191.
[172] A. Gulino, F. Lupo, G.C. Condorelli, A. Motta, I.L. Fragalà, J. Mater. Chem. 19 (2009) 3507.
[173] L.-N. Sun, Y. Zhang, J.-B. Yu, C.-Y. Peng, H.-J. Zhang, J. Photochem. Photobiol. 199 (2008) 57.
[174] L.-N. Sun, H.-J. Zhang, C.-Y. Peng, J.-B. Yu, Q.-G. Meng, L.-S. Fum, F.-Y. Liu, X.-M. Guo, J. Phys. Chem. B 110 (2006) 7249.
[175] P. Lenaerts, K. Driesen, R. Van Deun, K. Biennemans, Chem. Mater. 17 (2005) 2148.
[176] S.J. Lee, S.S. Lee, M.S. Lah, J.-M. Hong, J.H. Jung, Chem. Commun. (2006) 4539.
[177] S.J. Lee, D.R. Bae, W.S. Han, S.S. Lee, J.H. Jung, Eur. J. Inorg. Chem. (2008) 1559.
[178] N. Van Hoof, T.E. Keyes, R.J. Forster, A. McNally, N.R. Russell, Chem. Commun. (2001) 1156.
[179] M. Atmeh, N.R. Russell, R.J. Forster, J. Incl. Phenom. Macrocycl. Chem. 57 (2007) 607.

[180] T. Gunnlaugsson, J.P. Leonard, K. Sénéchal, A.J. Harte, J. Am. Chem. Soc. 125 (2003) 12062.
[181] T. Gunnlaugsson, J.P. Leonard, K. Sénéchal, A.J. Harte, Chem. Commun. (2004) 782.
[182] A.M. Nonat, A.J. Harte, K. Sénéchal-David, J.P. Leonard, T. Gunnlaugsson, Dalton Trans. (2009) 4703.
[183] K. Sénéchal-David, S.J.A. Pope, S. Quinn, S. Faulkner, T. Gunnlaugsson, Inorg. Chem. 45 (2006) 10040.
[184] A.M. Nonat, S.J. Quinn, T. Gunnlaugsson, Inorg. Chem. 48 (2009) 4646.
[185] M. Riklin, D. Tran, X. Bu, L.E. Laverman, P.C. Ford, J. Chem. Soc., Dalton Trans. (2001) 1813.
[186] B. Higgins, B.A. DeGraff, J.N. Demas, Inorg. Chem. 44 (2005) 6662.
[187] J. Bolger, A. Gourdon, E. Ishow, J.-P. Launay, Inorg. Chem. 35 (1996) 2937.
[188] S. Bodige, F.M. MacDonnell, Tetrahedron Lett. 38 (1997) 8159.
[189] Y. Pellegrin, A. Quaranta, P. Dorlet, M.F. Charlot, W. Leibl, A. Aukauloo, Chem. Eur. J. 11 (2005) 3698.
[190] W. Paw, R. Eisenberg, Inorg. Chem. 36 (1997) 2287.
[191] C.R. Rice, A. Guerrero, Z.R. Bell, R.L. Paul, G.R. Motson, J.C. Jeffery, M.D. Ward, New J. Chem. (2001) 185.
[192] T. Lazarides, T.A. Miller, J.C. Jeffery, T.K. Ronson, H. Adams, M.D. ward, Dalton Trans. (2005) 528.
[193] T. Lazarides, A. Barbieri, C. Sabatini, F. Barigelletti, H. Adams, M.D. Ward, Inorg. Chim. Acta 360 (2007) 814.
[194] J. Ettedgui, R. Neumann, J. Am. Chem. Soc. 131 (2009) 4.
[195] D.G. Markees, Helv. Chim. Acta 66 (1983) 620.
[196] T.J. Terry, G. Dubois, A. Murphy, T.D.P. Stack, Angew. Chem., Int. Ed. Engl. 46 (2007) 945.
[197] T.J. Terry, T.D.P. Stack, J. Am. Chem. Soc. 130 (2008) 4945.
[198] L. Shu, S. Pyo, J. Rivera, L. Echegoyen, Inorg. Chim. Acta 292 (1999) 34.
[199] D. Tzalis, Y. Tor, S. Failla, J.S. Siegel, Tetrahedron Lett. 36 (1995) 3489.
[200] L. Wang, W. You, W. Huang, C. Wang, X.-Z. You, Inorg. Chem. 48 (2009) 4295.
[201] D. Tzalis, Y. Tor, Tetrahedron Lett. 36 (1995) 6017.
[202] H.S. Joshi, R. Jamshidi, Y. Tor, Angew. Chem., Int. Ed. Engl. 38 (1999) 2722.
[203] D. Tzalis, Y. Tor, Chem. Commun. (1996) 1043.
[204] D. Tzalis, Y. Tor, J. Am. Chem. Soc. 119 (1997) 852.
[205] P.J. Connors, D. Tzalis, A.L. Dunnick, Y. Tor, Inorg. Chem. 37 (1998) 1121.
[206] M.J.E. Resendiz, J.C. Noveron, H. Disteldorf, S. Fischer, P.J. Stang, Org. Lett. 6 (2004) 651.
[207] S. Bonnet, J.-P. Collin, J.-P. Sauvage, Inorg. Chem. 45 (2006) 4024.
[208] M. Levis, U. Lüning, M. Müller, M. Schmittel, C. Wöhrle, Z. Naturforsch.,Teil B 49 (1994) 675.
[209] M. Schmittel, A. Ganz, Synth. Lett. (1997) 710.
[210] M. Schmittel, H. Ammon, J. Chem. Soc., Chem. Commun. (1995) 687.
[211] M. Schmittel, H. Ammon, C. Wöhrle, Chem. Ber. 128 (1995) 845.
[212] D. Pomeranc, V. Heitz, J.-C. Chambron, J.-P. Sauvage, J. Am. Chem. Soc. 123 (2001) 12215.
[213] C. Goze, J.-C. Chambron, V. Heitz, D. Pomeranc, X.J. Salom-Roig, J.-P. Sauvage, A. Farrán Morales, F. Barigelletti, Eur. J. Inorg. Chem. (2003) 3752.
[214] A.P. de Silva, H.Q.G. Gunaratne, T. Gunnlaugsson, A.J.M. Huxley, C.P. McCoy, J.T. Rademacher, T.E. Rice, Chem. Rev. 97 (2007) 1515.
[215] L. Prodi, F. Bolletta, M. Montalti, N. Zaccheroni, Coord. Chem. Rev. 205 (2000) 59.
[216] K. Rurack, Spectrochim. Acta, Part A 57 (2001) 2161.
[217] J. Mater. Chem. 15 (2005) (Theme Issue: Fluorescent Sensors).
[218] L. Prodi, New J. Chem. 29 (2005) 20.
[219] V. Amendola, L. Fabbrizzi, F. Foti, M. Licchelli, C. Mangano, P. Pallavicini, A. Poggi, D. Sacchi, A. Taglietti, Coord. Chem. Rev. 250 (2006) 273.
[220] C. Lodeiro, F. Pina, Coord. Chem. Rev. 253 (2009) 1353.
[221] M. Schmittel, H.-W. Lin, Angew. Chem., Int. Ed. Engl. 46 (2007) 893.
[222] M. Schmittel, H. Lin, Inorg. Chem. 46 (2007) 9139.
[223] V.P. Boricha, S. Patra, Y.S. Chouhan, P. Sanavada, E. Suresh, P. Paul, Eur. J. Inorg. Chem. (2009) 1256.
[224] M.-J. Li, B.W.-K. Chu, N. Zhu, V.W.-W. Yam, Inorg. Chem. 46 (2007) 720.
[225] M.-J. Li, C.-C. Ko, G.-P. Duan, N. Zhu, V.W.-W. Yam, Organometallics 26 (2007) 6091.
[226] P. Comba, R. Kramer, A. Mokhir, K. Naing, E. Schatz, Eur. J. Inorg. Chem. (2006) 4442.
[227] A. Bencini, A. Bianchi, C. Lodeiro, A. Masotti, A.J. Parola, F. Pina, J. Seixa de Melo, B. Valtancoli, Chem. Commun. (2000) 1639.
[228] A. Bencini, E. Berni, A. Bianchi, P. Fornasari, C. Giorgi, J.C. Lima, C. Lodeiro, M.J. Melo, J. Seixa de Melo, A.J. Parola, F. Pina, J. Pina, B. Valtancoli, Dalton Trans. (2004) 2180.
[229] J. Pina, J. Seixas de Melo, F. Pina, C. Lodeiro, J.C. Lima, A.J. Parola, C. Soriano, M.P. Clares, M.T. Albelda, R. Aucejo, E. García-España, Inorg. Chem. 44 (2005) 7449.
[230] R. Martínez-Mánez, F. Sancenón, Chem. Rev. 103 (2003) 4419.
[231] P.A. Gale, R. Quesada, Coord. Chem. Rev. 250 (2006) 3219.
[232] C. Caltagirone, P.A. Gale, Chem. Soc. Rev. (2009) 520.
[233] C.M.G. dos Santos, T. McCabe, T. Gunnlaugsson, Tetrahedron Lett. 48 (2007) 3135.
[234] C.M.G. dos Santos, T. Gunnlaugsson, Supramol. Chem. 21 (2009) 173.
[235] A. Ghosh, S. Verma, B. Ganguly, H.N. Ghosh, A. Das, Eur. J. Inorg. Chem. (2009) 2496.
[236] A. Ghosh, B. Ganguly, A. Das, Inorg. Chem. 23 (2007) 9912.
[237] K.K.-W. Lo, J.S.-Y. Lau, D.K.-K. Lo, L.T.-L. Lo, Eur. J. Inorg. Chem. (2006) 4054.
[238] H.D. Batey, A.C. Whitwood, A.-K. Duhme-Klair, Inorg. Chem. 46 (2007) 6516.
[239] X. Yu, H. Lin, Z. Cai, H. Lin, Tetrahedron Lett. 48 (2007) 8615.
[240] Y.-H. Qiao, H. Lin, H.-K. Lin, J. Incl. Phenom. Macrocycl. Chem. 59 (2007) 211.
[241] M. Yu, H. Lin, H.-K. Lin, Supramol. Chem. 20 (2008) 357.
[242] Y.-H. Qiao, H. Lin, H.-K. Lin, Can. J. Chem. 84 (2006) 1155.
[243] J. Shao, Y.-H. Qiao, H. Lin, H.-K. Lin, J. Lumin. 128 (2008) 1985.
[244] J. Shao, Y. -H- Qiao, H. Lin, H.-K. Lin, J. Fluoresc. 19 (2009) 183.
[245] Z. Xu, S. Kim, K.-H. Lee, J. Yoon, Tetrahedron Lett. 48 (2007) 3797.
[246] L.A. Cabell, M.B. Best, J.L. Lavigne, S.E. Schneider, D.M. Perreault, M.-K. Monahan, E.V. Anslyn, J. Chem. Soc., Perkin Trans. 2 (2001) 315.
[247] M. Takeuchi, M. Yamamoto, S. Shinkai, Chem. Commun. (1997) 1731.
[248] M. Takeuchi, M. Yamamoto, S. Shinkai, Tetrahedron 54 (1998) 3125.
[249] P. Linnane, T.D. James, S. Imazu, S. Shinkai, Tetrahedron Lett. 36 (1995) 8833.
[250] L. Fabbrizzi, M. Licchelli, G. Rabaioli, A. Taglietti, Coord. Chem. Rev. 205 (2000) 85.
[251] A.M. O'Mahony, M.D. Scanlon, A. Berduque, V. Beni, D.M.W. Arrigan, E. Faggi, A. Bencini, Electrochem. Commun. 7 (2005) 976.
[252] C. Bazzicalupi, A. Beconcini, A. Bencini, V. Fusi, C. Giorgi, A. Masotti, B. Valtancoli, J. Chem. Soc., Perkin Trans. 2 (1999) 1675.
[253] C. Bazzicalupi, A. Bencini, S. Biagini, E. Faggi, C. Giorgi, I. Matera, B. Valtancoli, Chem. Commun. (2006) 4087.
[254] C. Bazzicalupi, A. Bencini, S. Biagini, E. Faggi, S. Meini, C. Giorgi, A. Spepi, B. Valtancoli, J. Org. Chem. 74 (2009) 7349.
[255] A. Bencini, A. Bianchi, E. García-España, M. Micheloni, J.A. Ramírez, Coord. Chem. Rev. 188 (1999) 97.
[256] E. García-España, P. Díaz, J.M. Llinares, A. Bianchi, Coord. Chem. Rev. 250 (2006) 2952.
[257] A. Bianchi, K. Bowman-James, E. García-España (Eds.), Supramolecular Chemistry of Anions, Wiley-VCH, New York, 1997.
[258] C. Bazzicalupi, A. Bencini, E. Berni, A. Bianchi, P. Fornasari, C. Giorgi, B. Valtancoli, Eur. J. Inorg. Chem. (2003) 1974.
[259] C. Bazzicalupi, A. Bencini, E. Berni, A. Bianchi, P. Fornasari, C. Giorgi, C. Marinelli, B. Valtancoli, Dalton Trans. (2003) 2564.
[260] C. Cruz, R. Delgado, M.G.B. Drew, V. Félix, J. Org. Chem. 72 (2007) 4023.
[261] C. Cruz, V. Calisto, R. Delgado, V. Felix, Chem. Eur. J. 15 (2009) 3277.
[262] Y.-H. Guo, Q.-C. Ge, H. Lin, H.-K. Lin, S.-R. Zhu, C.-Y. Zhou, Biophys. Chem. 105 (2003) 119.
[263] Y.-H. Guo, Q.-C. Ge, H. Lin, H.-K. Lin, S.-R. Zhu, Can. J. Chem. 82 (2004) 504.
[264] M.W. Hosseini, J.-M. Lehn, L. Maggiora, K.B. Mertes, M.P. Mertes, J. Am. Chem. Soc. 109 (1987) 537.
[265] D.A. Bell, S.G. Diaz, V.M. Lynch, E.V. Anslyn, Tetrahedron Lett. 36 (1995) 4155.
[266] M. Mazik, A. Hartmann, J. Org. Chem. 73 (2008) 7444.
[267] M. Mazik, A. Hartmann, P.G. Jones, Chem. Eur. J. 15 (2009) 9147.
[268] Y. Engel, A. Dahan, E. Rozrnshine-Kemelmakher, M. Gozin, J. Org. Chem. 72 (2007) 2318.
[269] S. Goswami, R. Mkherjee, J. Ray, Org. Lett. 7 (2005) 1283.
[270] M. Scott Goodman, A.D. Hamilton, J. Weiss, J. Am. Chem. Soc. 117 (1995) 8447.
[271] M. Slim, H.F. Sleiman, Bioconj. Chem. 15 (2004) 949.
[272] D. Paul, F. Melin, C. Hirtz, J. Wytko, P. Ochsenbein, M. Bonin, K. Schenk, P. Maltese, J. Weiss, Inorg. Chem. 42 (2003) 3779.
[273] F. Melin, S. Choua, M. Bernard, P. Turek, J. Weiss, Inorg. Chem. 45 (2006) 10750.
[274] M. Lo, D. Mahajan, J.A. Wytko, C. Boudon, J. Weiss, Org. Lett. 11 (2009) 2487.
[275] D. Paul, J.A. Wytko, M. Koepf, J. Weiss, Inorg. Chem. 41 (2002) 3699.
[276] J. Brandel, A. Trabolsi, H. Traboulsi, F. Melin, M. Koepf, J.A. Wytko, M. Elhabiri, J. Weiss, A.-M. Albrecht-Gary, Inorg. Chem. 48 (2009) 3743.
[277] M. Koepf, A. Trabolsi, M. Elhabiri, J.A. Wytko, D. Paul, A.M. Albrecht-Gary, J. Weiss, Org. Lett. 7 (2005) 1279.
[278] D.S. Sigman, A. Mazunder, D.M. Perrin, Chem. Rev. 93 (1993) 2295.
[279] D.S. Sigman, T.W. Bruice, A. Mazunder, C.L. Sutton, Acc. Chem. Res. 26 (1992) 98.
[280] C.-H. Cen, L. Milne, R. Landgraf, D.M. Perrin, D.S. Sigman, Chem. Biol. Chem. 2 (2001) 735.
[281] K.E. Augustyn, V.C. Pierre, J.K. Barton, Metallointercalators as probes of DNA recognition and reactions, in: Wiley Encyclopedia of Chemical Biology, vol. 3, 2009, p. 34.
[282] B.M. Zeglis, V.C. Pierre, J.K. Barton, Chem. Commun. (2007) 4565.
[283] G. Pratviel, J. Bernadou, B. Meurnier, Angew. Chem., Int. Ed. Engl. 34 (1995) 746.
[284] G. Pratviel, J. Bernadou, B. Meurnier, Adv. Inorg. Chem. 45 (1998) 251.
[285] L. Herman, S. Ghosh, E. Defrancq, A. Kirsh-De Mesnaeker, J. Phys. Org. Chem. 21 (2008) 670.
[286] B. Armitage, Chem. Rev. 98 (1998) 1171.
[287] W.K. Pogozelski, T.D. Tullius, Chem. Rev. 98 (1998) 1089.
[288] F. Mancin, P. Scrimin, P. Tecilla, U. Tonellato, Chem. Commun. (2005) 2540.
[289] J. Chin, Curr. Opin. Chem. Biol. 1 (1997) 514.
[290] J.A. Cowan, Curr. Opin. Chem. Biol. 5 (2001) 634.
[291] C. Liu, M. Wang, T. Zhang, H. Su, Coord. Chem. Rev. 248 (2004) 147.
[292] D.S. Sigman, D.R. Graham, V. D'Aurora, A.M. Stern, J. Biol. Chem. 254 (1979) 12269.
[293] L.E. Marshall, D.R. Graham, K.A. Reich, D.S. Sigman, Biochemistry 20 (1981) 244.
[294] L.M. Pope, K.A. Reich, D.R. Graham, D.S. Sigman, J. Biol. Chem. 257 (1982) 12121.
[295] J.M. Veal, K. Merchant, R.L. Rill, Nucl. Acids Res. 19 (1991) 3383.
[296] L.E. Pope, D.S. Sigman, Proc. Natl. Acad. Sci. U.S.A. 81 (1984) 3.
[297] J.-C. François, T. Saison-Behmoaras, M. Chassignol, N.T. Thuong, J.-S. Sun, C. Hèlené, Biochemistry 27 (1988) 2272.

[298] B.G. Que, K.M. Downey, A.G. So, Biochemistry 19 (1980) 5987.
[299] D.R. Graham, L.E. Marshall, K.A. Reich, D.S. Sigman, J. Am. Chem. Soc. 102 (1980) 5419.
[300] T.B. Thedarahn, M.D. Kuwabara, T.A. Larsen, D.S. Sigman, J. Am. Chem. Soc. 111 (1989) 4941.
[301] M.M. Meijler, O. Zelenko, D.S. Sigman, J. Am. Chem. Soc. 119 (1997) 1135.
[302] O. Zelenko, J. Gallagher, Y. Su, D.S. Sigman, Inorg. Chem. 37 (1998) 2198.
[303] G.R.A. Johnson, N.B. Nazhat, J. Am. Chem. Soc. 109 (1987) 1990.
[304] K. Yamamoto, S. Kawanishi, J. Biol. Chem. 264 (1989) 15435.
[305] T.E. Goyne, D.S. Sigman, J. Am. Chem. Soc. 109 (1987) 2846.
[306] M. Kuwabara, C. Yoo, T. Goyne, T. Thedarahn, D.S. Sigman, Biochemistry 25 (1986) 7401.
[307] D.S. Sigman, Acc. Chem. Res. 19 (1986) 180.
[308] O. Zelenko, J. Gallagher, D.S. Sigman, Angew. Chem., Int. Ed. Engl. 36 (1997) 2776.
[309] T. Oyoshi, H. Sugiyama, J. Am. Chem. Soc. 122 (2000) 6313.
[310] G.J. Murakawa, C.H. Chen, M.D. Kuwabara, D.P. Nierlich, D.S. Sigman, Nucl. Acids Res. 17 (1989) 5361.
[311] J.M. Vaal, R.L. Rill, Biochemistry 27 (1988) 1822.
[312] J.M. Vaal, K. Mechant, R.L. Rill, Biochemistry 28 (1989) 28.
[313] M. Pitié, B. Donnadieu, B. Meunier, Inorg. Chem. 37 (1998) 3486.
[314] M. Pitié, B. Sudres, B. Meunier, Chem. Commun. (1998) 2597.
[315] J. Gallagher, C.B. Chen, C.Q. Pan, D.M. Perrin, Y. Cho, D.S. Sigman, Bioconj. Chem. 7 (1997) 413.
[316] M. Pitié, C. Boldron, H. Gornitzka, C. Hemmert, B. Donnadieu, B. Meunier, Eur. J. Inorg. Chem. (2003) 528.
[317] Y. Yao, M.W. Perkovic, D.P. Rillema, C. Woods, Inorg. Chem. 31 (1992) 2956.
[318] A. Robertazzi, A. Magistrato, P. de Hoog, P. Carloni, J. Reedijk, Inorg. Chem. 46 (2007) 5873.
[319] P. de Hoog, M.J. Louwerse, P. Gamez, M. Pitié, E.J. Baerends, B. Meunier, J. Reedijk, Eur. J. Inorg. Chem. (2008) 612.
[320] S.A. Ross, M. Pitié, B. Meunier, Eur. J. Inorg. Chem. (1999) 557.
[321] C. Boldron, S.A. Ross, M. Pitié, B. Meunier, Bioconj. Chem. 13 (2002) 1031.
[322] M.L. Edwards, R.D. Snyder, D.M. Stermerick, J. Med. Chem. 34 (1991) 2414.
[323] M. Musso, T. Thomas, A. Shirarata, L.H. Sigal, M.W. Van Dike, T.J. Thomas, Biochemistry 36 (1997) 1441.
[324] M. Pitié, B. Meunier, Bioconj. Chem. 9 (1998) 604.
[325] C. Bailly, C.B. Chaires, Bioconj. Chem. 9 (1998) 513.
[326] M. Pitié, J.D. Van Horn, D. Brion, C. Burrows, B. Meunier, Bioconj. Chem. 11 (2000) 892.
[327] E.E. Baird, P.B. Dervan, J. Am. Chem. Soc. 118 (1996) 6141.
[328] M. Pitié, C.J. Burrows, B. Meunier, Nucl. Acids. Res. 28 (2000) 4856.
[329] P. de Hoog, C. Boldron, P. Gamez, K. Sliedregt-Bol, I. Roland, M. Pitié, R. Kiss, B. Meunier, J. Reedijk, J. Med. Chem. (2007) 3148.
[330] G. Zhao, H. Sun, H.K. -Lin, S. Zhu, X. Su, Y.-T. Chen, J. Inorg. Biochem. 72 (1998) 173.
[331] Z.-M. Wang, H.-K. Lin, Z.-F. Zhou, M. Xu, T.-F. Liu, S.-R. Zhu, Y.-T. Chen, Bioorg. Med. Chem. 9 (2001) 2849.
[332] T. Hirohama, Y. Kuranuki, E. Ebina, T. Sugizaki, H. Arii, M. Chikira, P.T. Selvi, M. Palaniandavar, J. Inorg. Biochem. 99 (2005) 1205.
[333] W. Saenger, Principles of Nucleic Acid Structure, Springer, NY, USA, 1984.
[334] T. Biver, F. Secco, M.R. Tinè, M. Venturini, J. Inorg. Biochem. 98 (2004) 33.
[335] T. Biver, F. Secco, M.R. Tinè, M. Venturini, A. Bencini, A. Bianchi, C. Giorgi, J. Inorg. Biochem. 98 (2004) 1531.
[336] T. Biver, D. Lombardo, F. Secco, M.R. Tinè, M. Venturini, A. Bencini, A. Bianchi, B. Valtancoli, Dalton Trans. (2006) 1524.
[337] A. Zaid, J.-S. Sun, C.-H. Nguyen, E. Bisagni, T. Garestier, D.S. Grierson, R. Zain, Chem. Biol. Chem. 5 (2004) 1550.
[338] H. Amiri, N. Nekhotiaeva, J.-S. Sun, C.-H. Nguyen, D.S. Grierson, L. Good, R. Zain, J. Mol. Biol. 351 (2005) 776.
[339] H.E. Moser, P.B. Dervan, Science 238 (1987) 645.
[340] C. Giovannangeli, C. Hèlené, Curr. Opin. Mol. Ther. 2 (2000) 288.
[341] S.M. Murkin, M.D. Frank-Kamenetskii, Annu. Rev. Biophys. Biomol. Struct. 23 (1994) 541.
[342] M. Cossee, M. Schmitt, V. Campunzano, L. Reutenauer, C. Moutou, J.L. Mandel, M. Koenig, Proc. Natl. Acad. Sci. U.S.A. 94 (1997) 7452.
[343] H. Bergquist, A. Nigravesh, R.D. Fernandez, V. Larsson, C.-H. Nguyen, L. Good, R. Zain, Chem. Biol. Chem. 10 (2009) 2929.
[344] L. Gude, M.J. Fernandez, K.B. Grant, A. Lorente, Org. Biomol. Chem. (2005) 1856.
[345] G.W. Muth, W.E. Hill, Methods 23 (2001) 218.
[346] J.M. Bullard, W.A. van Waes, D.J. Bucklin, W.E. Hill, J. Mol. Biol. 252 (1995) 572.
[347] D.E. Bergstrom, N.P. Gerry, J. Am. Chem. Soc. 116 (1994) 12607.
[348] D.M. Perrin, A. Mazunder, F. Sadeghi, D.S. Sigman, Biochemistry 33 (1994) 3848.
[349] D.J. Bucklin, W.A. van Waes, J.M. Bullard, W.E. Hill, Biochemistry 37 (1998) 7951.
[350] J.-C. François, T. Saison-Behmoara, C. Barbier, M. Chassignol, N.T. Thuong, C. Hèlené, Proc. Natl. Acad. Sci. U.S.A. 86 (1989) 9702.
[351] J. Gallagher, C.-H.B. Chen, C.Q. Pan, D.M. Perrin, Y.M. Cho, D.S. Sigman, Bioconj. Chem. 7 (1996) 413.
[352] D.S. Sigman, R. Landgraf, D.M. Perrin, L. Pearson, Met. Ions Biol. Syst. 33 (1996) 485.
[353] P. Arimondo, A. Bouterine, J.-C. François, Rec. Res. Dev. Bioconj. Chem. 1 (2002) 29.
[354] G. Xiao, D.L. Cole, R.P. Gunsalus, D.S. Sigman, C.-H.B. Chen, Protein Sci. 11 (2002) 2427.
[355] C.-H.B. Chen, M.B. Gorin, D.S. Sigman, Proc. Natl. Acad. Sci. U.S.A. 90 (1993) 4206.
[356] D.S. Sigman, C.-H.B. Chen, M.B. Gorin, Nature 363 (1993) 474.
[357] R. Landgraf, C.-H.B. Chen, D.S. Sigman, Nucl. Acids. Res. 23 (1995) 3524.
[358] M. Faria, C. Giovannangeli, J. Gene Med. 3 (2001) 299.
[359] W.E. Hill, D.J. Bucklin, J.M. Bullard, A.L. Galbralth, N.V. Jammi, C.C. Rettberg, B.S. Sawyer, W.A. van Waes, Biochem. Cell. Biol. 73 (1995) 1033.
[360] J.M. Bullard, W.A. van Waes, D.J. Bucklin, W.E. Hill, Biochemistry 37 (1998) 1350.
[361] G.W. Muth, S.P. Hennelly, W.E. Hill, Biochemistry 39 (2000) 4068.
[362] J.-C. François, C. Hèlené, Biochemistry 34 (1995) 65.
[363] G. Godard, J.-C. François, I. Duroux, U. Asseline, M. Chassignol, T. Nguyen, C. Hèlené, T. Saison-Behmoaras, Nucl. Acids Res. 22 (1994) 4789.
[364] W.C. Putman, A.T. Daniher, B.N. Trawick, J.K. Bashkin, Nucl. Acids Res. 292 (2002) 2199.
[365] C.Q. Pan, S.E. Finkel, S.E. Crampton, J.A. Feng, D.S. Sigman, R.C. Johnson, J. Mol. Biol. 264 (1996) 675.
[366] R. Landgraf, C. Pan, C. Sutton, L. Pearson, D.S. Sigman, D.S. Protein, Engineering 9 (1996) 603.
[367] C.Q. Pan, R. Landgraf, D.S. Sigman, Protein Sci. 4 (1995) 2279.
[368] P.S. Pendergrast, Y.W. Ebright, R.H. Ebright, Science 265 (1994) 959.
[369] P. Harrison-McMonagle, N. Denissova, E. Marinez-Hackert, R.H. Ebright, A.M. Stock, J. Mol. Biol. 285 (1999) 555.
[370] Z. Shang, Y.W. Ebright, N. Ilerr, P.S. Pendergrast, Y. Echelard, A.P. McMaahon, R.H. Ebright, C. Abate, Proc. Natl. Acad. Sci. U.S.A. 9 (1994) 118.
[371] P. Dumoulin, R.H. Ebright, R. Knegtel, R. Kaptein, R.M. Granger-Schnarr, M. Schnarr, Biochemistry 35 (1996) 4279.
[372] J.-C. François, M. Faria, D. Perrin, G. Giovannangeli, Nucl. Acids Mol. Biol. 13 (2004) 224.
[373] J.K. Barton, J.J. Dannenberg, A.L. Raphael, J. Am. Chem. Soc. 104 (1982) 4967.
[374] J.K. Barton, A.T. Danishefsky, J.M. Goldberg, J. Am. Chem. Soc. 106 (1984) 2172.
[375] C.V. Kumar, J.K. Barton, N.J. Turro, J. Am. Chem. Soc. 107 (1985) 5518.
[376] J.K. Barton, J.M. Goldberg, C.V. Kumar, N.J. Turro, J. Am. Chem. Soc. 108 (1986) 2081.
[377] J.K. Barton, A.L. Raphael, Proc. Natl. Acad. Sci. U.S.A. 82 (1985) 6460.
[378] J.P. Rehmann, J.K. Barton, Biochemistry 29 (1990) 1701.
[379] J.P. Rehmann, J.K. Barton, Biochemistry 29 (1990) 1710.
[380] J.K. Barton, Science 233 (1986) 727.
[381] J.K. Barton, L.A. Basile, A.T. Danishefsky, A. Alexandrescu, Proc. Natl. Acad. Sci. U.S.A. 81 (1984) 1961.
[382] A.E. Friedman, J.-C. Chambron, J.-P. Sauvage, N.J. Turro, J.K. Barton, J. Am. Chem. Soc. 112 (1990) 4960.
[383] R.M. Hartshorn, J.K. Barton, J. Am. Chem. Soc. 114 (1992) 5919.
[384] Y. Jenkins, A.E. Friedman, N.J. Turro, J.K. Barton, Biochemistry 31 (1992) 10809.
[385] E. Tuite, P. Lincoln, B. Nordén, J. Am. Chem. Soc. 119 (1997) 239.
[386] C. Hiort, P. Lincoln, B. Nordén, J. Am. Chem. Soc. 115 (1993) 3448.
[387] F.R. Svensson, M. Li, B. Nordén, P. Lincoln, J. Phys. Chem. B 112 (2008) 10969.
[388] C.M. Dupureur, J.K. Barton, J. Am. Chem. Soc. 116 (1994) 10286.
[389] E.J. Merino, J.K. Barton, Biochemistry 47 (2008) 1511.
[390] B.P. Hudson, J.K. Barton, J. Am. Chem. Soc. 120 (1998) 6877.
[391] J.G. Collins, T.P. Shields, J.K. Barton, J. Am. Chem. Soc. 116 (1994) 9840.
[392] C.L. Kielkopf, K.E. Erkkila, B.P. Hudson, J.K. Barton, D.C. Rees, Nat. Struct. Biol. 7 (2000) 117.
[393] A.H. Krotz, L.Y. Kuo, T.P. Shields, J.K. Barton, J. Am. Chem. Soc. 115 (1993) 3877.
[394] A.H. Krotz, L.Y. Kuo, J.K. Barton, Inorg. Chem. 32 (1993) 5963.
[395] T.P. Shields, J.K. Barton, Biochemistry 34 (1995) 15037.
[396] T.P. Shields, J.K. Barton, Biochemistry 34 (1995) 15049.
[397] C. Turro, S.H. Bossmann, Y. Jenkins, J.K. Barton, N.J. Turro, J. Am. Chem. Soc. 117 (1995) 9026.
[398] E.J.C. Olson, D. Hu, A. Hormann, A.M. Jonkman, M.R. Arkin, E.D.A. Stemp, J.K. Barton, P.F. Barbara, J. Am. Chem. Soc. 119 (1997) 11458.
[399] J.K. Barton, R.E. Holmin, Inorg. Chem. 34 (1995) 7.
[400] C.M. Dupureur, J.K. Barton, Inorg. Chem. 36 (1997) 33.
[401] R.E. Holmlin, E.D.A. Stemp, J.K. Barton, Inorg. Chem. 37 (1998) 29.
[402] P. Lincoln, A. Broo, B. Nordén, J. Am. Chem. Soc. 118 (1996) 2644.
[403] I. Greguric, J.R. Aldrich-Wright, J.C. Collins, J. Am. Chem. Soc. 119 (1997) 3621.
[404] J.C. Collins, A.D. Sleeman, J.R. Aldrich-Wright, I. Greguric, T.W. Hambley, Inorg. Chem. 37 (1998) 3133.
[405] A. Sitlani, E.C. Long, A.M. Pyle, J.K. Barton, J. Am. Chem. Soc. 114 (1992) 2303.
[406] D. Campisi, T. Morii, J.K. Barton, Biochemistry 33 (1994) 4130.
[407] L.N. Ji, X.-H. Zou, J.-G. Liu, Coord. Chem. Rev. 216 (2001) 513.
[408] M. Waring, J. Mol. Biol. 54 (1970) 7012.
[409] J.-P. Lecompte, A. Kirsch-De Mesmaeker, M. Demeunynck, J. Lhomme, J. Chem. Soc., Faraday Trans. (1993) 3261.
[410] A.D. Guerzo, A. Kirsch-De Mesmaeker, M. Demeunynck, J. Lhomme, J. Chem. Soc., Dalton Trans. (2000) 1173.
[411] F. Pierard, A.D. Guerzo, A. Kirsch-De Mesmaeker, M. Demeunynck, J. Lhomme, Phys. Chem. Chem. Phys 3 (2001) 2911.
[412] M. Vrabel, M. Hocek, L. Havran, M. Fojta, I. Votruba, B. Klepetarova, R. Pohl, L. Rulek, L. Zendlova, P. Hobza, I.-H. Shih, E. Mabery, R. Mackman, Eur. J. Inorg. Chem. (2007) 1752.
[413] F. O'Reilly, J. Kelly, A. Kirsch-De Mesmaeker, Chem. Commun. (1996) 1013.
[414] F.M. O'Reilly, J.M. Kelly, New J. Chem. 22 (1998) 215.
[415] F.M. O'Reilly, J.M. Kelly, J. Phys. Chem. B 104 (2000) 7206.

[416] L.M. Wilhelmsson, F. Westerlund, P. Lincoln, B. Nordén, J. Am. Chem. Soc. 124 (2002) 12092.
[417] L.M. Wilhelmsson, E.K. Esbjoerner, F. Westerlund, B. Nordén, P. Lincoln, J. Phys. Chem. B 107 (2003) 11784.
[418] F. Westerlund, L.M. Wilhelmsson, B. Nordén, P. Lincoln, J. Am. Chem. Soc. 125 (2003) 3773.
[419] C. Rajput, R. Rutkaite, L. Swanson, I. Haq, J.A. Thomas, Chem. Eur. J. 12 (2006) 4611.
[420] B. Önfelt, P. Lincoln, B. Nordén, J. Am. Chem. Soc. 121 (1999) 10846.
[421] F. Westerlund, F. Pierard, M.P. Eng, B. Nordén, P. Lincoln, J. Phys. Chem. B 109 (2005) 17327.
[422] G. Telfer Shane, N. Tajima, R. Kuroda, J. Am. Chem. Soc. 126 (2004) 1408.
[423] J.A. Smith, J.G. Collins, B.T. Patterson, F.R. Keene, Dalton Trans. (2004) 1277.
[424] F.M. Foley, F.R. Keene, J.G. Collins, J. Chem. Soc., Dalton Trans. (2002) 2968.
[425] A. Brodkorb, A.K.-D. Mesmaeker, T.J. Rutherford, F.R. Keene, Eur. J. Inorg. Chem. (2001) 2151.
[426] B.T. Patterson, J.G. Collins, F.M. Foley, F.R. Keene, J. Chem. Soc., Dalton Trans. (2002) 4343.
[427] J.R. Aldrich-Wright, C. Brodie, E.C. Glazer, N.W. Luedtke, L. Elson-Schwab, Y. Tor, Chem. Commun. (2004) 1018.
[428] J.R. Aldrich-Wright, C. Brodie, Eur. J. Inorg. Chem. (2007) 4781.
[429] J. Lacour, C. Goujon-Ginglinger, S. Troche-Haldimann, J.J. Jordry, Angew., Chem. Int. Ed. Engl. 39 (2000) 3695.
[430] D.J. Hurley, S.E. Seaman, J.C. Mazura, Y. Tor, Org. Lett. 4 (2002) 2305.
[431] D.J. Hurley, Y. Tor, J. Am. Chem. Soc. 120 (1998) 2194.
[432] D.J. Hurley, Y. Tor, J. Am. Chem. Soc. 124 (2002) 3749.
[433] Y. Kitamura, T. Ihara, K. Ohada, Y. Tsujimara, Y. Shirasaka, M. Tazaki, A. Jyo, Chem. Commun. (2005) 4523.
[434] R.H. Terbrueggen, T.W. Johann, J.K. Barton, Inorg. Chem. 37 (1998) 6874.
[435] S.J. Franklin, J.K. Barton, Biochemistry 27 (1998) 16093.
[436] R.H. Terbrueggen, J.K. Barton, Biochemistry 34 (1995) 8227.
[437] N.Y. Sardesai, K. Zimmermann, J.K. Barton, J. Am. Chem. Soc. 116 (1994) 7502.
[438] N.Y. Sardesai, J.K. Barton, J. Biol. Inorg. Chem. 2 (1997) 762.
[439] C.Y. Hastings, J.K. Barton, Biochemistry 38 (1999) 10042.
[440] S. Yoon, P. Kukura, C.M. Stuart, R.A. Mathies, Mol. Phys. 104 (2006) 1275.
[441] C.-T. Lin, W. Böttcher, M. Chou, S. Creutz, N. Sutin, J. Am. Chem. Soc. 98 (1976) 6536.
[442] H. Yersin, E. Gallhuber, J. Am. Chem. Soc. 106 (1984) 6582.
[443] J.M. Kelly, D.J. McConnell, C. Oh Uigin, A.B. Tossi, A. Kirsch-De Mesmaeker, A. Masschelein, J. Nasielski, J. Chem. Soc., Chem. Commun. (1987) 1821.
[444] B. Elias, C. Creely, G.W. Doorley, M.M. Feeney, C. Moucheron, A. Kirsch-De Mesmaeker, J. Dyer, D.C. Grills, M.W. George, P. Matousek, A.W. Parker, M. Towrie, J.M. Kelly, Chem. Eur. J. 14 (2008) 369.
[445] M.S. Deshpande, A.A. Kumbhar, A.S. Kumbhar, Inorg. Chem. 46 (2007) 5450.
[446] H. Uji-i, P. Foubert, F.C. De Schryver, S. De Feyter, E. Gicquel, A. Etoc, C. Moucheron, A. Kirsch-De, Mesmaeker, Chem. Eur. J. 12 (2006) 758.
[447] L. Jacquet, J.M. Kelly, A. Kirsch-De Mesmaeker, J. Chem. Soc., Chem. Commun. (1995) 913.
[448] R. Blasius, H. Nierengarten, M. Luhmer, J.-F. Constant, E. Defrancq, P. Dumy, A. van Dorsselaer, C. Moucheron, A. Kirsch-De, Mesmaeker, Chem. Eur. J. 11 (2005) 1507.
[449] P. Vicendo, S. Mouysset, N. Paillous, Photochem. Photobiol. 65 (1997) 647.
[450] M.M. Feeney, J.M. Kelly, A.B. Tossi, A. Kirsch-De Mesmaeker, J.-P. Lecomte, J. Photochem. Photobiol. B Biol. 23 (1994) 69.
[451] A.D. Guerzo, A. Kirsch-De Mesmaeker, Inorg. Chem. 41 (2002) 938.
[452] M.E. Pauly, I. Kayser, M. Schmitz, M. Dicato, A. Del Guerzo, I. Kolber, C. Moucheron, A. Kirsch-De Mesmaeker, Chem. Commun. (2002) 1086.
[453] A.B. Tossi, J.M. Kelly, Photochem. Photobiol. 49 (1989) 545.
[454] A. Aboul-Enein, D. Schulte-frohlinde, Photochem. Photobiol. 48 (1988) 27.
[455] I. Ortmans, S. Content, N. Boutonnet, A. Kirsch-De Mesmaeker, W. Bannwarth, J.-F. Constant, E. Defrancq, J. Lhomme, Chem. Eur. J. 9 (1999) 2712.
[456] O. Lentzen, J.-F. Constant, E. Defrancq, M. Prevost, S. Schumm, C. Moucheron, P. Dumy, A. Kirsch-De Mesmaeker, Chem. Biol. Chem. 4 (2003) 195.
[457] O. Lentzen, E. Defrancq, J.-F. Constant, S. Schumm, D. García-Fresnadillo, C. Moucheron, P. Dumy, A. Kirsch-De Mesmaeker, J. Biol. Inorg. Chem. 9 (2004) 100.
[458] F.W. Hobbs, J. Org. Chem. 54 (1989) 3420.
[459] S. Schumm, M. Prevost, D. García-Fresnadillo, O. Lentzen, C. Moucheron, A. Kirsch-De Mesmaeker, J. Phys. Chem. B 106 (2002) 2763.
[460] D. García-Fresnadillo, N. Boutonnet, S. Schumm, C. Moucheron, A. Kirsch-De Mesmaeker, E. Defrancq, J.-F. Constant, J. Lhomme, Biophys. J. 82 (2002) 978.
[461] M. Villien, S. Deroo, E. Gicquel, E. Defrancq, C. Moucheron, A. Kirsch-De Mesmaeker, P. Dumy, Tetrahedron 63 (2007) 11299.
[462] S. Deroo, E. Defrancq, C. Moucheron, A. Kirsch-De Mesmaeker, P. Dumy, Tetrahedron Lett. 44 (2003) 8379.
[463] D. Forget, D. Boturyn, E. Defrancq, J. Lhomme, P. Dumy, Chem. Eur. J. 7 (2001) 3976.
[464] O.P. Edupuganti, Y. Singh, E. Defrancq, P. Dumy, Chem. Eur. J. 10 (2004) 5988.
[465] S. Deroo, S. Le Gac, S. Ghosh, M. Villien, P. Gerbaux, E. Defrancq, C. Moucheron, P. Dumy, A. Kirsch-De Mesmaeker, Eur. J. Inorg. Chem. (2009) 524.
[466] S. Deroo, V. Toncheva, E. Defrancq, C. Moucheron, E. Schacht, A. Kirsch-De Mesmaeker, Biomacromolecules 8 (2007) 3503.
[467] F.-H. Li, G.-H. Zhao, H.-X. Wu, S.-R. Zhu, H.-K. Lin, Trans. Met. Chem. 31 (2006) 630.
[468] F.-H. Li, G.-H. Zhao, H.-X. Wu, H. Lin, X.-X. Wu, S.-R. Zhu, H.-K. Lin, J. Inorg. Biochem. 100 (2006) 36.
[469] Z.-M. Wang, H. Lin, H.-K. Lin, S.-R. Zhu, T.F. Liu, Y.T. Chen, J. Inorg. Biochem. 89 (2002) 97.
[470] G.-H. Zhao, F.-H. Li, H. Lin, H.-K. Lin, Bioorg. Med. Chem. 15 (2007) 533.
[471] Y. Kitamura, T. Ihara, Y. Tsujimura, Y. Osawa, M. Tazaki, A. Jyo, Chem. Lett. 34 (2005) 1606.
[472] Y. Kitamura, T. Ihara, Y. Tsujimura, Y. Osawa, M. Tazaki, A. Jyo, Anal. Biochem. 359 (2006) 259.
[473] Y. Kitamura, T. Ihara, Y. Tsujimura, Y. Osawa, D. Sasahara, M. Yamamoto, K. Okada, M. Tazaki, A. Jyo, J. Inorg. Biochem. 102 (2008) 1921.
[474] S.J. Lippard, Acc. Chem. Res. 11 (1978) 211.
[475] J.C. Collins, R.M. Rixon, J. Aldrich-Wright, Inorg. Chem. 39 (2000) 4377.
[476] C.R. Brodie, J.C. Collins, J. Aldrich-Wright, Dalton Trans. (2004) 1145.
[477] D. Jaramillo, D.P. Buck, J.C. Collins, R.R. Fenton, F.H. Stootman, N.J. Wheate, J. Aldrich-Wright, Eur. J. Inorg. Chem. (2006) 839.
[478] S. Kemp, N.J. Wheate, D.P. Buck, M. Nikac, J.C. Collins, F.H. Stootman, J. Aldrich-Wright, J. Inorg. Biochem. 101 (2007) 1049.
[479] D.M. Fisher, P.J. Bednarski, R. Grünert, P. Turner, R.R. Fenton, J. Aldrich-Wright, Chem. Med. Chem. 2 (2007) 488.
[480] N.J. Wheate, R.I. Taleb, A.M. Krause-Heuer, R.L. Cook, S. Wang, J.G. Collins, J. Aldrich-Wright, Dalton Trans. (2007) 5055.
[481] A.M. Krause-Heuer, N.J. Wheate, M.J. Tilby, D.J. Pearson, C.J. Ottley, J. Aldrich-Wright, Inorg. Chem. 47 (2008) 6880.
[482] S. Kemp, N.J. Wheate, M.J. Pisani, J. Aldrich-Wright, J. Med. Chem. 51 (2008) 2787.
[483] A.M. Krause-Heuer, R. Grünert, S. Kühne, M. Buczkowska, N.J. Wheate, D.D. Le Pevelen, L.R. Booag, D.M. Fisher, J. Kasparkova, J. Malina, P.J. Bednarski, V. Brabec, J. Aldrich-Wright, J. Med. Chem. 52 (2009) 5474.
[484] J.E. Reed, S. Neidle, R. Vilar, Chem. Commun. (2007) 4366.
[485] J.E. Reed, A.J.P. White, S. Neidle, R. Vilar, Dalton Trans. (2009) 2558.
[486] J.F.J. Engbersen, A. Koudijs, M.H.A. Joosten, H.C. Van der Plas, J. Heterocycl. Chem. 23 (1986) 989.
[487] C. Bazzicalupi, A. Bencini, C. Bonaccini, C. Giorgi, P. Gratteri, S. Moro, M. Palumbo, A. Simionato, J. Sgrignani, C. Sissi, B. Valtancoli, Inorg. Chem. 47 (2008) 5473.
[488] Q.-X. Xiang, J. Zhang, P.-Y. Liu, C.-Q. Xia, Z.-Y. Zhou, R.-G. Xie, X.-Q. Yu, J. Inorg. Biochem. 99 (2005) 1661.
[489] C. Musetti, L. Lucatello, S. Bianco, A.P. Krapcho, S.A. Cadamuro, M. Palumbo, C. Sissi, Dalton Trans. (2009) 3657.
[490] S. Routier, V. Joanny, A. Zaparucha, H. Vezin, J.-P. Catteau, J.-L. Bernier, C. Bailly, J. Chem. Soc., Perkin Trans. 2 (1998) 863.
[491] F.A. Aldaye, H.F. Sleiman, J. Am. Chem. Soc. 129 (2007) 13376.
[492] F.A. Aldaye, H.F. Sleiman, J. Am. Chem. Soc. 129 (2007) 4130.
[493] F.A. Aldaye, H.F. Sleiman, Angew. Chem., Eng. Int. Ed. Engl. 45 (2006) 2204.
[494] H. Yang, A.Z. Rys, C.K. McLaughlin, H.F. Sleiman, Angew. Chem., Eng. Int. Ed. Engl. 48 (2009) 9919.
[495] H. Yang, H.F. Sleiman, Angew. Chem., Eng. Int. Ed. Engl. 47 (2008) 2443.
[496] H. Yang, C.K. McLaughlin, F.A. Aldaye, G.D. Amblin, A.Z. Rys, I. Rouiller, H.F. Sleiman, Nat. Chem. 1 (2009) 390.
[497] S. Neidle, S. Balasubramanian (Eds.), Quadruplex Nucleic Acids, RSC Publishing, Cambridge, 2006.
[498] J.L. Huppert, Chem. Soc. Rev. 37 (2008) 1375.
[499] D. Monchaud, M.-P. Teulade Fichou, Org. Biomol. Chem. 6 (2008) 627.
[500] A. De Cian, E. DeLemos, J.-M. Mergny, M.-P. Teulade Fichou, D. Monchaud, J. Am. Chem. Soc. 129 (2007) 1856.
[501] A. De Cian, G. Cristofari, P. Reichenbach, E. DeLemos, D. Monchaud, M.-P. Teulade Fichou, K. Shin-ya, L. Lacroix, J. Lingner, J.-M. Mergny, Proc. Natl. Acad. Sci. U.S.A. 104 (2007) 17347.
[502] A. De Cian, P. Grellier, E. Mouray, D. Depoix, H. Bertrand, D. Monchaud, M.-P. Teulade Fichou, J.-M. Mergny, P. Alberti, Chem. Biol. Chem. 9 (2008) 2730.
[503] A. Henn, A. Joachimi, D.P.N. Gonçalves, D. Monchaud, M.-P. Teulade Fichou, J.K.M. Sanders, J.S. Hartig, Chem. Biol. Chem. 9 (2008) 2722.
[504] M. Kaiser, A. De Cian, M. Sainlos, C. Renner, J.-M. Mergny, M.-P. Teulade Fichou, Org. Biomol. Chem. 4 (2006) 1049.
[505] K. Hayashi, H. Akutsu, H. Ozaki, H. Sawai, Chem. Commun. (2004) 1386.
[506] B. Baldyrou, C. Tardy, C. Bailly, P. Colson, C. Houssier, F. Charmantray, M. Demeunynck, Eur. J. Med. Chem. 37 (2002) 315.
[507] S.M. Langenegger, R. Häner, Tetrahedron Lett. 45 (2004) 9273.
[508] S.M. Langenegger, R. Häner, Chem. Biol. Chem. 6 (2005) 848.
[509] V. Esposito, A. Galeone, L. Mayol, G. Oliviro, A. Randazzo, M. Varra, Eur. J. Org. Chem. (2002) 4228.
[510] S.-X. Liu, C. Michel, M. Schmittel, Org. Lett. 2 (2000) 3959.
[511] M. Schmittel, C. Michel, A. Wiegrefe, V. Kalsani, Synthesis (2001) 1561.
[512] V. Kalsani, H. Bodenstedt, D. Fenske, M. Schmittel, Eur. J. Inorg. Chem. (2005) 1841.
[513] M. Schmittel, K. Mahata, Chem. Commun. (2008) 2550.
[514] M. Schmittel, K. Mahata, Inorg. Chem. 48 (2009) 822.
[515] M. Schmittel, V. Kalsani, D. Fenske, A. Wiegrefe, Chem. Commun. (2004) 490.
[516] M. Schamittel, H. Ammon, V. Kalsani, A. Wiegrefe, C. Michel, Chem. Commun. (2002) 2566.
[517] M. Schmittel, V. Kalsani, C. Michel, P. Mal, H. Ammon, F. Jäckel, J.P. Rabe, Chem. Eur. J. 13 (2007) 6223.
[518] M. Schmittel, B. He, Chem. Commun. (2008) 4723.
[519] M. Schmittel, P. Mal, Chem. Commun. (2008) 960.
[520] V. Kalsani, H. Ammon, F. Jäckel, J.P. Rabe, M. Schmittel, Chem. Eur. J. 10 (2004) 5481.
[521] R.S.K. Kishore, T. Paululat, M. Schmittel, Chem. Eur. J. 12 (2006) 8136.

[522] J.-C. Chambron, V. Heitz, J.-P. Sauvage, Tetrahedron Lett. 36 (1995) 9321.
[523] G. Hungerford, M. Van der Auweraer, J.-C. Chambron, V. Heitz, J.-P. Sauvage, J.-L. Pierre, D. Zurita, Chem. Eur. J. 5 (1999) 2089.
[524] E. Iengo, E. Zangrando, E. Alessio, J.-C. Chambron, V. Heitz, L. Flamifni, J.-P. Sauvage, Chem. Eur. J. 9 (2003) 5879.
[525] M. Shaul, Y. Cohen, J. Org. Chem. 64 (1999) 9358.
[526] C. Dietrich-Buchecker, B. Colasson, D. Jouvenot, J.-P. Sauvage, Chem. Eur. J. 11 (2005) 4374.
[527] M. Hutin, R. Frantz, J.R. Nitschke, Chem. Eur. J. 12 (2006) 4077.
[528] M. Hutin, C.A. Schalley, G. Bernardinelli, J.R. Nitschke, Chem. Eur. J. 12 (2006) 4069.
[529] J.R. Nitschke, Acc. Chem. Res. 40 (2007) 103.
[530] D. Schultz, F. Biaso, A.R.M. Shahi, M. Geoffroy, K. Rissanen, L. Gagliardi, C.J. Cramer, J.R. Nitschke, Chem. Eur. J. 14 (2008) 7180.
[531] V.E. Campbell, X. de Hatten, N. Delsuc, B. Kauffmann, I. Huc, J.R. Nitschke, Chem. Eur. J. 15 (2009) 6138.
[532] P. Pallavicini, V. Amendola, Y. Diaz Fernadez, M. Ghisalberti, L. Linati, C. Mangano, A. Manotti Lanfredi, C. Massera, Dalton Trans. (2003) 575.
[533] M.A. Heuft, A.G. Fallis, Angew. Chem., Int. Ed. Engl. 41 (2002) 4520.
[534] S.M. Hecht, I. Huc, Foldamers: Structure. Properties and Applications, Wiley-VCH, Weinheim, Germany, 2007.
[535] Z.-Q. Hu, H.-Y. Hu, C.-F. Chen, J. Org. Chem. 71 (2006) 1131.
[536] H.-Y. Hu, W. Xue, Z.-Q. Hu, J.-F. Xiang, C.-F. Chen, S.-G. He, J. Org. Chem. 74 (2009) 4949.
[537] H.-Y. Hu, J.-F. Xiang, Y. Yang, C.-F. Chen, Org. Lett. 10 (2008) 69.
[538] H. Stephan, G. Geipel, G. Bernhard, P. Comba, G. Rajaraman, U. Hahn, F. Vögtle, Eur. J. Inorg. Chem. (2005) 4501.
[539] U. Hahn, F. Vögtle, G.D.E. Paoli, M. Staffilani, L. De Cola, Eur. J. Inorg. Chem. (2009) 2639.
[540] M. Kimura, T. Shiba, T. Muto, K. Hanabusa, H. Shirai, Tetrahedron Lett. 41 (2000) 6809.
[541] N.D. McClenaghan, R. Passalacqua, F. Loiseau, S. Campagna, B. Verheyde, A. Hameurlaine, W. Dehaen, J. Am. Chem. Soc. 125 (2003) 5356.
[542] E. Gumienna-Kontecka, Y. Rio, C. Bourgogne, M. Elhabiri, R. Louis, A.-M. Albrecht-Gary, J.-F. Nierengarten, Inorg. Chem. 43 (2004) 3200.
[543] Y. Rio, G. Accorsi, N. Armaroli, D. Felder, E. Levillain, J.-F. Nierengarten, Chem. Commun. (2002) 2380.
[544] J.-F. Nierengarten, D. Felder, J.-F. Nicoud, Tetrahedron Lett. 40 (1999) 273.
[545] N. Armaroli, C. Boudon, D. Felder, J.-P. Gisselbrecht, M. Gross, G. Marconi, J.-F. Nicoud, J.-F. Nierengarten, V. Vicinelli, Angew. Chem., Int. Ed. Engl. 38 (1999) 3730.
[546] G. Pickaert, L. Douce, R. Ziessel, D. Guillon, Chem. Commun. (2002) 1584.
[547] G. Pickaert, M. Cesario, R. Ziessel, J. Org. Chem. 69 (2004) 5335.
[548] R. Ziessel, G. Pickaert, F. Camerel, B. Donnio, D. Guillon, M. Cesario, T. Prangé, J. Am. Chem. Soc. 126 (2004) 12403.